Université d'Ottawa • University of Ottawa

Université d'Ottawa · University of Ottawa

FACULTÉ DES ÉTUDES SUPÉRIEURES ET POSTDOCTORALES

FACULTY OF GRADUATE AND POSTDOCTORAL STUDIES

Esra DINCER
AUTEUR DE LA THÈSE - AUTHOR OF THESIS

M. A. Sc. (Civil Engineering)
GRADE - DEGREE

Department of Civil Engineering
FACULTÉ, ÉCOLE, DÉPARTEMENT - FACULTY, SCHOOL, DEPARTMENT

TITRE DE LA THÈSE - TITLE OF THE THESIS

Seismic Drift Demands of Reinforced Concrete Buildings

M. Saatcioglu
DIRECTEUR DE LA THÈSE - THESIS SUPERVISOR

CO-DIRECTEUR DE LA THÈSE - THESIS CO-SUPERVISOR

EXAMINATEURS DE LA THÈSE - THESIS EXAMINERS

J. Humar

N. Naumoski

H. Tanaka

J.-M. De Koninck, Ph.D.
LE DOYEN DE LA FACULTÉ DES ÉTUDES SUPÉRIEURES ET POSTDOCTORALES

SIGNATURE

DEAN OF THE FACULTY OF GRADUATE AND POSTDOCTORAL STUDIES

SEISMIC DRIFT DEMANDS OF REINFORCED CONCRETE BUILDINGS

by

Esra Dincer

A thesis presented to the
School of Graduate Studies and Research of the University of Ottawa in
partial fulfillment of the requirements for the degree of
Master of Applied Science in Engineering

Ottawa-Carleton Institute for Civil Engineering
Faculty of Engineering
University of Ottawa

Ottawa, Ontario, Canada
November 2003

Your file Votre référence
ISBN: 0-612-90057-6
Our file Notre référence
ISBN: 0-612-90057-6

Acknowledgements

This thesis was conducted under the supervision of Prof. Murat SAATCIOGLU, to whom I would like to express my gratitude for his helpful guidance and endless encouragement throughout the thesis. I also thank Prof. Jag HUMAR, Prof. Nove NAUMOSKI and Prof. Hiroshi TANAKA for their suggestions and comments. I also would like to thank Husham ALMANSOUR for his technical assistance and great help.

There are things that can not be expressed by words. Without any doubt, I would like to thank Ilhan GULCAN for his great understanding and support regardless the very long distance.

Living in another country brings many difficulties, but I would like to thank two friends, Aysegul OZBAKIR and Gunes KARABULUT, for their efforts in making the life easier and enjoyable.

Finally, I owe my special thanks to my family for their faith in me, continuous support, understanding and endless patience.

Abstract

The main objective of the current research is to establish drift demands for reinforced concrete buildings designed on the basis of the National Building Code of Canada (NBCC-2005). A total of 12 reinforced concrete buildings with three different heights and structural systems, consisting of moment resisting frames with and without shear walls and structures with core walls, were designed for eastern and western Canada. A comprehensive analytical research was conducted involving more than 140 analyses of buildings to investigate inelastic seismic drift demands in Canada.

The investigation consisted of three phases. The first phase included preparation of a Visual Basic pre-processor for an existing general purpose dynamic analysis software. The second phase involved the design of selected buildings. The third and final phase consisted of dynamic inelastic response history analysis of buildings under code compatible earthquake records. A large number of artificially generated earthquake records were selected, reflecting the seismicity of the two cities considered in design, i.e., Ottawa in the east and Vancouver in the west.

The results indicate that the buildings remained within the code specified maximum limit of 2.5% lateral drift ratio. Buildings in the east developed little inelasticity and showed a maximum interstorey drift ratio of 0.65%. The buildings in the west exhibited increased ductility demands, with maximum displacement ductility ratios ranging between 5.5 for beams and 6.5 for shear walls. The drift ratios remained below 1.14 %. Additional results obtained from dynamic analysis indicate that total static base shears, obtained on the basis of the equivalent static load approach, are close to those obtained from dynamic inelastic analyses of frame buildings in the east, though major differences do exist between the two for shear wall buildings in the east as well as all the buildings in the west. In general, dynamic base shears are higher than the static values, though base moments agree closely with static values, indicating discrepancies between the actual and assumed static distribution of seismic forces along building height.

Table of Contents

List of Tables

List of Figures

CHAPTER 1
Introduction

1.1 General

The main goal of structural design is to build safe structures that can withstand the imposed loads during their service life. This criterion is satisfied by selecting a proper structural system, understanding the behavior of the system and by identifying the possible failure modes under estimated loads. After the structure is designed for adequate strength, it is checked against serviceability limits. An important serviceability limit is an acceptable level of deflection. The deflection limit gains a new dimension in earthquake resistant construction where members experience inelastic deformations while dissipating seismic induced energy, without significant degradation in strength.

The level of damage sustained during an earthquake is closely related to the level of inelastic deformations developed. Thus, deformation control also results in damage control. This is especially true for nonstructural elements like partitions, stair enclosures and brittle materials which can become a source of potential injury or loss of life due to lack of inelastic deformability. Furthermore, structural stability is provided by limiting the flexibility of the system. Larger lateral deformations can result in secondary moment effects (P-Δ effects) on vertical load carrying members, creating potentially dangerous stability problems. Torsional effects increase the susceptibility of structures to high seismic deformation demands. Therefore, drift limits are often specified in building codes and standards for earthquake resistant structures.

Structures are designed to meet certain performance criteria while satisfying the functions for which they are designed. The most important criterion is life safety. While no structure is totally immune to structural collapse, since there is always a probability of failure due to overloads and abnormal loads. The acceptable level of this probability depends on the importance of the structure and the performance criteria adopted for design. Since the protection of life is the main objective in seismic design codes, reducing the property damage becomes a secondary goal. Bertero (1996b) explained the general philosophy of earthquake resistant design for nonessential facilities, as stated below, which has been accepted worldwide:

"...(1) structural and nonstructural damage in frequent minor earthquake ground shaking, (2) structural damage and minimization of nonstructural damage during occasional moderate earthquake ground shaking, and (3) collapse or serious damage in rare major earthquake ground-shaking."

Most current seismic design codes are based on a one-level design earthquake (life-safety level). It is desirable to also include lower level of design earthquakes to satisfy other performance criteria. The newly developed design methodology, known as "Performance-Based Seismic Engineering of Buildings," considers multi-level earthquakes and corresponding performance levels (Bertero 1996a). Bertero (1996b) gives the definition of this method as; "*Performance-based EQ-RD consists of selection of appropriate systems, layout, proportioning and detailing of a structure and its nonstructural components and contents so that at specified levels of ground motion and with defined levels of reliability, the structure will not be damaged beyond certain limiting states.*" Heidebrecht and Naumoski (1999) define the performance level as "*...an expression of the maximum permissible extent of damage to a building when subjected to specific earthquake design ground motions...*" Four performance levels are defined for this procedure (SEAOC Vision 2000 Committee 1995) as fully operational, operational, life-safe and near collapse. Performance levels are linked to the maximum permissible interstorey drifts, having 0.5%, 1.5%, and 2.5% drifts for operational, life-safe and near collapse levels, respectively. Displacement-based seismic design utilizes expected displacement response of a structure to display a given performance. Therefore, the focus is on the displacements. The structural and nonstructural damage can then be linked to interstorey drifts.

In conventional force-based design procedures the required strength of the structure is established first prior to the computation of displacements. The designer usually does not design for displacements but does perform a displacement check. In displacement based design approaches, the decision to control displacement demands is made in the planning stage (Moehle 1992). Chandler and Mendis (2000) indicated that the focus in displacement-based approaches is on achieving the required combination of elastic stiffness and inelastic energy-dissipation capacity, whereas the focus in force-based design is on required strength.

The current Canadian seismic design code (NBCC 1995) is based on a strength-controlled design approach that corresponds to an earthquake return period of 475 years. Required strength for this level of earthquake is reduced by the force modification factor R in anticipation of inelastic response and energy dissipation capabilities of the structure. The R factor depends only on the type of structural system adopted and is not explicitly tied in with the period of structure. Bertero (1996b) indicated that the currently used static equivalent lateral force approach did not always give conservative solutions and could overestimate performance.

Many changes are proposed for the Earthquake Design Provisions of the 2005 edition of the National Building Code of Canada (NBCC 2005); they are explained in greater detail in the following sections. In the new code, dynamic analysis has been adopted as the preferred method of analysis. Dynamic analysis has also been recognized as one of the analysis tools in an effort to improve the accuracy of design, including estimates of drift demands. The drift limit is increased from 2% to 2.5% for ordinary buildings as an acceptable level of deformability. However, the consequence of the proposed design approach, with the new seismicity information and associated Uniform Hazard Response Spectra (UHS), on deformation demands has not been established. The current research project has been undertaken to assess drift demands for concrete frame and shear wall structures under the new NBCC-2005 proposed design force levels.

1.2 Objective and Scope

The objective of current research is to establish drift demands for reinforced concrete structures designed on the basis of NBCC-2005. The objective also includes the modification of computer software DRAIN-RC, developed at the University of California, Berkeley (Kanaan and Powell, 1973) and later enhanced at the University of Ottawa by incorporating appropriate hysteretic models for inelastic response of reinforced concrete structures.

The following includes the scope of research:

- Literature survey on seismic deformation demands of structures and dynamic inelastic response history analysis of reinforced concrete structures.
- Preparation of a Visual Basic (Version 6.0) pre-processor for computer program DRAIN-RC to make it interactive and user friendly.
- Design of 12 reinforced concrete buildings, consisting of 3 moment resisting frame (MRF) buildings and 3 frame-shear wall (SHW) interactive systems located in Ottawa and the same number of buildings located in Vancouver. The buildings in Vancouver consisted of frame interactive systems with two levels of bracing provided by two different arrangements of shear walls and correspondingly different levels of lateral stiffness.
- Selection of artificial ground motion records, compatible with NBCC-2005 specified UHS for Ottawa, representative of eastern Canadian earthquakes and Vancouver, representative of western Canadian earthquakes.
- Dynamic inelastic history analyses of 12 buildings under proper ground motion records, resulting in a total of 144 analyses, providing data on drift demands.
- Review and evaluation of results to draw conclusions that are applicable to buildings and seismicity of Canada.
- Preparation and presentation of research results in the form of a thesis.

1.3 Literature Survey

A literature survey was conducted to find out previously generated information in the area of dynamic response and lateral drift demands of reinforced concrete structures. A summary of previous research in the area is provided in the following paragraphs.

Drift response of reinforced concrete structures was investigated by several researches analytically as well as experimentally. A pilot project was conducted by Heidebrecht (1997) on a six-storey reinforced concrete frame structure in Vancouver. A medium height office building with 7 bays in the longitudinal direction and 5 bays in the transverse direction was selected with a total of 8 moment resisting frames. The lateral loads were resisted by 6 frames in the longitudinal direction that were critical for both gravity and lateral loads. In the transverse direction, only two moment resisting frames were assumed to provide resistance to lateral loads. Despite the 2% lateral drift limit specified in NBCC (1995), an interstorey drift limit of 1% was used to limit damage. Inelastic response history analysis was conducted using the computer software IDARC (1992), which is capable of examining hysteretic characteristics of reinforced concrete elements. The transverse frame was subjected to scaled N00E component of the time-history recorded during the 1985 Mexico City Earthquake. P-Δ effects were not included in the analysis. The results indicated that when the peak ground acceleration was scaled to 0.40g the maximum roof displacement and interstorey drift were 0.77% and 1.18%, respectively, and column and beam curvature ductility ratios were 3.15 and 5.59, respectively.

Heidebrecht and Naumoski (1999) investigated seismic performance of the same building using the newly proposed performance based approach, comparing interstorey drifts with the drift criteria. Static pushover and dynamic analyses were conducted to investigate the relationship between local damage and maximum interstorey drift. Pushover analyses were conducted by applying monotonically increasing static lateral loads on the structure to determine possible locations for cracking and yielding. A total of 15 acceleration time-histories were used for dynamic analyses with a scaling factor of up to three times the design acceleration level. The results indicated that transverse and longitudinal frames met life safety performance criterion for excitations up to 2 and 2.5 times the design criterion, respectively. It was concluded that structures designed for the design earthquake (life-safety level) were able to conservatively withstand twice the design ground motions without compromising life safety performance level. The pushover analysis gave non-conservative values for maximum member deformations and maximum interstorey drifts as compared to dynamic analysis.

Zhu, Tso and Heidebrecht (1992) and Zhu (1994) conducted inelastic dynamic analyses for 4, 10 and 18 storey buildings with 45 strong motion records. The records had three groups; having low, intermediate, and high peak acceleration-to-velocity (A/V) ratios that represent different combinations of acceleration and velocity zones of NBCC-1995. The purpose of the study was to investigate seismic performance of high-rise, long-period buildings, as affected by different acceleration and velocity zones. The objective also included the comparison of NBCC procedure for calculating lateral drift ratios with those estimated for different zonal combination areas. Inelastic static analyses were conducted under monotically increasing lateral loads. Subsequently, inelastic dynamic analysis was conducted using software DRAIN-2D (1973) to determine response parameters. The computed interstorey drifts were compared with the code procedure. In low-rise buildings inelastic deformations occurred mostly in the lower storeys and the code procedure underestimated lateral drift ratios when the frame was subjected to high A/V ratios (located in Za>Zv areas). As the number of storeys increased, the code procedure became conservative irrespective of the actual zonal combinations. It was established that for high-rise buildings, low A/V ratio ground motions were more damaging than those with high ratios A/V. Non-structural elements were not included in the analyses.

Filiatrault, Lachapelle and Lamontagne (1998a, 1998b) conducted experimental and analytical seismic analyses to investigate the behavior of ductile and nominally ductile reinforced concrete buildings. Two half-scale reinforced concrete moment resisting frames were examined by conducting shaking table tests. The structures had two storeys and two bays with a 3 m height and a 5m width. One of the structures was designed to be a ductile structure with a force reduction factor of R=4 and contained strict seismic detailing. The other structure was designed to be nominally ductile with R=2 and nominal detailing. Two different earthquake intensities; 0.21 g and 0.42 g, were used for analyses. During the design level earthquake, both structures exhibited less than the maximum allowable interstorey drift. The ductile structure experienced a maximum interstorey drift of 1.58 % when the lower intensity level was used, and 2.74 % when the higher level was used. The structure with nominal ductility experienced 1.98 % and 4.67 % interstorey drift ratios, respectively. Nonlinear time-history dynamic analyses of these buildings were conducted using the computer program RUAUMOKO with acceleration time-histories recorded during shake table tests. The cyclic moment-curvature behavior of members and inelastic deformations of joints were included with a hysteretic model and nonlinear rotational springs at the end of the beams, respectively. The results were compared with those obtained from shake table tests. They indicated good correlation between the two sets of results.

Bariola (1992) studied drift response of medium-rise buildings by selecting six 8-storey concrete frames with different dimensions and base shear capacities. Five different ground motion components were used to conduct nonlinear seismic analyses by using computer program LARZ. The program could consider only planar frames with member models consisting of elastic portions and rotational springs, incorporating flexural response. Anchorage slip effects were not included in the analyses and ground motions were specified in the horizontal direction. The results indicated that for low and medium-rise buildings, weak structures experienced higher drift than strong structures, whereas for high structures the opposite was observed for some ground motions. This indicates dependency of drift response in medium and high-rise structures on their strength. Drift responses were also obtained by linear dynamic analyses assuming an effective period equal to twice the natural period computed on the basis of gross sections and a damping ratio of 2 %. Comparison of results obtained from nonlinear and linear analyses indicated that, for most of the ground motions considered, the difference in drift responses was acceptably small.

Lee and Woo (2002) conducted analytical and experimental studies to investigate the seismic performance of a three-storey reinforced concrete building that was not designed for earthquake effects. A 1:5 scale frame was subjected to shake table simulations. The damping ratios and natural periods were estimated by performing free vibration tests. The roof drift was estimated as the average of values obtained from two frames. The maximum interstorey drift was 1.68 % and was calculated when the structure underwent maximum roof drift of 30 mm, whereas the maximum allowable value was 1.5 %. IDARC-2D computer program was used to conduct dynamic inelastic analysis. The comparison showed smaller peak drift at the roof level for analytical studies. Pushover tests were also conducted to determine strength and deformation under increased earthquake motions. The results indicated that nonlinear dynamic analysis did not provide a higher level of accuracy or reliability. The first storey developed 3.7 % interstorey drift ratio under Pushover analysis before collapsing.

Chandler and Mendis (2000) conducted analyses to compare the performance characteristics of frames designed with conventional force-based and newly proposed displacement-based design procedures. A typical 6-storey building was selected with three different ductility levels, reflecting low, medium and highly ductile structures on the basis of the Australian Code. The design of buildings was done with an equivalent static method. Nonlinear dynamic analysis computer program DRAIN-2D (1973) was used to conduct time history analysis. Effective period, effective equivalent damping and effective damping ratio were required to develop the displacement spectra. The results indicated that the displacement-based approach predicted overall drifts accurately for these typical frames.

Moehle (1992) conducted a study to compare the displacement-based design approach, which uses expected displacements as a direct design tool, with the conventional ductility-based approach, which uses the required strength for elastic response directly. The displacement response of SDOF and MDOF systems were investigated with examples. The design procedure for ductility and displacement based approaches were compared and it was concluded that the displacement-based design approach was an effective and simple tool to design structures.

Medhekar and Kennedy (2000) performed a critical overview of currently used design approaches. It was indicated that, to conduct seismic analysis with a spectral acceleration based method the fundamental period T of the structure should be found before beginning the analysis. There are approximate formulas in building codes to estimate its value, mostly using only the height of the structure, without any consideration of the structural system and geometry. Thus, the period value does not reflect the exact period of the structure, but rather provide a conservative estimate. The determination of the force modification factor R, specified in most building codes to account for available ductility in the system, the structural system and the characteristics of the construction material used need to be established, which are difficult to establish properly. The design is based on these values that are calculated at the beginning. The displacements are then checked at the end of the design process. Although the structure is designed for sufficient strength, excessive displacements can lead to stability problems and partial or complete collapse of structural and/or non-structural elements. It can be said that the deformations rather than the forces may be a more proper parameter to indicate potential damage. It is therefore recommended to employ a displacement-based design method. This method does not require the computation of fundamental period T with approximate expressions and define an arbitrary R value. The acceptable level of deformation is established at the beginning of the design process with due consideration given to the displaced shape of the building and estimates of drift tolerances for non-structural elements. The deformation demand can be met by selecting the strength and stiffness of the lateral load resisting system. The overall displacement of the structure may be controlled by the displacement-based design method.

Shooshtari (1998) investigated drift demands in concrete buildings designed in Eastern and Western Canada. He designed three frame and three shear wall buildings in Ottawa and Vancouver, using the requirements of NBCC-1995. The buildings were then subjected to artificial earthquake records representative of Eastern and Western Canada, as well as actual records of California earthquakes. The results indicated that none of the buildings exceeded the 2% drift limit specified in NBCC-1995. The buildings in Eastern Canada showed interstorey drifts of 0.2% and those in the Western Canada showed 1.2% under artificial records.

The current research program involves the use of a modified version of computer software DRAIN-2D. Therefore, the development of this software and its use in earlier phases of the same investigation was also reviewed as part of the literature survey. DRAIN-2D was developed by Kanaan and Powell (1973) as a general purpose computer program for dynamic inelastic analysis of two dimensional structures under earthquake type ground motions. Five different types of elements were introduced, consisting of truss bars, beam-column elements, semi-rigid connection elements, shear panel elements representing infill panels and beam element. Subsequently, Powell (1975) introduced a beam element with degrading stiffness characteristics for reinforced concrete, where the moment-rotation relationship for each hinge is based on the extended version of Takeda's model (Powell 1975).

The program was later modified at the University of Ottawa by Alsiwat (1993), while also making it run on personal computers. The reinforced concrete beam element was modeled as an elastic line element having three inelastic springs at each end to account for inelasticity due to flexure, shear and anchorage slip, as described below.

- *Flexural Modeling:* Each element was modeled as an elastic line element having inelastic flexural springs at each end to form plastic hinges. The modified version of Takeda's model was used to account for flexural hysteretic behavior of reinforced concrete elements.
- *Shear Modeling:* To incorporate inelastic shear effects, the beam element was modeled to have an elastic line element and two inelastic shear springs at each end of member. The hysteretic model assigned to shear springs was that developed by Ozcebe and Saatcioglu (1989), consisting of a tri-linear primary curve with break points at cracking and yielding.

- *Anchorage Slip Modeling:* Inelastic behaviour of the extension and/or slip of anchored reinforcement in adjoining members was incorporated by adding a third group of inelastic springs at each end of the elastic beam element. The hysteretic model used was that developed by Saatcioglu, Alsiwat and Ozcebe (1992). The model was based on a bilinear primary curve that was computed on the basis of the strain distribution along the bar (Alsiwat and Saatcioglu, 1992).

Shooshtari (1998) further modified DRAIN-2D to incorporate additional models applicable to reinforced concrete structures. The modified version was referred to as DRAIN-RC as it was essentially meant for reinforced concrete (RC) structures. The new modifications were introduced in the following topics:

- *Axial Force-Moment Interaction Model*: The hysteretic model that was developed by Saatcioglu et al. (1983), incorporating P-M interaction on strength and stiffness of members, was included in the program.
- *Hysteretic Model for Infill Panels:* The hysteretic model that was developed by Klingner and Bertero (1978), consisting of two equivalent diagonal struts replacing the infill panel in each direction, was introduced.
- *Static Inelastic (Pushover) Analysis:* Incremental inelastic static analysis was introduced to be able to conduct pushover analysis of reinforced concrete structures.
- *P-Δ Effects:* Secondary deformations caused by P-Δ effects were introduced to account for changes in both flexural and axial stiffness matrices.

1.4 Outline of Thesis

The thesis consists of 5 chapters. Following Chapter1, Chapter 2 describes the capabilities and features of computer software DRAIN-RC that was used in the current investigation to conduct dynamic inelastic analysis. The hysteretic models, solution techniques and features of the program are explained. The chapter also includes the description of Windows-based pre-processor that was developed as part of the scope of this thesis. The details of the pre-processor are presented by printing example windows. The user's guide of the program, outlining input instructions, is presented in Appendix A.

Chapter 3 includes the selection and design of 12 reinforced concrete buildings with different heights and lateral force resisting systems, consisting of frames and frame-shear wall interactive systems with different levels of lateral rigidity provided by different types of shear walls. Artificially generated ground motion records, representative of Eastern and Western Canada and compatible with design response spectra proposed in the 2005 edition of NBCC are selected and described in this Chapter.

Chapter 4 includes dynamic inelastic response history analyses of selected buildings under the selected ground motion records to examine overall structural drift and interstorey drift demands. The relationships between drift index and structural parameters are studied. The static base shears are compared with dynamic base shears.

Chapter 5 presents the results of current investigation. Further research is recommended for continued investigation of drift demands in reinforced concrete structures.

CHAPTER 2
Computer Program Used in the Analysis

2.1 Introduction

The computer program DRAIN-RC was used to conduct dynamic inelastic response history analysis. A new version of this program was developed for the current research project by preparing a pre-processor to be able to input data within the Windows Operating System environment in a more user friendly and interactive manner. The original version of the program (DRAIN-2D) was developed by Kanaan and Powell (1973) to conduct dynamic analysis of inelastic plane structures. Alsiwat (1993) modified the original version of the program by adding new hysteretic models for shear and anchorage slip. This version was then modified by Shoostari (1998) and called DRAIN-RC (RC for reinforced concrete). DRAIN-RC includes hysteretic models that are applicable to reinforced concrete response and also includes new features, consisting of inelastic static analysis (push-over) and P-Δ effects. The solution technique and features of hysteretic models employed in the computer software are discussed in the following sections. The new development, in the form of Windows based pre-processor is also explained in this Chapter.

2.2 Program Concept

Computer software DRAIN-RC is a general purpose program intended for inelastic static and dynamic analysis of reinforced concrete structures. The program is limited to structures that can be idealized in two-dimensions, having discrete elements. Each node of the structure can have up to three degrees of freedom that are considered only at the nodes. To decrease the number of unknowns, degrees of freedom at supports can be restrained so that no degree of freedom is assigned, or can be combined with the translational or rotational displacements of any group of nodes to have identical displacements. To have a diagonal mass matrix, the structural mass is assumed to be lumped at the nodes. The earthquake excitation is defined by time histories of ground acceleration that may be different in the horizontal and vertical directions. Analysis is done by using the Direct Stiffness Method that is a special form of the Displacement Method where the state of deformation of the structure can be completely defined in terms of a finite number of displacement parameters associated with the nodes. The global stiffness matrix is assembled from individual element stiffness matrices by a simple addition process. Displacements of some nodes may be assumed to be zero without introducing significant errors, such as those of supports that are stiff in comparison with the frame, or those that are known to be zero, such as axial deformations of certain members. The commonly used idealization of modeling floors as rigid diaphragms can be done by assuming displacements of all beams in the horizontal direction equal to each other. Therefore, all degrees of freedom of nodes in the same floor in X direction become identical.

The dynamic response is established by step-by-step integration, with the average acceleration assumption (see Fig. 2.1) within any time step. The tangent stiffness of the structure is used for each time step, and linear structural behavior is assumed within a time step. Any unbalanced loads resulting from errors in the assumed linear behavior within a time step are eliminated by applying corrective loads in the subsequent time step.

For a finite time step, Δt, the incremental equation of motion can be written as follows:

$$[M]\{\Delta\ddot{u}\}+[C]\{\Delta\dot{u}\}+[K]\{\Delta u\}=\{\Delta P\} \tag{2.1}$$

in which $\{\Delta u\}$,$\{\Delta u\}$,$\{\Delta \mathrm{u}\}$and$\{\Delta \mathrm{P}\}$ are finite increments of acceleration, velocity, displacement and load, respectively. The average acceleration method has the advantage of being stable for all periods and time steps, and not introducing damping into the system. The average of accelerations at time t=0 and t=1 can be written as:

$$\ddot{u} = \frac{1}{2}(\ddot{u}_0 + \ddot{u}_1) \tag{2.2}$$

The change in velocity may be defined as following:

$$\dot{u} = \dot{u}_0 + \int_0^t \ddot{u}dt \tag{2.3}$$

The velocity at time t=1 can be given by the following equation as:

$$\dot{u}_1 = \dot{u}_0 + \frac{\Delta t}{2}(\ddot{u}_0 + \ddot{u}_1) \tag{2.4}$$

The change in displacement value is described by:

$$u = u_0 + \int_0^t \dot{u}dt \tag{2.5}$$

The displacement at time t=1 is expressed below:

$$u_1 = u_0 + \Delta t\dot{u}_0 + \frac{\Delta t^2}{4}(\ddot{u}_0 + \ddot{u}_1) \tag{2.6}$$

Re-arranging Eqs. 2.4 and 2.6 in terms of Δu, gives:

$$\Delta\dot{u} = -2\dot{u}_0 + \frac{2}{\Delta t}\Delta u \tag{2.7}$$

$$\Delta\ddot{u} = -2\ddot{u}_0 - \frac{4}{\Delta t}\dot{u}_0 + \frac{4}{\Delta t^2}\Delta u \tag{2.8}$$

Substituting Eqs. 2.7 and 2.8 into Eq. 2.1 results in the following equation.

$$[K']\{\Delta u\} = [P'] \tag{2.9}$$

in which:

$$[K'] = \frac{4}{\Delta t^2}[M] + \frac{2}{\Delta t}[C] + [K] \tag{2.10}$$

and

$$[P'] = \{\Delta P\} + \left[\frac{4}{\Delta t}\{\dot{u}_0\} + 2\{\ddot{u}_0\}\right][M] + 2\{\dot{u}_0\}[C] \tag{2.11}$$

The damping matrix is expressed as a combination of mass and stiffness dependent matrices as illustrated below having α and β as constants to be specified by the program user. The details of the damping matrix are given in Section 2.8.

$$[C] = \alpha[M] + \beta[K] \tag{2.12}$$

Substituting Eq. 2.12 into Eqs. 2.10 and 2.11 leads to the equilibrium equation for each time step.

$$[K^*]\{\Delta u\} = [P^*] \tag{2.13}$$

in which [K*] and [P*] are the effective stiffness and force at the beginning of each time step, respectively.

$$[K^*] = \left[\left\{\frac{4}{\Delta t^2} + \frac{2\alpha}{\Delta t}\right\}[M] + \left\{\frac{2\beta}{\Delta t} + 1\right\}[K]\right] \tag{2.14}$$

$$[P^*] = \left[\{\Delta P\} + \left[\frac{4}{\Delta t}\{\dot{u}_0\} + 2\{\ddot{u}_0\} + 2\alpha\{\dot{u}_0\}\right][M] + 2\beta\{\dot{u}_0\}[K]\right] \tag{2.15}$$

The effective stiffness [K*] and effective load vector [P*] are assembled at the beginning of each time step, based on Eqs. 2.14 and 2.15. Eq. 2.13 is used to determine the incremental displacement whereas Eqs 2.7 and 2.8 are used to establish the initial velocity and acceleration for the following time step. Greater accuracy can be attained with reduced integration time step. For nonlinear increments, equilibrium is be satisfied and the unbalance can be expressed in terms of unbalanced nodal forces. To avoid errors that may arise from accumulating equilibrium unbalances over many time steps, a corrective load is added to the load vector within the next time step to restore equilibrium.

The analytical models used in computer program DRAIN-RC and their features are explained in the following sections.

2.3 Flexural Modeling

Each member is modeled for flexure as an elastic line element and inelastic flexural springs at each end to form plastic hinges. Fig. 2.2 shows three different inelastic springs at beam ends, one of which simulates flexural behaviour. The elastic part of the element is activated within the elastic region and the inelastic springs do not rotate in this region because of their high initial stiffnesses. One or both of the springs are activated when the force level exceeds the prescribed yield level. The element stiffness formulation for flexure is done in terms of end moments M_A and M_B. The moment-chord rotation relationship for an actual beam element can be defined as the sum of M-ϕ relationships for an elastic beam element and a flexural spring that can be seen in Fig. 2.3. Since the flexural hinges become active when the applied moment M on the actual beam is greater than the yield moment M_y, the relationship between the incremental chord rotations and end moments can be defined as:

$$\begin{bmatrix} \Delta\theta_A \\ \Delta\theta_B \end{bmatrix} = \begin{bmatrix} \dfrac{L}{3rEI} & \dfrac{-L}{6rEI} \\ \dfrac{-L}{6rEI} & \dfrac{L}{3rEI} \end{bmatrix} \begin{bmatrix} \Delta M_A \\ \Delta M_B \end{bmatrix} \tag{2.16}$$

where "r" is the strain hardening ratio for the real beam. At end A the incremental chord-rotation can be expressed as:

$$\Delta\theta_A = \frac{L}{3rEI}(\Delta M_A - \frac{\Delta M_B}{2}) \tag{2.17}$$

The two end moments are related. The ratio of these two end moments can be defined by coefficient ξ:

$$\xi = \frac{\Delta M_B}{\Delta M_A} \tag{2.18}$$

Substituting Eq.2.18 into Eq.2.17 gives:

$$\Delta\theta_{A_{actual}} = \frac{L}{3rEI}(1-\frac{\xi}{2})\Delta M_A \tag{2.19}$$

For the elastic beam element (r =1):

$$\Delta\theta_{A_{elastic}} = \frac{L}{3EI}(1-\frac{\xi}{2})\Delta M_A \tag{2.20}$$

For the flexural hinge rotation, the following equation can be written as:

$$\Delta\theta_{A_{hinge}} = \frac{\Delta M_A}{K_{sp}} \tag{2.21}$$

where K_{sp} is the flexural spring stiffness beyond yield at end A. The chord-rotation of the actual element is the sum of the chord-rotations of the elastic element and hinge as illustrated in Fig. 2.3.

$$\Delta\theta_{A_{actual}} = \Delta\theta_{A_{elastic}} + \Delta\theta_{A_{hinge}} \tag{2.22}$$

Another expression for the flexural stiffness can be written by substituting Eqs. 2.19, 2.20 and 2.21 into Eq. 2.22 :

$$K_{sp} = pK_{se} = \frac{3EI}{L(1-\frac{\xi}{2})}(\frac{r}{1-r}) \tag{2.23}$$

in which "p" is the strain hardening ratio of flexural spring and can be determined as:

$$p = \frac{3EI}{L(1-\frac{\xi}{2})K_{se}}(\frac{r}{1-r}) \tag{2.24}$$

When the end moments are equal to each other, the inflection point is in the center of the member and it deforms in double curvature. For this simple case "p" can be defined as following:

$$p = \frac{6EI}{LK_{se}}\left(\frac{r}{1-r}\right) \tag{2.25}$$

DRAIN-RC uses Eq. 2.25 as default. For a generalized loading, the inflection point need not be located at the center of the beam. For the purpose of modeling post-yield deformations, the inflection point is assumed to remain at the center for simplicity, while the variation in the location of inflection point is accounted for in computing elastic deformations. When Eq. 2.25 is used in the program the real location of the point of inflection is calculated by entering an "r" value. This value results in the correct value of "p" when used in Eq. 2.25 for the real location of the inflection point. The actual strain hardening ratio can be defined as r_a (actual "r") where the input value is defined as r_i (input "r"). These two values can be related to each other by the following expression:

$$p_{actual} = \frac{3EI}{L(1-\frac{\xi}{2})K_{se}}\left(\frac{r_a}{1-r_a}\right) \tag{2.26}$$

DRAIN-RC calculates "p" as:

$$p_{computed} = \frac{6EI}{LK_{se}}\left(\frac{r_i}{1-r_i}\right) \tag{2.27}$$

Since computed and actual "p" values should be equal to each other, Eq. 2.26 and Eq. 2.27 are set equal to each other. For known quantities of ξ and r_a, an input value r_i can be computed and entered as input data.

$$r_i = \frac{r_a}{2(1-\frac{\xi}{2})(1-r_a)+r_a} \tag{2.28}$$

If ξ = 1.0, the point of inflection is in the center and the following expression is described:

$$r_i = r_a \tag{2.29}$$

The post yield stiffness of the flexural spring is defined by "p" that is calculated from Eq. 2.27. The total flexibility of the member is established by superimposing elastic and inelastic flexibilities for flexure, shear and anchorage slip. By taking the inverse of the flexibility matrix the stiffness matrix is determined. Direct stiffness method is used to express the total stiffness of the whole structure.

The modified version of Takeda's model was used in original DRAIN-2D (Powell 1975) to account for flexural hysteretic behavior of beam elements with degrading stiffness. The modifications introduced by Powell (1975) include the reduction of the unloading stiffness and incorporation of a variable reloading stiffness. The model was created using a bilinear primary curve with an initial stiffness and following strain hardening stiffness that are characteristics of monotonic loading condition. The unloading stiffness depends on the maximum hinge rotation and is controlled by input parameter α_1. The reloading stiffness also depends on the maximum hinge rotation and is governed by the input parameter β_1. The modified Takeda model for small amplitude cycles can be seen in Fig. 2.4.

2.4 Inelastic Shear Modeling

Inelastic shear effects are modeled by an elastic line element and two inelastic shear springs, one at each end of member, as seen in Fig. 2.2. Elastic deformations are developed by elastic beam element and springs rotate after diagonal cracking of concrete. The inelastic deformations within the post-cracking and post-yielding portions are created by shear springs. The moment-shear distortion relationship for an actual beam element is plotted in Fig. 2.5 by having components due to elastic beam element and inelastic shear spring. For $M_y > M > M_{cr}$ the relationship between incremental chord-rotations and end moments for an actual beam is defined as:

$$\begin{bmatrix} \Delta\theta_A \\ \Delta\theta_B \end{bmatrix} = \begin{bmatrix} \dfrac{1}{s_1 GAL} & \dfrac{1}{s_1 GAL} \\ \dfrac{1}{s_1 GAL} & \dfrac{1}{s_1 GAL} \end{bmatrix} \begin{bmatrix} \Delta M_A \\ \Delta M_B \end{bmatrix} \tag{2.30}$$

where s_1 is the ratio of post-cracking stiffness to pre-cracking stiffness of the primary moment-shear distortion curve. At end A, the incremental chord-rotation due to shear is expressed as:

$$\Delta\theta_A = \frac{1}{s_1 GAL}(\Delta M_A + \Delta M_B) \tag{2.31}$$

Using coefficient ξ from Eq. 2.18 and substituting into Eq. 2.31 gives:

$$\Delta\theta_{A_{actual}} = \frac{1}{s_1 GAL}(1+\xi)\Delta M_A \tag{2.32}$$

For the elastic part of the element:

$$\Delta\theta_{A_{elastic}} = \frac{1}{GAL}(1+\xi)\Delta M_A \tag{2.33}$$

The chord rotation due to shear spring can be established in much the same manner as for flexural spring as:

$$\Delta\theta_{A_{hinge}} = \frac{\Delta M_A}{K_{p_1}} \tag{2.34}$$

in which K_{p1} is the inelastic shear spring stiffness beyond cracking but prior to yielding at end A. The two components contributing to the incremental chord-rotation of the actual beam are defined as follows:

$$\Delta\theta_{A_{actual}} = \Delta\theta_{A_{elastic}} + \Delta\theta_{A_{hinge}} \tag{2.35}$$

Using the above defined equations and solving for K_{p1} gives:

$$K_{p_1} = p_1 K_{se} = \frac{GAL}{(1+\xi)}\left(\frac{s_1}{1-s_1}\right) \tag{2.36}$$

We can define p_1 as follows:

$$p_1 = \frac{GAL}{(1+\xi)K_{se}}\left(\frac{s_1}{1-s_1}\right) \tag{2.37}$$

When ξ=1.0, the expression for p_1 becomes:

$$p_1 = \frac{GAL}{2K_{se}}\left(\frac{s_1}{1-s_1}\right) \tag{2.38}$$

This simple approach is used in DRAIN-RC as default. As it was mentioned for the case of flexure, the inflection point does not need to be located in the middle of the beam. A value for s_1 should be defined and entered in the program by the user to use Eq.2.38 for other cases. When the actual and input ratios of post-cracking stiffness to elastic stiffness

s_1 is expressed as s_a and s_i respectively, an equation can be obtained for s_i in terms of s_a and ξ from Eq. 2.37 as shown below:

$$p_{1_{actual}} = \frac{GAL}{(1+\xi)K_{se}}\left(\frac{s_a}{1-s_a}\right) \tag{2.39}$$

DRAIN-RC computes this value as:

$$p_{1_{computed}} = \frac{GAL}{2K_{se}}\left(\frac{s_i}{1-s_i}\right) \tag{2.40}$$

Because these two values should be equal to each other, the following equation is obtained for the input value:

$$s_i = \frac{2s_a}{(1+\xi)(1-s_a)+2s_a} \tag{2.41}$$

For equal end moments, the above expression is simplified as follows:

$$s_i = s_a \tag{2.42}$$

The same procedure may be used for $M > M_y$ using K_{p2}, p_2, s_2 instead of K_{p1}, $p_1$and s_1, respectively. After obtaining the pre-yield and post-yield flexibilities of each spring, they are added to the member flexibility matrix where the member stiffness matrix is obtained.

The hysteretic model for shear was developed by Ozcebe and Saatcioglu (1989), consisting of tri-linear primary curve with break points at cracking and yielding (See Fig. 2.6). Pinching of hysteresis curves caused by the slippage of inclined cracked surfaces was incorporated in the model. The effect of axial compression, reducing ductility and promoting strength decay, were also included. The rules of the hysteretic model were developed on the basis of test data. Stiffness degradation during reloading and unloading was specified as a function of the previous peak displacement.

2.5 Anchorage Slip Modeling

Hysteretic behaviour of anchorage slip was introduced by means of a third pair of inelastic springs, one at each end of the elastic beam element. Anchorage slip deformations occur near the critical section like interior and exterior beam column joints and column foundation interfaces. These deformations can be lumped in the form of concentrated rotations at the ends of each member. The hysteretic model developed by Saatcioglu, Alsiwat and Ozcebe (1992) was assigned to each anchorage slip spring. The model consists of a primary moment-slip relationship, which can be computed by establishing a nonlinear strain distribution along the bar. The rotations due to anchorage slip effect may be based on reinforcement extension or the slippage in the adjoining member or both. The unloading slope is calculated based on residual steel strain whereas reloading slopes are based on experimental analysis. Fig. 2.7 illustrates the model.

DRAIN-RC needs the pre-yield and post-yield stiffnesses of the slip spring as input data. Furthermore, the unloading slope at a control point on the primary curve and the coordinates of that point must also be input into the computer program. By interpolating and extrapolating the input slope of this control point, the unloading slope at any other point on the post yield primary curve is determined.

2.6 Axial Force-Moment Interaction Model

The previous version of computer program DRAIN-2D included degrading stiffness characteristics for members under constant level of axial load. During earthquakes, vertical members of structures experience changing axial forces. Therefore, a model was developed by Saatcioglu et al. (1983) to introduce the P-M interaction effects on strength and stiffness of members. The model is illustrated in Fig. 2.8. The interaction of axial forces with moments is such that, up to the balanced load the increase in axial compression produces an increase in yield level. This trend reverses itself above the balance point. In the model, it is accepted that the stiffness change within the elastic region was negligible whereas yield moment was changed significantly due to the P-M interaction effects. In the first time step of analysis, the axial load caused by gravity is used. In subsequent time steps, any increase or decrease in axial load is considered with its effect on concurrent yield moment level. At the end of each time increment the computed element moment is compared with the concurrent level of yield moment. If the yield moment is exceeded, the element enters into the inelastic range. Beyond the yield point any change in axial load level defines a new primary moment rotation curve with increased or decreased yield level. Since the loading and reloading in the inelastic range is aimed at previous deformation on the primary curve, the updating of primary curves on the basis of concurrent level of axial load results in stiffness changes. Higher axial compression results in steeper slopes (increased stiffness) and lower axial compression (or increased tension) results in flatter slopes (decreased stiffness) of the force-deformation hysteretic relationship.

2.7 Hysteretic Model for Infill Panels

A hysteretic model was developed and experimentally verified by R. E. Klingner and V. V. Bertero (1978). The model simulates an infill wall by replacing it with two equivalent diagonal strut elements in each direction. These elements are designed to represent the strength and stiffness characteristics of infill walls observed in experiments. The hysteretic behavior of the strut has rules that were explained by Shooshtari (1998). The element type number assigned to the infill element in DRAIN-RC is #11.

2.8 Damping Matrix, [C]

Damping forces resist the motion of a structure during dynamic response, and are difficult to measure in nature because of their complexity. They are usually classified as viscous damping, and are expressed as a function of velocity. In the equation of motion, damping forces are related to the velocity vector through damping matrix [C], which is defined as a combination of mass [M] and stiffness [K] matrices, with coefficients obtained from orthogonality conditions of these matrices as seen below:

$$[C] = \alpha[M] + \beta[K] \tag{2.43}$$

The expressions for these coefficients are given by:

$$\alpha = \frac{4\pi(T_i\Psi_i - T_j\Psi_j)}{T_i^2 - T_j^2} \tag{2.44}$$

and

$$\beta = \frac{T_iT_j(T_j\Psi_i - T_i\Psi_j)}{\pi(T_j^2 - T_i^2)} \tag{2.45}$$

where;

Ti, Tj = periods of vibration for modes i and j, respectively.

Ψi, Ψj =damping ratios for modes i and j, respectively.

By assuming a damping ratio (say 5%), and the periods for the first two modes (for example as computed by computer software SAP2000) one can establish the above coefficients. Using Eqs.2.44 and 2.45, the coefficients α and β were computed for 5% critical damping for the 12 buildings designed in the current investigation and entered in DRAIN-RC as part of input to conduct nonlinear dynamic analysis.

2.8.1 Stiffness Matrix, [K]

In DRAIN-RC, the Direct Stiffness Method is used to construct the structure stiffness matrix. The stiffness matrix for individual elements of the structure is evaluated first to assemble the global stiffness matrix. The element stiffness matrix is obtained by establishing the element flexibility matrix in local coordinates and inverting it. This matrix is then transformed to global coordinates using a transformation matrix. The stiffness matrix of the structure is assembled from individual element stiffness matrices by matching the element degrees of freedom to the global degrees of freedom of the structure. The stiffness matrix of each element is added to the global stiffness matrix based on the coincidence between the element and global degrees of freedom.

2.8.2 Mass Matrix, [M]

Mass in any structure is distributed throughout the entire structure. The structure must be divided in an infinite number of degrees of freedom to account for this distribution. Nevertheless, this is impossible and unnecessary for the purpose of structural analysis. Instead, mass is assumed to be concentrated at each floor level and it is divided between the joints according to the respective tributary area. For rotational degrees of freedom, the mass moment of inertia is taken as zero and the corresponding entry in the mass matrix is set to zero.

2.9 Ductility Ratio

Ductility is the amount of plastic deformation that can be experienced by elements of a structure without a significant loss in strength during seismic response. Ductility ratio is computed as the ratio of maximum deformation to deformation at first yield. Three types of ductility ratios are often used and defined as displacement, rotation and curvature ductility ratios. The rotational ductility ratio is used in this research program as the ratio of maximum chord rotation to chord rotation at initial yield as expressed below:

$$\mu_\theta = \frac{\theta_{\max}}{\theta_y} \tag{2.46}$$

The rotations referred to are the chord rotations of a cantilever beam (over shear span) with moment M applied at the support. The chord rotation at each end is calculated based on the end moment and a cantilever length of L/2. The chord rotation can be expressed by summing the inelastic deformations of three different components as flexural ductility ratio, shear ductility ratio and slip ductility ratio, each of which is explained in the following sections.

2.9.1 Flexural Ductility Ratio

The ratio of maximum flexural rotation to flexural rotation at first yield is defined as the flexural ductility ratio as given by:

$$\mu_{fl} = \frac{(\theta_{\max})_{fl}}{(\theta_y)_{fl}} \tag{2.47}$$

in which:

$$(\theta_y)_{fl} = M_y\left(\frac{L}{6EI} + \frac{1}{K_{efl}}\right) \tag{2.48}$$

and

$$(\theta_{\max})_{fl} = (\theta_y)_{fl} + (M_{\max} - M_y)\left(\frac{L}{6EI} + \frac{1}{K_{pfl}}\right) \tag{2.49}$$

where K_{efl} and K_{pfl} are the pre-yield and post-yield stiffness of the flexural spring, respectively.

2.9.2 Shear Ductility Ratio

The shear ductility ratio is determined in a similar manner to flexure, as indicated below:

$$\mu_{sh} = \frac{(\theta_{\max})_{sh}}{(\theta_y)_{sh}} \tag{2.50}$$

where:

$$(\theta_y)_{sh} = M_{cr}\left(\frac{2}{GAL} + \frac{1}{K_{e_{sh}}}\right) + (M_y - M_{cr})\left(\frac{2}{GAL} + \frac{1}{K_{p_{1sh}}}\right) \tag{2.51}$$

and

$$(\theta_{\max})_{sh} = (\theta_y)_{sh} + (M_{\max} - M_y)\left(\frac{2}{GAL} + \frac{1}{K_{p_{2sh}}}\right) \tag{2.52}$$

in which $K_{e_{sh}}$ is the elastic stiffness, $K_{p_{1sh}}$ is the post-cracking stiffness and $K_{p_{2sh}}$ is the post-yield stiffness of the shear spring.

2.9.3 Slip Ductility Ratio

The anchorage slip ductility ratio is defined by taking the ratio of maximum and yield rotation values as follows:

$$\mu_{sl} = \frac{(\theta_{\max})_{sl}}{(\theta_y)_{sl}} \tag{2.53}$$

in which:

$$(\theta_y)_{sl} = \frac{M_y}{K_{e_{sl}}} \tag{2.54}$$

and

$$(\theta_{\max})_{sl} = (\theta_y)_{sl} + \frac{(M_{\max} - M_y)}{K_{p_{sl}}} \tag{2.55}$$

where $K_{e_{sl}}$ is the elastic stiffness and $K_{p_{sl}}$ is the post-yield stiffness in the slip model.

2.9.4 Combined Ductility Ratio

The combined ductility ratio is defined by considering all the inelastic deformation components (flexure, shear and slip deformations) and superimposing them as follows:

$$\mu_{com} = \left(\frac{(\theta_{\max})_{fl} + (\theta_{\max})_{sl} + (\theta_{\max})_{sh}}{(\theta_y)_{fl} + (\theta_y)_{sl} + (\theta_y)_{sh}}\right) \tag{2.56}$$

The first yield can be due to flexure, shear or anchorage slip, whichever occurs first. Then this stage of loading is marked as initial yield and the rotations for the other two components are calculated for this stage and added to the rotation of the first yielding component.

Ductility ratios are computed by DRAIN-RC automatically. If the inelastic spring of any deformation components is not included in the model, the rotation value is set equal to zero and does not have any contribution to the combined ductility ratio.

2.10 P-Δ Effect

With increasing lateral deformations during an earthquake, and in the presence of axial loads, P-Δ effects generate secondary moments. Secondary moments can be quite significant in structures that experience inelastic deformations and may result in additional moments. This may severely reduce the capacity to resist lateral loads and may result in stability failures under high axial loads. The P-Δ effect was incorporated into program DRAIN-RC by considering the geometric stiffness properties of a beam-column element. Since DRAIN-RC has the capability of doing push-over analysis, P-Δ effect was introduced to the static analysis as well. The geometric stiffness is updated during the analysis. Within the elastic range, the geometric stiffness matrix is formed and subtracted from the flexural stiffness matrix at the beginning of the analysis to introduce the effects of geometric stiffness. If the level of axial force changes in an element, the geometric stiffness is calculated at each time step and load steps for dynamic and push-over analyses, respectively.

If yielding occurs in an element, the effect of geometric stiffness should be included in the flexibility matrix. This matrix consists of two components as flexural flexibility and geometric flexibility matrices. The total flexibility matrix of each element is constructed by including the effects of flexure, shear, anchorage slip and P-Δ. By taking the inverse of the flexibility matrix, the stiffness matrix for each element is determined. The global stiffness matrix is established by using the element stiffness matrices in the beginning of each analysis. The details on assembling the element flexibility matrix may be found elsewhere (Shoostari 1998).

2.11 Static Inelastic Analysis (Push-Over)

This method consists of incremental loads being applied statically well into the inelastic range of deformations. It was proposed as an alternative to costly and difficult nonlinear time history analysis. The lateral loads may be entered in equal increments or varying arbitrarily in several load steps. For each load step, the global stiffness matrix is updated and unbalanced loads resulting from yielding are computed and added to the load vector at the following time step. Before performing incremental analysis, vertical loads, like gravity loads, may be applied on the structure with their full magnitudes. At first load step the structure is analyzed only under these load effects. Afterwards the structure is also analyzed under incrementally changing loads and the effects of both analyses are then superimposed.

2.12 Development of a Pre-Processor for DRAIN-RC

The input data required for computer software DRAIN-RC consisted of a large number of data to be entered sequentially using a text editor and separating the data items with commas. An input file had to be created all at once on the basis of input instructions. This was found to be cumbersome. One of the objectives of the current thesis was to develop a user friendly and interactive pre-processor to be used with DRAIN-RC. It was felt that a pre-processor that worked in Microsoft Windows environment would enhance the usability of the program quite considerably. Therefore a pre-processor was developed using the computer programming language Visual Basic 6.0. This programming language was designed to allow the programmer to develop applications that would run under the Windows operating system. The pre-processor was developed by designing windows with standard Windows elements such as *text boxes, menus, command buttons, check boxes* and *option boxes*. Bradley and Millspaugh (1999) indicate that each of these Windows objects operates by producing a "standard" Windows user interface.

Microsoft Windows uses a "graphical user interface" that defines how the various elements look and function. New windows are named as 'forms', elements added are called 'controls' and the projects following a new type of programming are called 'event-driven programming'.

As indicated in Bradley and Millspaugh (1999), there are hundreds of programming languages, each developed to solve a particular type of problem. Languages like BASIC, FORTRAN, C, COBOL and Pascal are known as procedural languages in which the program specifies the exact sequence of all operations. The next instruction to execute in response to conditions and user requests is determined by the program logic. A different approach is used for the newly developed programming languages like C++, Java and Visual Basic and is referred to as object-oriented programming (OOP) and event-driven programming. Visual Basic is not really an OOP language, because it does not have all elements of an OOP language so it is referred as event-driven programming. In contrast to the procedural languages, event-driven programming does not follow a sequential logic. The user can press keys and click on various buttons and boxes in a window and cause an event to occur with a Basic procedure written for it. The steps followed in preparing the pre-processor for DRAIN-RC with Visual Basic (VB), are summarized in Fig. 2.9.

The VB project includes one or more forms, which are saved in a file with a .FRM extension. These forms contain descriptions of all objects and their properties for the form and the Basic code that is written to respond to the events. One of the forms containing different objects is given in Fig. 2.10. In that form, the definitions are given by placing labels. Data input boxes are created from text boxes, check boxes are created to select or deselect options and option buttons are used when only one button of a group is selected. Frames are used as containers for option boxes to group them. Command buttons are used to execute an event by following a prescribed Basic code for the command button. The caption of the form is changed to a meaningful title.

Different windows are used for different types of information. The input data for DRAIN-RC is entered in many forms that were created for each type of information. The first form a project displays is called the startup form, which is selected as the main window containing the menus to display all the forms. This is done by using a multiple document interface (MDI) project. The project has a *parent form* (the main window) and *child forms* (other forms). Multiple child windows may be opened, maximized, minimized, restored or closed while staying within the boundaries of the parent window. When the parent window is closed, all child windows are closed automatically. In Fig. 2.11, the parent window and one of the child windows is described, in which a menu bar with menu names may be seen, each of which drops down to display a list of menu commands. The menu names for this project are 'file', 'input', 'analysis' and 'run'. The menu commands for 'input' may be seen on the screen as an example. When a command on the menu has another list of commands that pops up, the new list is called a *submenu.* A filled triangle to the right of the command refers that a menu command has a submenu. By clicking menu commands, the form consistent with that command is displayed on the main form by using Show method, which is one of the dialog boxes of a Common Dialog control placed on the form.

Visual Basic uses various types of data, such as variables and constants that should be defined in specific places. Variables can be changed during project execution, whereas constants cannot be changed. The declaration statements determine the project's variables and constants, giving names and specifying the type of data they hold. All the data used in this project are variables that are defined with different data types, such as *double, integer, variant* and *string.* The first three of them must be used when the data is used in a calculation (numeric) mode and the string is used otherwise.

Once the input data is entered, by using text boxes in the forms, these data should be stored in specific files to build a document that contains all the input data. The data entered in each form is saved in a text file, which appears on the form. A small Fortran code is written and added to the original DRAIN-RC that reads the data from text files and summarizes them in input file naming 'project'. When the 'start' button in DRAIN-

RC is pressed, the original DRAIN-RC starts executing, including the newly added Fortran code. The program does transform the data and prepare the input file automatically.

Random File Organization is used to organize, store and retrieve data in text files. To process data files, three commands must be used in the following order:

- *Open the file:* To place data on disk or read from the disk. The file must first be open.
- *Read or Write the data records:* Data will be read from or written to, following the save procedure associated with the data entry form.
- *Close the file:* When a process is finished with a file, it should be closed.

Each form contains command buttons referring to these operations. In some forms (for ex. Fig. 2.11) pressing OK button activates all three operations sequentially. The related code is given in Fig. 2.12. For most forms the input data is more than one line. In other words, there should be a loop to enter, save the data and clear the boxes to enter the following data, until the end of data is encountered. One of the sample forms illustrating data entry, as explained above, and the code for save command of this form, are given in Figs. 2.13 and 2.14, respectively. These forms are created using the example forms from Sinclair (1999).

Input instructions and the modifications introduced are explained with examples in DRAIN-RC User's Guide, provided in Appendix A.

CHAPTER 3
Selection of Structures and Earthquake Records

3.1 Introduction

The main objective of the research project reported in this thesis was to establish inelastic drift demands for reinforced concrete buildings in Canada. Previously developed computer software DRAIN-RC was used to conduct dynamic inelastic response history analysis. Selection and design of structures form an important task towards attaining the objective for research. For this purpose, three different structural systems were designed and detailed, consisting of moment resisting frames with and without shear walls and structures with core walls. The structural properties of buildings, including the geometry, mass, stiffness, strength and damping characteristics were required for the analysis. Furthermore, the ground motion records used play an important role in attaining realistic results. Therefore, the selection of proper ground motions formed an important second step towards conducting dynamic analysis. This chapter explains the details of the structures and the ground motion records selected.

3.2 Selection of Structures

Structures are divided in groups based on their height; as low-rise, medium-rise and high-rise buildings. Building height plays an important role on dynamic response of structures as it affects the periods of vibration. It is essential to cover different building heights in arriving at conclusions that are applicable to buildings in general. Similarly, different structural types may behave differently and this should be recognized. In this research program, where drift demands of reinforce-concrete buildings in Canada are assessed, different types of structural systems were selected in different height groups. Commonly used structural systems, consisting of moment resisting frames with and without shear and core walls, were selected with 5-storey, 10-storey and 15-storey building heights, representing low, medium and high-rise buildings, respectively.

Canada is approximately divided into two different seismic regions as west and east, reflecting different seismicity. Two different cities were selected to represent these two regions; Ottawa for Eastern Canada and Vancouver for Western Canada. The designs of buildings were done using the requirements of the proposed 2005 edition of the National Building Code of Canada (NBCC). For Ottawa, three moment resisting frame structures and three frame-shear wall structures were designed as nominally ductile. Because of the drift limitations it was not feasible to design a frame structure for Vancouver. For this reason, three frame-shear wall structures were designed for Vancouver having one shear wall in each exterior frame. In addition, three frame-core wall structures (CW) were designed with stiff core walls in addition to the one shear wall in each exterior frame, creating a structure with enhanced stiffness and shorter fundamental period. The buildings in Vancouver are designed as ductile structures. In the end the following 12 buildings were designed on the basis of NBCC-2005:

1. 5 - Storey frame building in Ottawa.
2. 10 - Storey frame building in Ottawa.
3. 15 - Storey frame building in Ottawa.
4. 5 - Storey frame-shear wall building in Ottawa.
5. 10 - Storey frame-shear wall building in Ottawa.
6. 15 - Storey frame-shear wall building in Ottawa.
7. 5 - Storey frame-shear wall building in Vancouver.
8. 10 - Storey frame-shear wall building in Vancouver.
9. 15 - Storey frame-shear wall building in Vancouver.
10. 5 - Storey frame-shear wall building with additional core walls in Vancouver.
11. 10 - Storey frame-shear wall building with additional core walls in Vancouver.
12. 15 - Storey frame-shear wall building with additional core walls in Vancouver.

The plan views and elevations of the buildings are given in Figs. 3.1 to 3.5. A symmetrical floor plan was selected to eliminate the effect of torsion in analysis. The load combinations considered were based on NBCC - 1995, since the proposed edition of NBCC -2005 (which was not available in its entirety at the time) was not likely to have changes in load combinations. The design data are presented in Table 3.1.

The seismic base shear was determined using the provisions proposed for the 2005 edition of the NBCC, which permit the use of an equivalent static load procedure for the following classes of structures:

- Structures located in zones of low seismicity, that is, $IEF_aS_a(0.2) < 0.35$
- Regular structures that are less than 60 m in height and have $T_a < 2$ sec,
- Irregular structures that are less than 20 m in height, have $T_a < 0.5$ sec and are not torsionally sensitive.

Accordingly, the earthquake design base shear for the structures selected in the current research program were calculated using Eq. 3.1.

$$V = \frac{S(T_a)M_vIW}{R_dR_o} \tag{3.1}$$

where;

T_a = Fundamental period

$S(T_a)$ = The design spectral response acceleration, expressed as a ratio to gravitational acceleration, for the fundamental lateral period of the building T_a

M_v = Higher mode effect factor

I = Importance factor

W = Weight of structure

R_d = Ductility related force modification factor

R_o = Overstrength related force modification factor

As described in Heidebrect (2003), the product $S(T_a)M_vIW$ represents the elastic base shear in the proposed edition of NBCC, comparable to the product vSIFW in NBCC - 1995. Two force modification factors; R_d and R_o are introduced in NBCC-2005 and the calibration factor U is eliminated for calculating inelastic base shear. The rationale for introducing these force modification factors are given in Mitchell et al. (2003). Design spectral response acceleration values, $S(T_a)$ are determined from a site-specific uniform hazard spectrum (UHS) as explained by Adams and Atkinson (2003). The 5% damped spectral response acceleration $S_a(T)$ is modified by acceleration and velocity-based site coefficients F_a and F_v, respectively. For the current study, the soil type was selected as very dense soil and soft rock (Site Class C). The fundamental period, T_a, for design purposes was computed based on the code specified empirical expressions. These expressions are shown below:

For concrete frames;

$$T = 0.075(h_n)^{3/4} \tag{3.2}$$

For shear wall buildings;

$$T = 0.05(h_n)^{3/4} \tag{3.3}$$

More accurate estimation of fundamental periods of structures were calculated by solving the eigen value problem using computer software SAP2000 where the eigen solution included the effects of potential cracking in members. The effect of cracking was taken into account by reducing flexural rigidities to 0.35 EI for beams and 0.7 EI for columns and shear walls, where EI was computed on the basis of gross cross-sectional properties and elastic modulus of concrete.

The buildings were analyzed using equivalent static loads and computer software SAP2000 for design purposes. Two-dimensional static analyses were conducted using preliminary member dimensions to determine critical values of bending moments, axial forces and shear forces at each joint. These values were used to design the beams and columns, based on CSA Standard A23.3 (1994). The analyses were repeated with revised member sizes when necessary. The design results are summarized in Tables 3.2 to 3.13.

3.3 Selection of Earthquake Records

The main objective of the present research was to estimate realistic drift demands under Canadian seismic conditions. In both eastern and western Canada, the strong-motion database for earthquakes is very sparse. Although a large database is available for California earthquakes, they may not be applicable because of differences in their frequency content. Therefore, the use of actual earthquake records is not feasible. Instead, simulated records can be used to match the target spectra.

Two different types of simulated records were selected. The first type was based on seismological history and geological make up of the region and was generated for 10% in 50 year probability level by Atkinson and Beresnev (1998). Subsequently the researchers used the same method of generating artificial records and developed a new set corresponding to probability of exceedance of 2% in 50 years that are compatible with the uniform hazard spectra (UHS) specified in 2005 edition of NBCC. Compatible time histories may be generated using engineering simulation programs from a specified response spectrum without using other seismological information. However, Atkinson and Beresnev (1998) state that "they produce an artificial composite record which is unlike any actual ground motion that might be experienced..." and "to produce physically realistic time histories, it is necessary to simulate motions which not only match the spectrum, but which are representative of motions for specific magnitude-distance scenerios in the region of interest."

Geological Survey of Canada updated Canada's current seismic hazard maps, which were developed in 1988, by proposing a new seismic hazard model that included new knowledge from recent earthquakes, new strong motion relations and better understanding of site conditions as explained in Adams and Atkinson (2003). The newly proposed hazard computation was made for 2% in 50 year probability level instead of the 10% in 50 years used earlier. They presented uniform hazard spectra that can be thought of as a composite of the types of earthquakes that contribute most strongly to the hazard at the specified probability level. These spectra were adopted by the National Building Code of Canada in its 2005 edition in an idealized manner. Accordingly, the spectral accelerations are specified at 0.2, 0.5, 1.0 and 2.0 second periods. These four spectral parameters allow the construction of approximate uniform hazard spectra for each location.

It is important to select ground motion records that are compatible with these spectra, in order to conduct time history analyses consistent with the provisions of NBCC-2005. Atkinson and Beresnev (1998) describe that the artificially generated records provide a realistic representation of ground motion for the earthquake magnitudes and distances that contribute to hazard at the selected cities and probability level. To match the target uniform hazard spectra (UHS) more than one record is needed. For this purpose, four horizontal components are generated for a moderate earthquake nearby, and four horizontal components are generated for a larger earthquake farther away, with a total of eight records, for every selected city. This was found to be necessary from the fact that moderate nearby earthquakes would not produce sufficiently long-period energy to match the long-period band, whereas the larger distant earthquakes would have lost too much high-frequency energy to match the short-period band.

For eastern cities of Canada, an event of M6.0 and an event of M7.0 were selected to represent the short-period hazard and long-period hazard, respectively. It is assumed that these events occur at certain distances for each city considered. The best distance value for the M6.0 event was selected by matching the average spectrum for the four simulated records to the short-period end of the target most closely. For M7.0 event, the best distance value was determined by matching the long-period end of the target UHS. In the current study, Ottawa was selected to illustrate the ground motion characteristics in eastern Canada. For Ottawa, the hypocentral distance (R) for M6.0 was selected as 30 km whereas for M7.0, R was defined as 70 km. The resulting time histories were then scaled up or down by a "fine tuning factor" to match the target spectra as much as possible. The artificial records generated by Atkinson and Beresnev (1998) are referred to as A-B artificial records, hereafter.

Vancouver was selected as the city to represent western Canada. Eight artificial earthquake records were generated for short and long-period structures for 2% probability of exceedance in 50 year. The records were based on M6.5 and M7.2 for short-period and long-period hazard with hypocentral distances of 30 km and 70 km, respectively. These two scenario events represented only the hazard due to the crustal and subcrustal earthquakes, and did not include the hazard due to a great future earthquake along the Cascadia subduction zone. A great earthquake on the Cascadia subduction zone was simulated separately with a magnitude of M8.5. Four artificial records for Cascadia earthquake were used with a modification factor of 2.2. All the artificially generated earthquake records used in the analyses are listed in Table 3.14.

The compatibility of artificial records with the UHS specified in NBCC-2005 was verified by computing spectral values with the UHS developed by the Geological Survey of Canada (Adams and Halchuk, 2003). Response spectra were calculated using computer software BISPEC (1999) for Ottawa in the east and for Vancouver in the west. The results are shown in Figs. 3.6 and 3.7 for the selected cities and for every artificial record. The response spectra are then compared with the UHS in Fig. 3.8. The comparison indicates reasonably good agreement between UHS and computed spectral curves. The response spectra for Vancouver indicate that the short event records are governing the UHS also in the long period range. To find out the cumulative effect of the duration of longer ground motions, Long and Cascadia events were used.

A second set of artificial records, also matching with UHS, was considered to investigate the effect of the type of artificial record on structural response. The second set consisted of artificial records generated by different researchers, using a different technique. Naumoski (2001) developed computer program SYNTH to generate artificial records based on actual strong motion records, to maintain similar frequency content. Hence, a previously recorded earthquake motion is specified as input and a spectra compatible artificial record is obtained as output. Amiri (2003) used this program and generated artificial records using actual ground motions for eastern and western Canada. To generate artificial accelerograms, an initial accelerogram and the target spectrum should be specified for the program. By using the initial accelerogram and by iterating until matching the target spectrum, the artificial accelerogram is generated. Each ground motion generated for use in the current investigation, using this procedure is compatible with the design spectra specified, hence one ground motion record is sufficient to cover short and long period ranges.

The artificial ground motions were generated for Richmond in Vancouver and for Montreal. The artificial ground motions generated for Montreal were used in this study as representative of ground motions for Ottawa. The PGA values for Ottawa and Montreal are very close; 0.42 and 0.43, respectively. The response spectra for these cities also show very good agreement especially after 1 sec as illustrated in Fig. 3.9. Two records for each city were selected for dynamic analysis. These records are referred as N-A artificial records, hereafter.

The acceleration-time histories of sample N-A and A-B artificial records are plotted in Figs. 3.10 and 3.11. The time histories for A-B records have nearly a rectangular shape whereas N-A records have intensities at specific times resembling actual earthquake records. The current research also examined the effects of artificial records generated by using different techniques, on structural response, as reported in Chapter 4.

CHAPTER 4
Drift Demands

4.1 Introduction

The computation of drift demands for the reinforced concrete buildings designed for eastern and western Canada was done by conducting dynamic inelastic time history analyses. This was done by using computer software DRAIN-RC. A comprehensive investigation was conducted by analyzing the 12 buildings considered under the effects of UHS compatible earthquake records. The results provide inelastic drift demands for different structural systems having different building heights and subjected to Canadian seismic conditions. The drift demands were recorded for both overall structural drift ratios and interstorey drift ratios. The results also included assessment of the degree of inelasticity experienced, if any, by identifying ductility demands in vertical and horizontal framing elements. The dynamic base shear was compared with static design shear values. The analytical models, modeling parameters and analyses results are presented in the following sections.

4.2 Dynamic Analysis

Three different types of concrete structures were analyzed, consisting of frame structures, frame-shear wall and frame-core wall interactive systems. The difference between the latter two structural systems was the degree of lateral bracing provided by structural walls where the core wall structure represented the most rigid framing system. Three different building heights were considered as 5-storey, 10-storey, and 15-storey. This results in a total of 12 buildings. Half the buildings were located in eastern Canada and were subjected to 10 different earthquake records, while the other half were located in western Canada and were subjected to 14 different earthquake records. The rationale for the selection of different earthquake records is discussed in Section 3.3. These earthquake records were specified as horizontal seismic records for computer software DRAIN-RC. No vertical earthquake record was used.

Each structure was modeled for analysis as planar frames, linked by rigid links, with and without structural walls. The geometric and structural properties were determined based on building designs. Among the features for deformation components that could be incorporated in DRAIN-RC inelastic flexure, inelastic shear and inelastic anchorage slip components were considered. The interaction of varying axial forces with flexural strength and stiffness was also considered through the P-M interaction hysteretic model.

4.3 Modeling Structures for Inelastic Analysis

Modeling a structure for computer software DRAIN-RC is done by following certain steps. First, the entire structure is modeled by discrete elements, where each element represents either a beam (horizontal members), or a column or wall (vertical member). Each element is further modeled for the purpose of defining strength and stiffness characteristics. This is done by an elastic line element with three inelastic springs at each end, incorporating different components of inelastic deformations. Each spring is assigned a hysteretic model, defining the change in strength and stiffness of each element under reversed cyclic loading. The springs incorporate inelastic force-deformation relationships for flexure, anchorage slip and shear.

Analysis of structures due to earthquake motions should be done in two orthogonal directions, separately and independently. Most of the computer programs include planar frame models. In DRAIN-RC the structure is idealized as a planar assemblage of discrete elements. Three-dimensional structures should be modeled as a series of two-dimensional frames linked together to reflect the actual strength and stiffness in each direction. The buildings designed in the current investigation all have four interior and two exterior frames with three bays in the short direction. Due to the rigid slab diaphragm assumption, each frame was assumed to have the same horizontal deflection. Hence, the frames were modeled by connecting them in series with rigid links. The links were modeled by specifying rigid beam elements having infinitely high axial rigidities and infinitely small flexural rigidities. These elements transfer lateral forces without moment connections between the frames. Each structure can be modeled having six frames connected to each other by rigid links. Nevertheless, it is not necessary to model individual frames separately. Identical frames with the same member sizes, strengths and stiffness parameters can be lumped into one frame to reduce the number of elements and the required analysis time. Thus, for moment resisting frames with and without shear walls, two frames were connected by rigid link elements, where one of the frames represented strength and stiffness of four interior frames and the other represented the same for two exterior frames. This is shown in Fig. 4.1 and 4.2 for the 10-storey moment resisting frame building without and with shear walls, respectively. The core wall buildings designed for Vancouver were modeled with three lumped frames, one representing two moment resisting interior frames, the other representing two interior frames with core walls and the third one representing the two exterior moment resisting frame-shear walls. This model is shown in Fig. 4.3. The elements of each lumped frame had double the stiffness of the actual interior and exterior frames. These stiffnesses included flexural, shear and anchorage slip stiffnesses. The strength of each element of the lumped frames was increased to have the same cracking and yielding characteristics as those for individual frames.

Element modeling requires the consideration of elastic beam and spring properties. The properties of elastic line elements can be found easily by applying the principles of mechanics, although inelastic springs require more elaborate idealization of inelastic force-deformation relationships. The hysteretic models assigned to member end springs consist of a primary inelastic force-deformation relationship, which defines the initial stiffness and strength boundary and a set of rules defining stiffnesses during many cycles of unloading and reloading of hysteretic response. The rules have already been incorporated into the program as part of hysteretic models and need not be specified. However, the primary force-deformation relationship needs to be computed for each member and for each deformation component, and input into the program.

Structural mass was assumed to be concentrated at each floor level and was specified at each node. Damping was specified as stiffness and mass dependent mass, as explained in Section 2.8, and calculated on the basis of the first two periods of vibration and 5% of critical damping. The periods used for this purpose was computed using SAP 2000 computer software (Habibullah 2001). Table 4.1 lists the fundamental periods obtained from the empirical expressions recommended by NBCC-2005 and those computed by SAP 2000. In almost all cases the NBCC values give shorter periods.

4.3.1 Moment-Curvature Relationship

The flexural properties of each element, consisting of an elastic element and two plastic springs are determined through moment-curvature analysis. Although the springs simulate member end chord rotations, the post-yield properties of moment-curvature relationship can be used in terms of defining the post-yield stiffness because of the similarity between the post-yield slope of moment-curvature relationship and the moment plastic hinge rotation relationship. Indeed, the assumption of uniform distribution of curvatures within the plastic hinge region makes the relative slope of moment-curvature relationship the same as that of moment-chord rotation relationship. The moment-curvature relationship is established through sectional analysis. The initial linear portion, prior to cracking, is determined by the beam theory and by considering a transformed section. Strain compatibility analysis is used for post cracking regions. For a selected value of extreme fibre strain and an assumed location of neutral axis, the internal strain diagram is developed. The corresponding stress diagram and internal forces are computed and equilibrium is checked. The assumption of neutral axis location is revised until the internal equilibrium of forces is satisfied. Flexural strength is computed from these internal forces. Accordingly, plane sections of a reinforced concrete member before bending are assumed to remain plane after bending. After considering sufficient number of strain conditions the complete moment-curvature diagram can be plotted. The diagram is made of a smooth curve with distinct changes in slope at cracking and yield points, which can be idealized as a tri-linear relationship where the initial line represents the elastic branch, the second line represents the post-cracking region and the third line represents the post-yield region. However, a bi-linear idealization of moment-rotation relationship is adopted in DRAIN-RC for simplicity, with initial slope representing the effective flexural rigidity EI_{eff} which accounts for initially elastic concrete with subsequent reductions in rigidity due to cracking. The strain hardening ratio r is also required to define the post-yield rigidity as a fraction of the effective elastic rigidity. The ratio of post-yield rigidity to effective elastic rigidity (r) can be found from the idealized moment-curvature relationship.

The flexural primary curve for each element was established for the structures considered by conducting sectional moment-curvature analyses, using computer software, RC-SECTION (1997). The strain-hardening ratio of 5% (of effective elastic rigidity) was found to be appropriate for all members. The effective elastic rigidities, incorporating the effects of concrete cracking was found to be approximately the same as those recommended in CSA A23.3 (1994). Therefore, the recommended values were used as 0.7 of gross EI for columns and walls and 0.35 of gross EI for beams.

One of the short coming of DRAIN-RC is that the so called "single-component" modeling adopted does not allow the change in point of inflection for the purpose of inelastic hinge modeling. While the change in point of inflection is considered appropriately by the elastic beam element, this is not reflected on the post-yield stiffnesses of springs. It was argued by Powell (1975) that this approximation would not yield to any significant inaccuracy. Therefore, this ratio is entered as input for each element, as the ratio of two end moments (ξ). By defining the ratio of bending moment at far end to that at near end (ξ), and entering "ξ" and "r" for the actual member into Eq.2.28, the strain hardening ratio "r" for flexural spring is established. The ξ ratio is computed based on the load combination that includes dead load, 0.5 live load and earthquake loading.

4.3.2 Shear Force-Shear Displacement Relationship

The shear force-shear displacement primary curve is idealized as a tri-linear relationship in DRAIN-RC, consisting of an initial elastic segment up to cracking, a reduced slope beyond cracking up to yielding, and a line segment with further reduced slope beyond yielding. There is no simple approach available to establish inelastic shear force-shear distortion relationship of a reinforced concrete member analogous to the plane section analysis for flexure. Therefore, often it may be appropriate to rely on empirical observations. After examining the approach followed by Shoostari (1998), the primary shear curve was idealized to have elastic shear rigidity GA, followed by 0.5 GA as post cracking rigidity and 0.05 GA as the post-yield shear rigidity. It is important to note that shear and flexural yielding was observed to be coupled by Ozcebe and Saatcioglu (1989) who suggested that the onset of shear yielding within the plastic hinge region be assumed to coincide with shear yielding. Therefore, the shear yield level was specified as the value of shear at which flexural yielding occurred or shear at yielding of transverse shear reinforcement, whichever occurred first. In the buildings designed for the current investigation proper seismic design procedure was followed, which avoided premature shear yielding prior to flexural yielding.

4.3.3 Moment-Anchorage Slip Rotation Relationship

The primary curve for moment-anchorage slip relationship was established from the information generated in sectional flexural analysis. According to the procedure developed by Alsiwat and Saatcioglu (1992), the primary moment-anchorage slip curve can be idealized as a bi-linear relationship, where the first line segment represents the extension of flexural reinforcement within the adjoining member. This segment can be established by finding the distribution of strains along the anchored reinforcement and integrating to find the area. Upon yielding of reinforcement, while flexural deformations increase, the extension of reinforcement does not change significantly. However, beyond the onset of steel strain hardening, the extension increases substantially giving rise to higher extension of anchored reinforcement, which results in anchorage slip rotations and related softening in the member. This procedure was followed to establish the yield and post-yield slopes of the moment-anchorage slip primary curve and input into DRAIN-RC.

4.4 Analysis of Buildings in Eastern Canada

4.4.1 Under A-B Artificial Records

The buildings in eastern Canada were first analyzed using the artificial records generated by Atkinson and Beresnev (1998), matching the UHS with a probability of exceedance of 2% in 50 years. The set for each region in Canada includes four records for structures with long periods and four others for short periods, with a total of eight records. The results are presented in Figs. 4.4 to 4.9 in terms of maximum lateral drift and maximum interstorey drift, as well as the maximum ductility ratios for beams and columns of 5, 10 and 15-storey frame structures with fundamental periods 1.64 sec, 2.97 sec and 4.22 sec, respectively. The structures were designed without any consideration of possible contributions coming from non-structural elements. Therefore, these structures have somewhat longer periods than those expected in practice for buildings of similar height and structural system, but may be braced unintentionally by various non-structural elements. The periods calculated using the proposed NBCC-2005 requirements and SAP2000 computer software are shown in Table 4.1. The results indicate that the maximum lateral drift was limited to approximately 0.34% in all cases except for 5-storey structure where long event number 3 caused a lateral drift ratio of 0.57%. The maximum interstorey drift ratio was approximately 0.35% for all buildings except for the 5-storey structure, which had a 0.64% interstorey drift ratio. All the columns remained elastic during response with maximum moments reaching 83%, 45% and 30% of yield moments for 5, 10 and 15-storey buildings, respectively. For 10 and 15-storey buildings, all the beams remained elastic with approximately 82% and 78% of yield moments, whereas 5-storey building beams experience minor yielding at the bottom storey with a maximum ductility ratio of 1.06.

Three frame-shear wall buildings with different building heights were analyzed next. The reinforced concrete walls provided lateral bracing for the buildings. Figs. 4.10 to 4.21 display maximum lateral drift and interstorey drift responses along the height of 5, 10 and 15-storey buildings with fundamental periods of 0.52 sec, 1.36 sec and 2.41 sec, respectively. The maximum lateral drift was limited to 0.19%, whereas the interstorey drift was limited to 0.27% for all buildings. All the columns in the buildings remained elastic under the applied ground motions. The beams for 5-storey building remained elastic with a maximum 78% of the yield moment at the roof level. The beams of 10-storey and 15-storey buildings experienced maximum ductility ratio of 1.56 and 1.44, respectively. The wall response indicated minor yielding for 10 and 15-storey buildings whereas 5-storey building developed maximum ductility ratio of 1.5 at the base.

4.4.2 Under N-A Artificial Records

Earthquake records that were generated artificially by Amiri (2003) using computer software SYNTH (Naumoski 2001) were also used to investigate drift and ductility responses for the selected structures. The ground motion records were compatible with the UHS. Two such records were selected for use in the current investigation. Figs. 4.22 to 4.24 show drift and ductility responses of frame buildings analyzed under N-A records. The results indicate maximum drift ratios of 0.45 %, 0.41 % and 0.32 % for 5, 10 and 15-storey frame buildings. The interstorey drift demands were 0.52 %, 0.49 % and 0.39 % for 5, 10 and 15-storey frame buildings, respectively. The columns and beams for all buildings remained elastic during response, developing a maximum of 63% and 91% of yield moments, respectively.

The same three frame-shear wall buildings analyzed under A-B artificial earthquake records were also analyzed under N-A ground motion records. Drift and ductility responses are plotted in Figs. 4.25 to 4.30. The maximum drift demand was limited to 0.21 % in all cases. The interstorey drift demands were higher than the overall drift demands, as expected, and were limited to 0.3 % for all buildings. The columns remained elastic in all cases, developing a maximum of 52 % of yield moment, which occurred in the 10-storey building. The beams developed inelasticity in 10 and 15-storey buildings with maximum ductility ratios of 1.8 and 1.4, respectively. The beams of 5-storey building remained elastic with maximum moment reaching 80 % of yield moment. The walls of 5-storey building experienced limited inelasticity at the base, with a ductility ratio of 1.7, whereas the walls of 10 and 15-storey buildings remained elastic developing a maximum of 97 % of their yield moment.

4.4.3 Conclusions on Drift Demands in Eastern Canada

The drift response of buildings designed for Ottawa is re-evaluated in this section in an attempt to draw conclusions that can be generalized. Maximum drift demands of all 6 buildings, with and without shear walls, are plotted in Fig. 4.31. This figure is plotted only using the results of A-B artificial records. The results indicate a clear trend of increase in lateral drift with fundamental period. Also, interstorey drift response is always higher than overall lateral drift ratios. Fig. 4.32 shows the comparison between computed maximum drifts from dynamic analysis and proposed NBCC-2005 drift limit. The results indicate that the maximum computed drift ratio of 0.57% for buildings located in Ottawa is significantly below the NBCC-2005 limit of 2.5%. Drift for longer period frame structures are higher than the shorter period shear wall structures within the same height. However, low-rise buildings show higher drift ratios than medium-rise buildings which show higher drift demands than high-rise buildings. The relationship between drift and interstorey drift ratios, shown in Fig. 4.33 as a function of building period, indicate that the interstorey drift ratio is always higher than the overall drift ratio by about 30% in shear wall structures and 5 to 13% in frame buildings.

Table 4.2 and 4.3 summarize maximum roof and interstorey displacements, respectively under static and dynamic load conditions, while also showing the NBCC limits. For all cases frame buildings show higher lateral displacements than shear wall structures except for the 15-storey shear wall structure, which shows higher lateral displacement than the companion frame building under dynamic loading. In all cases, however, lateral displacements stay below the NBCC limits. The artificially generated N-A earthquake ground motions generally produce higher lateral displacements than A-B ground motions, except for the 5-storey frame building. All dynamic drift ratios are below the static drift ratios. While some variations exist between structural responses to various artificial records, in general large differences in drift and ductility responses do not occur under A-B and N-A records although their frequency contents are significantly different.

4.5 Analysis of Buildings in Western Canada

4.5.1 Under A-B Artificial Records

Two different types of frame-shear wall interactive systems, each having three different building heights were designed for Vancouver. The buildings were subjected to the A-B artificial records generated for Vancouver, representing seismic characteristics of western Canada. Four records for short period structures and additional four records for long period structures had been generated as discussed in Section 3.3. Furthermore, four additional records had been developed to represent a probable earthquake scenario in the Cascadia subduction zone. Fig. 3.8 shows that the short period events govern the entire period range, including the long period range. On the other hand, the ground motions for long period events have longer durations. Therefore, the long period events were also considered in analysis to examine the effects of ground motion duration on response, making the total number of records used 12.

The frame-shear wall structures had fundamental periods of 0.52 sec, 1.36 sec and 2.41 sec. for 5, 10 and 15-storey buildings, respectively. Figs. 4.34 to 4.51 show maximum lateral drift, maximum interstorey drift, and maximum ductility responses for frame-shear wall interactive structures. The results indicated that the maximum lateral drift was approximately 0.55%, 0.68% and 0.87%, and the maximum interstorey drift was limited to 0.59%, 0.88% and 1.14% for 5, 10 and 15-storey buildings, respectively. All structures experienced inelasticity in beams with a ductility ratio ranging between 2.0 and 5.5. The columns remained elastic for all cases with maximum yield moments of 94%, 85% and 90% for 5, 10 and 15-storey buildings, respectively. The shear walls in 5-storey building experienced inelasticity with a maximum ductility ratio of 6.5 whereas the shear walls in 10 and 15-storey buildings developed a maximum ductility ratio of 3.4 and 2.5, respectively.

Three core wall buildings with different building heights were also analyzed using the previously mentioned artificial records. The fundamental periods of core wall buildings were 0.33 sec, 0.90 sec and 1.71 sec for 5, 10 and 15-storey buildings, respectively. For the 5-storey core wall building the period calculated by SAP2000 was shorter than that computed based on the empirical expression in NBCC-2005. The results for the core wall buildings are presented in Figs. 4.52 to 4.69 for drift and ductility responses. The 5, 10 and 15-storey buildings developed maximum drift ratios of 0.19 %, 0.48 % and 0.59 %, respectively. The storey drift demands were higher, showing 0.21 %, 0.52 % and 0.79 % for 5, 10 and 15-storey buildings, respectively. The columns remained elastic, with maximum moments approaching 94 % of the yield moment, except at the 15th floor of the 15-storey building, where the columns experienced a ductility ratio of 2.1. The beams experienced yielding, showing ductility demands of 1.2 to 2.9. The shear walls and core walls developed some inelasticity at the base with a maximum ductility ratio ranging between 2.0 and 3.4.

4.5.2 Under N-A Artificial Records

The same three frame-shear wall buildings and three core wall buildings, designed for Vancouver, were also analyzed under the N-A artificial records. Two records were selected for use in the current research program. The analysis results for frame-shear wall buildings indicated that the maximum lateral drift was approximately 0.28 % in the 5-storey building, and approached 0.5 % in 10 and 15-storey buildings. This is illustrated in Figs. 4.70 to 4.75. The maximum interstorey drift was 0.33 % for the 5-storey building, whereas it approached 0.59% and 0.72 % for 10 and 15-storey buildings, respectively. In all cases, the columns remained elastic during response with maximum moments ranging between 60 % and 95% of yield moments. The beams however, experienced inelasticity with maximum ductility ratios ranging between 1.4 and 4.9. The walls for 5 and 10-storey buildings developed inelasticity with a ductility ratio of 3.0 while the walls for the 15-storey building experienced inelasticity with only a ductility ratio of 1.2 at the 11th floor level.

The drift and ductility responses for core walls are plotted in Figs. 4.76 to 4.81. The 5, 10 and 15-storey buildings showed maximum drift demands of 0.14 %, 0.29 % and 0.41 %, and maximum interstorey drift ratios of 0.17%, 0.35% and 0.53%, respectively. The columns for 5 and 10-storey buildings remained elastic developing 85% of yield moments whereas 15-storey building columns experienced limited inelasticity with a ductility ratio slightly higher than 1.0. The beams for all buildings experienced inelasticity with ductility ratios ranging between 1.0 and 2.2. The shear walls and core walls experienced inelasticity at the base with a maximum ductility ratio of 1.5 to 2.6.

4.5.3 Conclusions on Drift Demands in Western Canada

Maximum drift demands for all 6 structures designed for Vancouver are re-evaluated in this section in an attempt to draw generalized conclusions. Fig. 4.82 shows the drift demands obtained from analyses of structures with shear walls and core walls. The results are plotted in terms of maximum drift and maximum interstorey drift ratios as a function of the fundamental period using the results of A-B artificial records. Irrespective of the structural type, drift demands increase with increasing fundamental period. Hence, frame-shear wall and frame-core wall buildings can be combined in the same plot, while the structural differences in these buildings are reflected by their initial fundamental periods. The results also indicate that interstorey drift response is higher than lateral drift response. The interstorey drift quantities are of more significance to structural engineers and are also more critical. The results show that storey drift demands vary between approximately 0.21% and 1.14%.

Fig. 4.83 shows the comparison between the computed maximum drifts from dynamic analysis and proposed NBCC drift limit of 2.5%. The results show a maximum drift of 0.87% for frame-shear wall buildings in Vancouver. The relationship between the ratio of drift to interstorey drift and the fundamental period of buildings, shown in Fig. 4.84 indicates that the interstorey drifts are about 5% to 30% higher than the overall drift ratios.

Table 4.2 summarizes the maximum roof displacements for buildings under static and dynamic load conditions, while also showing the NBCC-2005 limits. In all cases the frame-shear wall buildings show higher lateral displacements than those for core wall buildings. Maximum displacements of buildings remain below the NBCC limits required for design. The N-A earthquake ground motions produce lower lateral displacements than those of A-B records. Drift demands obtained by dynamic analysis are below the values computed through static analysis with the exception of 5-storey buildings. Maximum interstorey displacements are summarized in Table 4.3. The results show the same trends as overall drift demands. Both dynamic and static analysis results are below the NBCC-2005 limit.

The drift response of structures designed for Vancouver was the highest under Short Event records. The long event records, in spite of their longer duration did not govern response in any of the buildings analyzed. The Cascadia Event was not critical for any of the structures either. Drift and ductility demands under A-B records were 1.5 to 2.0 times higher than those obtained under N-A records, the highest difference being for the 5-storey frame-shear wall building. This indicates that responses obtained under different artificial records can be significantly different even if the records matched the same spectrum.

4.6 Base Shear Calculations

One of the important design quantities for seismic design is the design base shear. Therefore, the outcome of the analyses conducted was further evaluated to compare design base shears computed by dynamic analyses with those obtained on the basis of the equivalent static load procedure. The equivalent static load procedure is limited in NBCC-2005 to structures with periods and heights below a certain limit, where the limits change with the level of seismicity of the region and the regularity of the building layout. All the buildings designed in the current investigation met the NBCC-2005 requirements for equivalent static load procedure since they were regular and had periods less than 2 sec and heights less than 60m. However, dynamic analysis is the primary analysis approach specified in NBCC-2005, with some apprehension on the part of designers concerning the base shear quantities that are obtained form dynamic analysis (Heidebrecht 2003). The empirical expressions suggested in the code for the computation of fundamental period would yield conservative values and result in design force levels that are compatible with the values used over the years as acceptable values. In conducting dynamic analysis the actual building periods computed are often significantly longer than those used in design. This may result in lower base shear values, necessitating the limit of 0.8 times the static base shear obtained from the equivalent static load procedure. Therefore, it is important to compare the base shear results of analyses of 12 buildings designed in the current investigation with the design values obtained by the equivalent static approach.

Table 4.4 summarizes base shear forces obtained from dynamic and static analyses for all 12 buildings considered in the current study. The dynamic shears were obtained under the A-B generated ground motions (compatible with UHS specified in NBCC-2005). Dynamic and static base shear values computed for MRF structures in Ottawa were similar, with dynamic analysis showing 14% lower and 39% higher quantities than those generated by static analysis for 5-storey and 15-storey buildings, respectively. This difference increased in shear wall buildings designed for Ottawa, with dynamic analyses resulting in 24% to 46% higher base shear values than those obtained statically. Buildings designed for Vancouver consistently developed much higher base shear values when dynamic analysis was employed. Dynamic base shears were 2.72 to 3.76 times the static base shears for these buildings. It should be noted however, the dynamic base shear values used in the latter case were obtained from an artificial record that resulted in somewhat higher values than those suggested by the UHS in the long period range. This is believed to contribute to the observed difference between static and dynamic shears. Furthermore, the comparison is made with static design base shear value, rather than the results of a static analysis. Therefore the static value does not incorporate additional shear forces due to frame-shear wall interactive effects.

Dynamic analysis results were further analyzed in detail to illustrate base shear time histories and the distribution of storey shears along the height when maximum base shear is attained. Fig. 4.85 depicts base shear time history for the 15-storey frame-shear wall building in Vancouver. The same figure also illustrates the static base shear. Also included in the figure is base moment history divided by 2/3 the building height, reflecting the variation of base shear if seismic forces were to be distributed in an inverted triangular manner to simulate the first mode response. The latter history shows a significant divergence from computed dynamic base shear history, indicating that the distribution of storey shears does not necessarily agree with the inverted triangular distribution assumption employed in the equivalent static load procedure. A similar observation was made by Naeim (2001), who indicated that the response of an isolated structural wall obtained from dynamic inelastic analyses show "...the maximum calculated shear at the base of walls can be from 1.5 to 3.5 times greater than the shear necessary to produce flexural yielding at the base, when such shear is distributed in a triangular manner over the height of the wall..." The static base shear is nearly the same as shear calculated from dynamic moment response using 2/3 the height as the lever arm. Dynamic and static base shears are compared for all other buildings in Figs. 4.86 through 4.89. In all cases, with the exception of moment resisting frames designed for Ottawa, dynamic based shears are higher than those computed on the basis of equivalent static load method. Distribution of dynamic storey shears is shown in Figs. 4.90 through 4.93 for specific times in response, corresponding to maximum base shear values. It is clear from these figures that higher mode effects result in variable locations of resultant lateral force, leading to higher dynamic base shear quantities.

4.7 Hysteretic Models and Force-Time Histories

15-storey frame-shear wall building designed for Vancouver is selected to study the moment, shear force and axial force time histories and flexure, shear and anchorage slip hinge hysteretic models for typical column, shear wall and beam elements. These include a first storey shear wall, a first storey exterior column and a fifth storey exterior beam under Short Event. No.3. In this particular case the shear wall and beam experienced yielding, while the column remained elastic. Figs. 4.94 to 4.96 show moment and force-time histories of selected members. The force and moment values correspond to lumped frames. At time zero, vertical members are subjected to gravity axial forces. Similarly, the columns and beams are subjected to member end forced generated by static gravity loads (prior to the onset of seismic excitation). These are distributed to adjoining members on basis of relative member stiffnesses.

Hysteretic relationships, recorded during response are shown in Figs. 4.97 to 4.99 for selected members and for all deformation components. These plots confirm that the hysteretic models do generate the expected force-deformation hysteresis loops, with appropriate yield levels, stiffness degradation and pinching of hysteresis loops.

4.8 Contributions of Deformation Components

Flexure, shear and anchorage slip deformations may constitute significant components of total deformation response. Neglect of one or more of these deformation components may result in inaccuracies in computed response. Shoostari (1998) showed the importance of these deformation components on reinforced concrete response. The significance of each deformation component is illustrated in Figs. 4.100 to 4.102 for selected members of the 15-storey frame-shear wall structure in Vancouver. The results show significant contributions of flexure, shear and slip components on overall deformation response. The contributions of deformation components vary with inelasticity and the characteristics of each structure considered.

CHAPTER 5
Summary and Conclusion

5.1 Summary

Drift demands of reinforced concrete buildings in Canada were investigated. Three different structural systems were considered in two seismologically different regions of Canada. Ottawa was selected as a city representative of eastern Canadian seismicity and Vancouver was selected as representative of western Canada. Three building heights were considered in each city, covering low, medium and high-rise buildings. A total of 12 buildings were designed using the seismic provisions of proposed NBCC-2005 Building Code and CSA Standard A23.3 for reinforced concrete design. Dynamic inelastic response history analyses of all 12 buildings were conducted to assess drift demands of these buildings. The proposed design response spectra, in the form of Uniform Hazard Response Spectra, were considered for the appropriate locations of buildings. Artificial records, compatible with UHS and with earthquake probability of exceedance of 2% in 50 years, were employed for the analyses. The results were evaluated for overall drift and interstorey drift ratios. Inelasticity in buildings was monitored and rotational ductility ratios were presented to assess the degree of inelasticity attained. The results are presented in the form of maximum response quantities.

Computer software DRAIN-RC was employed for dynamic analysis. The program is well equipped with hysteretic models appropriate for inelastic behaviour of reinforced concrete structures. A pre-processor was developed for the software, as part of the current work to make it more user-friendly and interactive. Visual Basic 6.0 programming language was used to develop a Windows-based pre-processor.

5.2 Conclusions

The following conclusions can be derived from the analytical research conducted in this research project:

- Seismic storey drift demands in Ottawa are below 0.65% for frame structures and 0.3% for frame-shear wall buildings, under the artificial earthquake records considered in this investigation, matching the proposed UHS and having 2% probability of exceedance in 50 years as defined in the 2005 edition of NBCC.
- Seismic storey drift demands in Vancouver are below 1.14% for frame-shear wall structures and 0.79% for frame-core wall buildings, under the artificial earthquake records considered in this investigation, matching the proposed UHS and having 2.0% probability of exceedance in 50 years as expressed in the 2005 edition of NBCC.
- Seismic interstorey drift demands were close to but higher than the overall drift demand in all buildings, by about 5% to 20%.
- Reinforced concrete buildings designed on the basis of the National Building Code of Canada (NBCC 2005) develop lower drift levels under the code spectra compatible earthquake records than the 2.5% drift limit specified in the code.
- The characteristics of earthquake records play a major role in assessing drift demands as well as other dynamic response quantities. Matching a design response spectrum may not necessarily be sufficient for an artificial record to reflect the intended design earthquake. Two different techniques were used to generate the artificial records used in the current investigation. While the results produced by the two different sets of records were somewhat in agreement in eastern Canada, they were significantly different in the west. The A-B records produced by approximately a factor of 2 higher response than the N-A records.
- Static and dynamic base shears obtained by equivalent static load approach and dynamic inelastic analysis can be substantially different. This implies that the equivalent static approach, essentially based on the first mode response as empirically modified for higher mode effects does not agree with the distribution of dynamic shear forces along the height of the building.

- ➢ Dynamic analysis results indicate that the resultant lateral seismic force required to attain base moment resistance is not necessarily acting at $2/3^{rd}$ of the building height as recommended in the static load analysis.
- ➢ Components of deformation components caused by flexure anchorage slip and shear can be important in dynamic analysis of reinforced concrete structures. A hysteretic model for each of these deformations should be considered for improved accuracy of results.

5.3 Recommendations for Further Research

The research program carried out in this study covered a large number of reinforced concrete buildings. Nonetheless, a number of cases were not studied, including buildings stiffened by non-structural elements and buildings with different structural configurations, as well as strength and stiffness characteristic. Of particular importance is the lack of the consideration of torsional effects and coupled wall systems. Building irregularities also constitute a challenge for the investigation of drift demands. Consequently, the following recommendations are made for future research:

- Investigation of buildings with different structural configurations, including coupled wall systems.
- Investigation of the effects of non-structural elements on structural stiffness and resulting changes in drift demands.
- Consideration of structural irregularities in the form of strength and stiffness taper along building height, as well as plan.
- Consideration of torsional effects on drift demands.
- Consideration of the effects of different ground motions on elastic and inelastic drift demands.

Additional work is also recommended in terms of computer software development. It is recommended that a post-processor be developed for computer software DRAIN-RC and integrated fully with the pre-processor developed as part of the current work and the main program.

References

Adams, J., and Atkinson, G. (2003). "Development of seismic hazard maps for the proposed 2005 edition of the National Building Code of Canada." *Canadian Journal of Civil Engineering*, **30:** 255-271.

Adams, J., and Halchuk, S. (2003). Fourth generation seismic hazard maps of Canada: Values for over 650 Canadian localities intended for the 2005 National Building Code of Canada. Geological Survey of Canada Open File 4459. 155 p. Available from http://www.seismo/nrcan.gc.ca/hazards/OF4459 as of 1 April 2003.

Alsiwat, J. M. (1993). Effect of Anchorage Slip and Inelastic Shear on Seismic Response of Reinforced Concrete Frames. PhD. dissertation, University of Ottawa, Ottawa, Canada, pp367

Alsiwat, J. M., Saatcioglu, M. (1992). "Reinforcement Anchorage Slip Under Monotonic Loading." *Journal of Structural Engineering*, **118:** 2421-2438

Amiri, K. (2003). Effects of Scaling of Earthquake Excitations on Dynamic Response of Reinforced Concrete Frame Buildings. Master Thesis, University of Ottawa, Ottawa, Canada

Atkinson, G., Beresnev, I. (1998). "Compatible ground-motion time histories for new national seismic hazard maps." *Canadian Journal of Civil Engineering*, **25**: 305-318.

Bariola, J. (1992). "Drift response of medium-rise reinforced concrete buildings during earthquakes." *ACI Structural Journal*, **89:** 384-390

Bertero, V. V. (1996a). "State-of-the-art report on: design criteria." *Report No. UCB/EERC-96/01*, Earthquake Engineering Research Center, University of California at Berkeley

Bertero, V. V. (1996b). "The need for multi-level seismic design criteria." *Report No. UCB/EERC-96/01*, Earthquake Engineering Research Center, University of California at Berkeley

Bradley, J. C., Millspaugh, A. C. (1999). Programming in Visual Basic, Version 6.0. Irwin/Mc Graw-Hill, Boston

Chandler, A. M., Mendis, P. A. (2000). "Performance of reinforced concrete frames using force and displacement based seismic assessment methods." *Engineering Structures*, **22:** 352-363

CSA Standard A23.3-94, (1994). Design of Concrete Structures. Canadian Portland Cement Association, Ottawa, Canada

Filiatrault, A., Lachapelle, E., and Lamontagne, P. (1998a). "Seismic performance of ductile and nominally ductile reinforced concrete moment resisting frames I. experimental study." *Canadian Journal of Civil Engineering*, **25:** 331-341

Filiatrault, A., Lachapelle, E., and Lamontagne, P. (1998b). "Seismic performance of ductile and nominally ductile reinforced concrete moment resisting frames II. analytical study." *Canadian Journal of Civil Engineering*, **25:** 342-352

Goudreault, P. A., Saatcioglu, M. (1997). Computer program RC-SECTION, developed by Picasso Inc., Ottawa, Canada

Habibullah, A. et al. (2001). SAP 2000 Nonlinear Structural Analysis Program Version 7.44. Computer Structures Inc., Berkeley, California

Hachem, M. M. (1999). An Interactive Computer Program for Computation of Bi-directional Nonlinear Spectra, BISPEC. University of California, Berkeley, Available from http://www.ce.berkeley.edu/ ~hachem/bispec/

Heidebrecht, A. C. (1997). "Seismic level of protection for building structures." *Canadian Journal of Civil Engineering*, **24:** 20-33

Heidebrecht, A. C. (2003). "Overview of seismic provisions of the proposed 2005 edition of the National Building Code of Canada." *Canadian Journal of Civil Engineering*, **30:** 241-254

Heidebrecht, A. C., Naumoski, N. (1999). "Seismic performance of ductile medium height reinforced concrete frame buildings designed in accordance with the provisions of the 1995 National Building Code of Canada." *Canadian Journal of Civil Engineering*, **26:** 606-617

Kanaan, A. E., Powell, G. H. (1973). DRAIN-2D: General Purpose Computer Program for Dynamic Analysis of Inelastic Plane Structures. University of California, Berkeley, California

Klingner, R. E., Bertero, V. V. (1978). "Earthquake Resistance of Infilled Frames." *Journal of the Structural Division*, **104:** 973-989

Lee, H. S., Woo, S. W. (2002). "Seismic performance of a 3-story RC frame in a low-seismicity region." *Engineering Structures*, **24:** 719-734

Medhekar, M. S., Kennedy, D. J. L. (2000). "Displacement-based seismic design of buildings-application." *Engineering Structures,* **22:** 210-221

Mitchell, D., Tremblay, R., Karacabeyli, E., Paultre, P., Saatcioglu, M., Anderson, D. L. (2003). "Seismic force modification factors for the proposed 2005 edition of the National Building Code of Canada." *Canadian Journal of Civil Engineering*, **30:** 308-327

Moehle J. P. (1992). "Displacement-based design of RC structures subjected to earthquakes." *Earthquake Spectra*, **8:** 403-428

Naeim, F. (2001). The Seismic Design Handbook. Kluwer Academic Publishers

NBCC. (1995). National Building Code of Canada 1995. Institute for Research in Construction , National Research Council of Canada, Ottawa, Ontario, Canada

Naumoski, N. (2001). Program SYNTH, Generation of Artificial Accelerograms Compatible with a Target Spectrum.

Ozcebe, G., Saatcioglu, M. (1989). "Hysteretic Shear Model for Reinforced Concrete Members." *Journal of Structural Engineering*, **115:** 132-148

Powell, G. H. (1975). Supplement to Computer Program DRAIN-2D. Supplement to Report, DRAIN-2D User's Guide, University of California, 36pp

Saatcioglu, M., Alsiwat, J. M., Ozcebe, G. (1992). "Hysteretic Behavior of Anchorage Slip in R/C Members." *Journal of Structural Engineering*, **118:** 2439-2458

Saatcioglu, M., Derecho, A. T., Corley, W. G. (1983). "Modelling Hysteretic Behaviour of Coupled Walls for Dynamic Analysis." *Earthquake Engineering and Structural Dynamics*, **11:** 711-726

Shooshtari, A. (1998), Seismic Drift Demands of Reinforced Concrete Buildings. PhD. dissertation, University of Ottawa, Ottawa, Canada, pp385

Sinclair, D. (1999). How to Program Visual Basic 6. Prentice Hall

Zhu, T. J. (1994). "Seismic storey drift estimation." *Canadian Journal of Civil Engineering*, **21:** 1081-1083

Zhu, T. J., Tso, W. K., and Heidebrecht, A. C. (1992). "Seismic performance of reinforced concrete ductile moment-resisting frame buildings located in different seismic regions." *Canadian Journal of Civil Engineering*, **19:** 688-710

Tables

Table 3.1 Data Used for Design of Buildings

	Floor	Roof
Dead Loads (kN/m²)	5	3.5
Live Loads (kN/m²)	2.4	2.2
Concrete Compressive Strength (MPa)	30	
Reinforcement Yield Strength (MPa)	400	

Table 3.2 Reinforcement Arrangements and Sectional Sizes of 5-Storey Moment Resisting Frame Building for Ottawa

Frame	Floor	Beam Section and Reinforcement	Column Section and Reinforcement	
			Interior	Exterior
Interior	1-4	300x450 3#25 top, 2#20 bottom	450x450 8#25	400x400 8#20
	5	300x400 3#20 top, 2#15 bottom	450x450 8#25	400x400 8#20
Exterior	1-4	300x450 3#25 top, 2#20 bottom	400x400 8#20	300x300 8#20
	5	300x400 3#20 top, 2#15 bottom	400x400 8#20	300x300 8#20

Table 3.3 Reinforcement Arrangements and Sectional Sizes of 10-Storey Moment Resisting Frame Building for Ottawa

Frame	Floor	Beam Section and Reinforcement	Column Section and Reinforcement	
			Interior	Exterior
Interior	1-5	300x450 3#25 top, 2#20 bottom	500x500 12#25	400x400 8#25
	6-9	300x450 3#25 top, 2#20 bottom	500x500 12#20	400x400 8#20
	10	300x400 3#20 top, 2#15 bottom	500x500 12#20	400x400 8#20
Exterior	1-5	300x500 3#25 top, 2#20 bottom	400x400 8#25	350x350 8#25
	6-9	300x450 3#25 top, 2#20 bottom	400x400 8#20	350x350 8#20
	10	300x400 3#20 top, 2#15 bottom	400x400 8#20	350x350 8#20

Table 3.4 Reinforcement Arrangements and Sectional Sizes of 15-Storey Moment Resisting Frame Building for Ottawa

Frame	Floor	Beam Section and Reinforcement	Column Section and Reinforcement	
			Interior	Exterior
Interior	1-5	300x450 3#25 top, 2#20 bottom	600x600 12#25	500x500 12#25
	6-14	300x450 3#25 top, 2#20 bottom	600x600 12#20	500x500 12#20
	15	300x400 3#20 top, 2#15 bottom	600x600 12#20	500x500 12#20
Exterior	1-5	300x450 3#25 top, 2#20 bottom	450x450 8#25	400x400 8#25
	6-14	300x450 3#25 top, 2#20 bottom	450x450 8#20	400x400 8#20
	15	300x400 3#20 top, 2#15 bottom	450x450 8#20	400x400 8#20

Table 3.5 Reinforcement Arrangements and Sectional Sizes of 5-Storey Frame-Shear Wall Building for Ottawa

Frame	Floor	Beam Section and Reinforcement	Column Section and Reinforcement	
			Interior	Exterior
Interior	1-4	300x450 3#25 top, 2#20 bottom	350x350 8#25	350x350 8#20
	5	300x400 3#20 top, 2#15 bottom	350x350 8#25	350x350 8#20
Exterior	1-4	300x450 3#25 top, 2#20 bottom	shear wall 250x7000	300x300 8#20
	5	300x400 3#20 top, 2#15 bottom	shear wall 250x7000	300x300 8#20

Table 3.6 Reinforcement Arrangements and Sectional Sizes of 10-Storey Frame-Shear Wall Building for Ottawa

Frame	Floor	Beam Section and Reinforcement	Column Section and Reinforcement	
			Interior	Exterior
Interior	1-5	300x450 3#25 top, 2#20 bottom	500x500 15#25	350x350 8#25
	6-9	300x450 3#25 top, 2#20 bottom	500x500 12#20	350x350 8#20
	10	300x400 3#20 top, 2#15 bottom	500x500 12#20	350x350 8#20
Exterior	1-5	300x450 3#25 top, 2#20 bottom	shear wall 350x7000	350x350 8#25
	6-9	300x450 3#25 top, 2#20 bottom	shear wall 250x7000	350x350 8#20
	10	300x400 3#20 top, 2#15 bottom	shear wall 250x7000	350x350 8#20

Table 3.7 Reinforcement Arrangements and Sectional Sizes of 15-Storey Frame-Shear Wall Building for Ottawa

Frame	Floor	Beam Section and Reinforcement	Column Section and Reinforcement	
			Interior	Exterior
Interior	1-5	300x450 3#25 top, 2#20 bottom	600x600 12#25	400x400 8#25
	6-14	300x450 3#25 top, 2#20 bottom	600x600 12#20	400x400 8#20
	15	300x400 3#20 top, 2#15 bottom	600x600 12#20	400x400 8#20
Exterior	1-5	300x450 3#25 top, 2#20 bottom	shear wall 450x7000	350x350 8#25
	6-10	300x450 3#25 top, 2#20 bottom	shear wall 350x7000	350x350 8#20
	11-14	300x450 3#25 top, 2#20 bottom	shear wall 250x7000	350x350 8#20
	15	300x400 3#20 top, 2#15 bottom	shear wall 250x7000	350x350 8#20

Table 3.8 Reinforcement Arrangements and Sectional Sizes of 5-Storey Frame-Shear Wall Building for Vancouver

Frame	Floor	Beam Section and Reinforcement	Column Section and Reinforcement	
			Interior	Exterior
Interior	1-4	300x450 3#25 top, 2#20 bottom	350x350 8#25	350x350 8#20
	5	300x400 3#20 top, 2#15 bottom	350x350 8#25	350x350 8#20
Exterior	1-4	300x450 3#25 top, 2#20 bottom	shear wall 250x7000	300x300 8#20
	5	300x400 3#20 top, 2#15 bottom	shear wall 250x7000	300x300 8#20

Table 3.9 Reinforcement Arrangements and Sectional Sizes of 10-Storey Frame-Shear Wall Building for Vancouver

Frame	Floor	Beam Section and Reinforcement	Column Section and Reinforcement	
			Interior	Exterior
Interior	1-5	300x450 3#25 top, 2#20 bottom	500x500 15#25	350x350 8#25
	6-9	300x450 3#25 top, 2#20 bottom	500x500 12#20	350x350 8#20
	10	300x400 3#20 top, 2#15 bottom	500x500 12#20	350x350 8#20
Exterior	1-5	300x450 3#25 top, 2#20 bottom	shear wall 350x7000	350x350 8#25
	6-9	300x450 3#25 top, 2#20 bottom	shear wall 250x7000	350x350 8#20
	10	300x400 3#20 top, 2#15 bottom	shear wall 250x7000	350x350 8#20

Table 3.10 Reinforcement Arrangements and Sectional Sizes of 15-Storey Frame-Shear Wall Building for Vancouver

Frame	Floor	Beam Section and Reinforcement	Column Section and Reinforcement	
			Interior	Exterior
Interior	1-5	300x450 3#25 top, 2#20 bottom	600x600 12#25	400x400 8#25
	6-14	300x450 3#25 top, 2#20 bottom	600x600 12#20	400x400 8#20
	15	300x400 3#20 top, 2#15 bottom	600x600 12#20	400x400 8#20
Exterior	1-5	300x450 3#25 top, 2#20 bottom	shear wall 450x7000	350x350 8#25
	6-10	300x450 3#25 top, 2#20 bottom	shear wall 350x7000	350x350 8#20
	11-14	300x450 3#25 top, 2#20 bottom	shear wall 250x7000	350x350 8#20
	15	300x400 3#20 top, 2#15 bottom	shear wall 250x7000	350x350 8#20

Table 3.11 Reinforcement Arrangements and Sectional Sizes of 5-Storey Core Wall Building for Vancouver

Frame	Floor	Beam Section and Reinforcement	Column Section and Reinforcement	
			Interior	Exterior
Interior	1-4	300x450 3#20 top, 2#20 bottom	350x350 8#25	350x350 8#20
	5	300x400 3#20 top, 2#15 bottom	350x350 8#25	350x350 8#20
Exterior (Shear Wall)	1-4	300x450 3#20 top, 2#20 bottom	shear wall 250x7000	300x300 4#20
	5	300x400 3#20 top, 2#15 bottom	shear wall 250x7000	300x300 4#20
Interior (Core Wall)	1-4	300x500 4#20 top, 2#25 bottom	core wall 250x7000	300x300 8#20
	5	300x450 3#20 top, 2#25 bottom	core wall 250x7000	300x300 8#20

Table 3.12 Reinforcement Arrangements and Sectional Sizes of 10-Storey Core Wall Building for Vancouver

Frame	Floor	Beam Section and Reinforcement	Column Section and Reinforcement	
			Interior	Exterior
Interior	1-5	300x450 3#25 top, 2#20 bottom	500x500 12#25	350x350 8#25
	6-9	300x450 3#25 top, 2#20 bottom	500x500 12#20	350x350 8#20
	10	300x400 3#20 top, 2#15 bottom	500x500 12#20	350x350 8#20
Exterior (Shear Wall)	1-5	300x450 3#25 top, 2#20 bottom	shear wall 350x7000	350x350 8#20
	6-9	300x450 3#25 top, 2#20 bottom	shear wall 250x7000	350x350 4#20
	10	300x450 3#25 top, 2#25 bottom	shear wall 250x7000	350x350 4#20
Interior (Core Wall)	1-5	300x500 3#25 top, 2#25 bottom	core wall 350x7000	350x350 8#25
	6-9	300x500 3#25 top, 2#25 bottom	core wall 250x7000	350x350 8#20
	10	300x450 3#20 top, 2#25 bottom	core wall 250x7000	350x350 8#20

Table 3.13 Reinforcement Arrangements and Sectional Sizes of 15-Storey Core Wall Building for Vancouver

Frame	Floor	Beam Section and Reinforcement	Column Section and Reinforcement	
			Interior	Exterior
Interior	1-5	300x450 3#25 top, 2#20 bottom	600x600 12#25	400x400 8#25
	6-14	300x450 3#25 top, 2#20 bottom	600x600 12#20	400x400 8#20
	15	300x400 3#20 top, 2#15 bottom	600x600 12#20	400x400 8#20
Exterior (Shear Wall)	1-5	300x450 3#25 top, 2#20 bottom	shear wall 450x7000	350x350 8#25
	6-10	300x450 3#25 top, 2#20 bottom	shear wall 350x7000	350x350 8#20
	11-14	300x450 3#25 top, 2#20 bottom	shear wall 250x7000	350x350 8#20
	15	300x400 3#20 top, 2#15 bottom	shear wall 250x7000	350x350 8#20
Interior (Core wall)	1-5	300x500 3#25 top, 2#25 bottom	core wall 450x7000	450x450 8#25
	6-10	300x500 3#25 top, 2#25 bottom	core wall 350x7000	450x450 8#20
	11-14	300x500 3#25 top, 2#25 bottom	core wall 250x7000	450x450 8#20
	15	300x450 3#25 top, 2#25 bottom	core wall 250x7000	450x450 8#20

Table 3.14 Artificial Ground Motion Records Used in Dynamic Analyses

Location	Ground Motion Record	PGA (cm/s^2)	ΔT (sec)	Duration (sec)
EAST	Short Event No.1	422.1	0.01	8.87
	Short Event No.2	512.3	0.01	8.87
	Short Event No.3	461.1	0.01	8.87
	Short Event No.4	430.9	0.01	8.87
	Long Event No.1	295.3	0.01	24.06
	Long Event No.2	280.4	0.01	24.06
	Long Event No.3	335.5	0.01	24.06
	Long Event No.4	286.1	0.01	24.06
	N-A Event No.6	421.83	0.005	35.00
	N-A Event No.14	421.83	0.005	35.00
WEST	Short Event No.1	523.5	0.01	8.52
	Short Event No.2	526.8	0.01	8.52
	Short Event No.3	567.5	0.01	8.52
	Short Event No.4	380.0	0.01	8.52
	Long Event No.1	241.5	0.01	18.17
	Long Event No.2	254.3	0.01	18.17
	Long Event No.3	225.9	0.01	18.17
	Long Event No.4	247.1	0.01	18.17
	Cascadia Event No.1	43.90	0.01	121.62
	Cascadia Event No.2	49.04	0.01	106.25
	Cascadia Event No.3	40.81	0.01	132.99
	Cascadia Event No.4	53.24	0.01	142.30
	N-A Event No.5	490.5	0.01	75.00
	N-A Event No.10	490.5	0.01	75.00

Table 4.1 The Fundamental Period of Buildings Calculated Using NBCC and SAP2000.

Location	Frame Type	No. of Storey	T_{NBCC} (sec)	$T_{SAP2000}$ (sec)
EAST	MRF	5	0.709	1.64
		10	1.193	2.97
		15	1.617	4.22
	SHW	5	0.473	0.52
		10	0.795	1.36
		15	1.078	2.41
WEST	SHW	5	0.473	0.52
		10	0.795	1.36
		15	1.078	2.41
	CW	5	0.473	0.33
		10	0.795	0.90
		15	1.078	1.71

Table 4.2 Maximum Roof Displacement of Buildings under Static and Dynamic Load Conditions

Location	Frame Type	No. of Storey	Maximum Roof Displacement (mm)			
			Δ_{STATIC}	$\Delta_{DYNAMIC}$ (A-B)	$\Delta_{DYNAMIC}$ (N-A)	Δ_{NBCC}
EAST	MRF	5	221.9	92.0	74.1	500
		10	468.6	78.0	106.1	1000
		15	709.1	93.0	104.0	1500
	SHW	5	33.6	27.8	31.1	500
		10	212.2	76.9	85.8	1000
		15	491.7	101.8	102.3	1500
WEST	SHW	5	75.6	113.4	56.5	500
		10	472.1	268.0	180.0	1000
		15	1089.7	521.0	311.0	1500
	CW	5	25.7	35.9	28.7	500
		10	199.9	184.0	119.0	1000
		15	528.6	342.0	248.0	1500

Table 4.3 Maximum Interstorey Displacement of Buildings under Static and Dynamic Load Conditions

Location	Frame Type	No. of Storey	Maximum Interstorey Displacement (mm)			
			Δ_{STATIC}	$\Delta_{DYNAMIC}$ (A-B)	$\Delta_{DYNAMIC}$ (N-A)	Δ_{NBCC}
EAST	MRF	5	60.6	25.6	20.3	100
		10	65.2	14.1	19.0	100
		15	64.9	12.2	14.9	100
	SHW	5	19.2	7.9	7.92	100
		10	28.3	10.8	11.9	100
		15	43.0	9.6	11.1	100
WEST	SHW	5	19.6	24.1	13.3	100
		10	63.0	34.6	23.5	100
		15	95.4	45.4	29.6	100
	CW	5	6.5	8.34	6.5	100
		10	27.2	21.3	13.9	100
		15	48.8	30.6	21.8	100

Table 4.4 Maximum Base Shear of Buildings under Static and Dynamic Load Conditions

Location	Frame Type	No. of Storey	Maximum Base Shear (kN)		
			V_{STATIC}	$V_{DYNAMIC}$	V_{ST}/V_{DY}
EAST	MRF	5	1110	1286	0.863
		10	1178	1085	1.086
		15	1289	926	1.392
	SHW	5	2045	3761	0.544
		10	2727	4074	0.669
		15	2917	3828	0.762
WEST	SHW	5	2112	6054	0.349
		10	3026	8232	0.367
		15	3268	10848	0.301
	CW	5	2208	8293	0.266
		10	3195	11197	0.285
		15	3488	10800	0.323

Figures

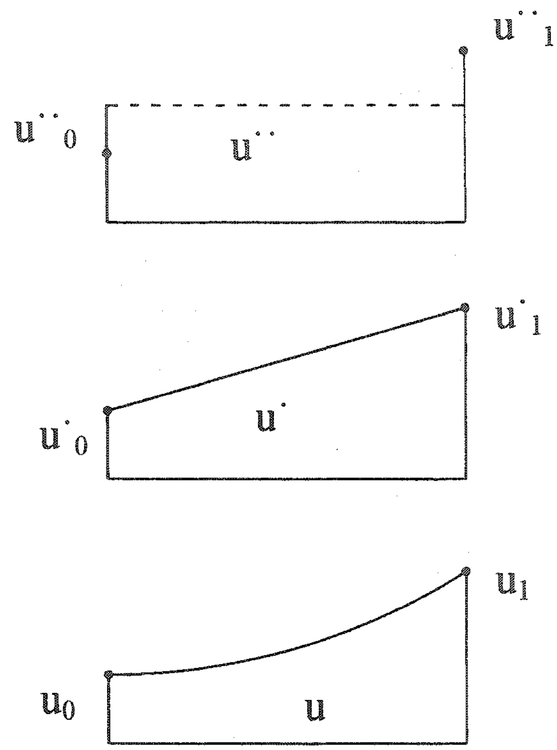

Fig. 2.1 Average Acceleration Method

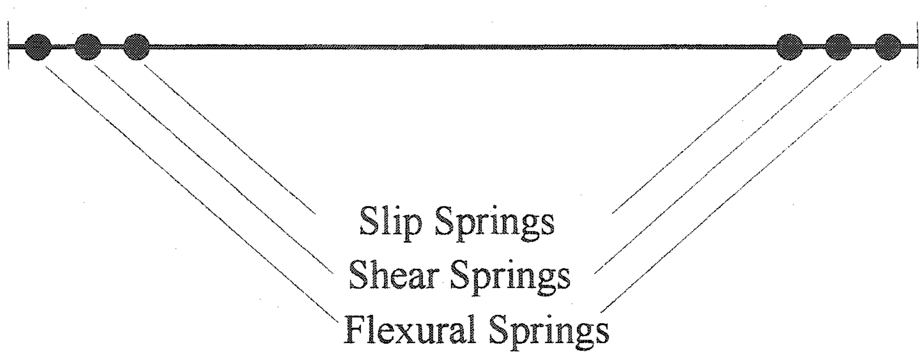

Fig. 2.2 Elastic Beam Element with Three Inelastic Springs at Each End

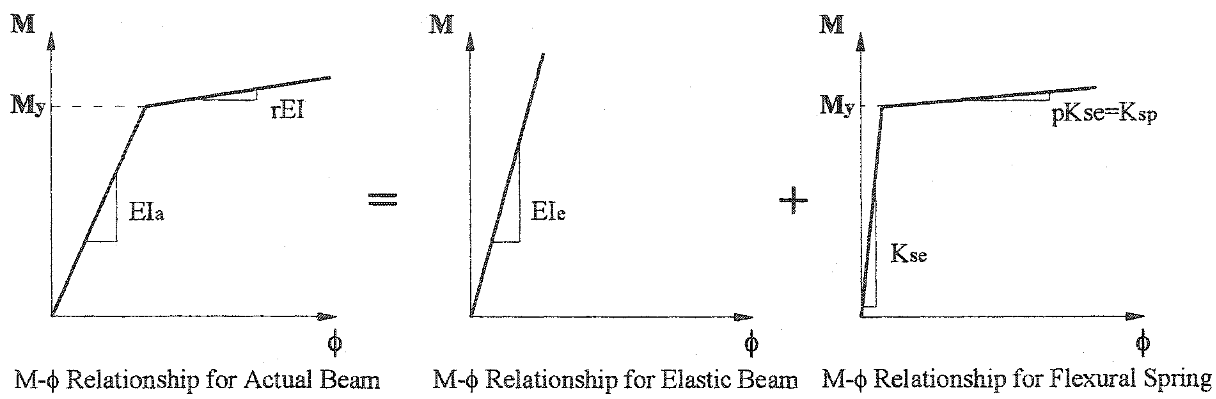

Fig. 2.3 Moment-Curvature Relationship for Actual and Idealized Beam (Shoostari 1998)

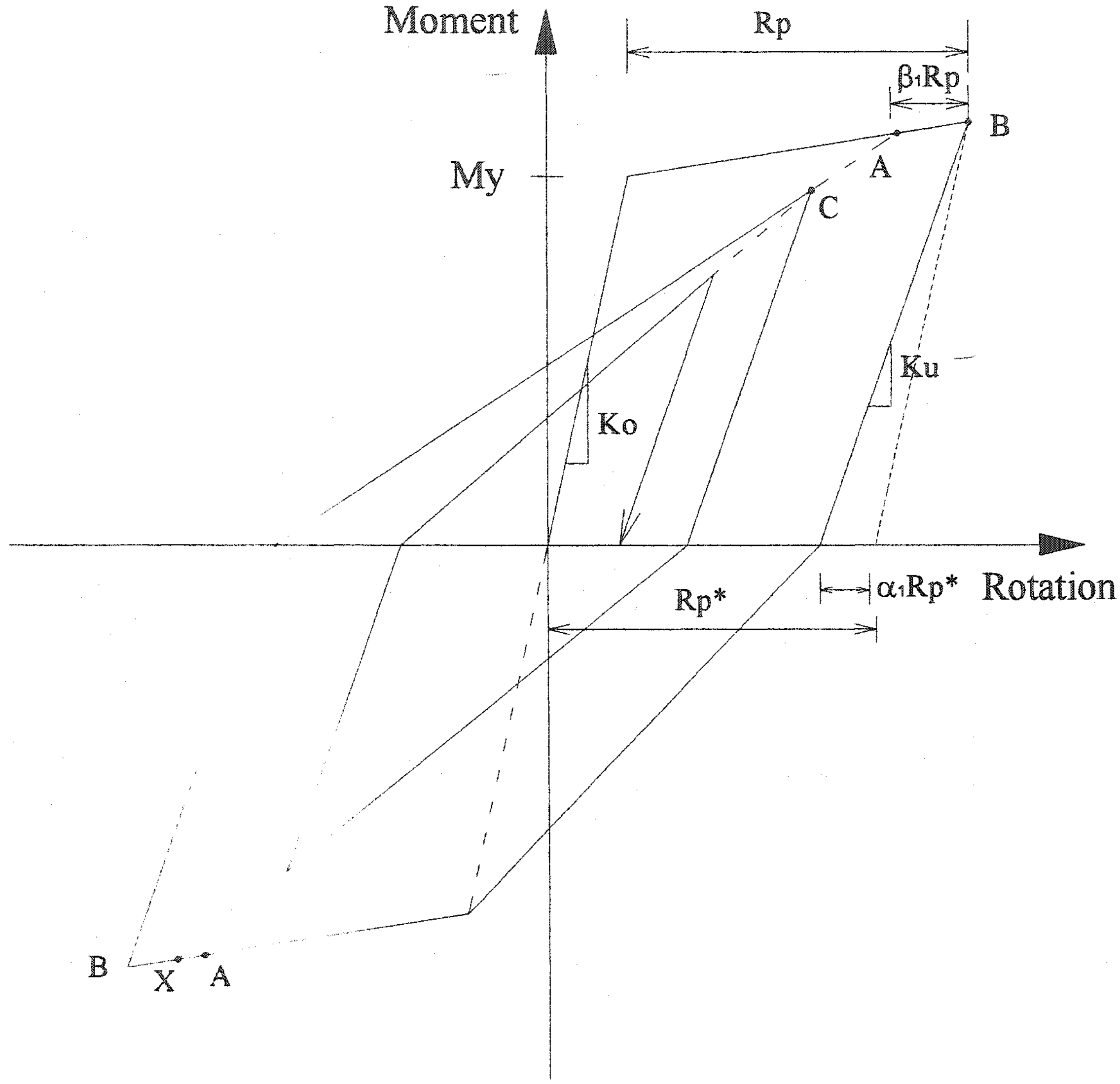

Fig. 2.4 Extended Version of Takeda's Hysteretic Model (Powell 1975)

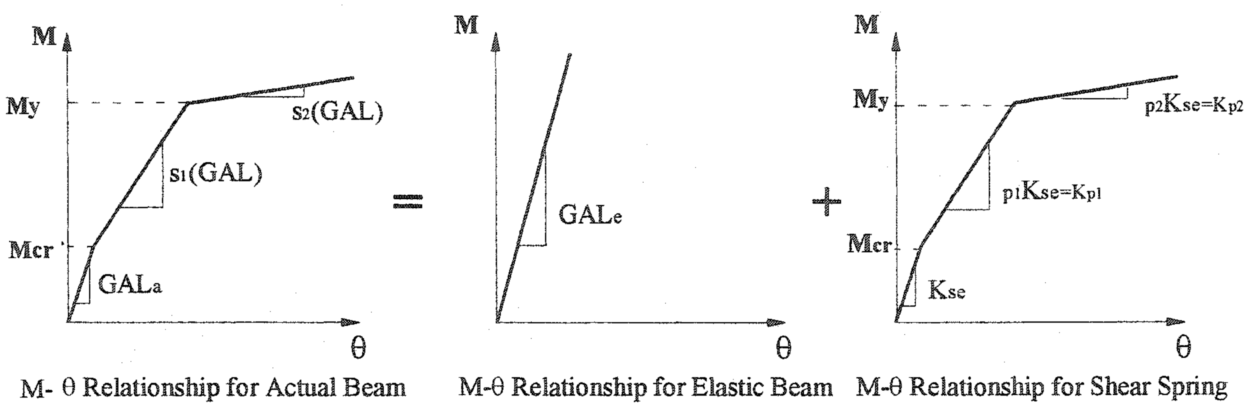

Fig. 2.5 Moment-Shear Cord Rotation Relationship for Actual and Idealized Beam (Shoostari 1998)

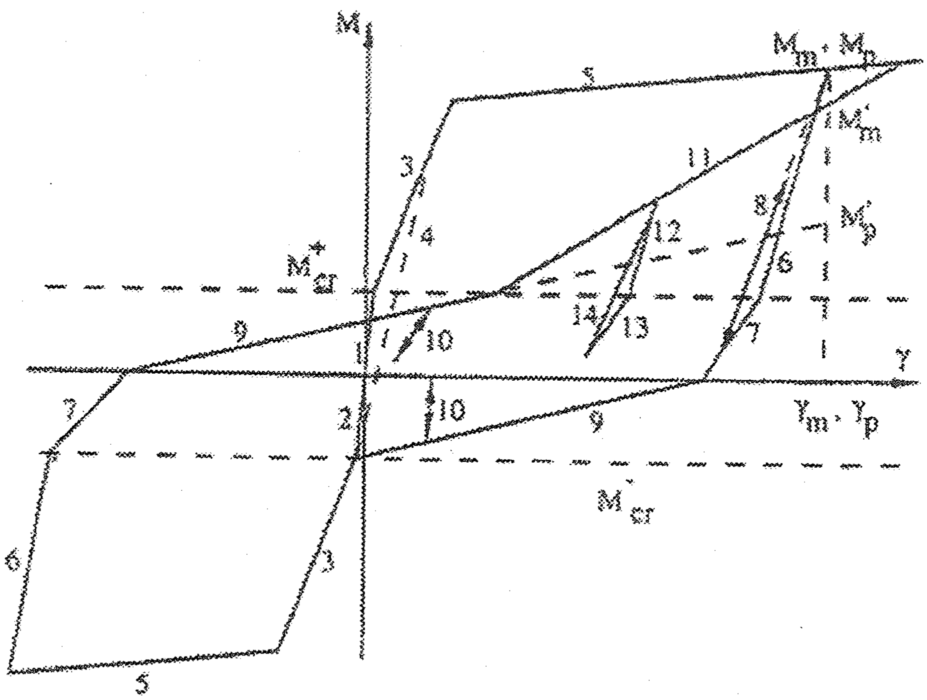

Fig. 2.6 Hysteretic Model for Shear (Ozcebe, Saatcioglu 1989)

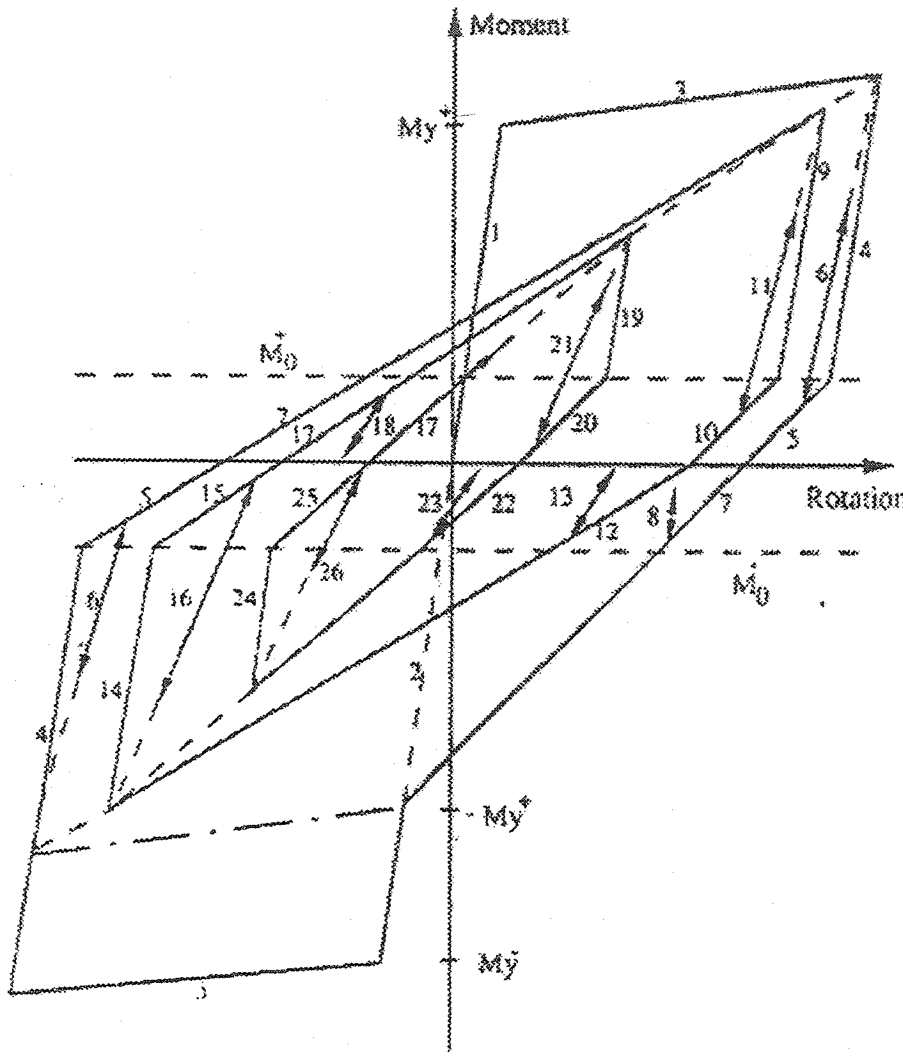

Fig. 2.7 Hysteretic Model for Anchorage Slip (Saatcioglu, Alsiwat, Ozcebe 1992)

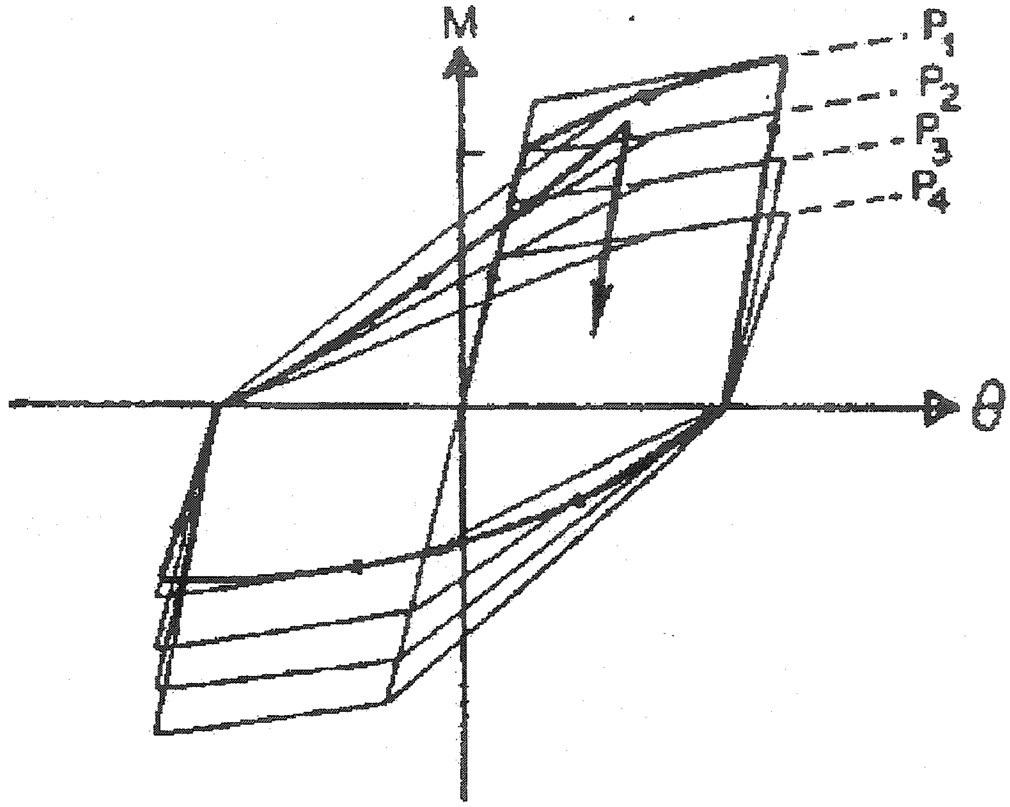

Fig. 2.8 Axial Force-Moment Interaction Model (Saatcioglu et al. 1983)

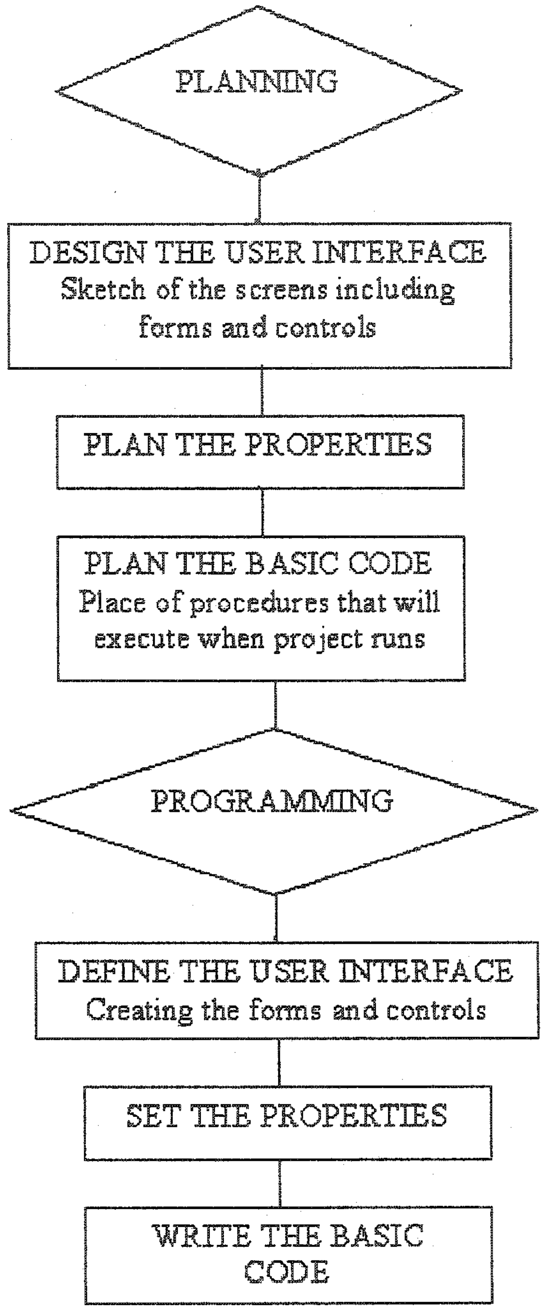

Fig. 2.9 The Flowchart of Preparing the Pre-processor

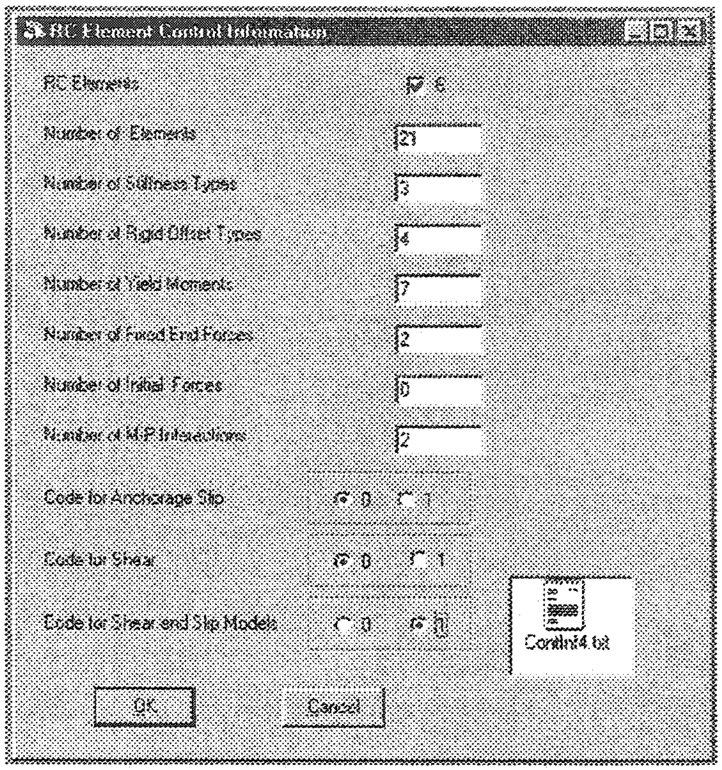

Fig. 2.10 The Form Containing Labels, Text Boxes, Check Boxes and Option Boxes

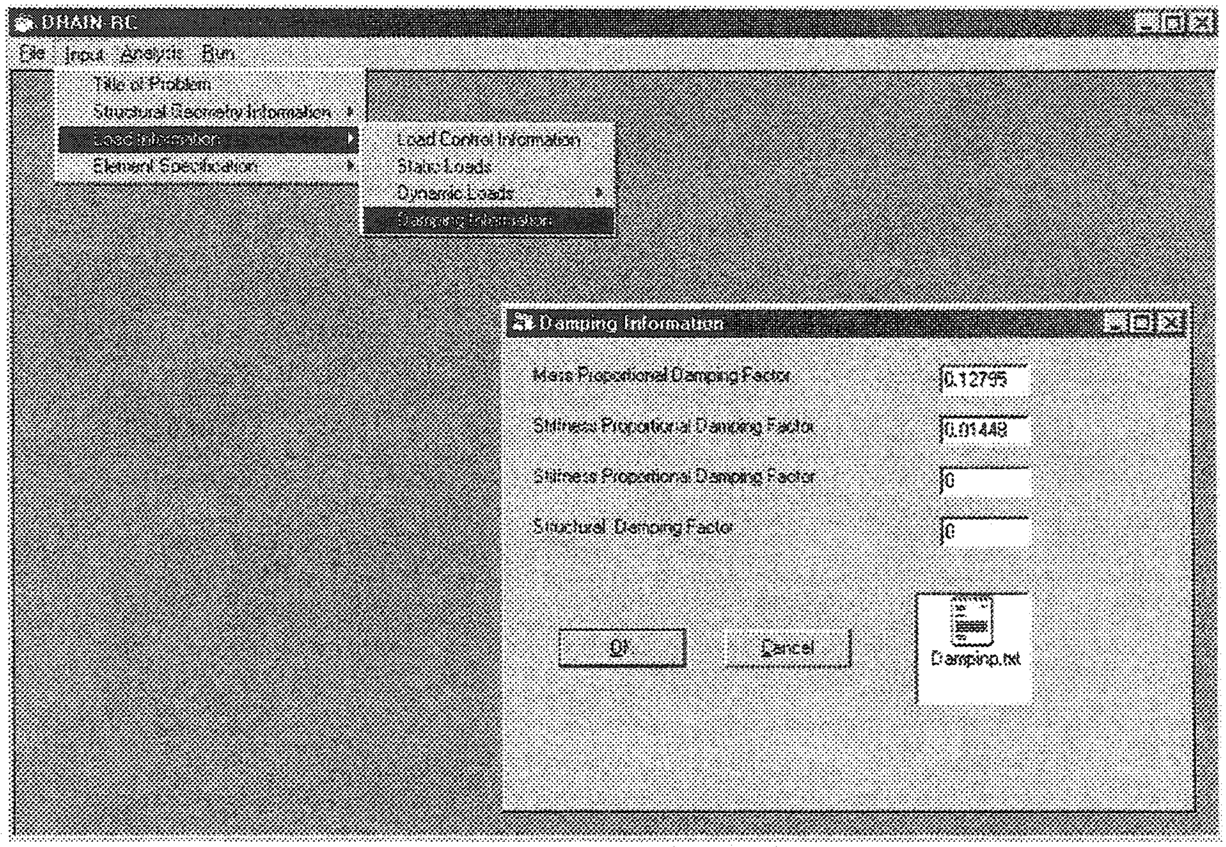

Fig. 2.11 The Window Containing Parent Form and One of The Child Forms

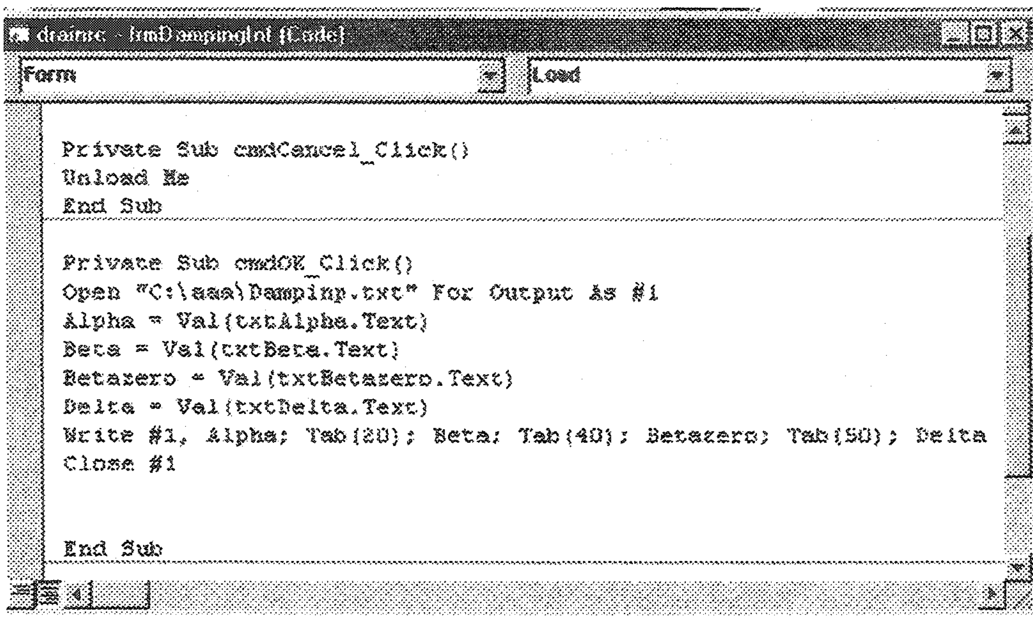

Fig. 2.12 Code for Save Command of the Damping Information Form

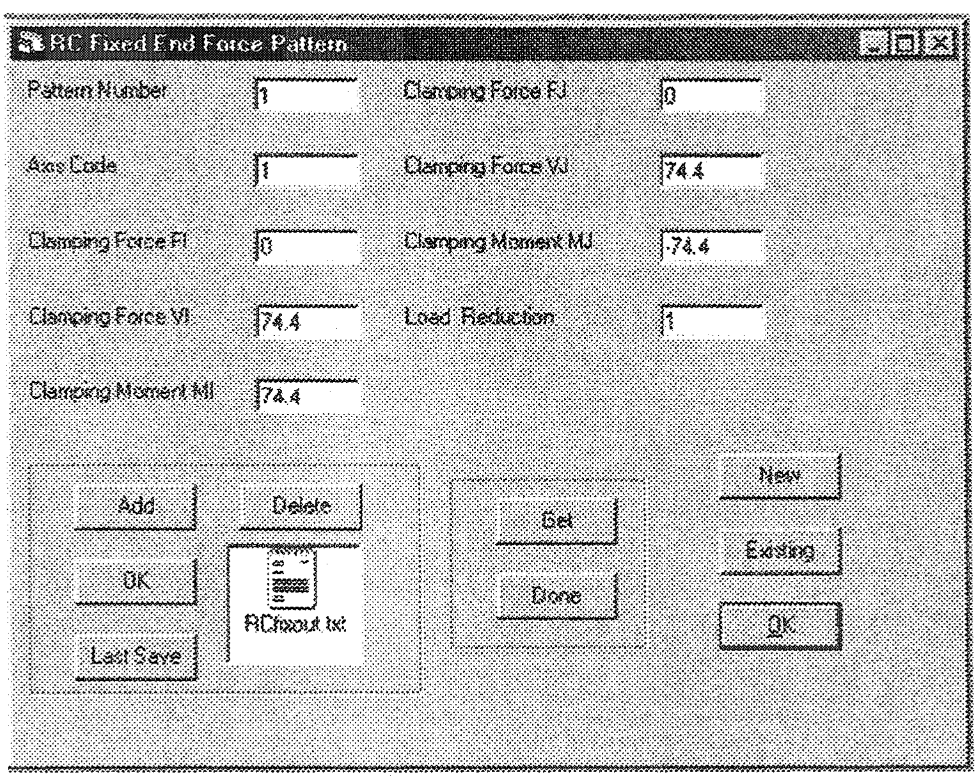

Fig. 2.13 One of the Forms that Data is Entered Subsequently

(General) cmdLastSave_Click

```
Private Sub cmdLastSave_Click()
 On Error Resume Next
 ' Open file for writing
 Open "C:\aaa\fixinp.txt" For Output Access Write As #2

 Seek #1, 1 ' reposition to start of file
 Get #1, , mFixedEnd ' read first record

 While Not EOF(1)
 If mFixedEnd.Pattern <> 0 Then
 Write #2, mFixedEnd.Pattern;
 Write #2, Tab(10); mFixedEnd.Axis;
 Write #2, Tab(20); mFixedEnd.ClamFI;
 Write #2, Tab(30); mFixedEnd.ClamVI;
 Write #2, Tab(40); mFixedEnd.ClamFJ;
 Write #2, Tab(50); mFixedEnd.ClamVJ
 End If

 Get #1, , mFixedEnd 'read next record
 Wend

 Close #2
 End Sub
```

Fig. 2.14 Code for Save Command of the Fixed End Force Pattern Form

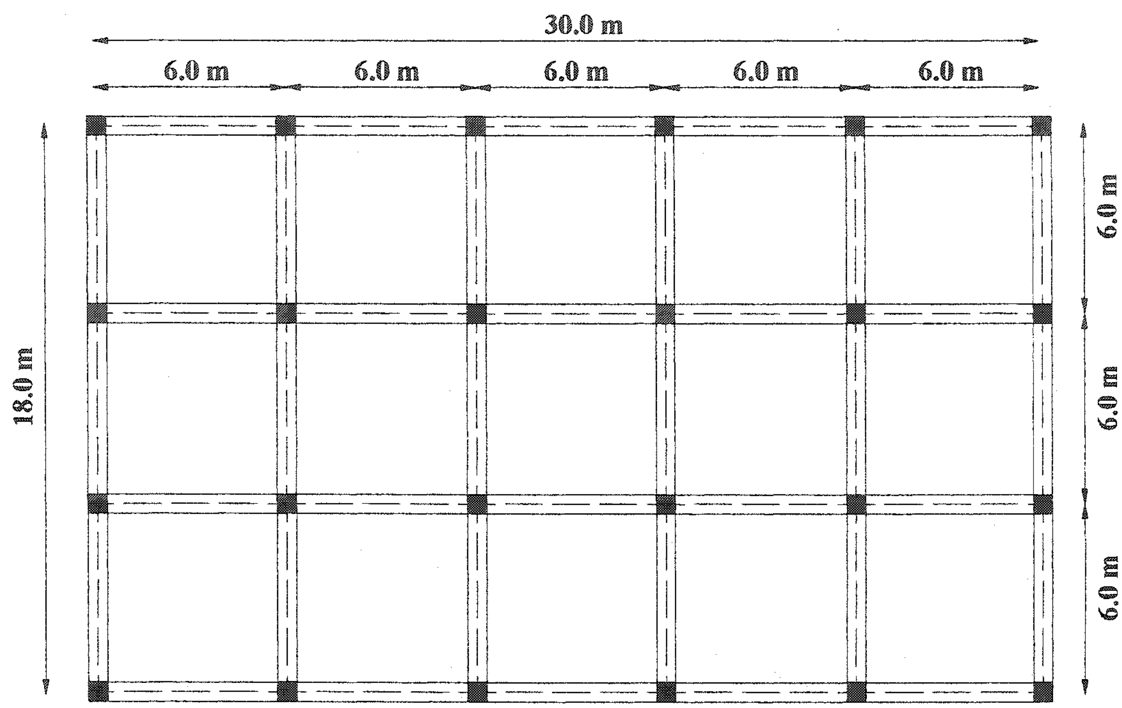

Fig.3.1 Plan of Moment Resisting Frame Building

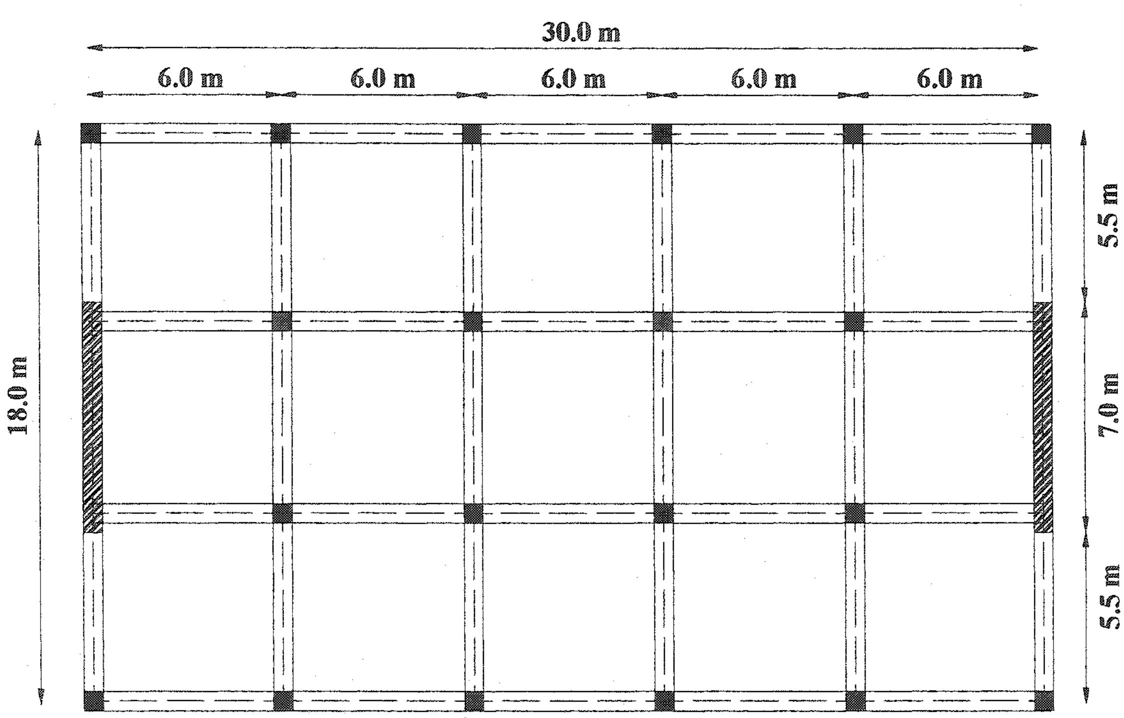

Fig.3.2 Plan of Frame-Shear Wall Building

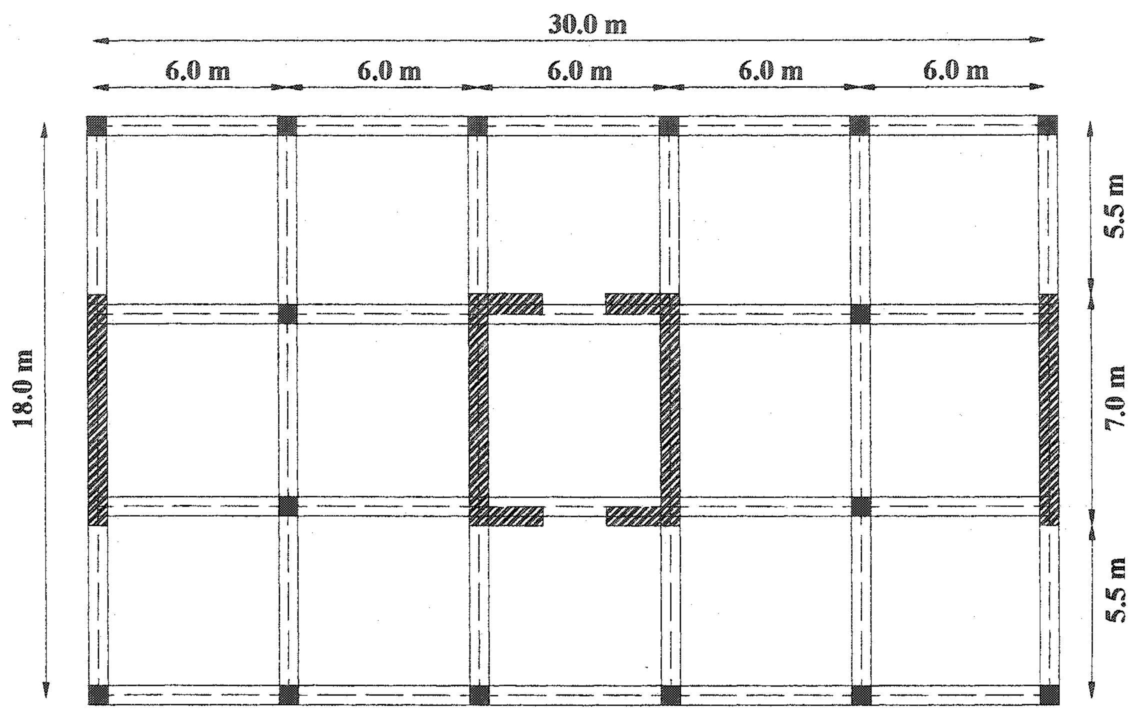

Fig. 3.3 Plan of Core Wall Building

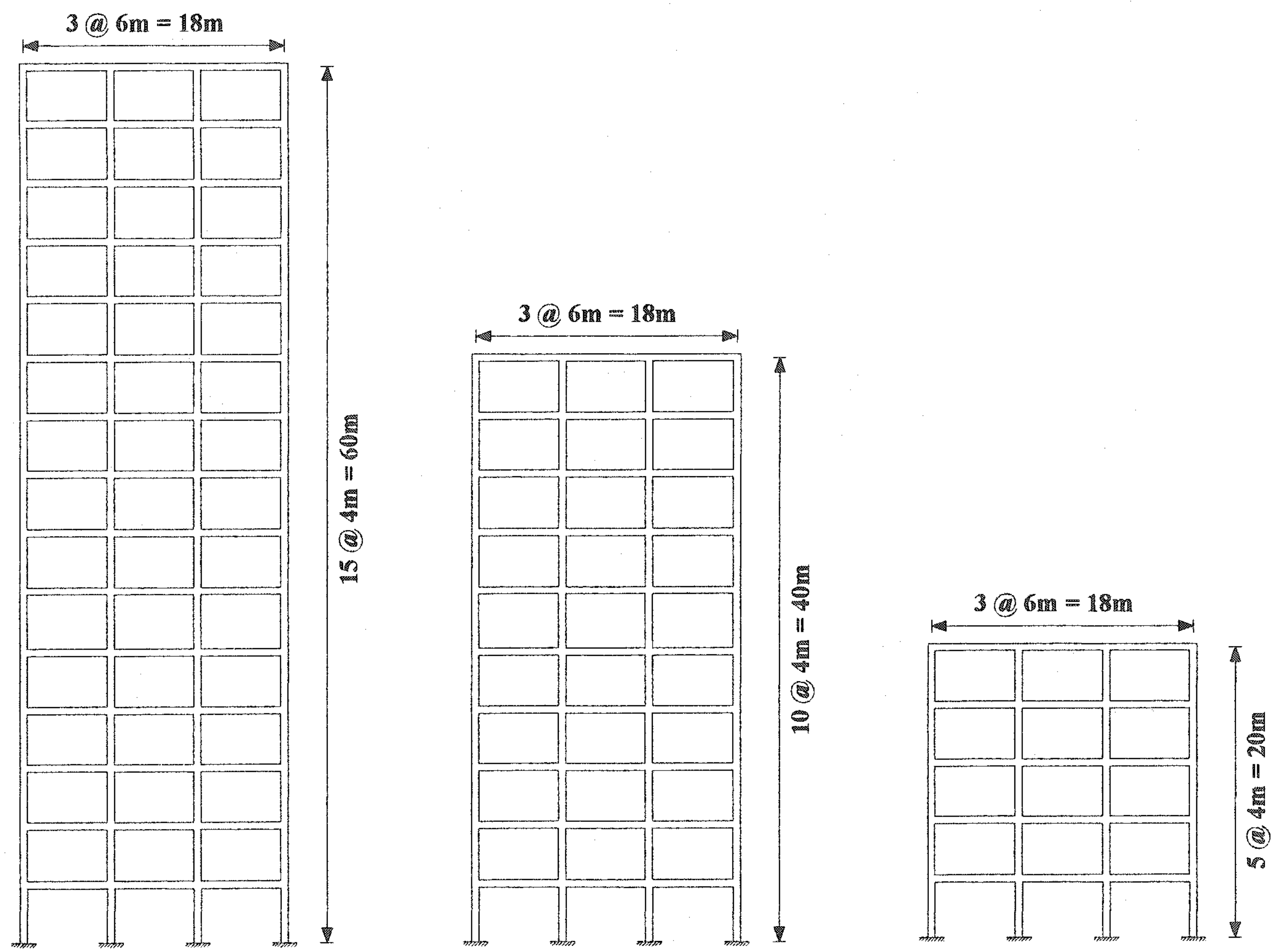

Fig. 3.4 Elevation View of 15, 10 and 5-Storey Frame Buildings

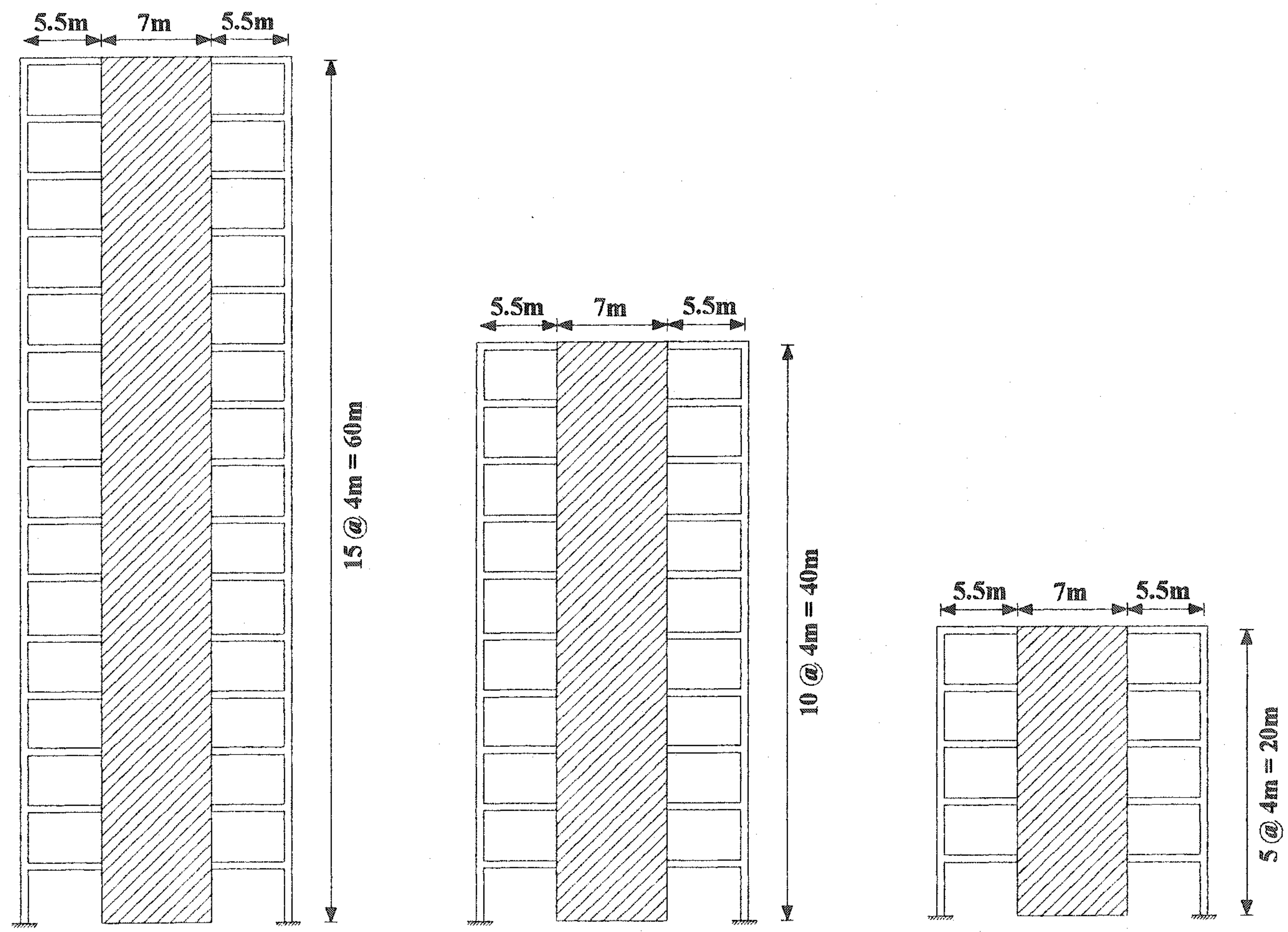

Fig. 3.5 Elevation View of 15, 10 and 5-Storey Frame-Shear Wall and Core Wall Buildings

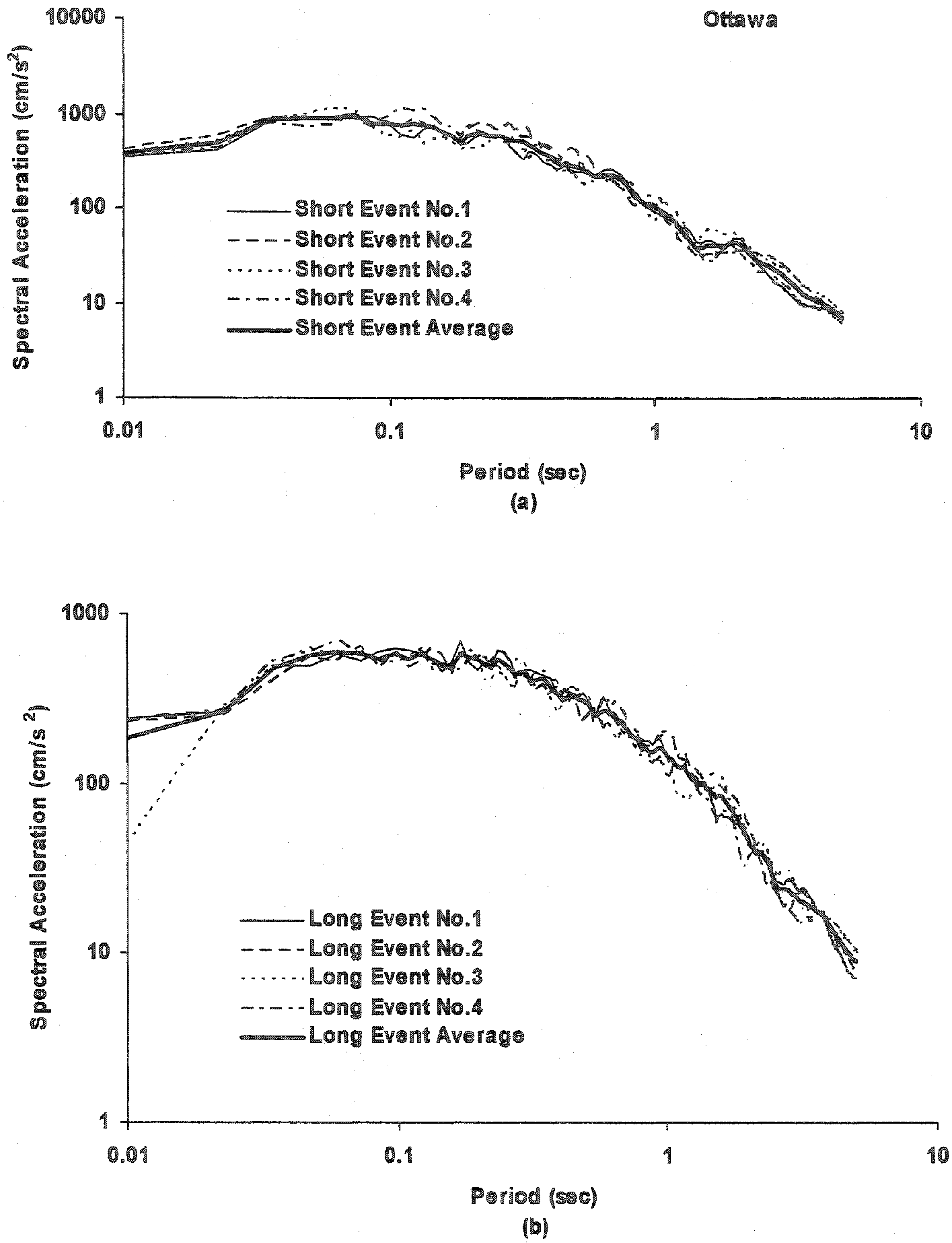

Fig. 3.6 Response Spectra of A-B Artificial Records for Ottawa

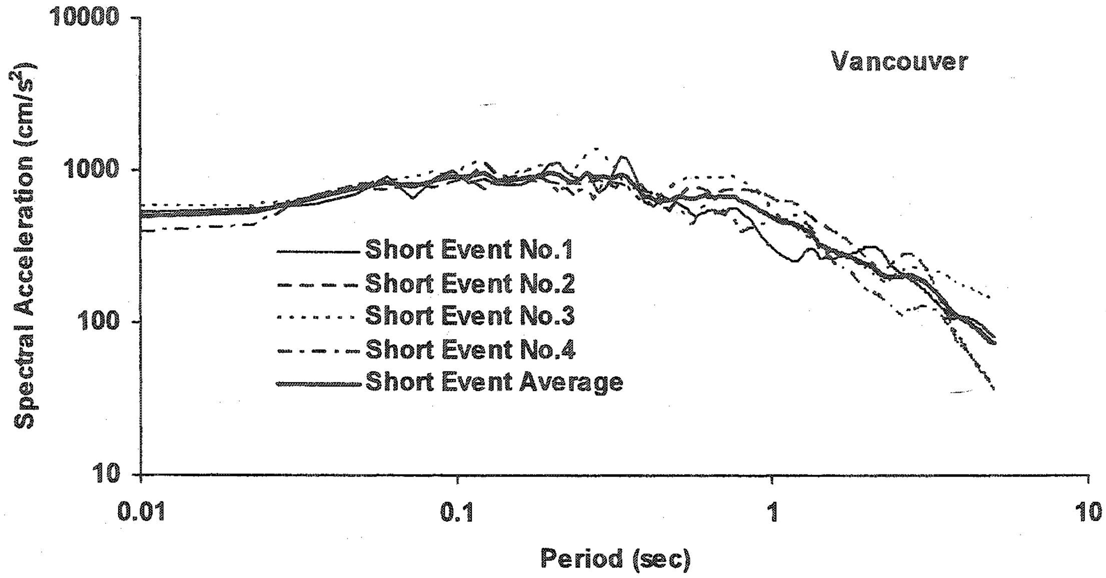
Vancouver
Short Event No.1
Short Event No.2
Short Event No.3
Short Event No.4
Short Event Average
Spectral Acceleration (cm/s²)
10000
1000
100
10
0.01
0.1
1
10
Period (sec)

(a)

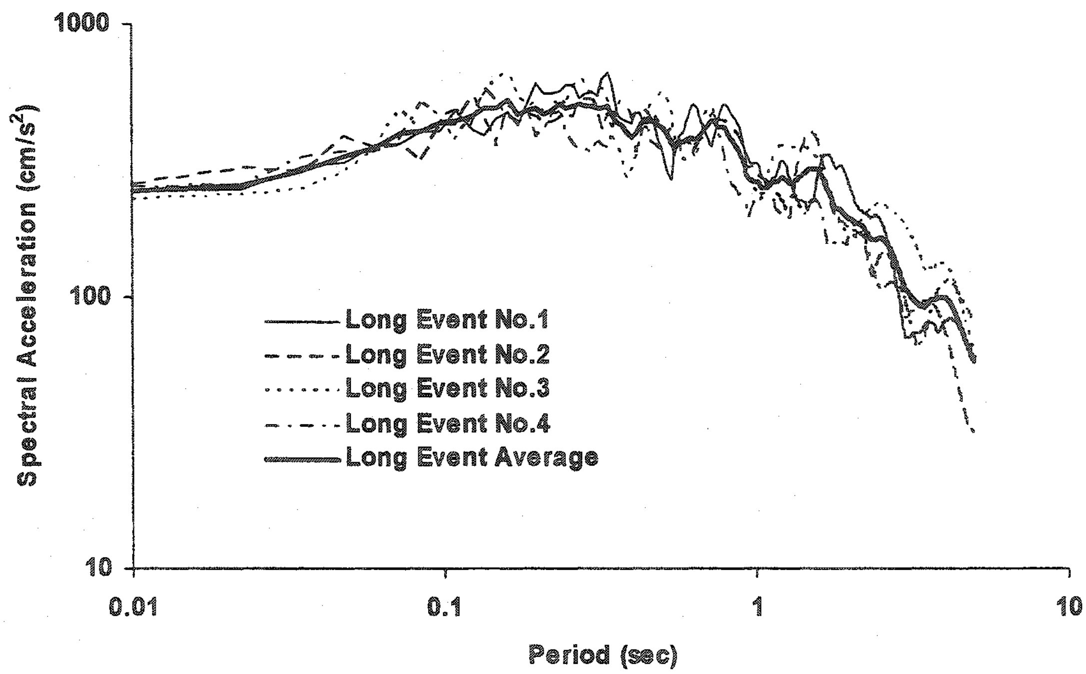
Long Event No.1
Long Event No.2
Long Event No.3
Long Event No.4
Long Event Average
Spectral Acceleration (cm/s²)
1000
100
10
0.01
0.1
1
10
Period (sec)

(b)

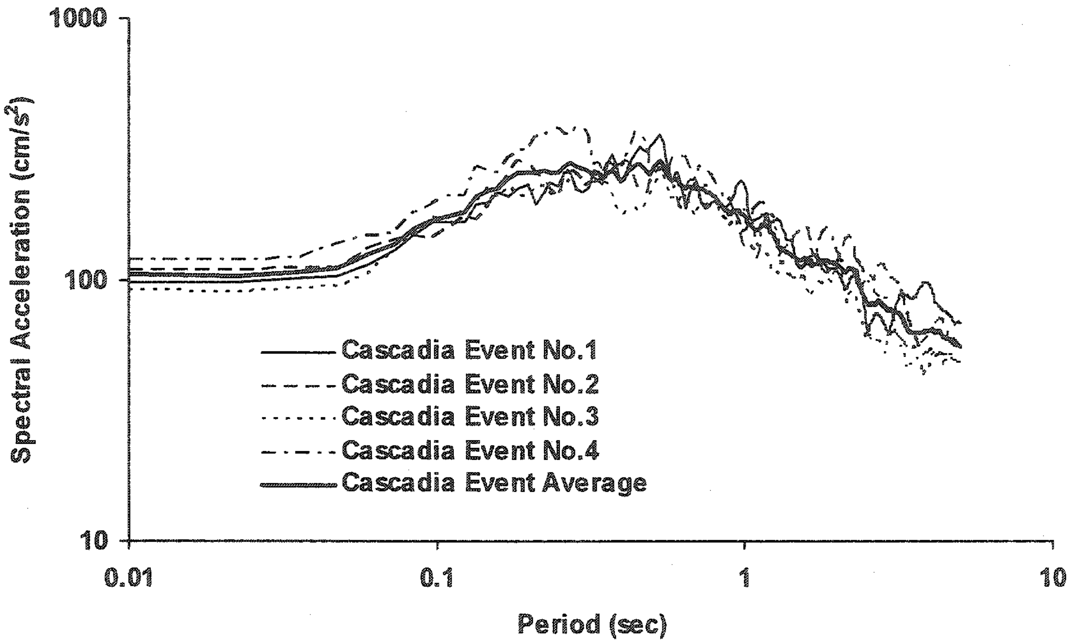

(c)

Fig. 3.7 Response Spectra of A-B Artificial Records for Vancouver

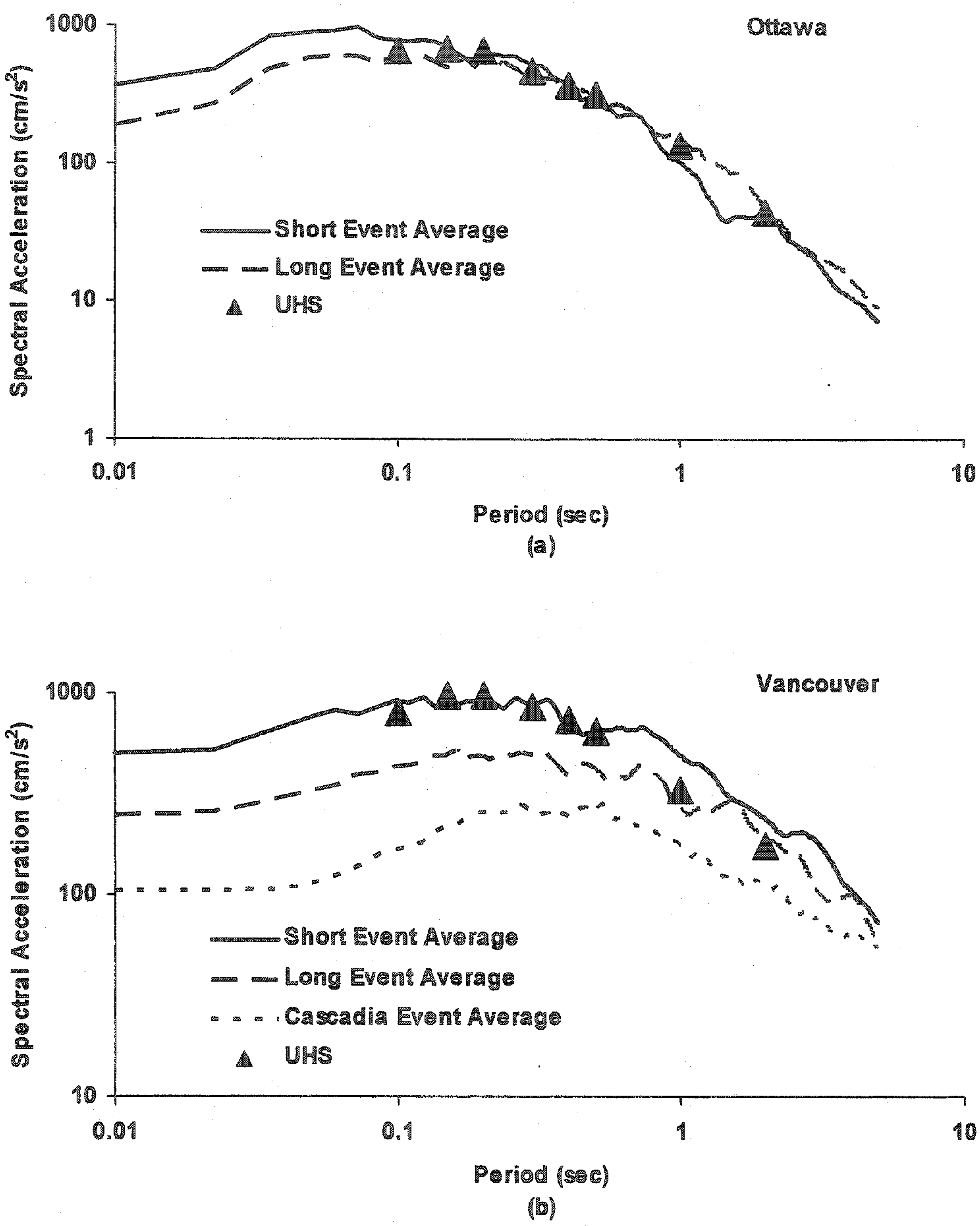

Fig. 3.8 Comparison of Response Spectra of A-B Artificial Records and UHS for Ottawa and Vancouver

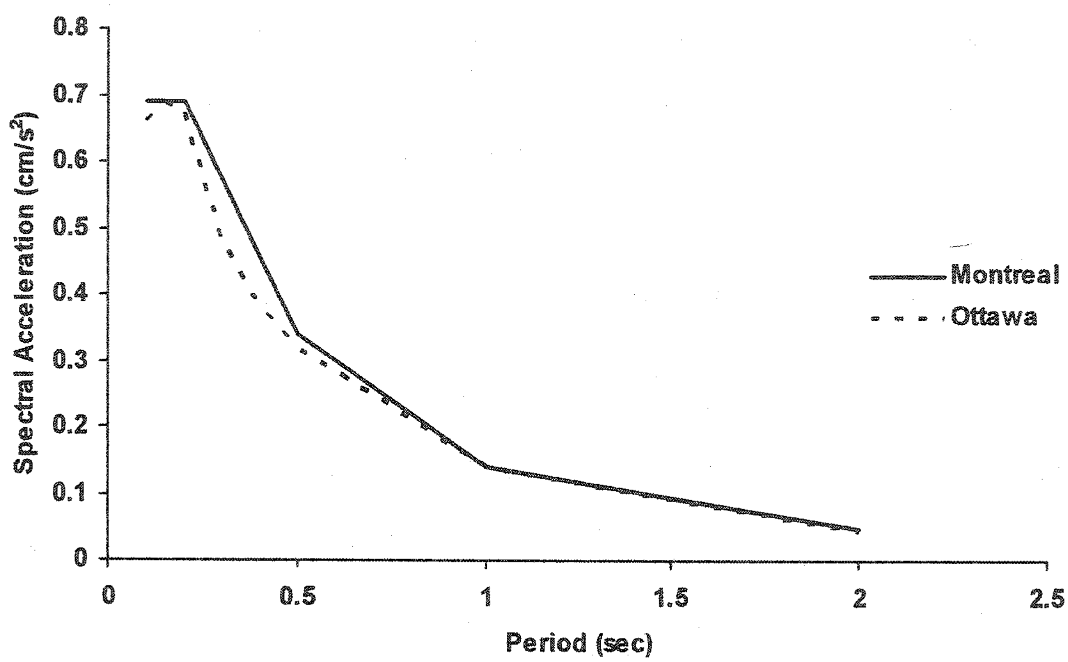

Fig. 3.9 Response Spectra for Ottawa and Montreal

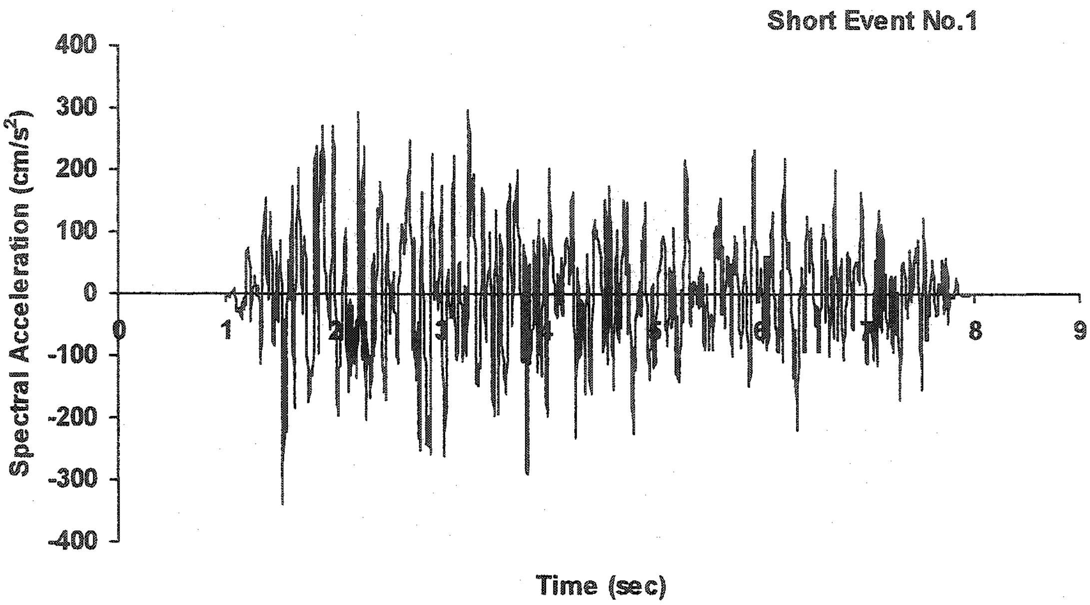

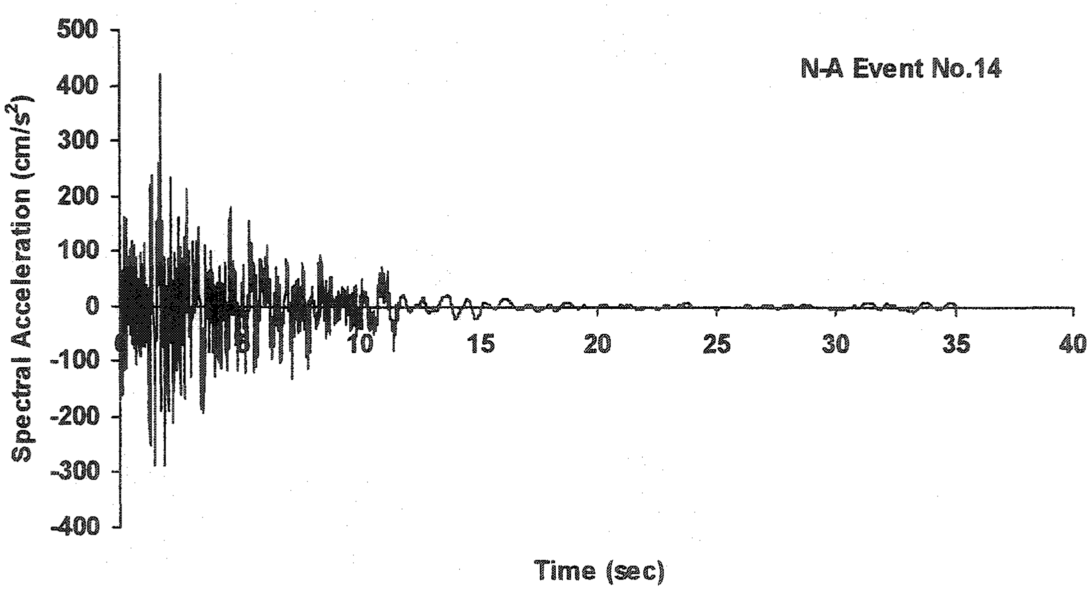

(b)

Fig. 3.10 The Comparison of Acceleration Time Histories of A-B and N-A Artificial Records used for Ottawa

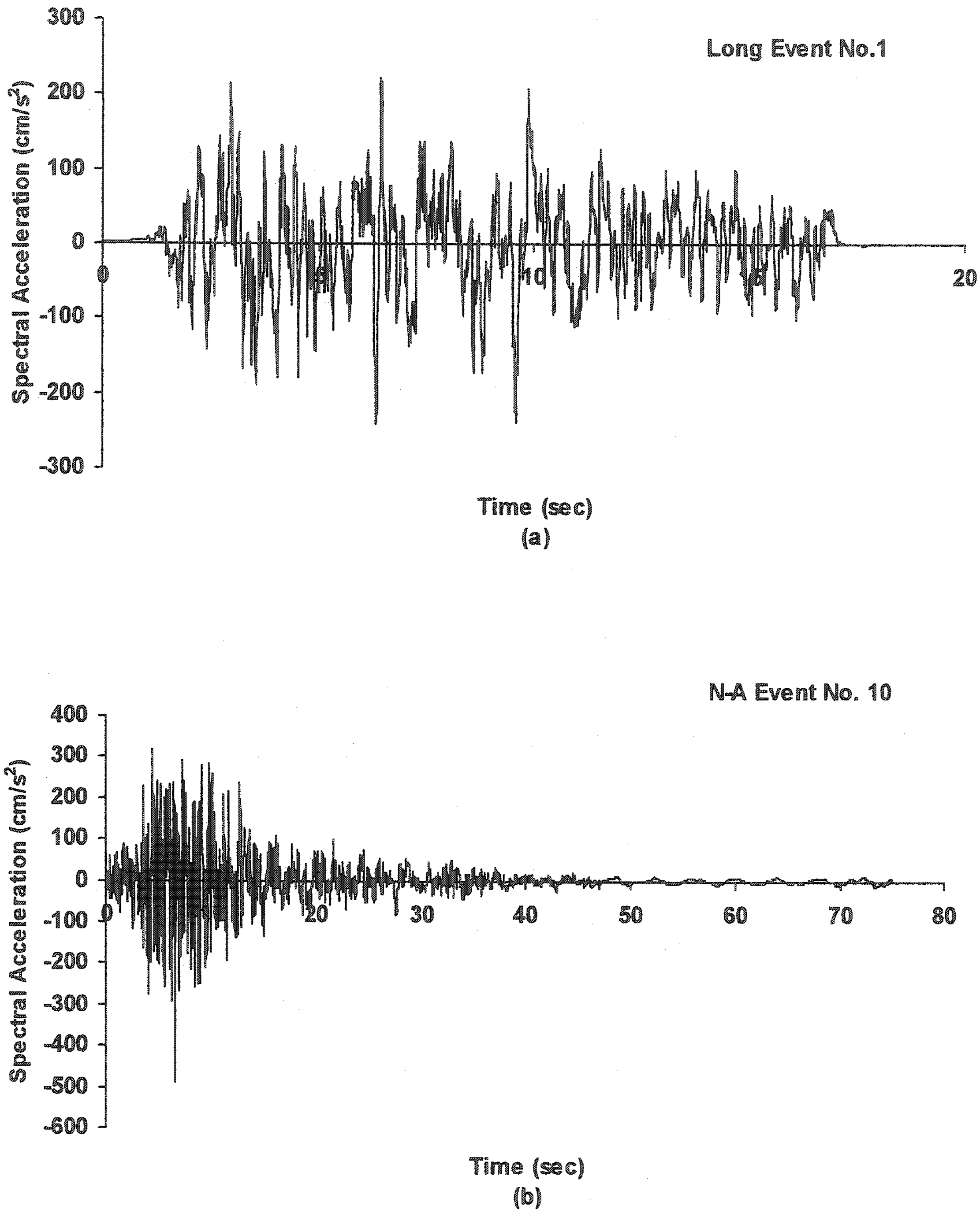

Fig. 3.11 The Comparison of Acceleration Time Histories of A-B and N-A Artificial Records used for Vancouver

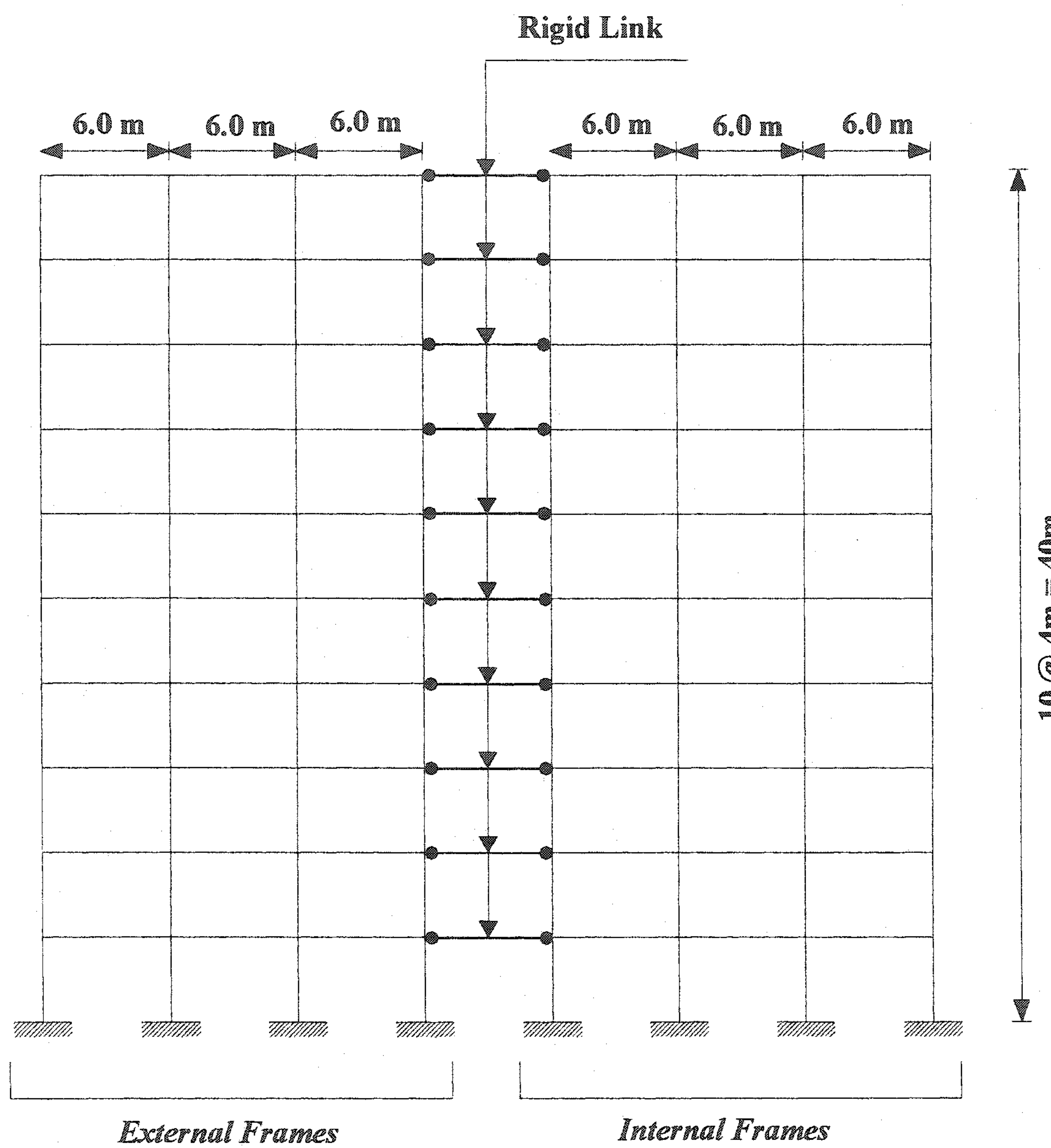

Fig. 4.1 Two Dimensional Lumped Frame Used in Analysis

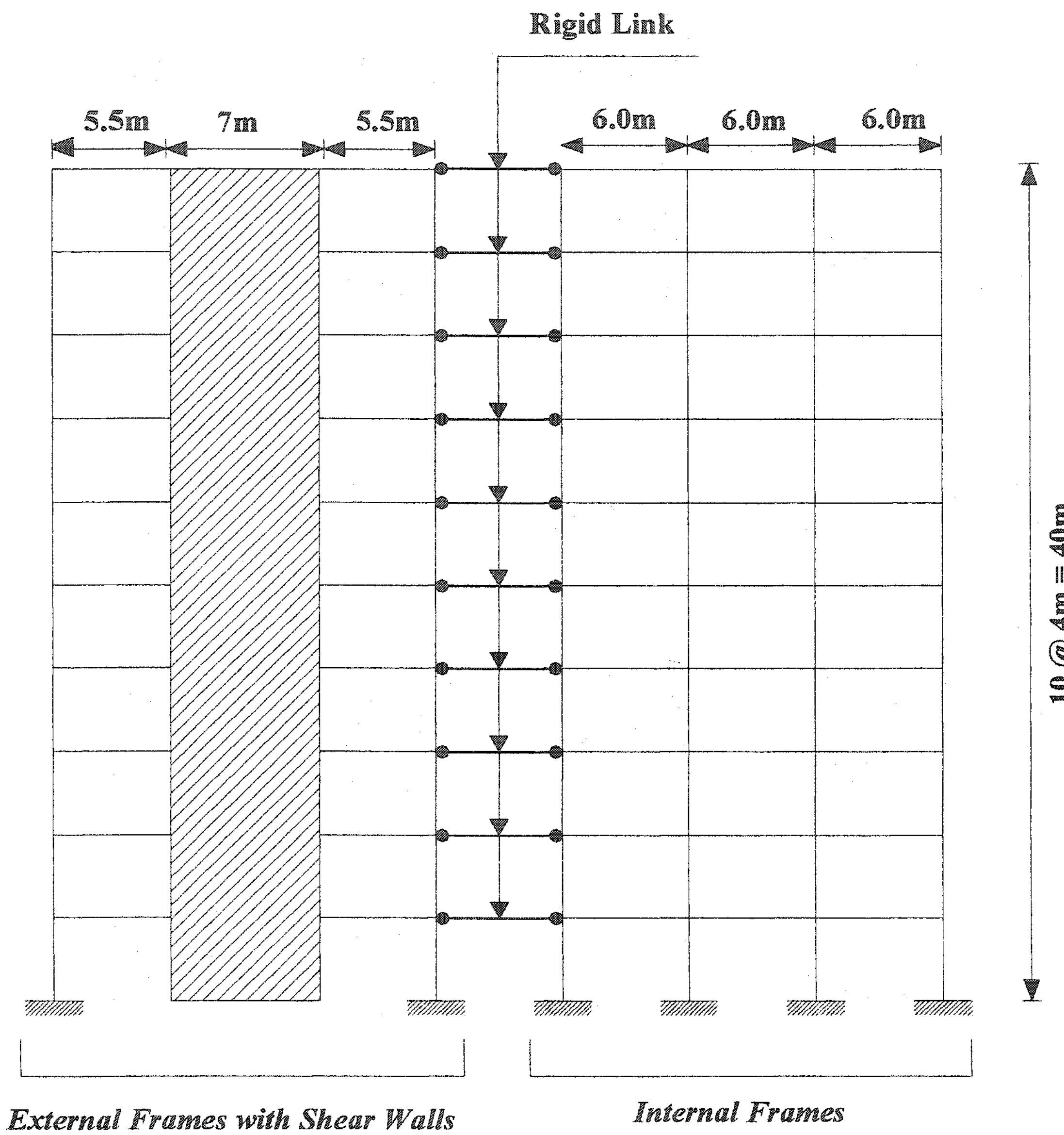

Fig. 4.2 Two Dimensional Lumped Frame-Shear Wall Used in Analysis

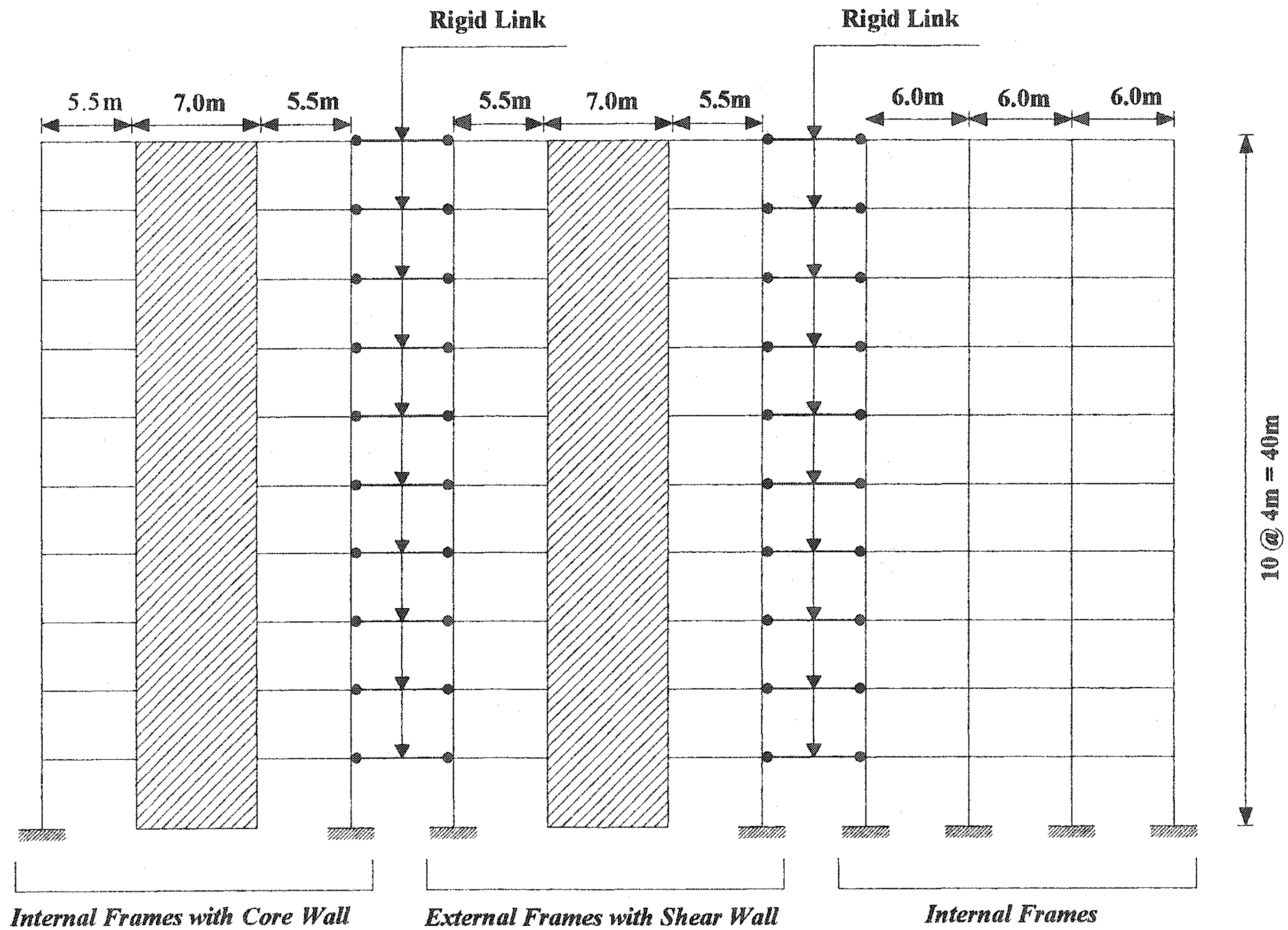

Fig. 4.3 Two Dimensional Lumped Core Wall Used in Analysis

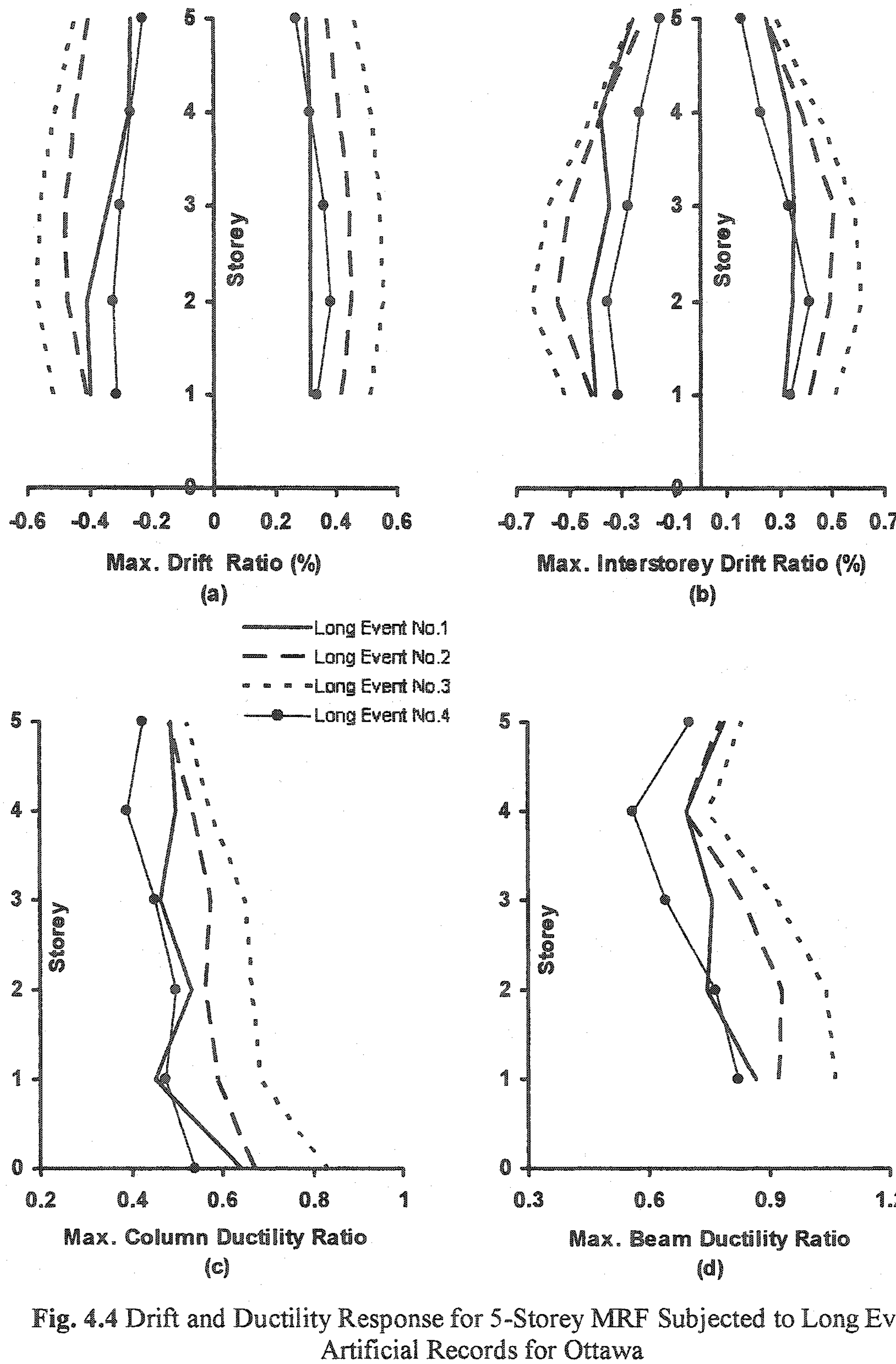

Fig. 4.4 Drift and Ductility Response for 5-Storey MRF Subjected to Long Event Artificial Records for Ottawa

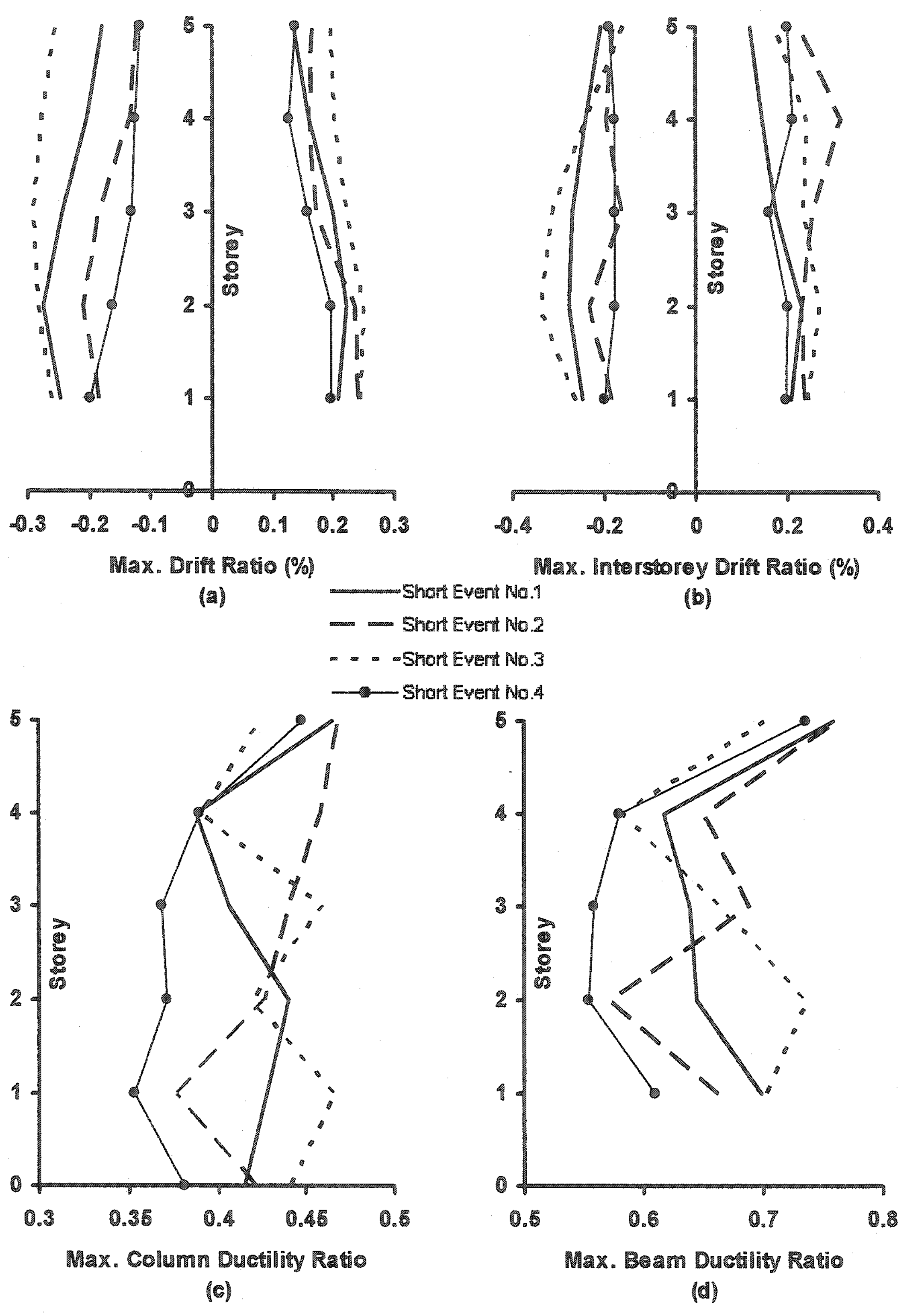

Fig. 4.5 Drift and Ductility Response for 5-Storey MRF Subjected to Short Event Artificial Records for Ottawa

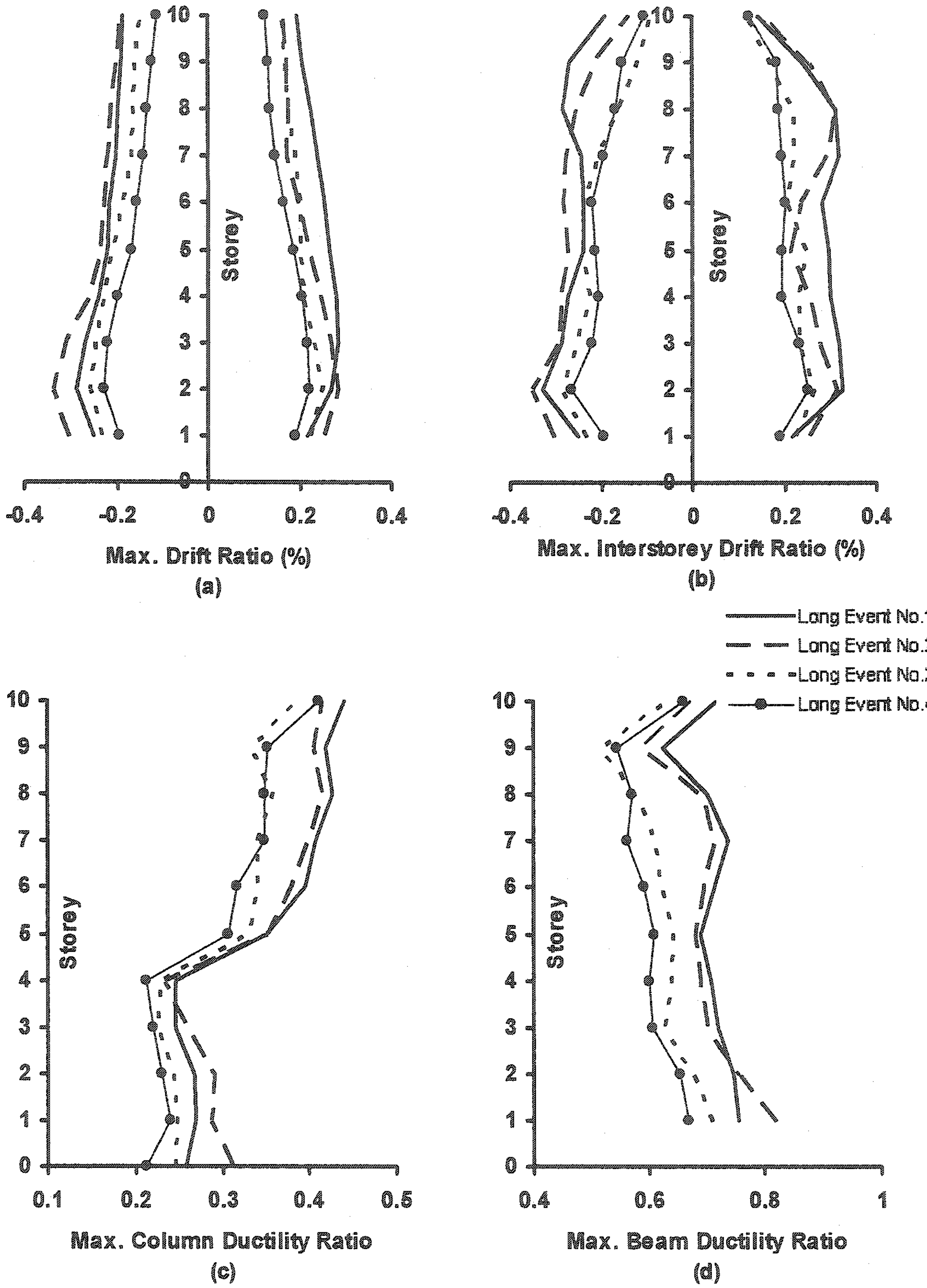

Fig. 4.6 Drift and Ductility Response for 10-Storey MRF Subjected to Long Event Artificial Records for Ottawa

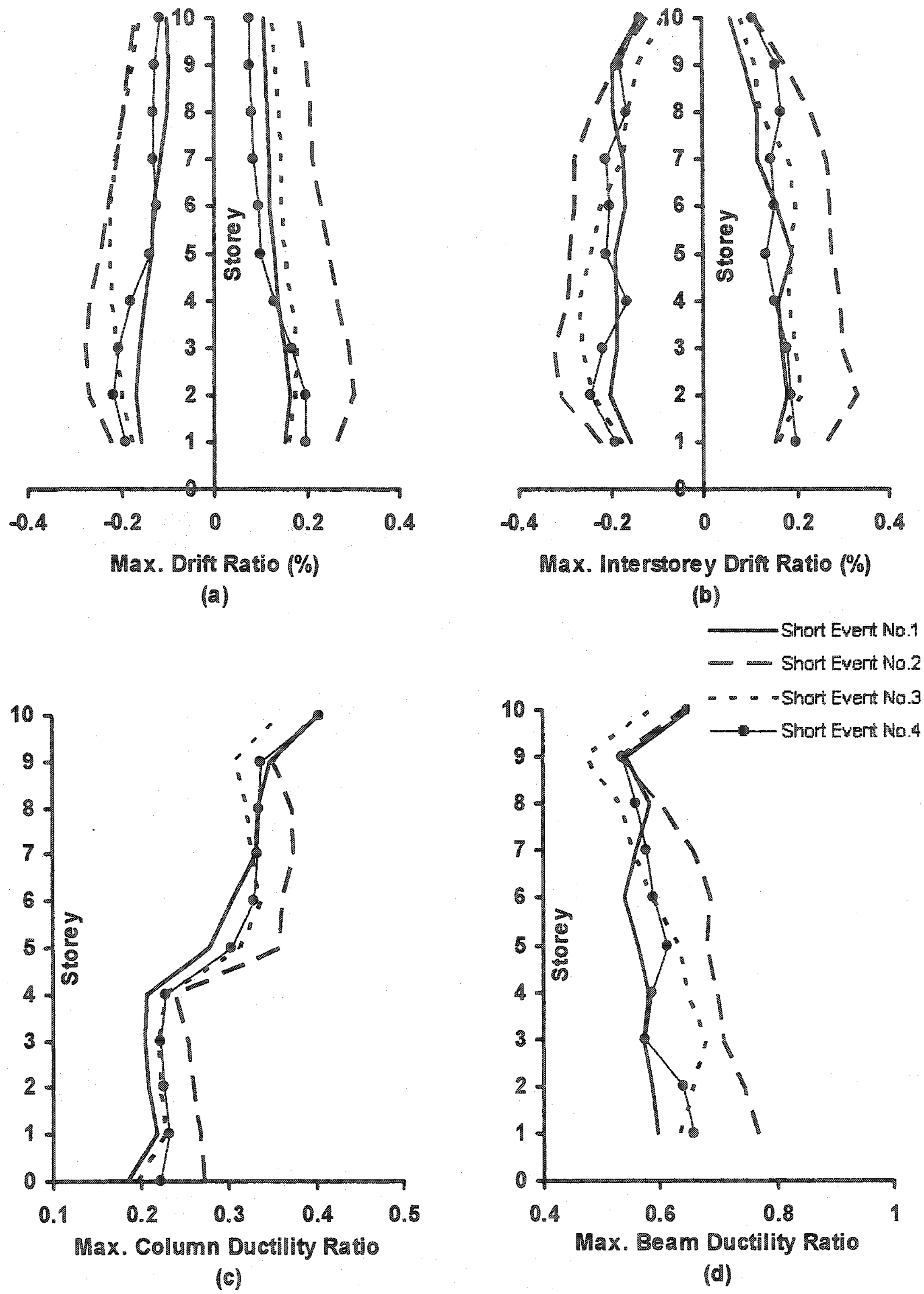

Fig. 4.7 Drift and Ductility Response for 10-Storey MRF Subjected to Short Event Artificial Records for Ottawa

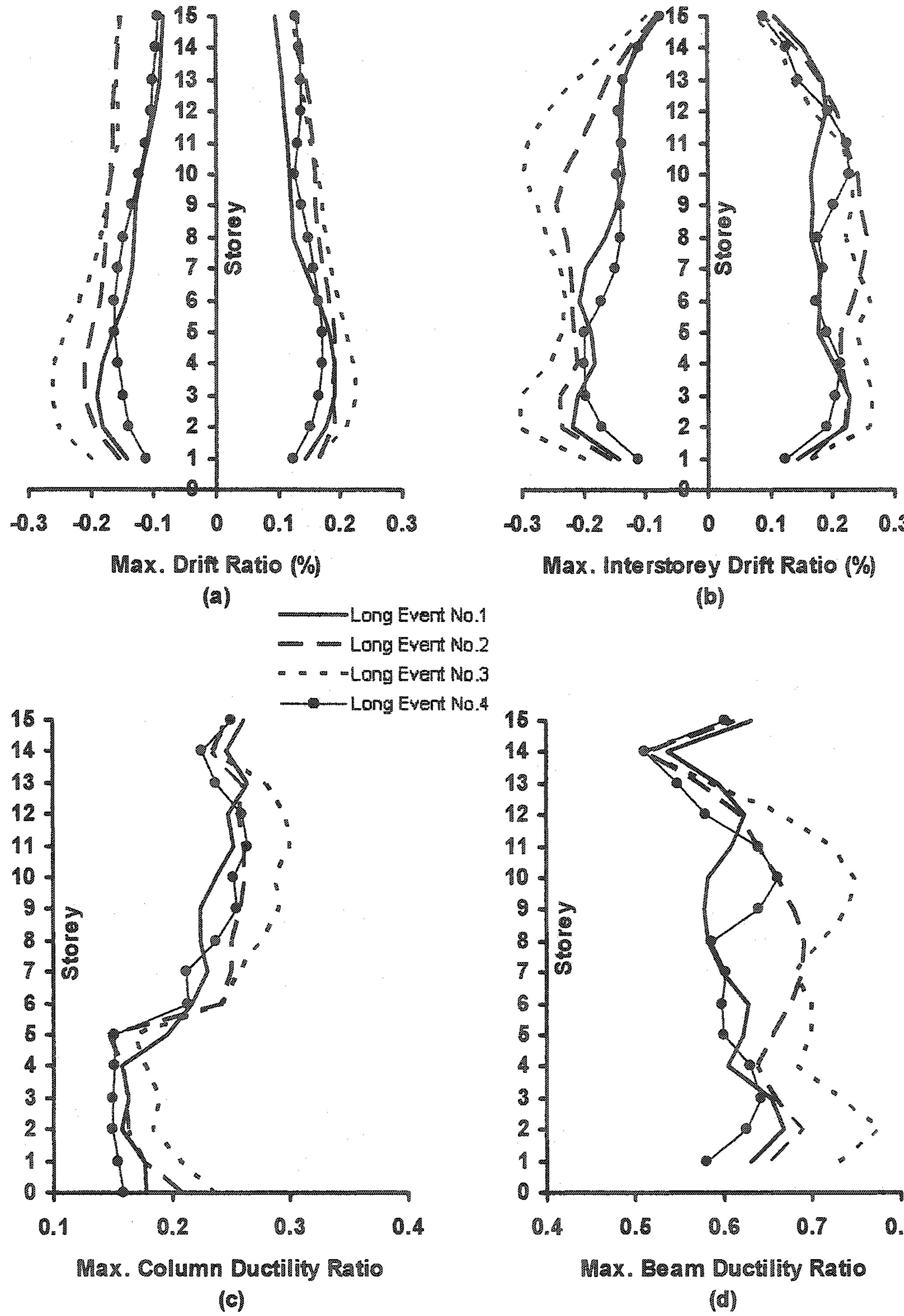

Fig. 4.8 Drift and Ductility Response for 15-Storey MRF Subjected to Long Event Artificial Records for Ottawa

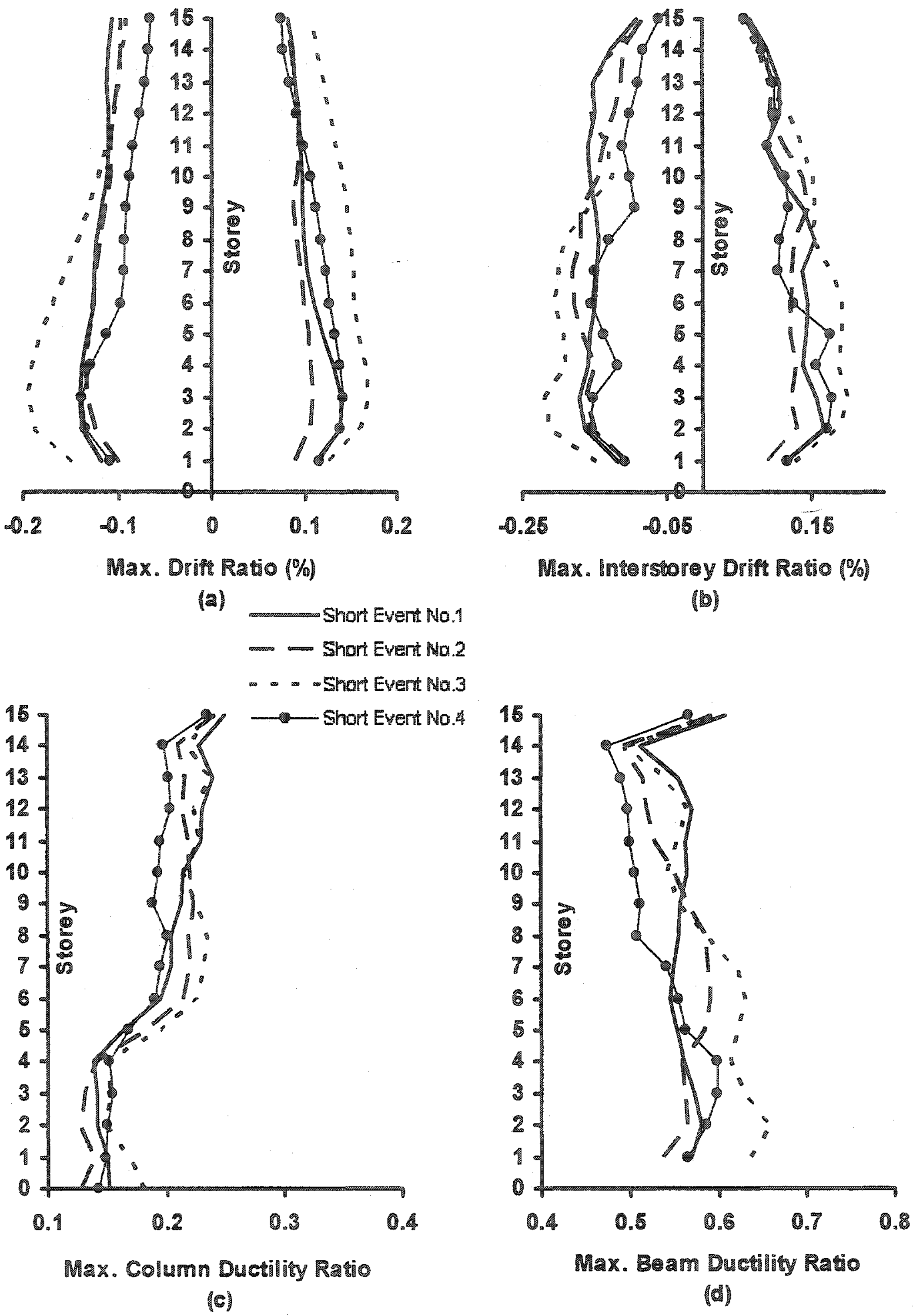

Fig. 4.9 Drift and Ductility Response for 15-Storey MRF Subjected to Short Event Artificial Records for Ottawa

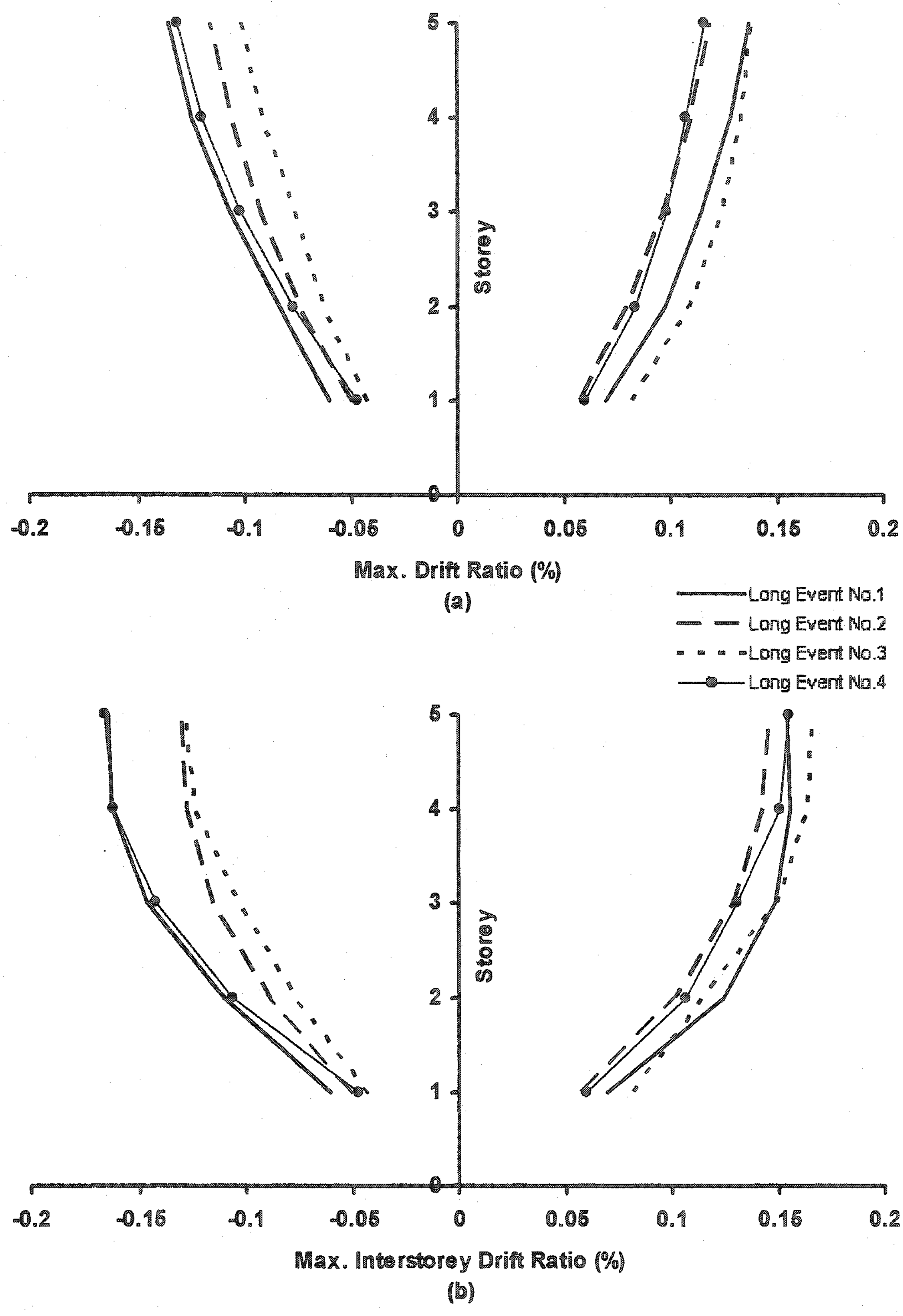

Fig. 4.10 Drift Response for 5-Storey SHW Subjected to Long Event Artificial Records for Ottawa

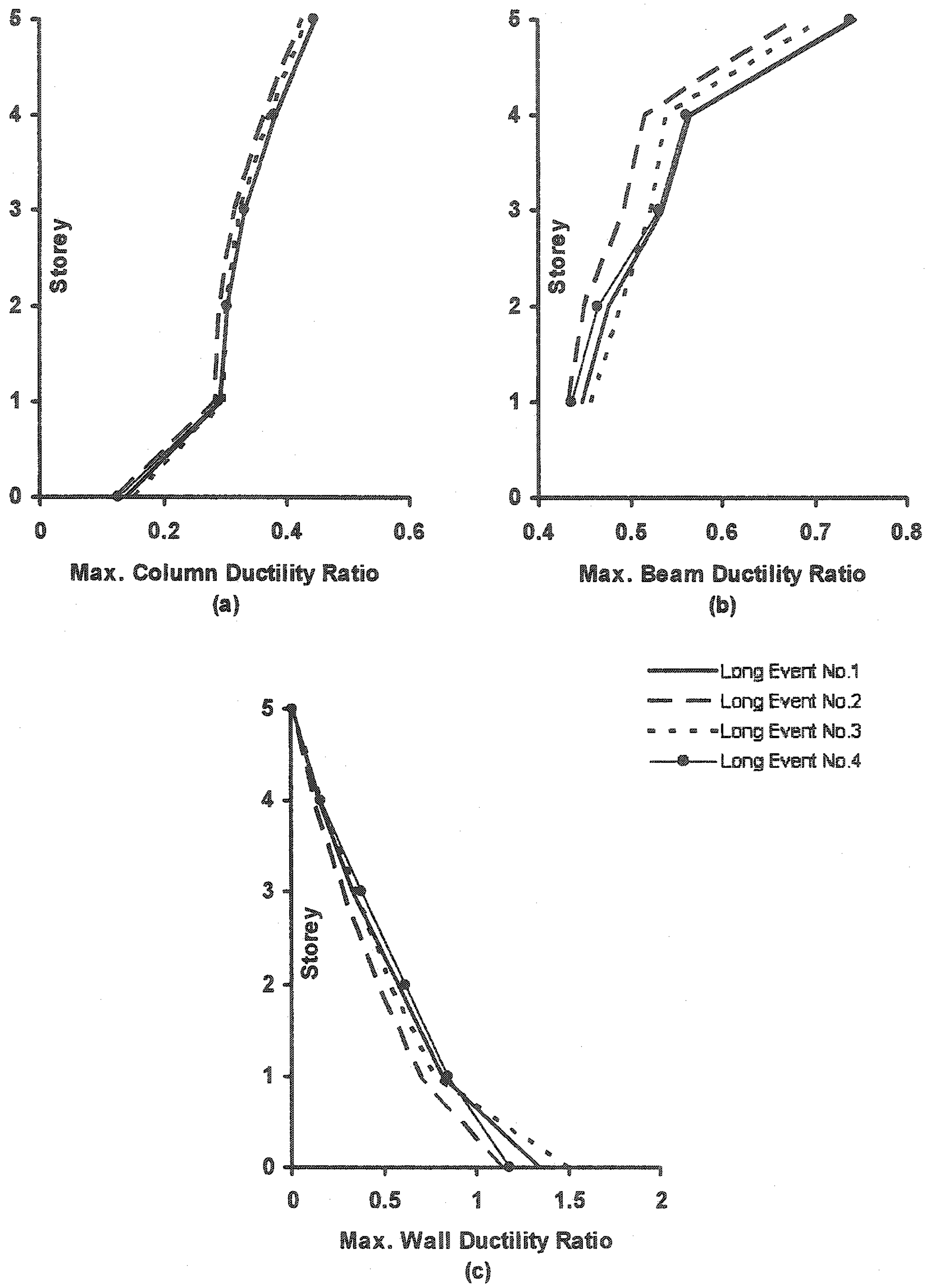

Fig. 4.11 Ductility Response for 5-Storey SHW Subjected to Long Event Artificial Records for Ottawa

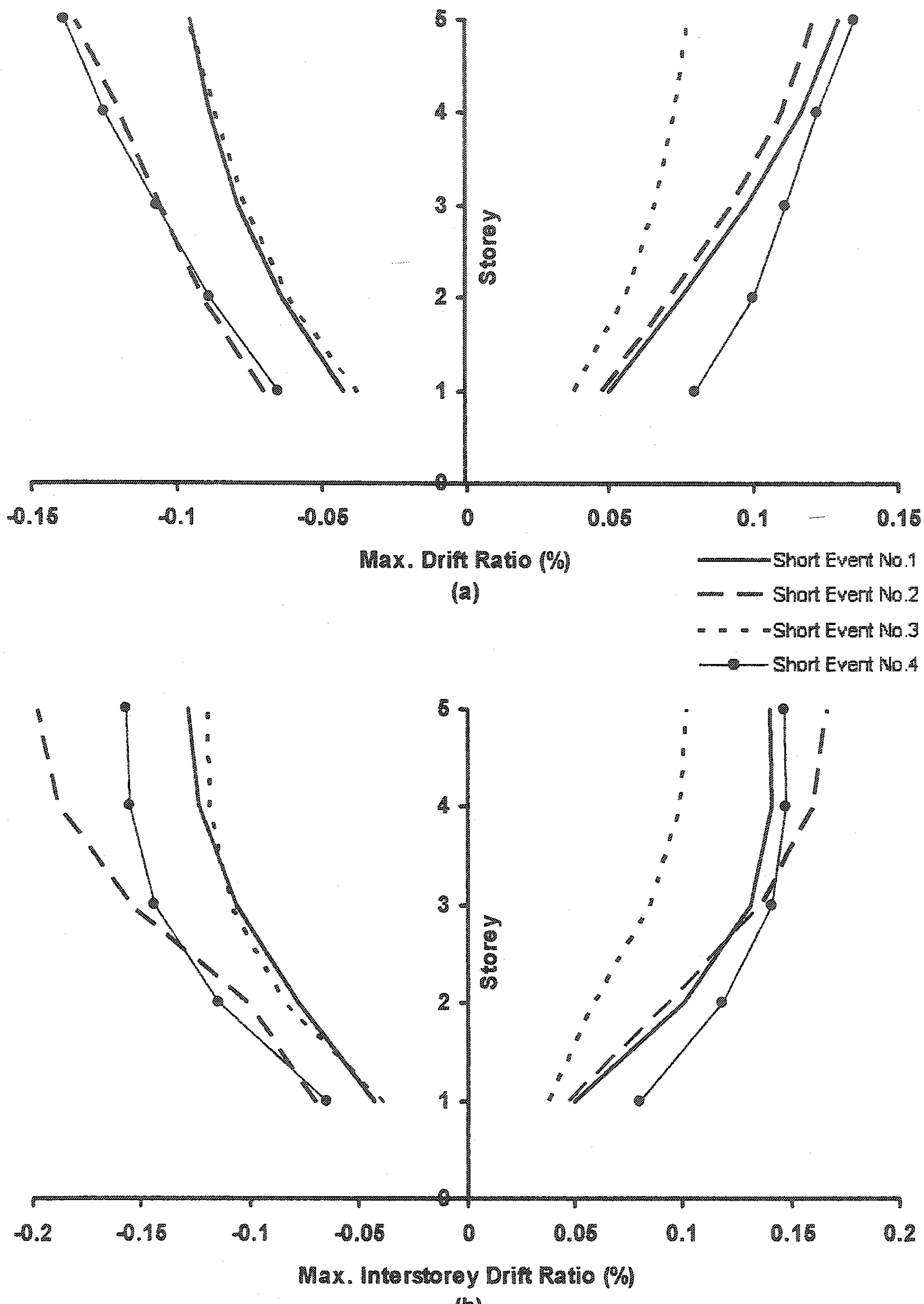

Fig. 4.12 Drift Response for 5-Storey SHW Subjected to Short Event Artificial Records for Ottawa

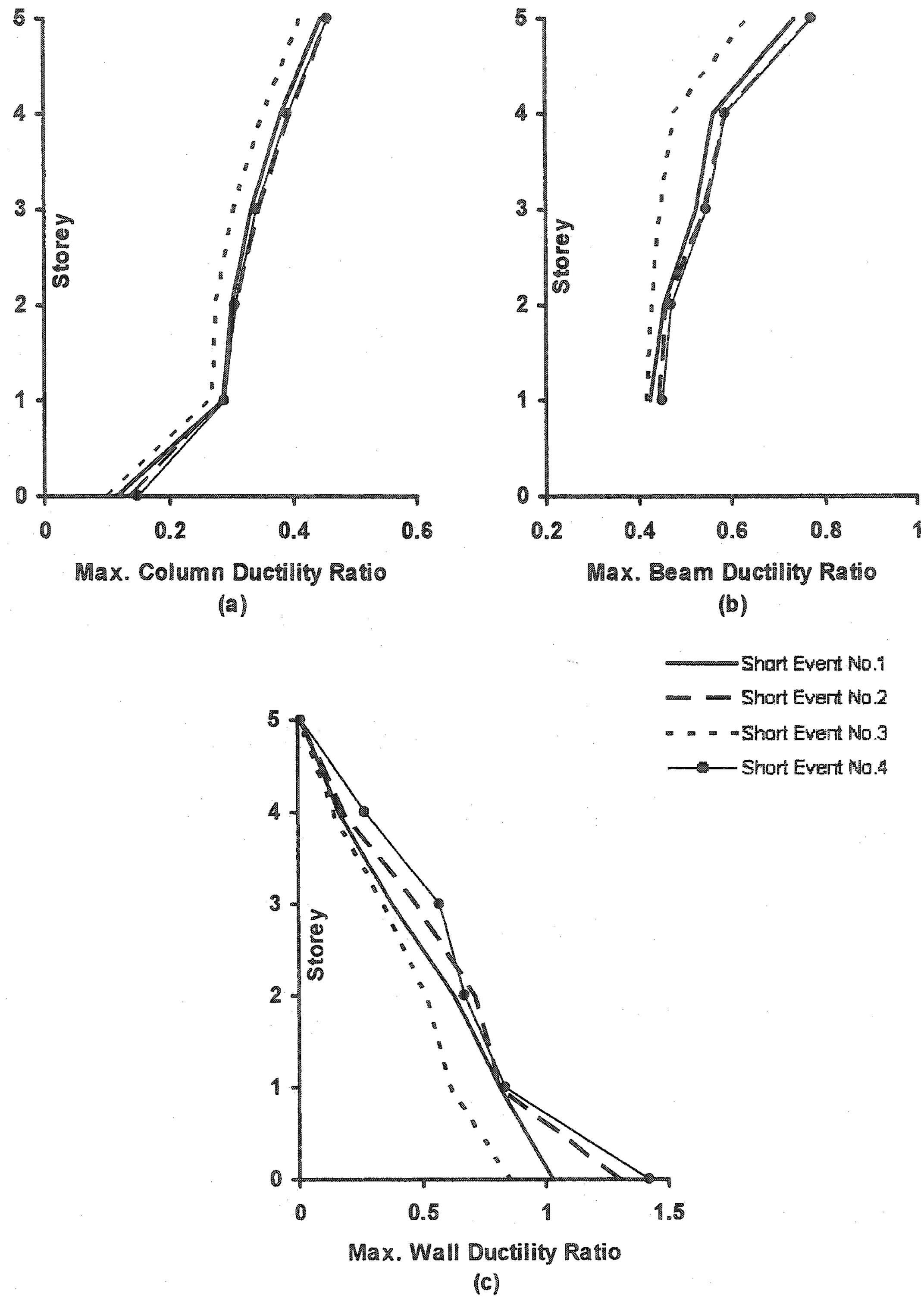

Fig. 4.13 Ductility Response for 5-Storey SHW Subjected to Short Event Artificial Records for Ottawa

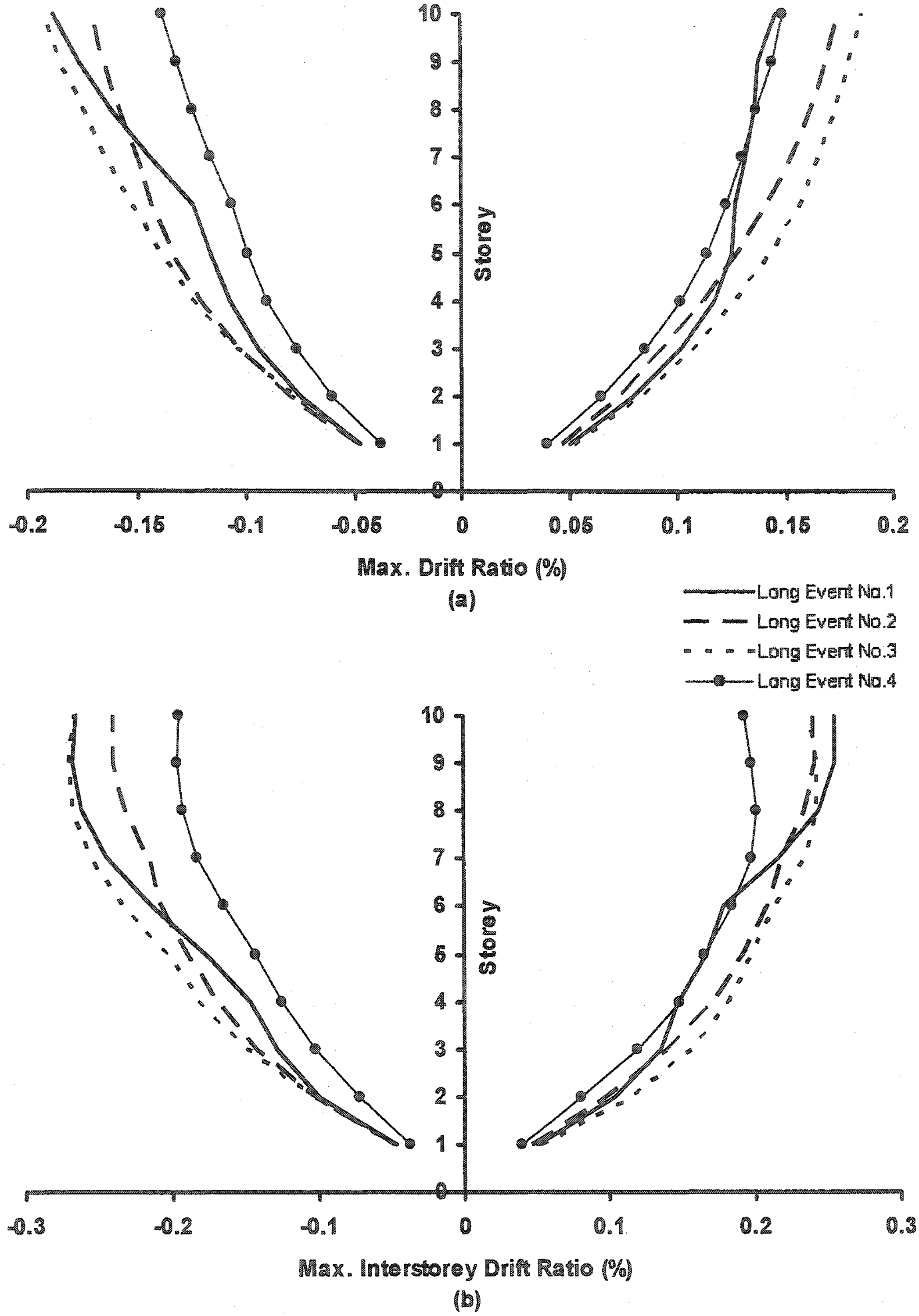

Fig. 4.14 Drift Response for 10-Storey SHW Subjected to Long Event Artificial Records for Ottawa

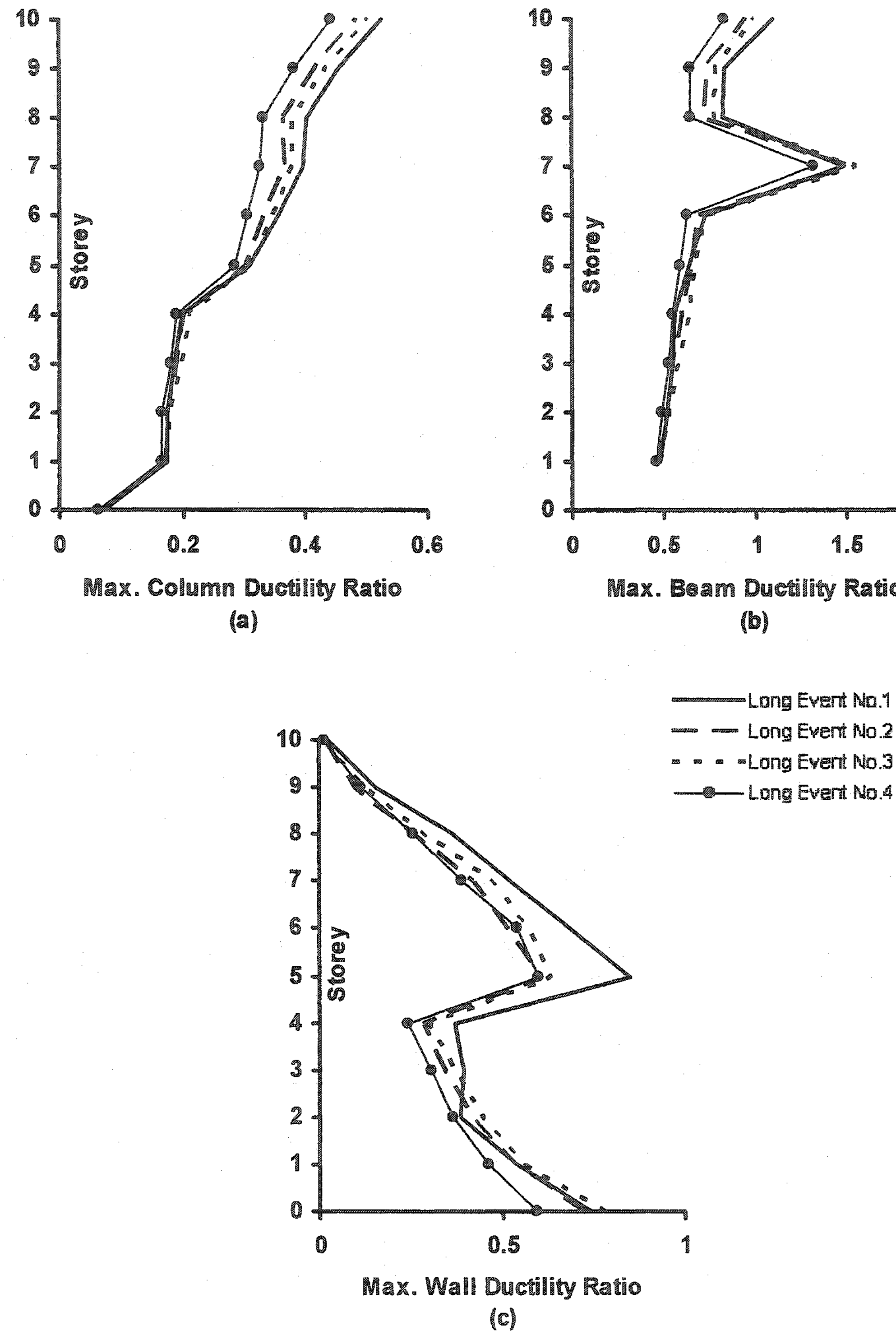

Fig. 4.15 Ductility Response for 10-Storey SHW Subjected to Long Event Artificial Records for Ottawa

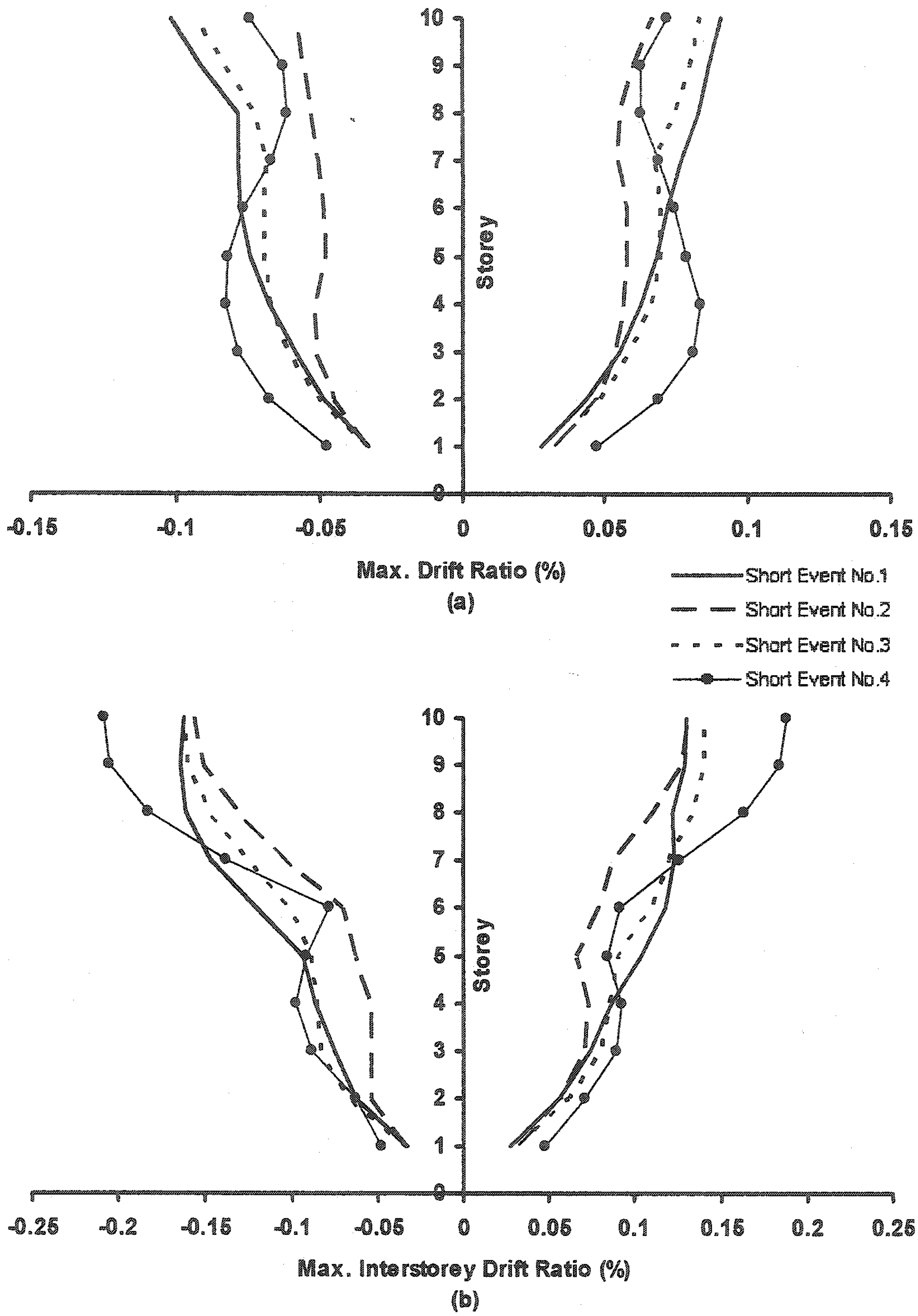

Fig. 4.16 Drift Response for 10-Storey SHW Subjected to Short Event Artificial Records for Ottawa

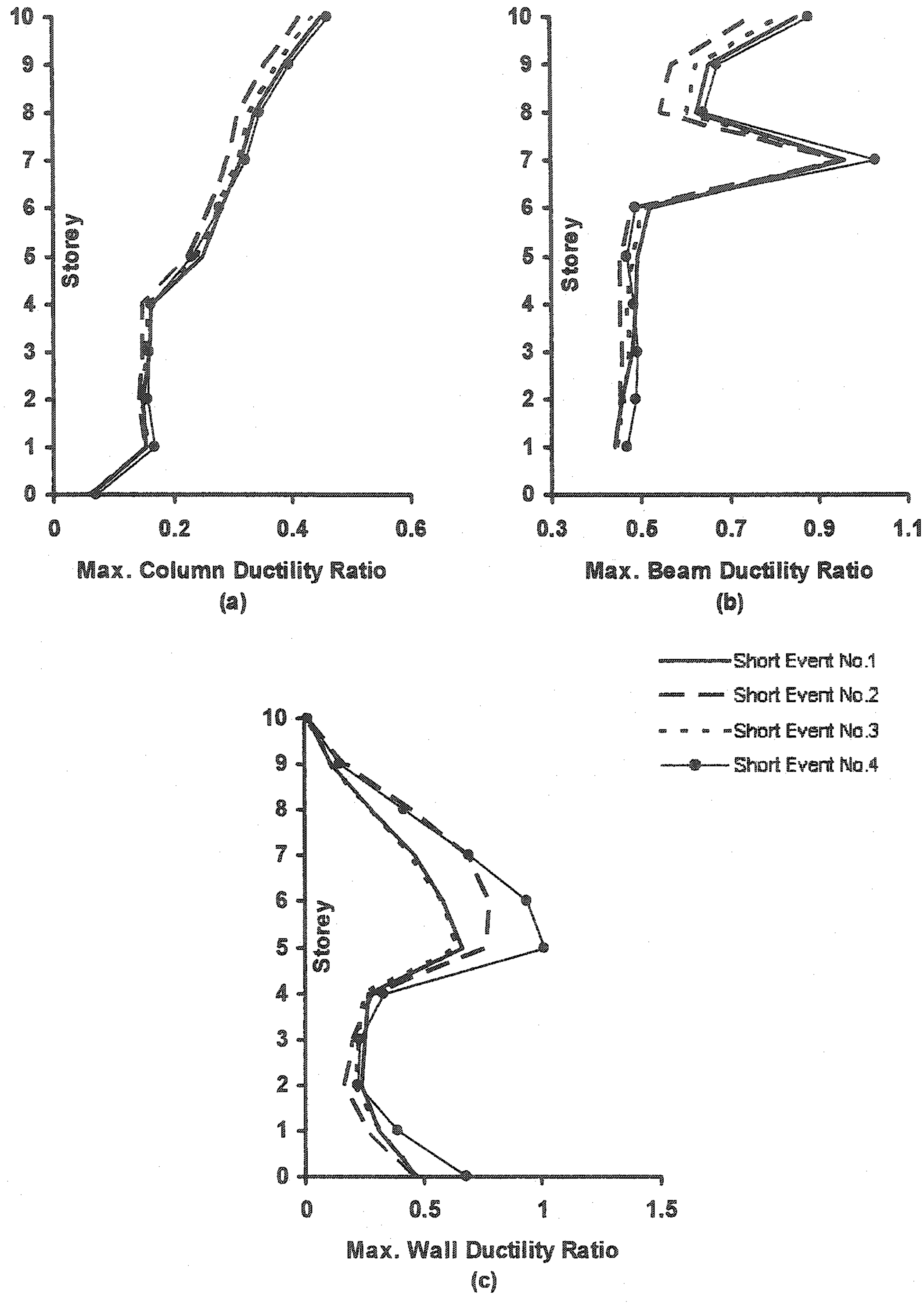

Fig. 4.17 Ductility Response for 10-Storey SHW Subjected to Short Event Artificial Records for Ottawa

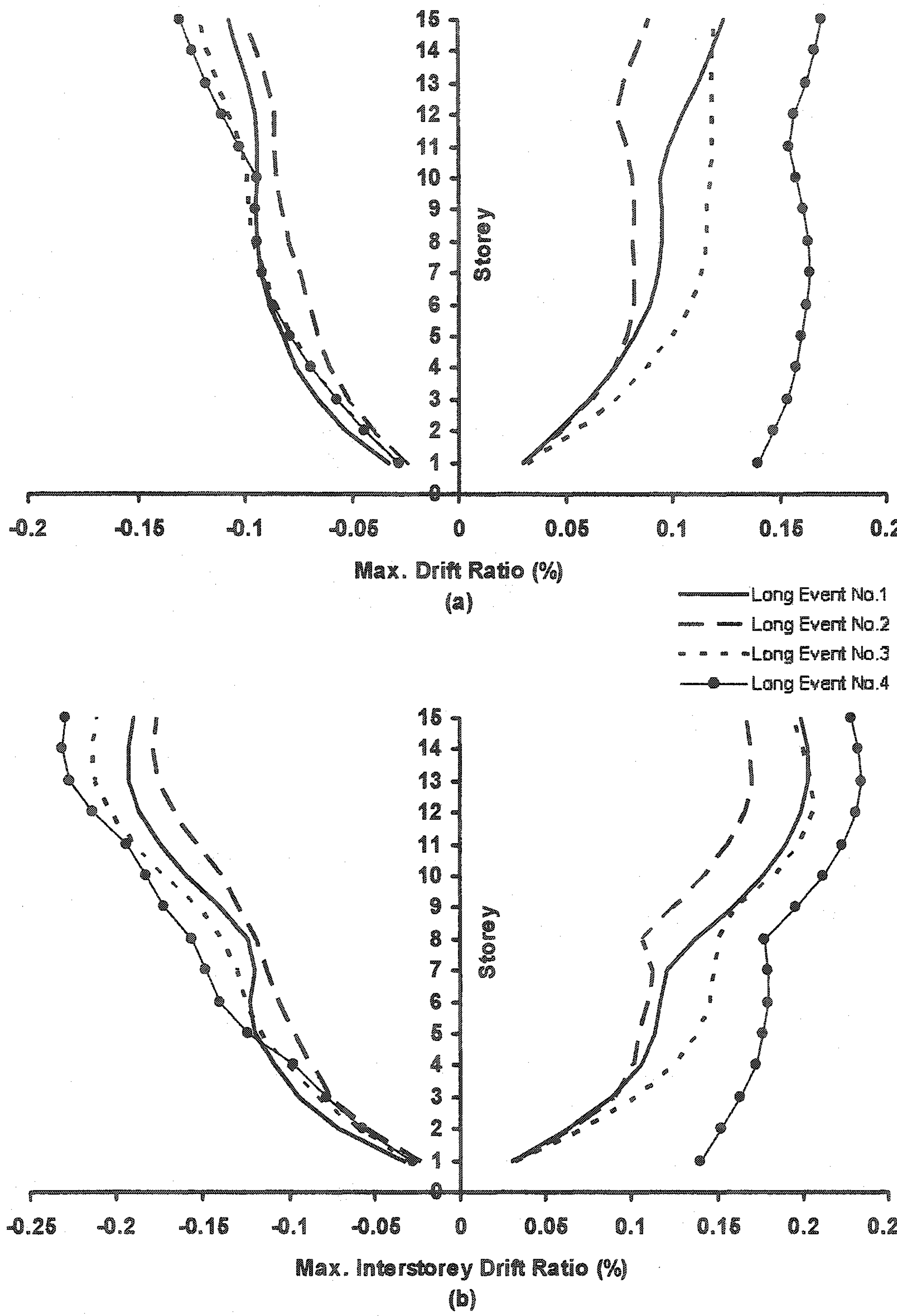

Fig. 4.18 Drift Response for 15-Storey SHW Subjected to Long Event Artificial Records for Ottawa

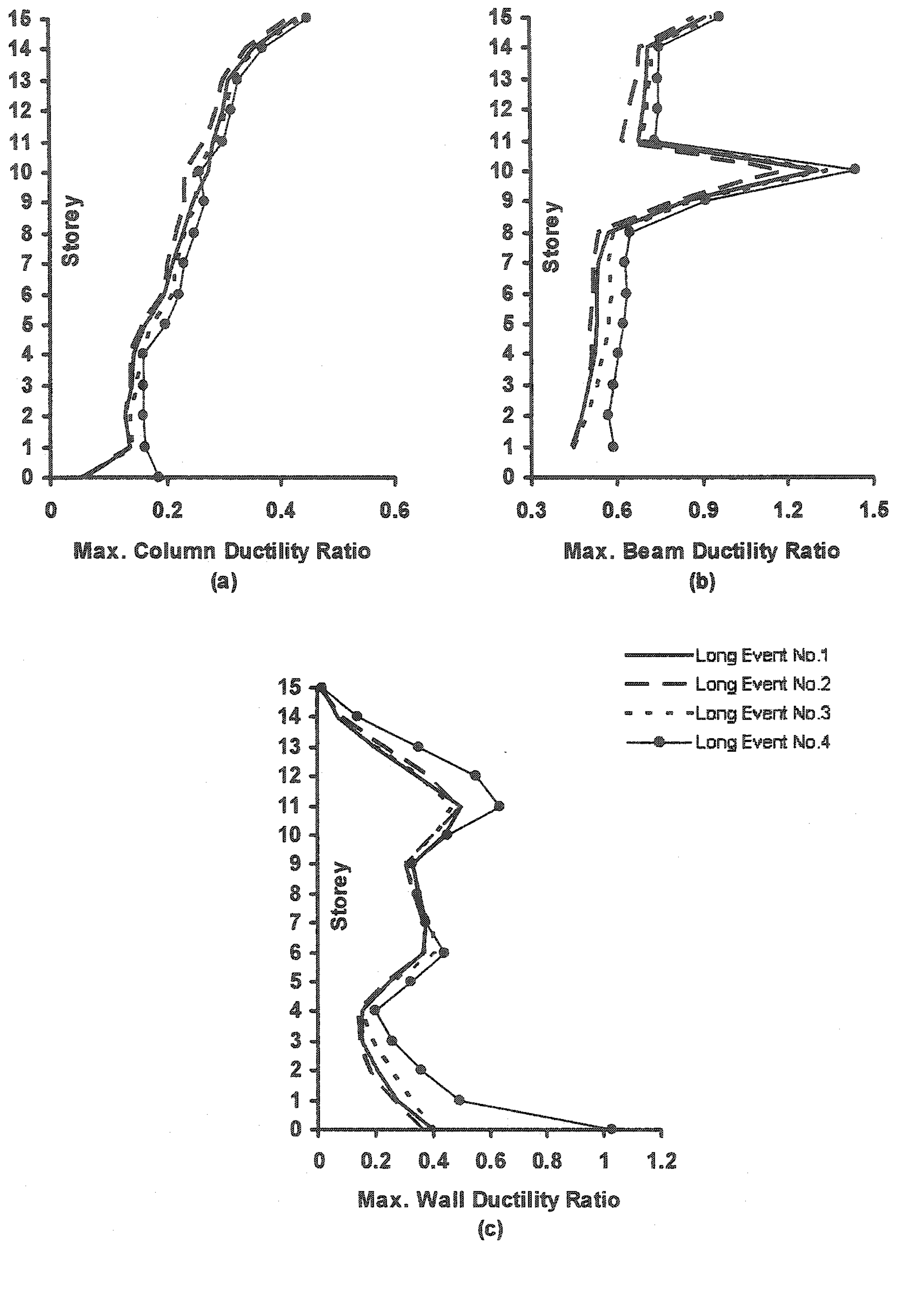

Fig. 4.19 Ductility Response for 15-Storey SHW Subjected to Long Event Artificial Records for Ottawa

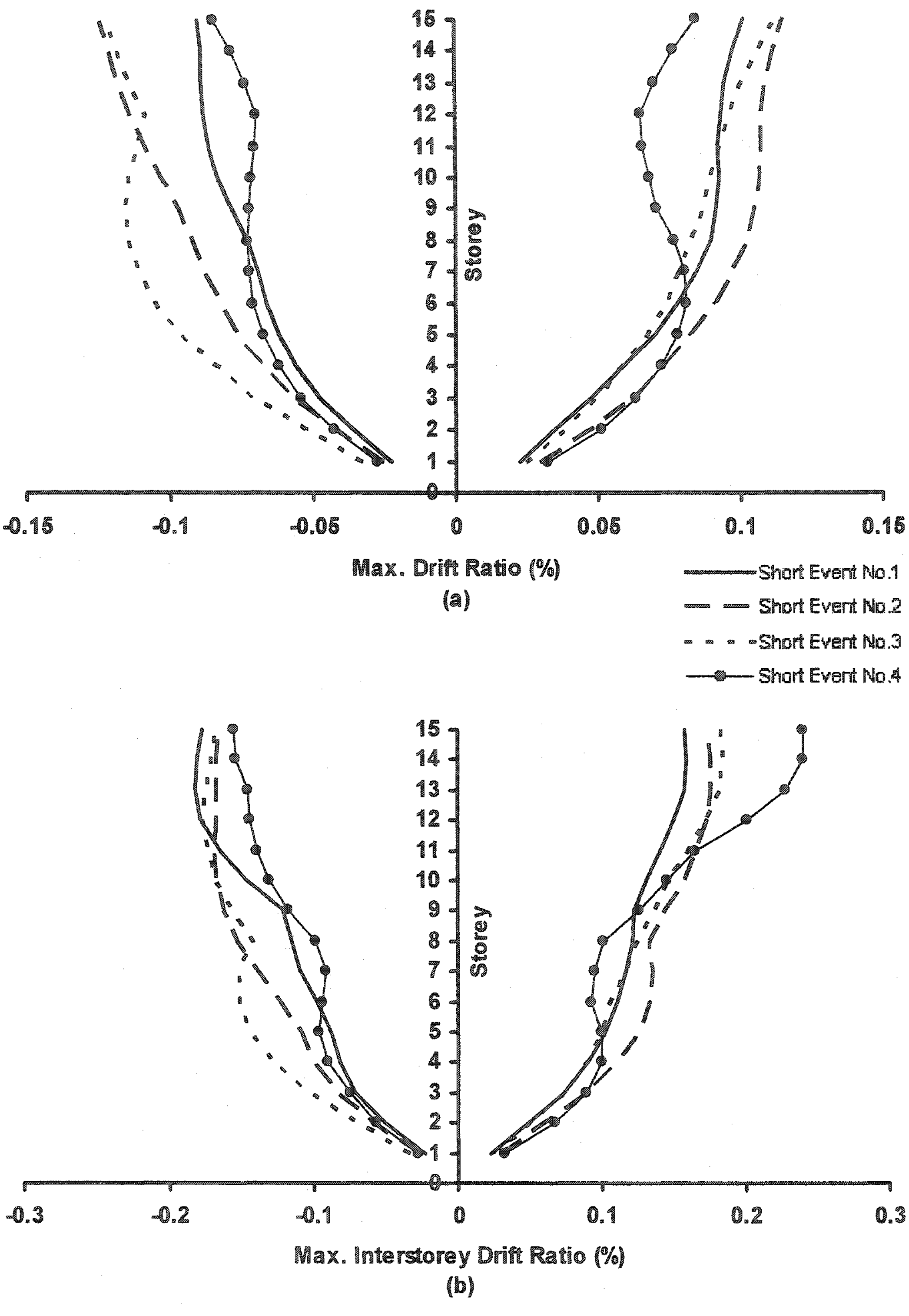

Fig. 4.20 Drift Response for 15-Storey SHW Subjected to Short Event Artificial Records for Ottawa

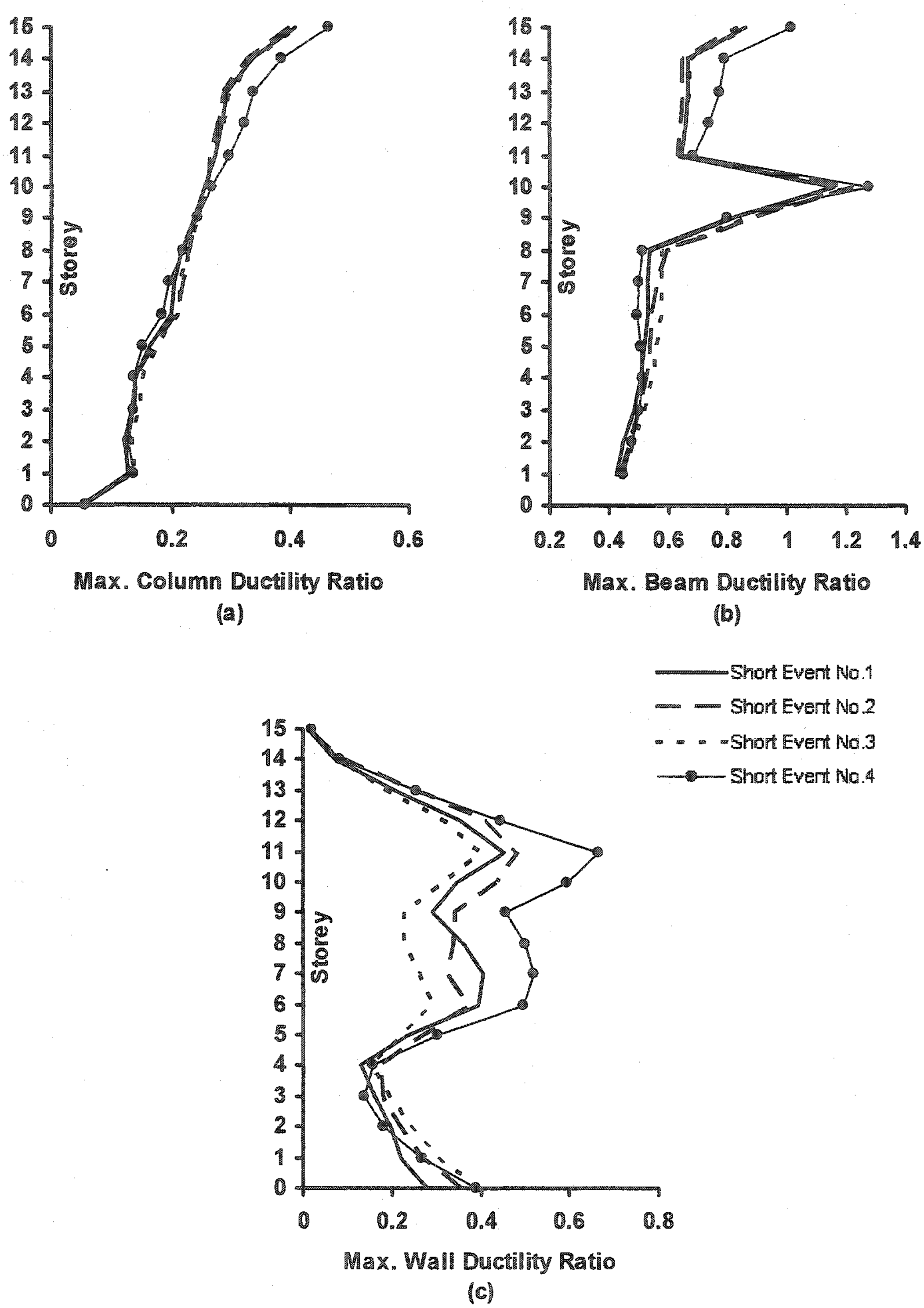

Fig. 4.21 Ductility Response for 15-Storey SHW Subjected to Short Event Artificial Records for Ottawa

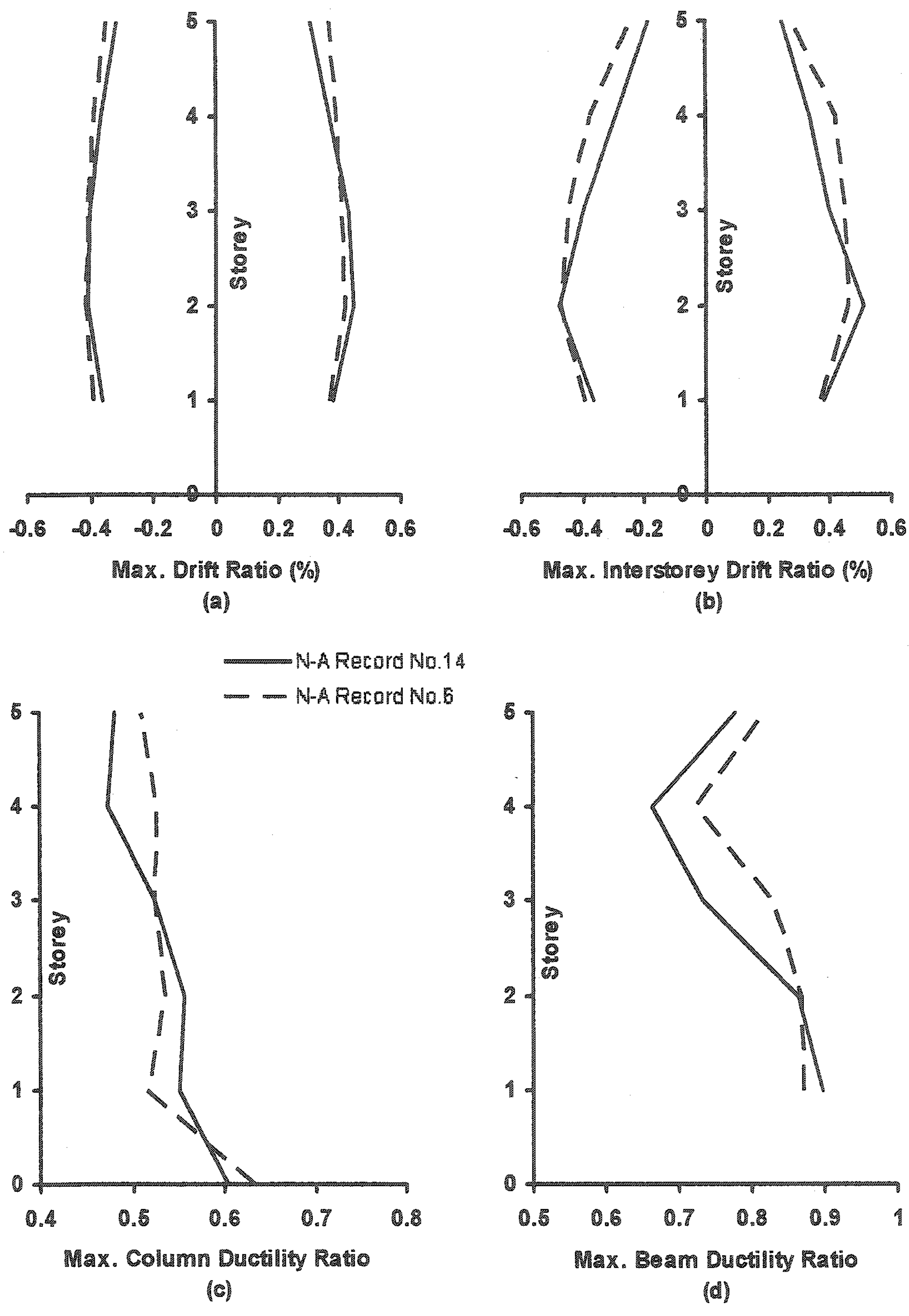

Fig. 4.22 Drift and Ductility Response for 5-Storey MRF Subjected to N-A Artificial Records for Ottawa

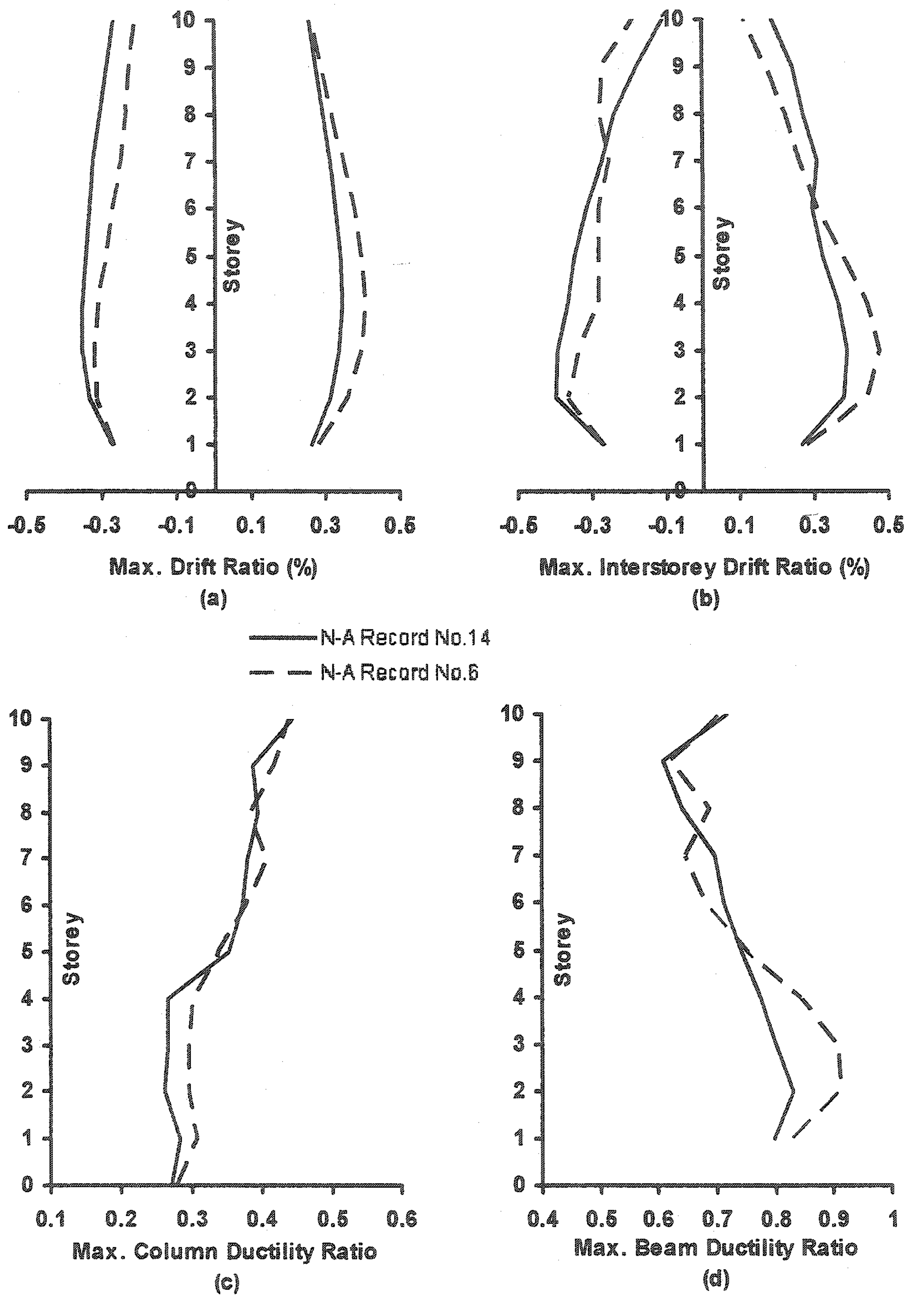

Fig. 4.23 Drift and Ductility Response for 10-Storey MRF Subjected to N-A Artificial Records for Ottawa

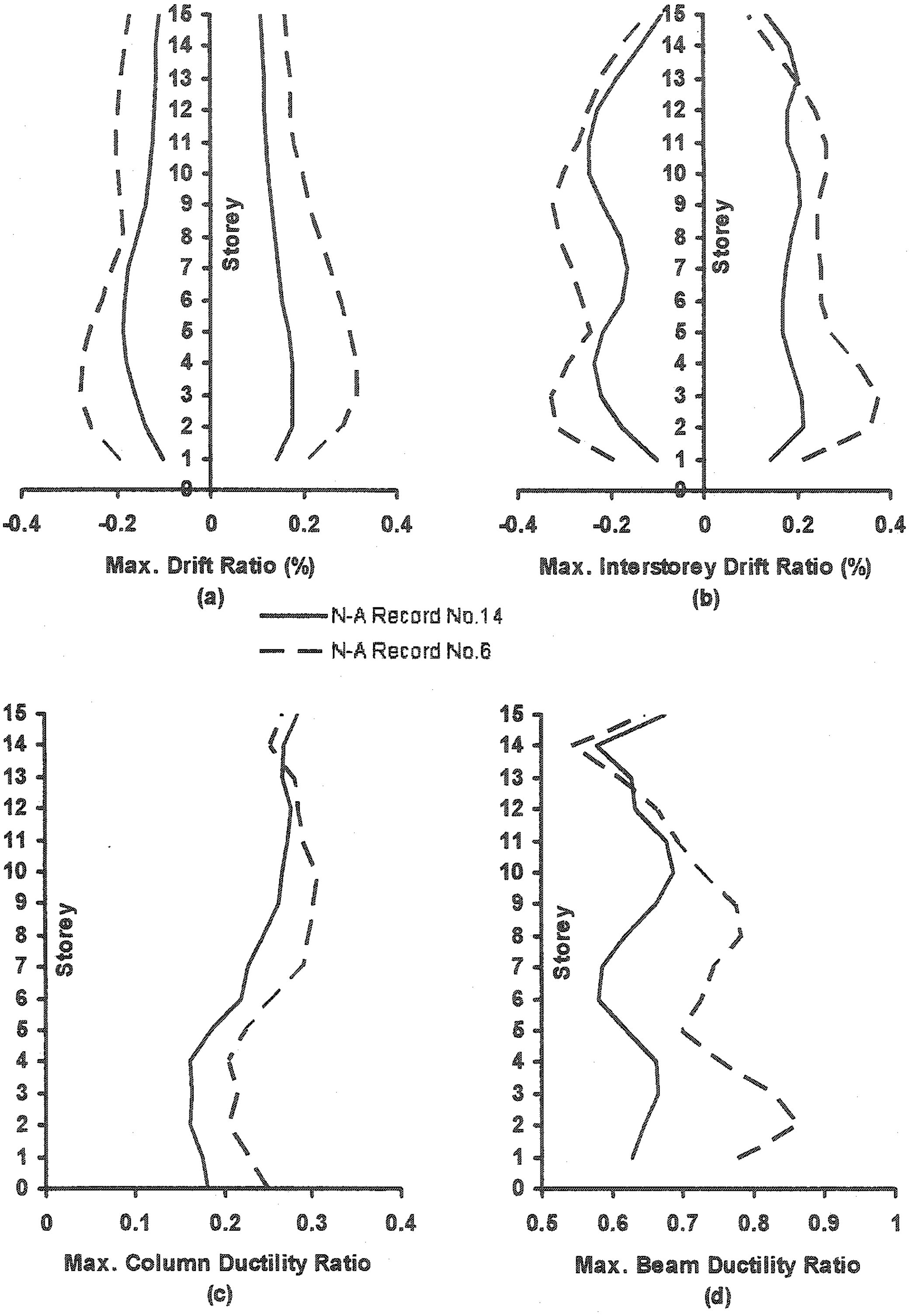

Fig. 4.24 Drift and Ductility Response for 15-Storey MRF Subjected to N-A Artificial Records for Ottawa

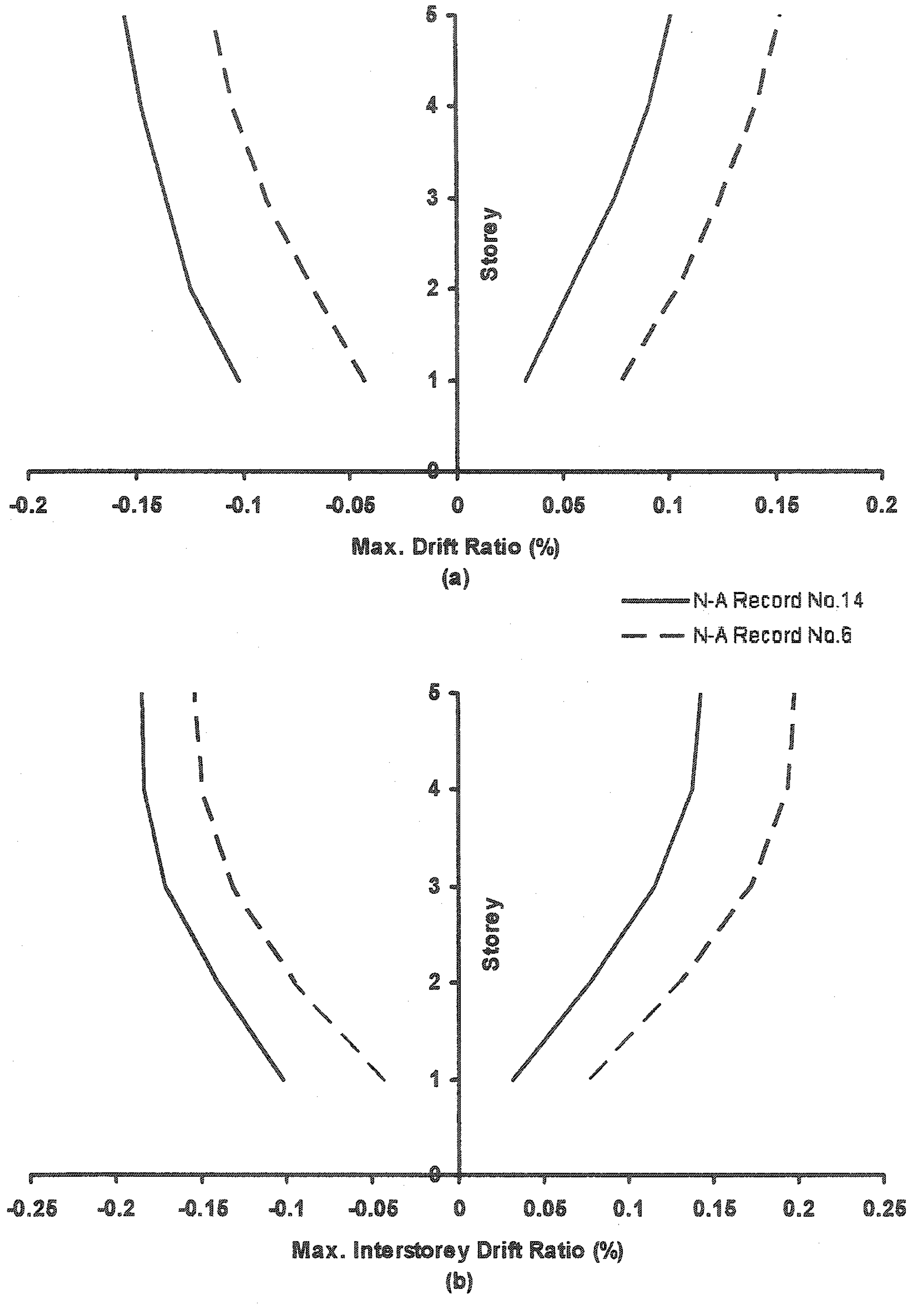

Fig. 4.25 Drift Response for 5-Storey SHW Subjected to N-A Artificial Records for Ottawa

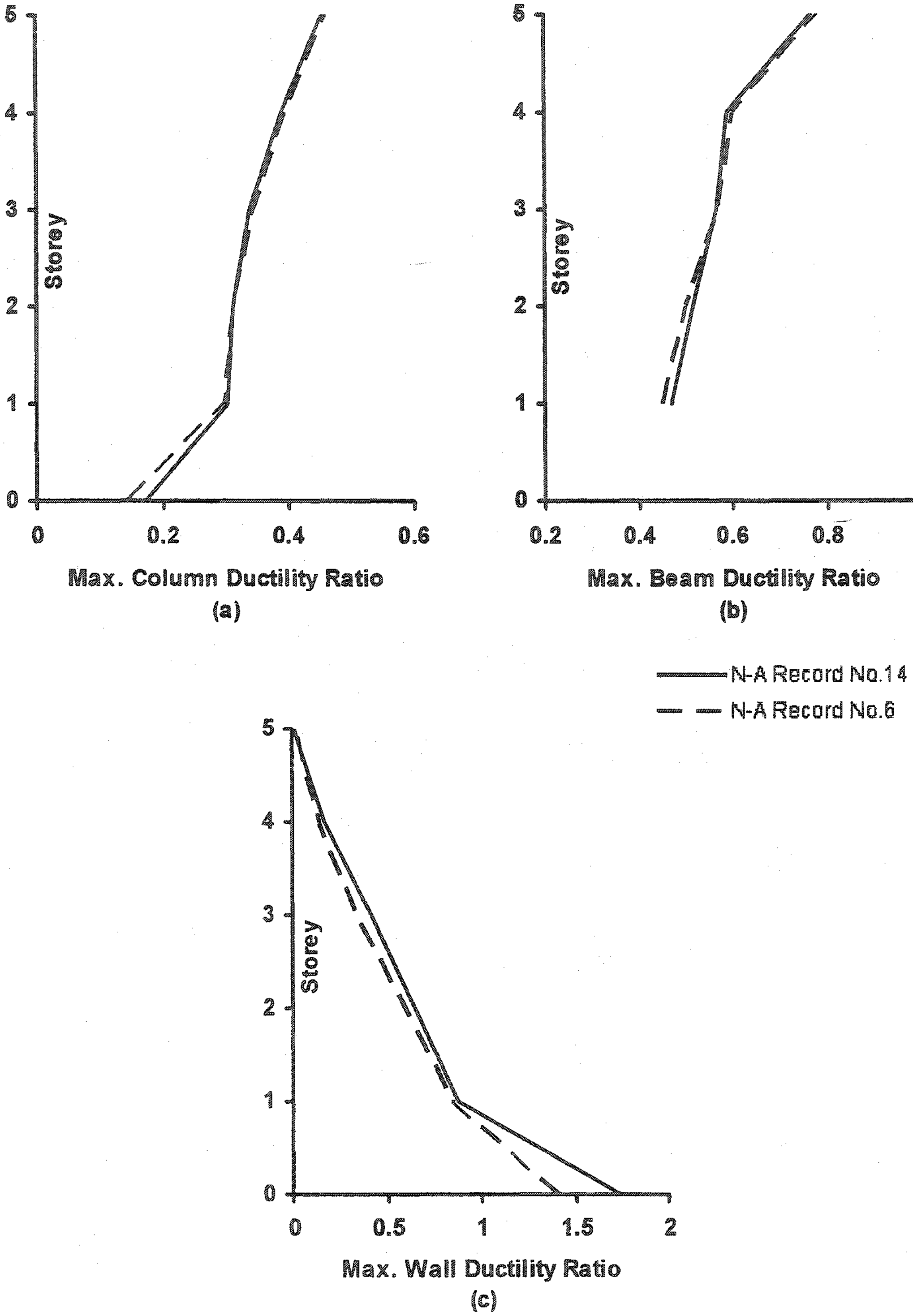

Fig. 4.26 Ductility Response for 5-Storey SHW Subjected to N-A Artificial Records for Ottawa

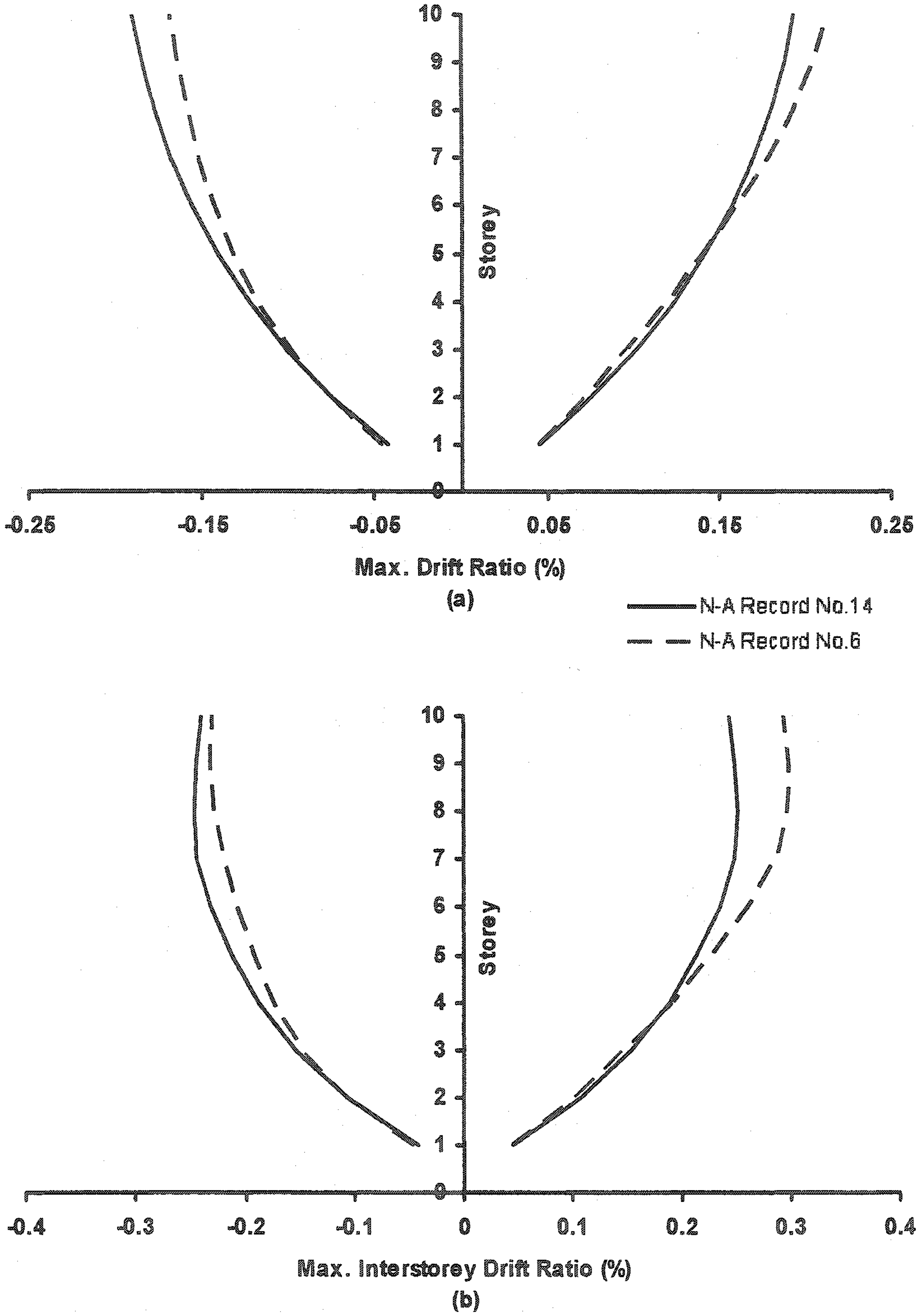

Fig. 4.27 Drift Response for 10-Storey SHW Subjected to N-A Artificial Records for Ottawa

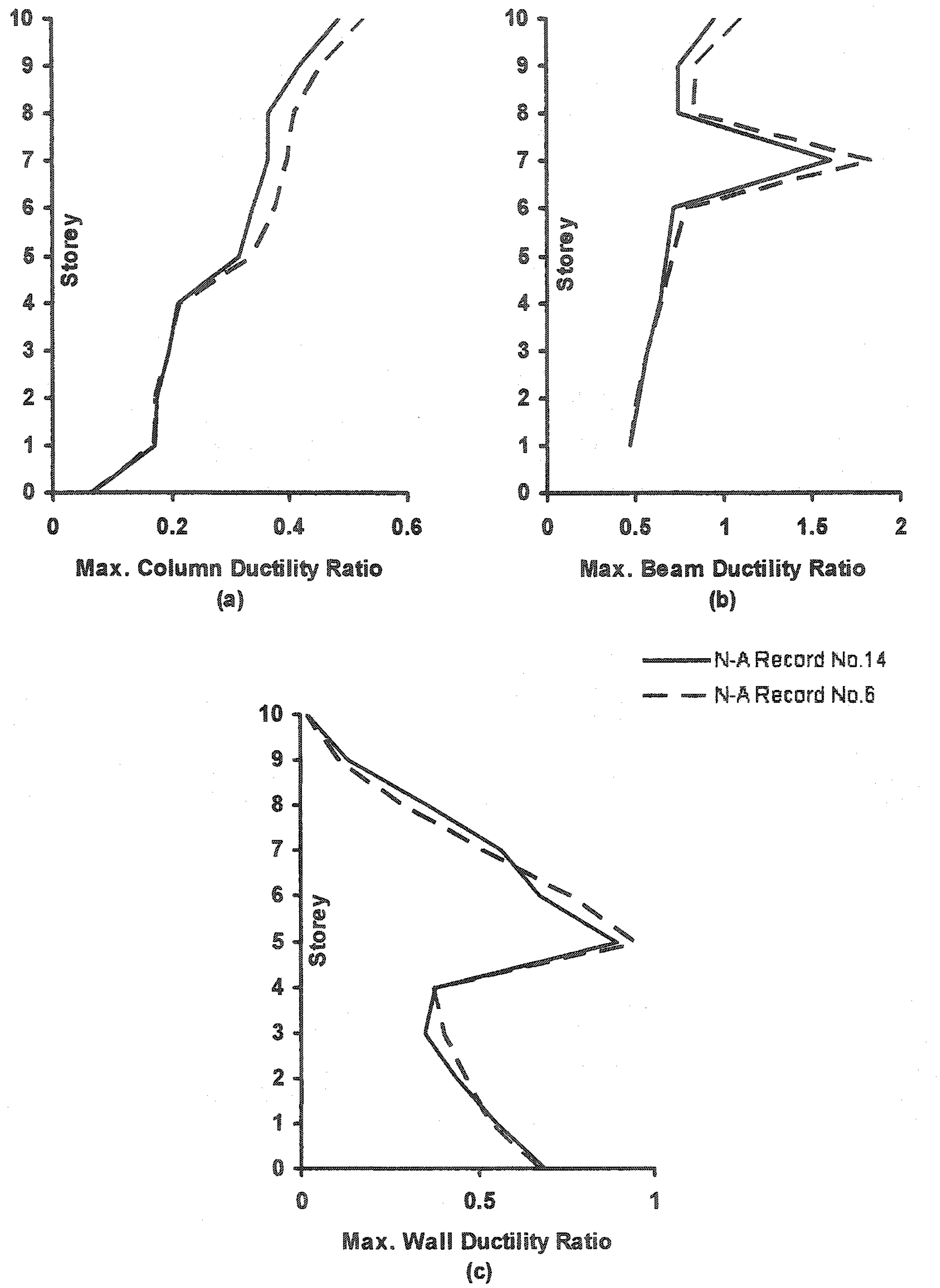

Fig. 4.28 Ductility Response for 10-Storey SHW Subjected to N-A Artificial Records for Ottawa

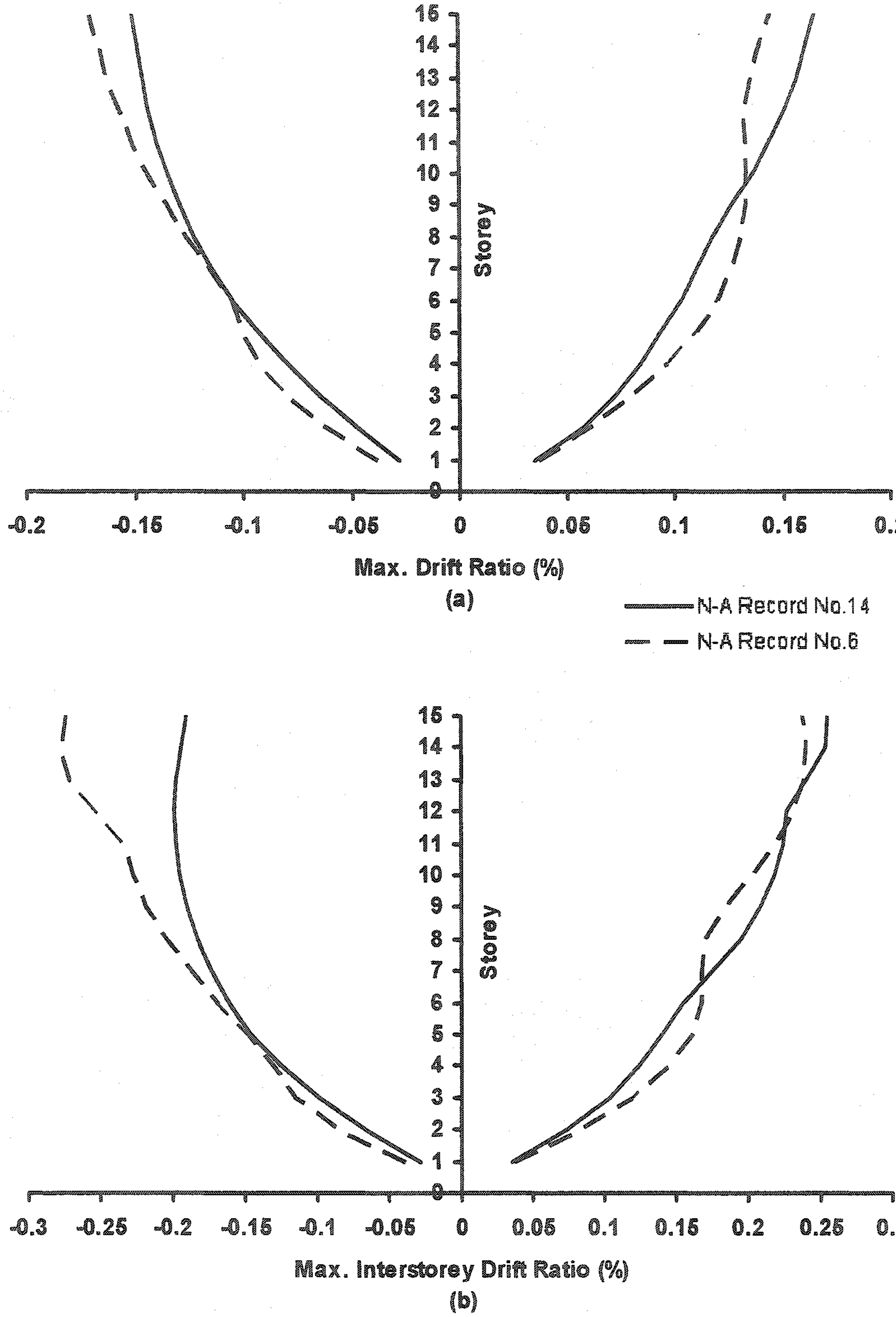

Fig. 4.29 Drift Response for 15-Storey SHW Subjected to N-A Artificial Records for Ottawa

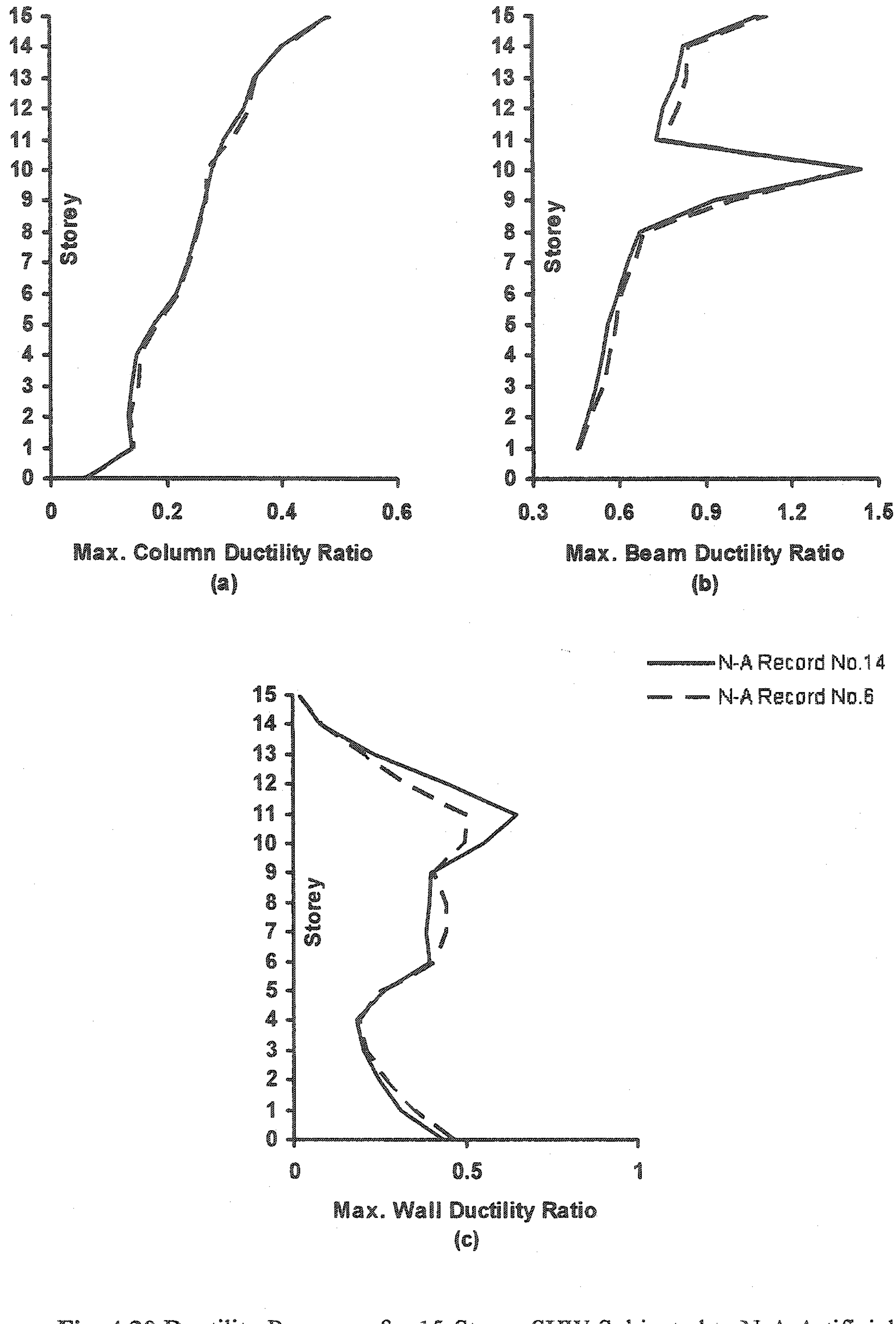

Fig. 4.30 Ductility Response for 15-Storey SHW Subjected to N-A Artificial Records for Ottawa

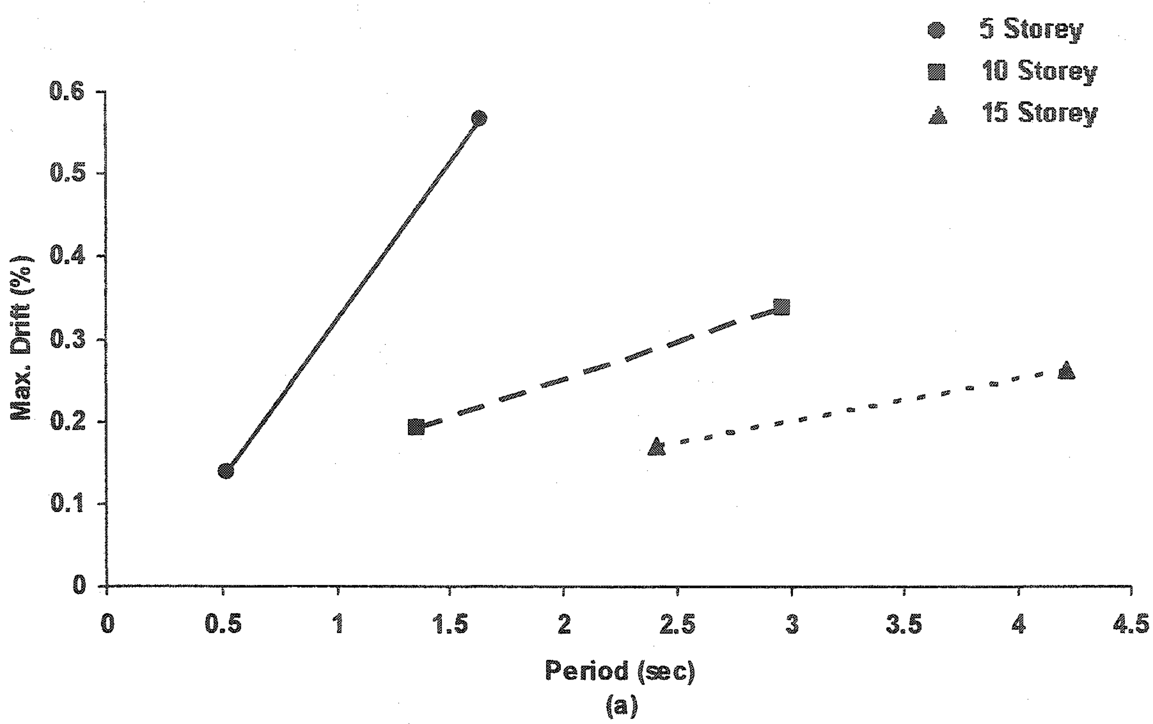

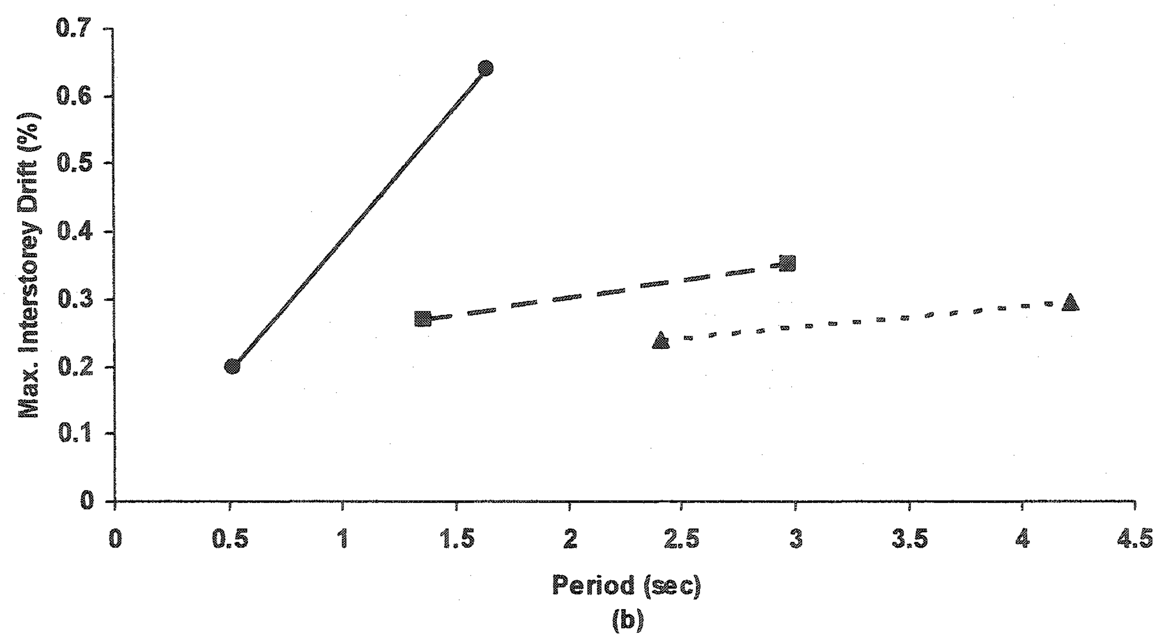

Fig. 4.31 The Relationship Between Maximum Drift Ratios and The Fundamental Period of Structures Subjected to A-B Artificial Records for Ottawa

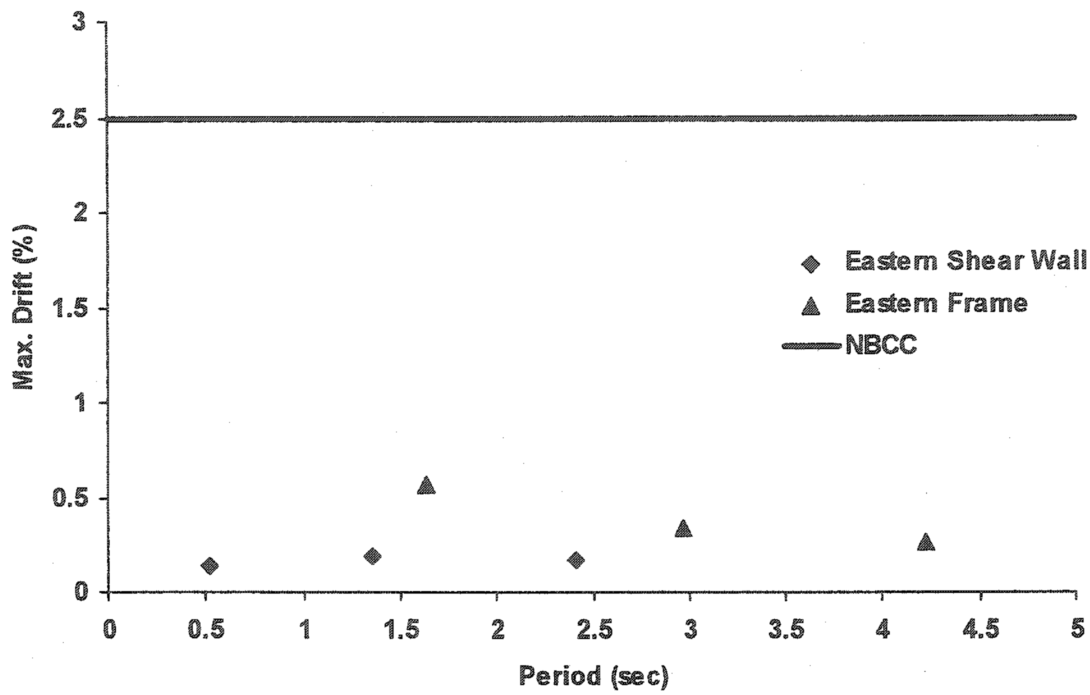

Fig. 4.32 The Relationship Between Computed Maximum Drift Ratios, NBCC Drift Limit and The Fundamental Period of Structures Subjected to A-B Artificial Records for Eastern Canada

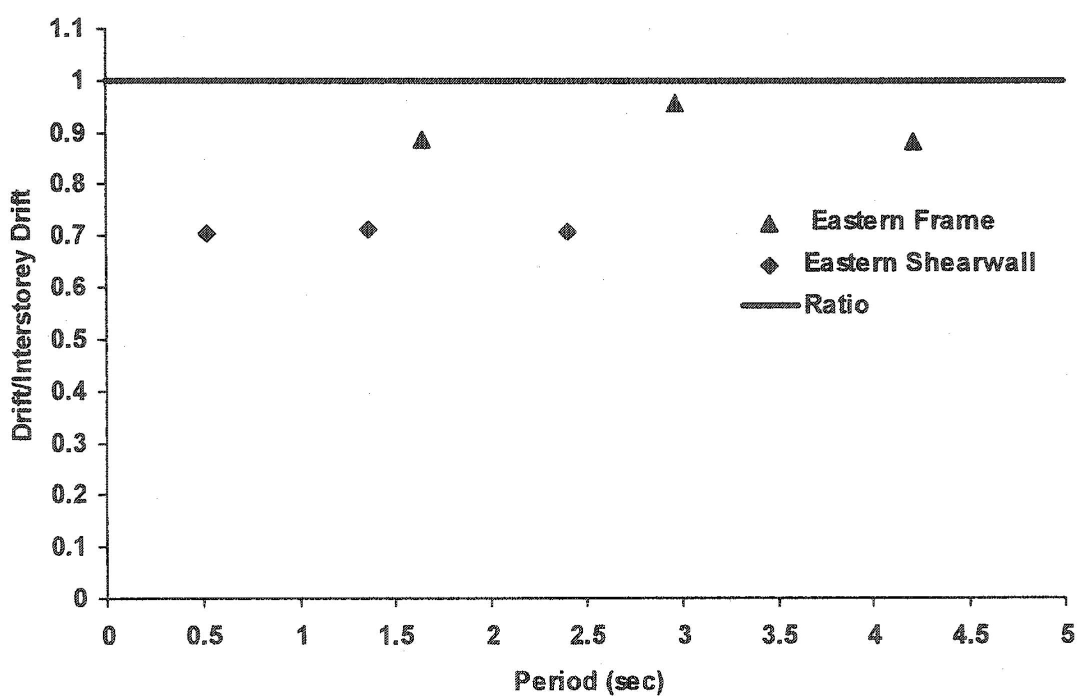

Fig. 4.33 The Relationship Between The Ratio of Drift to Interstorey Drift and The Fundamental Period of Buildings Subjected to A-B Artificial Records for Eastern Canada

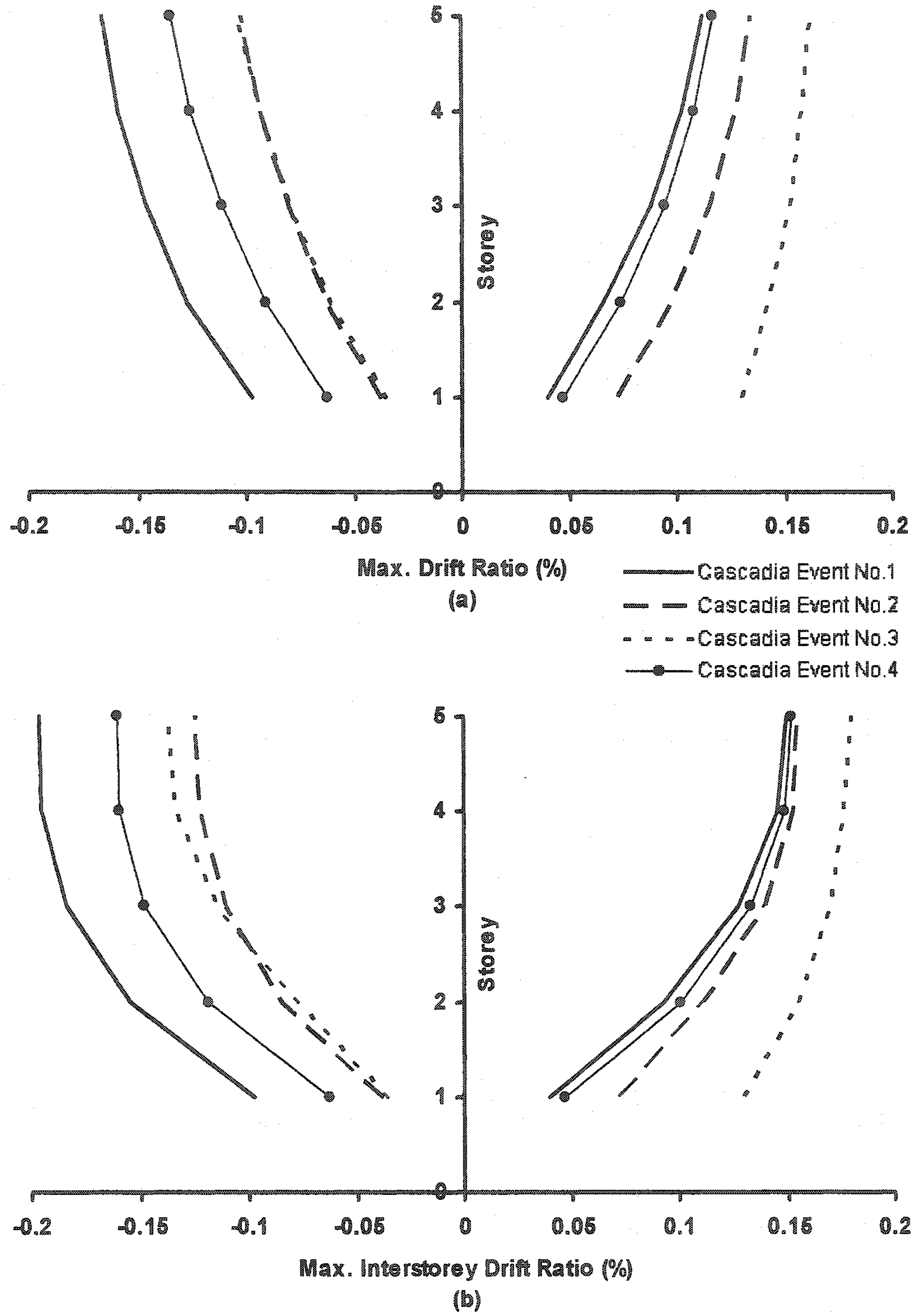

Fig. 4.34 Drift Response for 5-Storey SHW Subjected to Cascadia Event Artificial Records for Vancouver

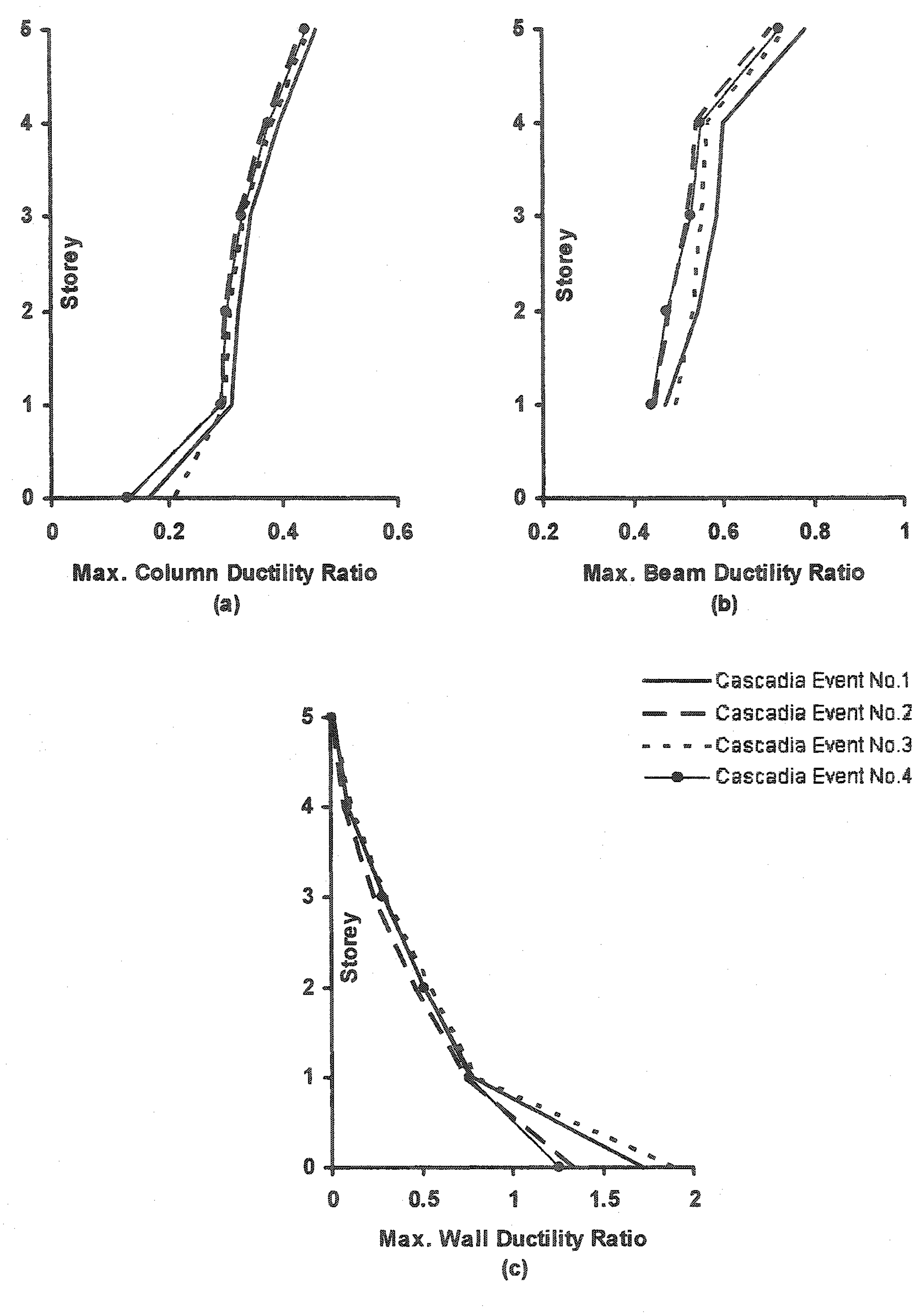

Fig. 4.35 Ductility Response for 5-Storey SHW Subjected to Cascadia Event Artificial Records for Vancouver

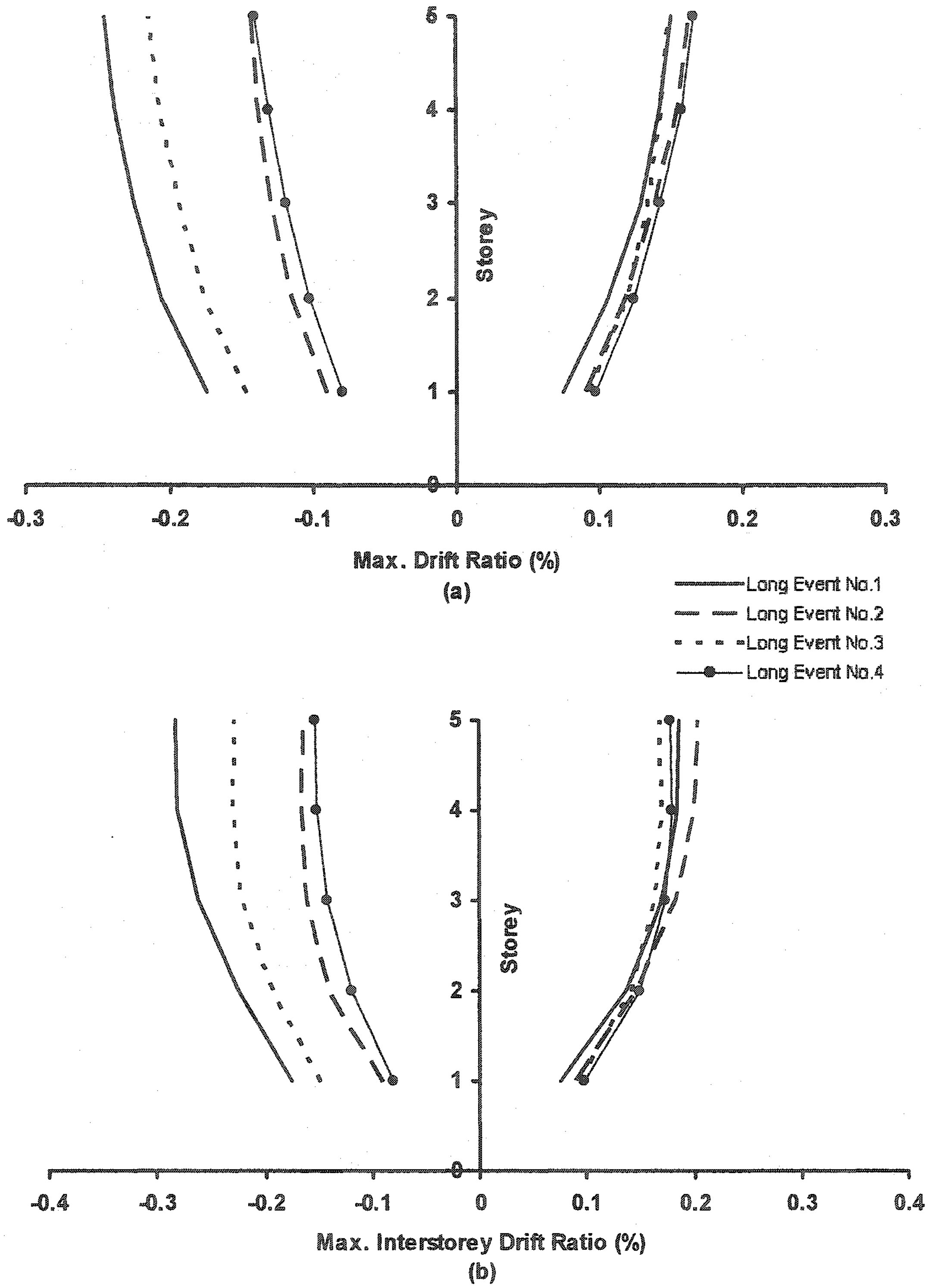

Fig. 4.36 Drift Response for 5-Storey SHW Subjected to Long Event Artificial Records for Vancouver

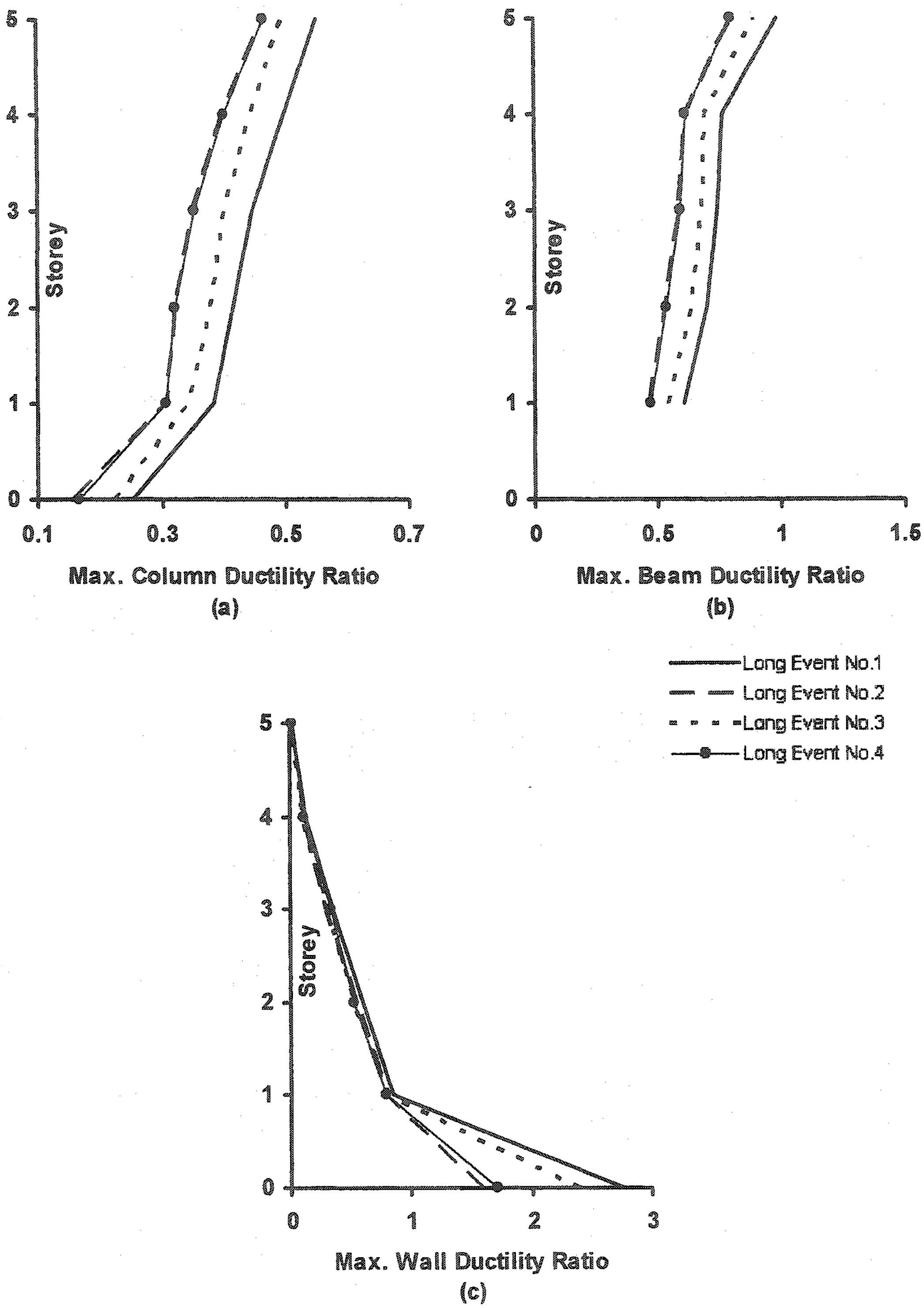

Fig. 4.37 Ductility Response for 5-Storey SHW Subjected to Long Event Artificial Records for Vancouver

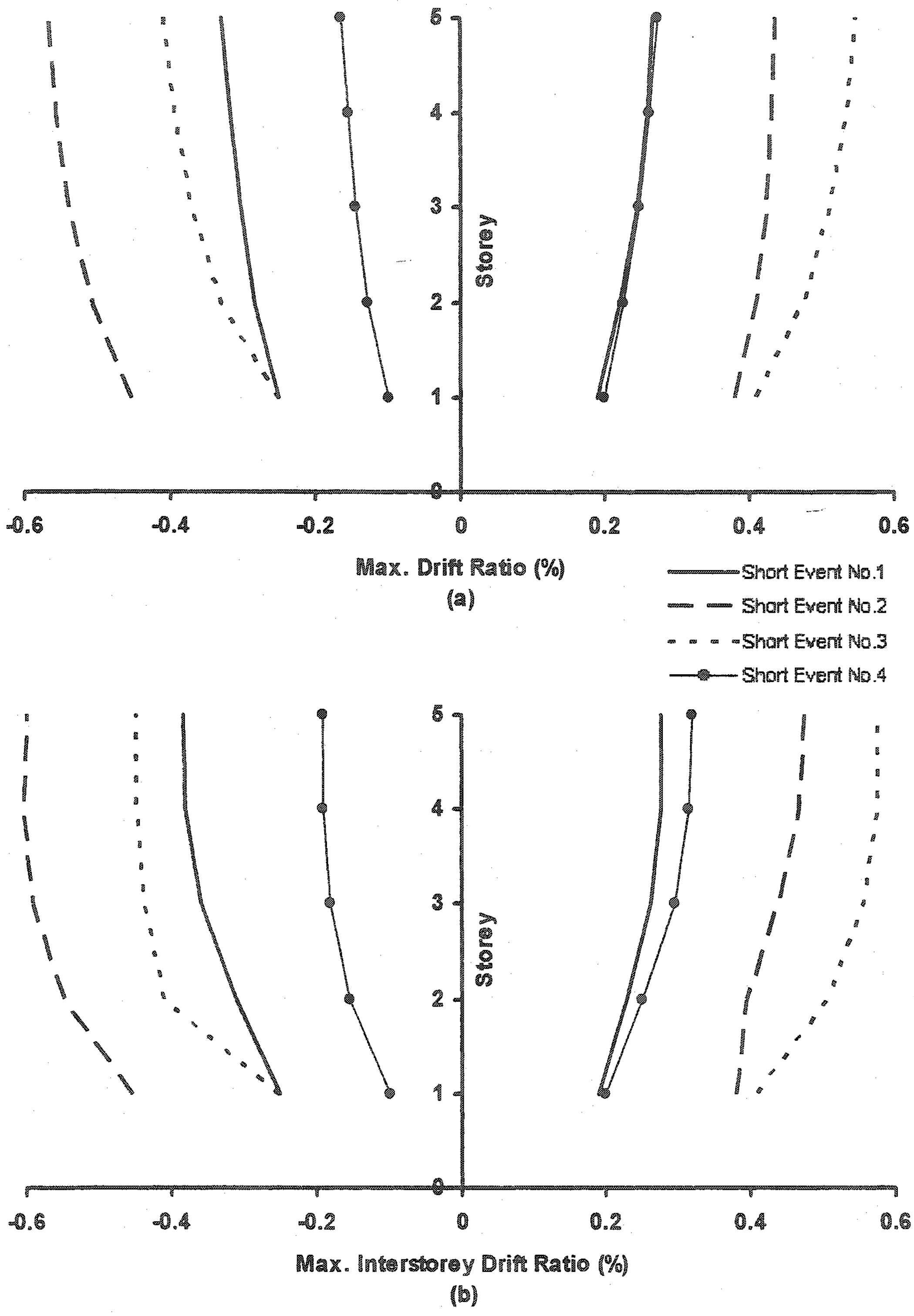

Fig. 4.38 Drift Response for 5-Storey SHW Subjected to Short Event Artificial Records for Vancouver

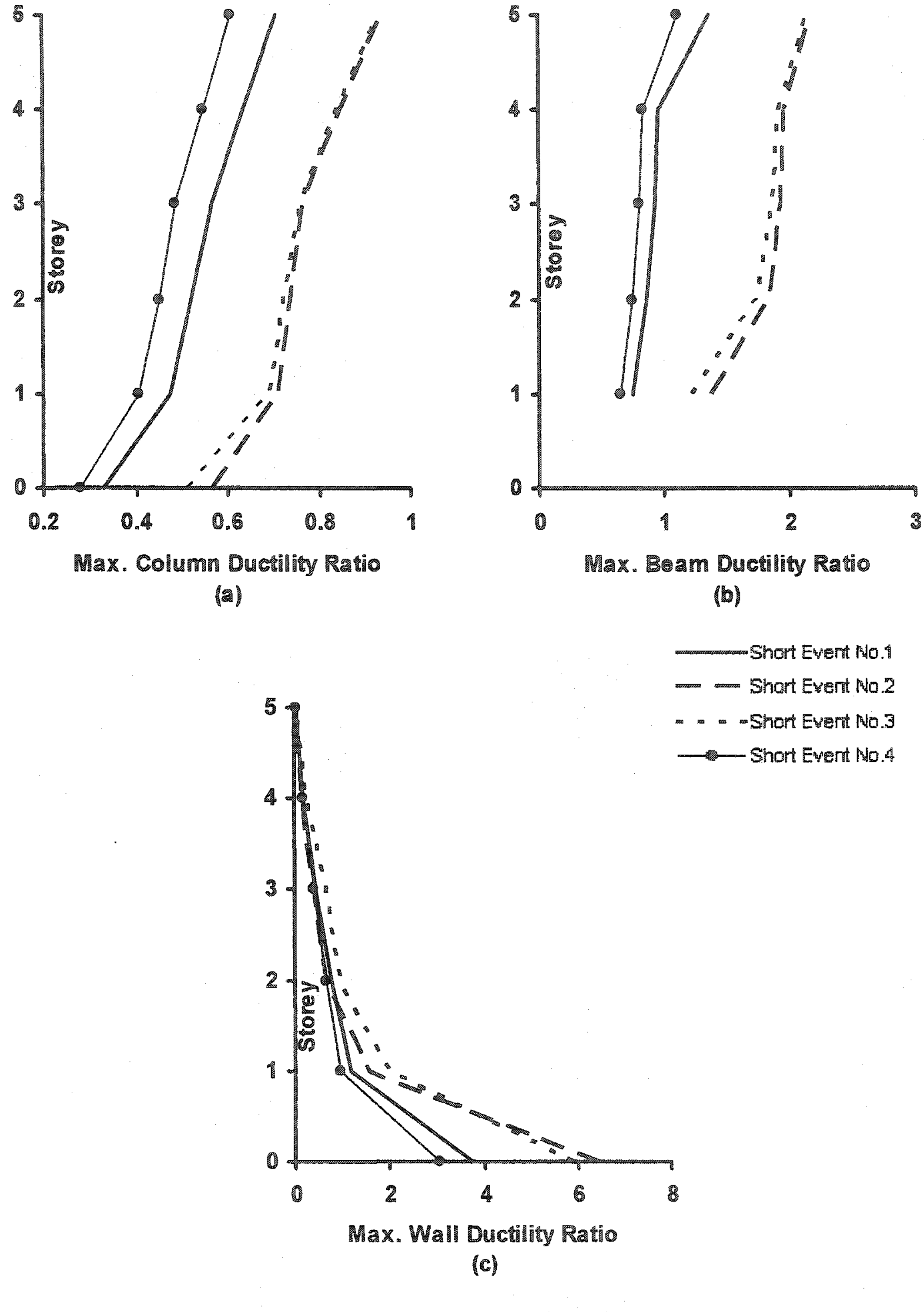

Fig. 4.39 Ductility Response for 5-Storey SHW Subjected to Short Event Artificial Records for Vancouver

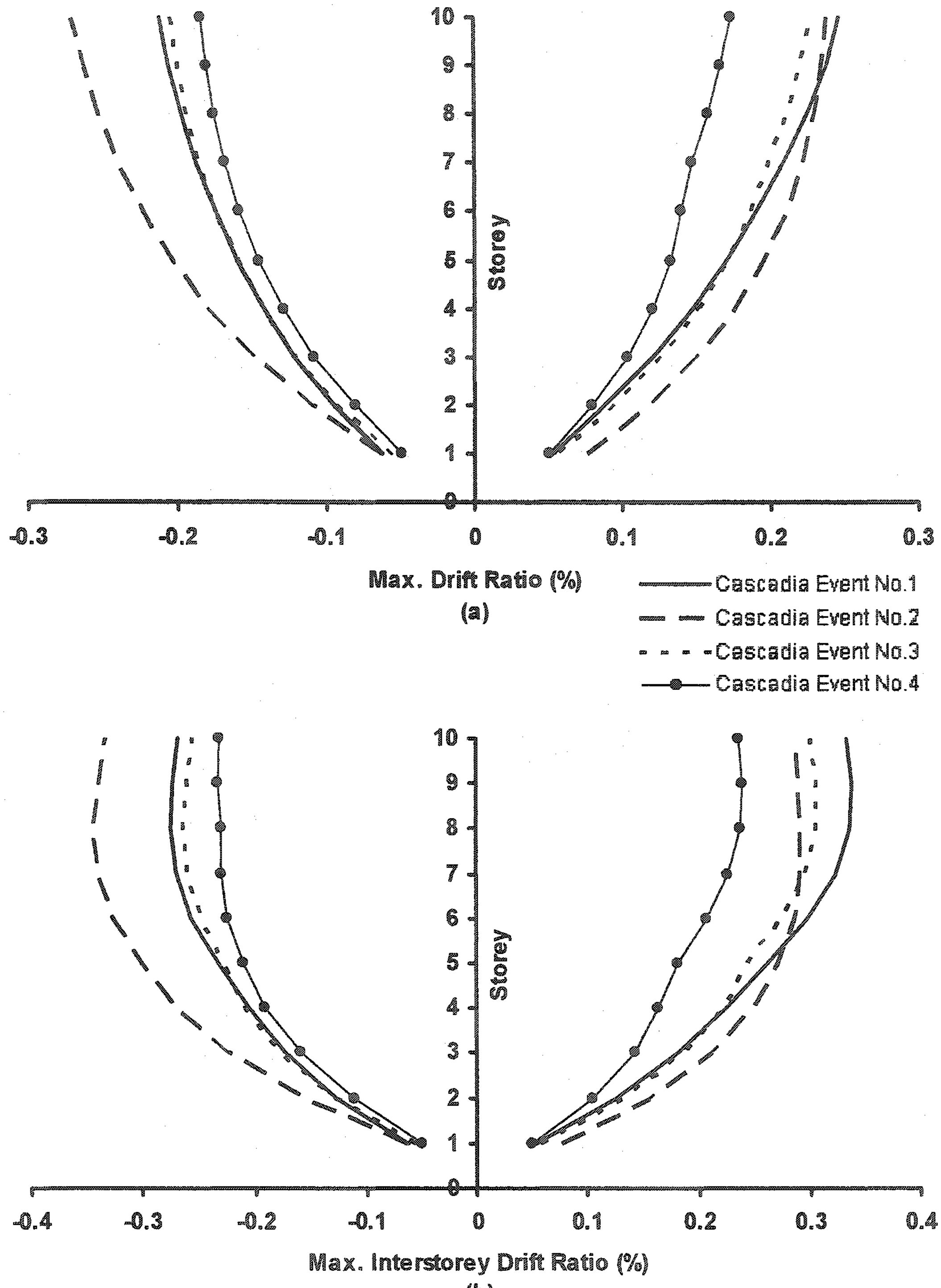

Fig. 4.40 Drift Response for 10-Storey SHW Subjected to Cascadia Event Artificial Records for Vancouver

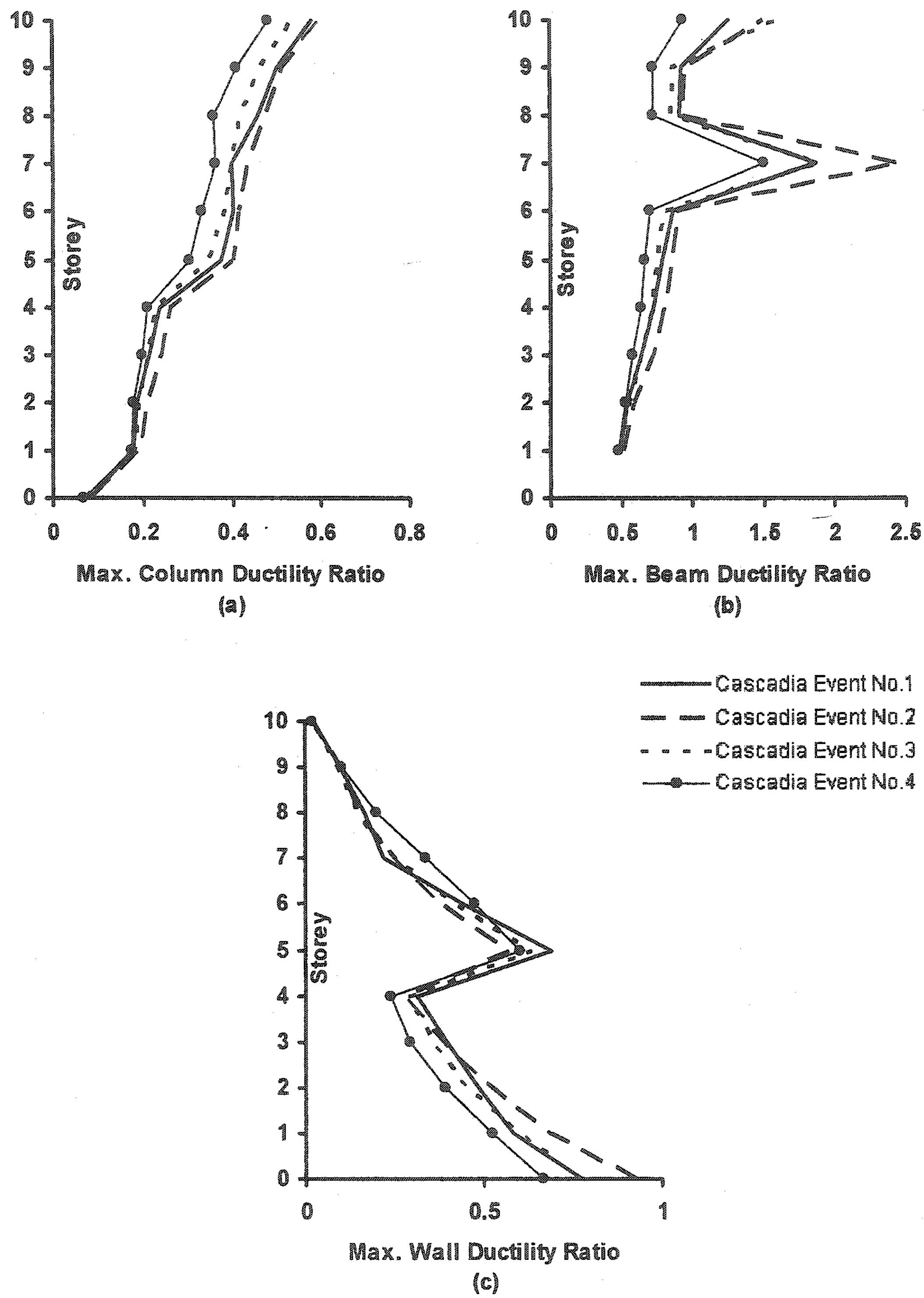

Fig. 4.41 Ductility Response for 10-Storey SHW Subjected to Cascadia Event Artificial Records for Vancouver

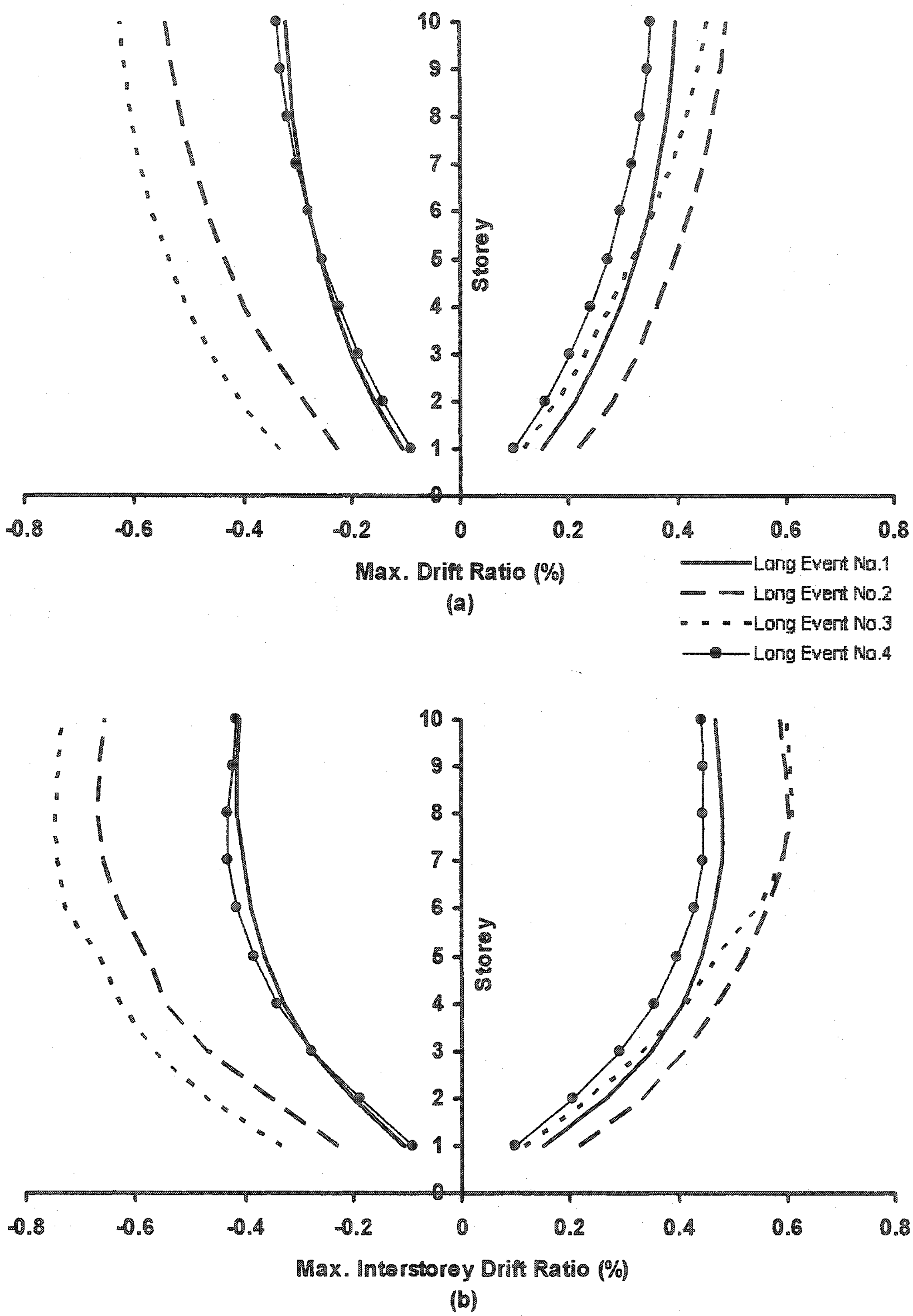

Fig. 4.42 Drift Response for 10-Storey SHW Subjected to Long Event Artificial Records for Vancouver

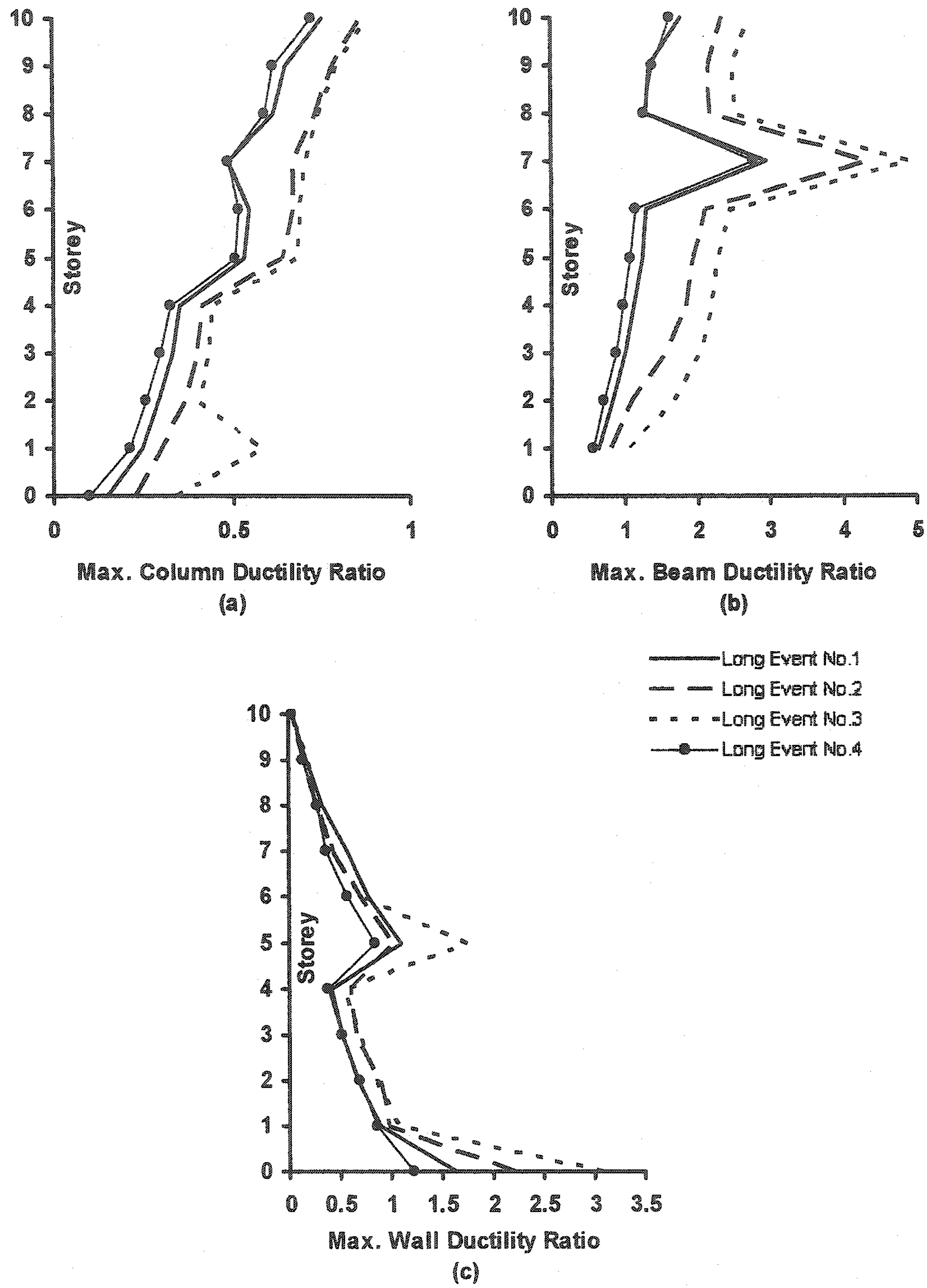

Fig. 4.43 Ductility Response for 10-Storey SHW Subjected to Long Event Artificial Records for Vancouver

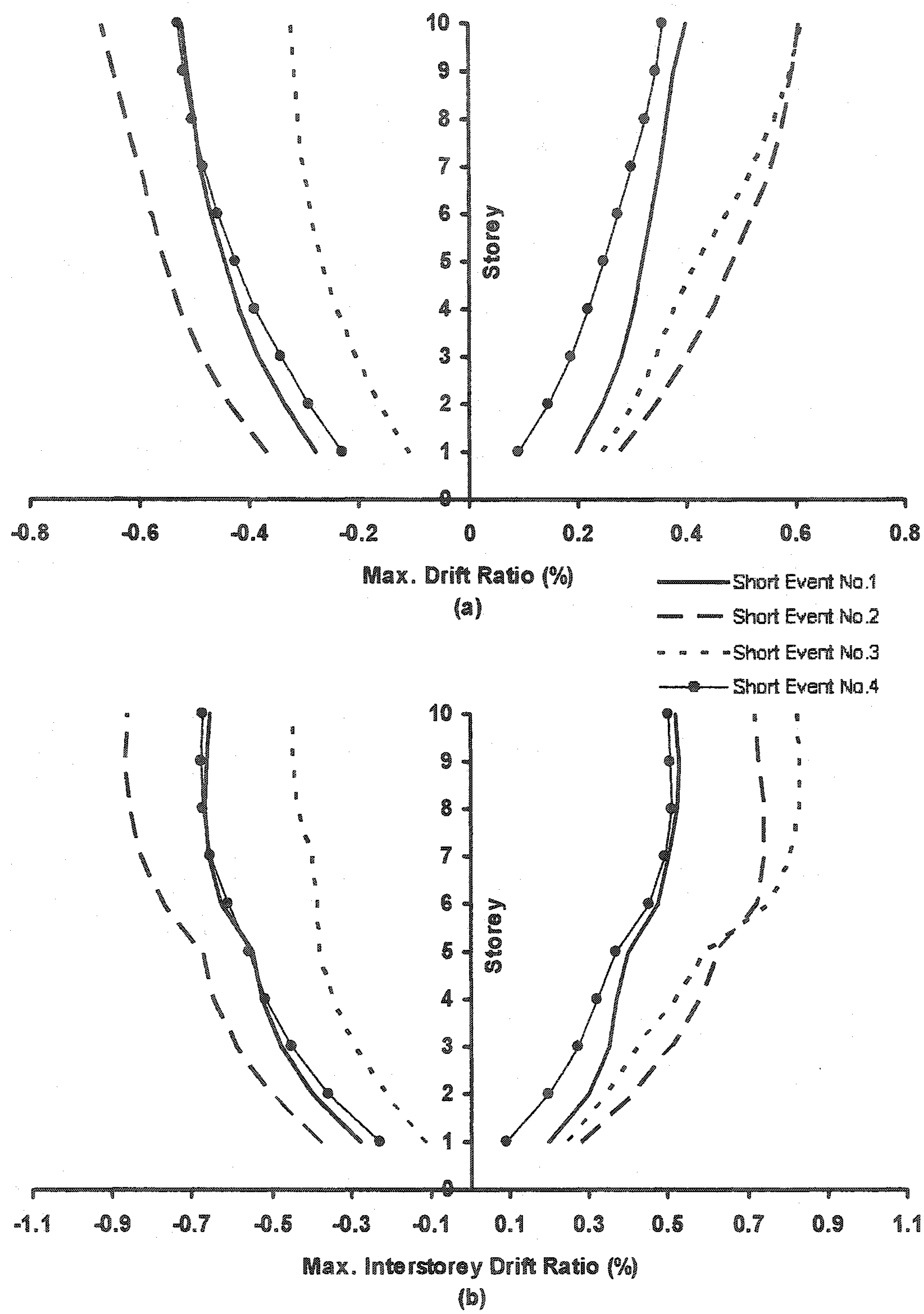

Fig. 4.44 Drift Response for 10-Storey SHW Subjected to Short Event Artificial Records for Vancouver

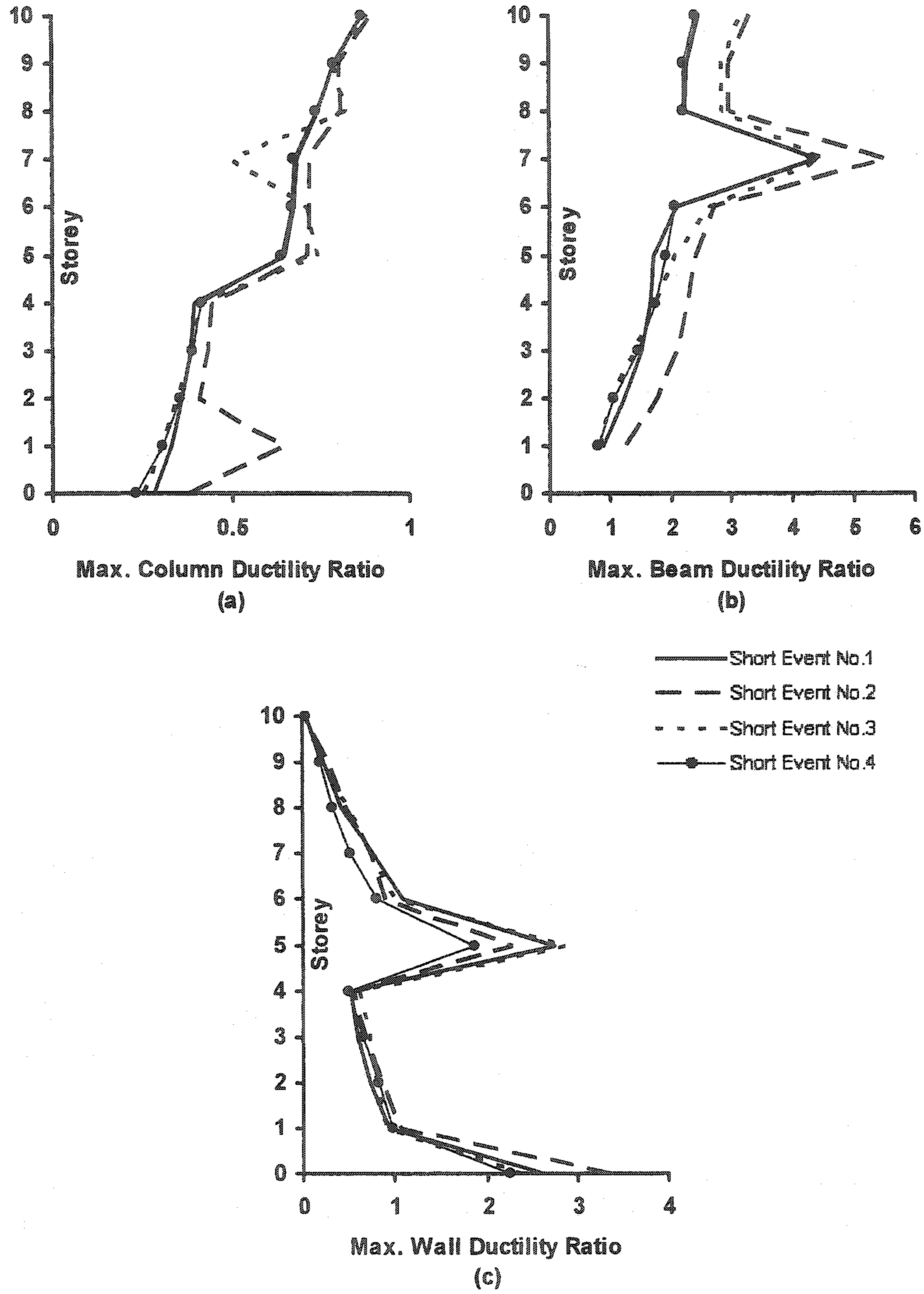

Fig. 4.45 Ductility Response for 10-Storey SHW Subjected to Short Event Artificial Records for Vancouver

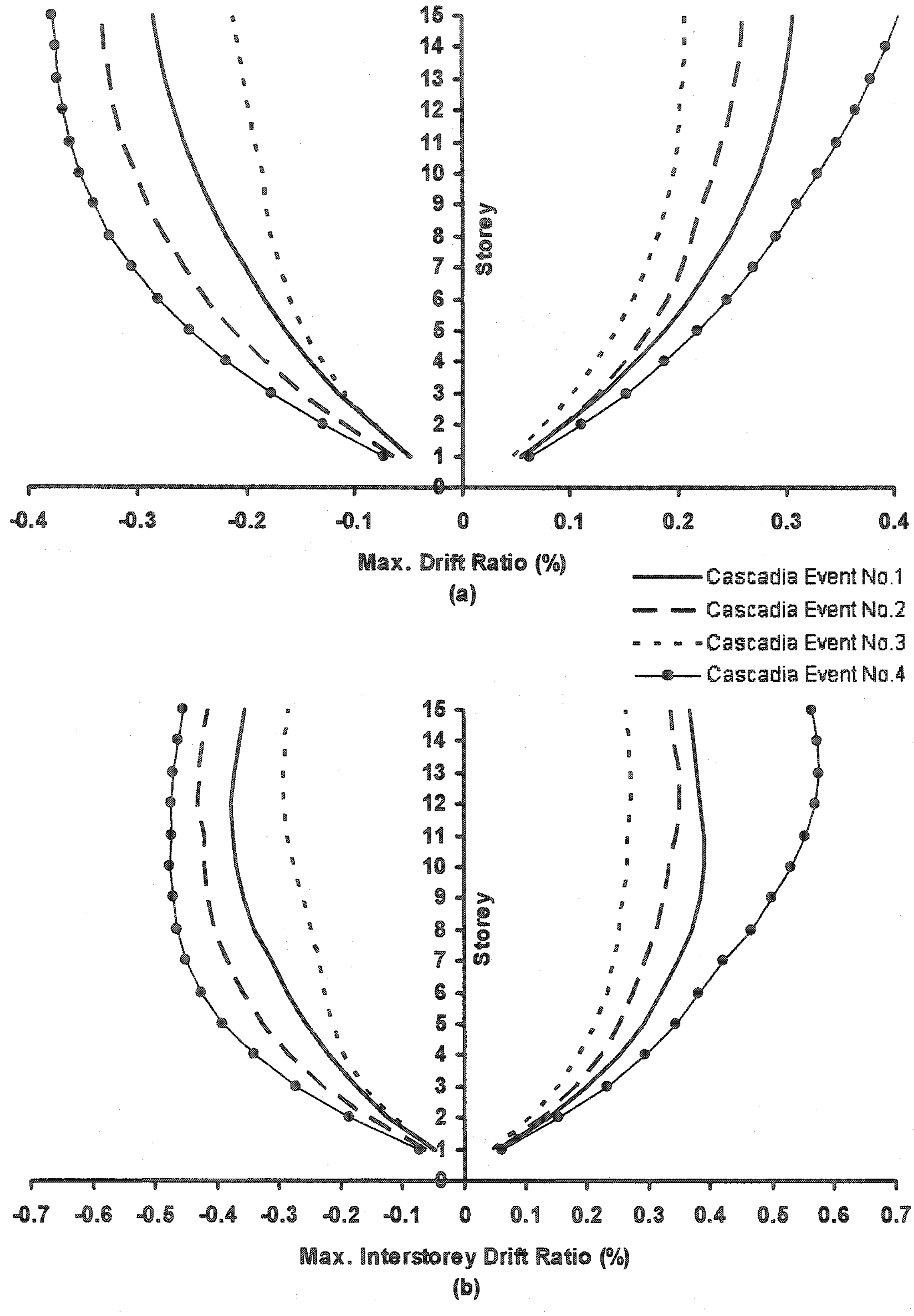

Fig. 4.46 Drift Response for 15-Storey SHW Subjected to Cascadia Event Artificial Records for Vancouver

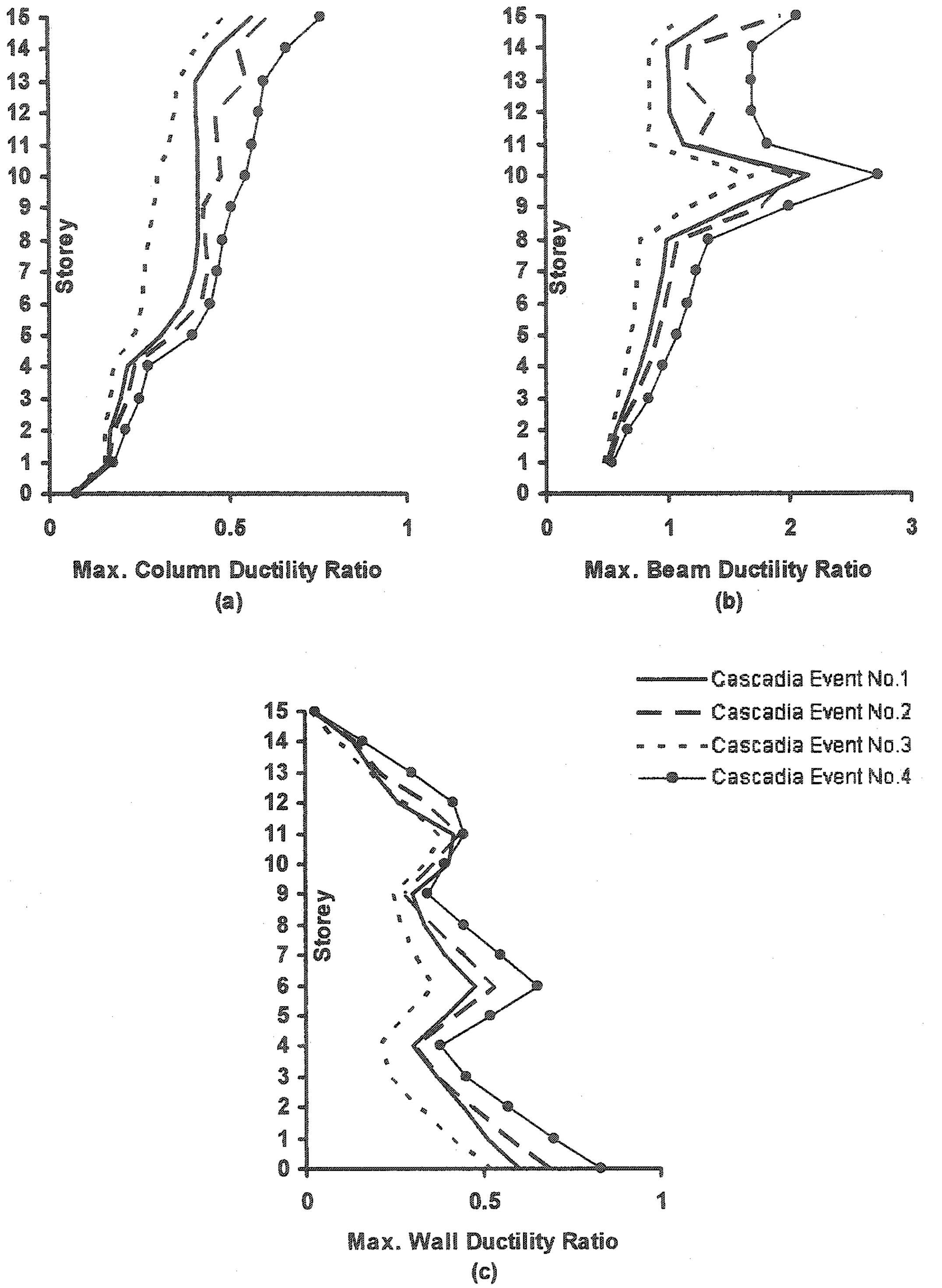

Fig. 4.47 Ductility Response for 15-Storey SHW Subjected to Cascadia Event Artificial Records for Vancouver

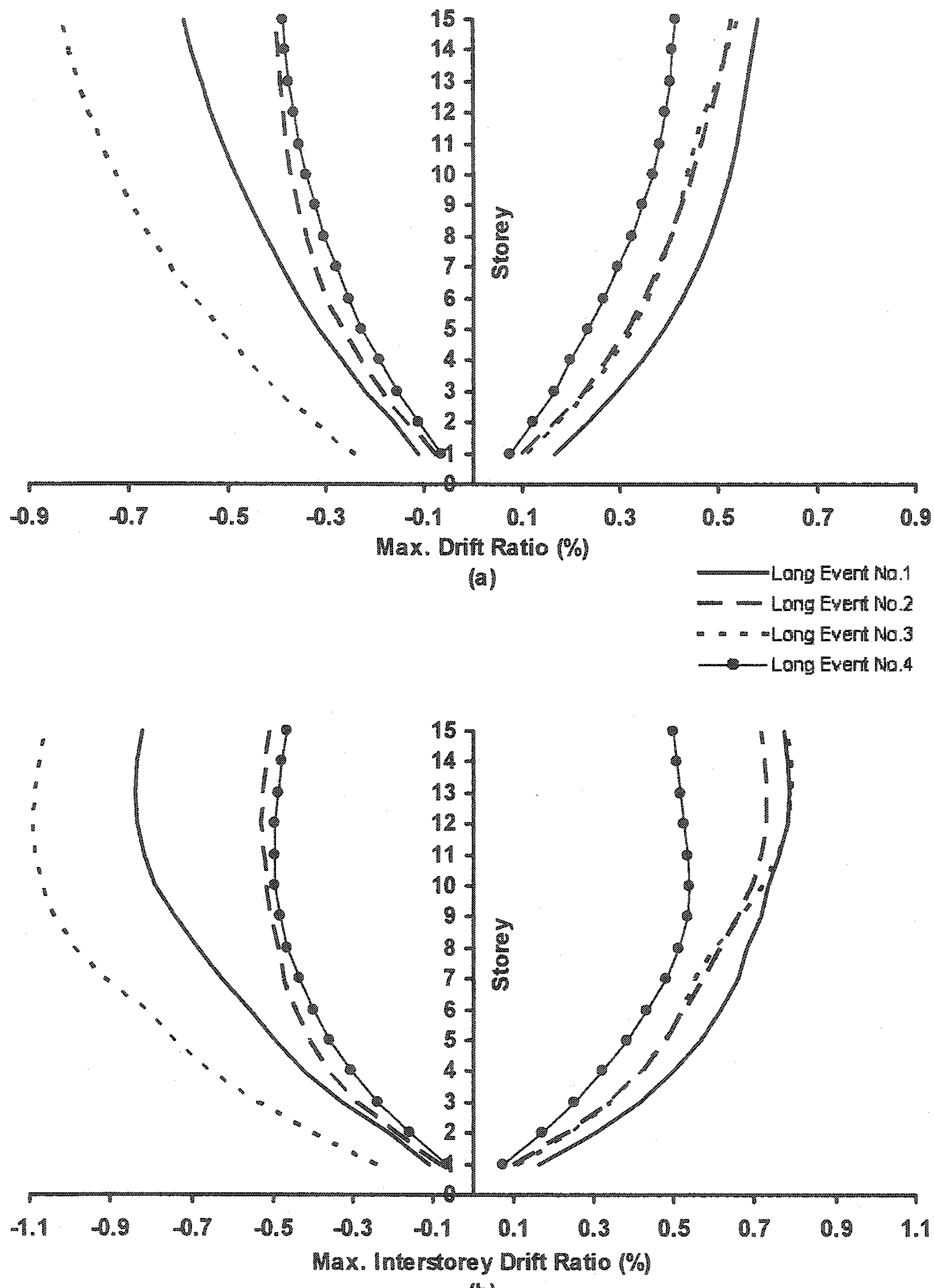

Fig. 4.48 Drift Response for 15-Storey SHW Subjected to Long Event Artificial Records for Vancouver

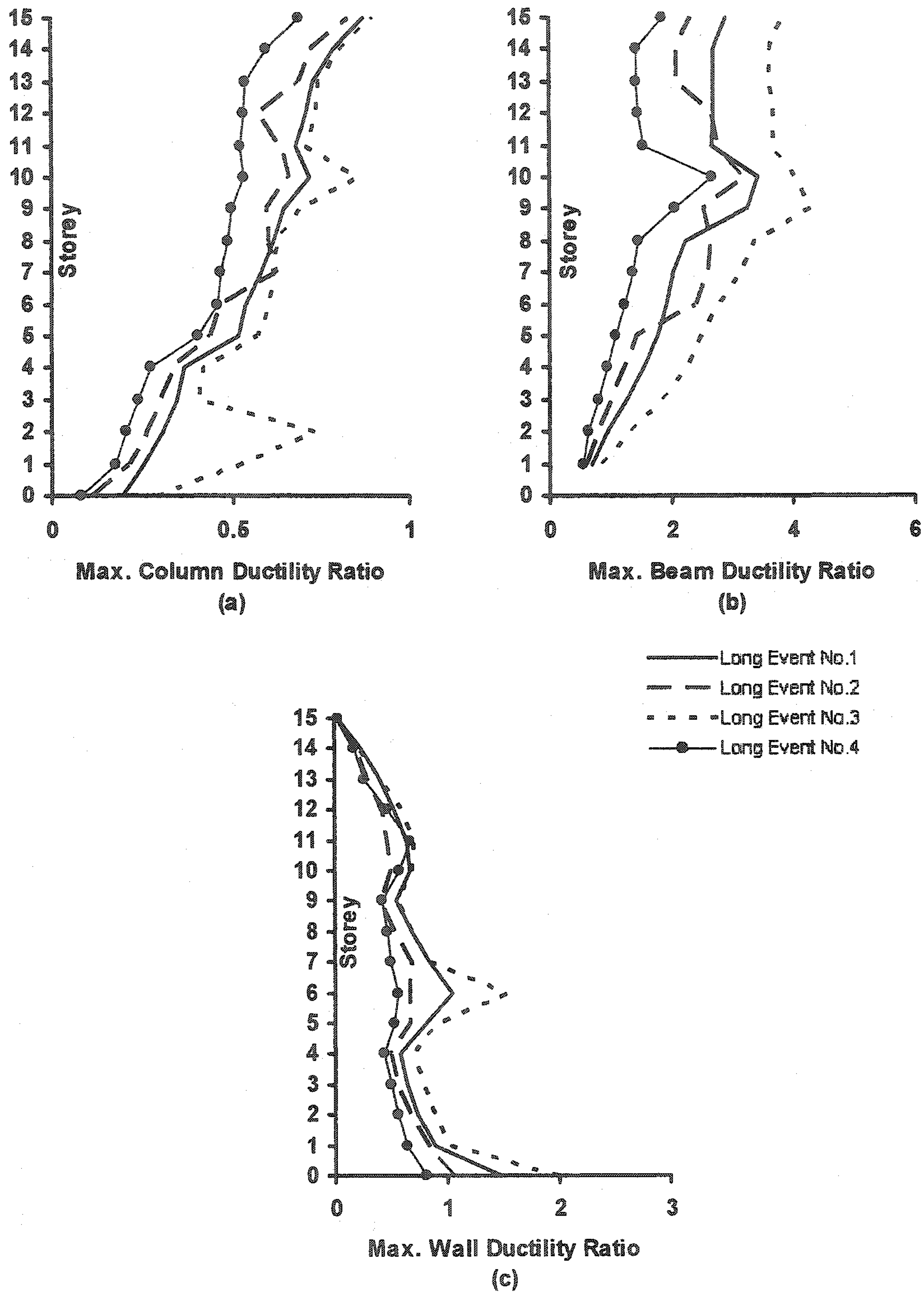

Fig. 4.49 Ductility Response for 15-Storey SHW Subjected to Long Event Artificial Records for Vancouver

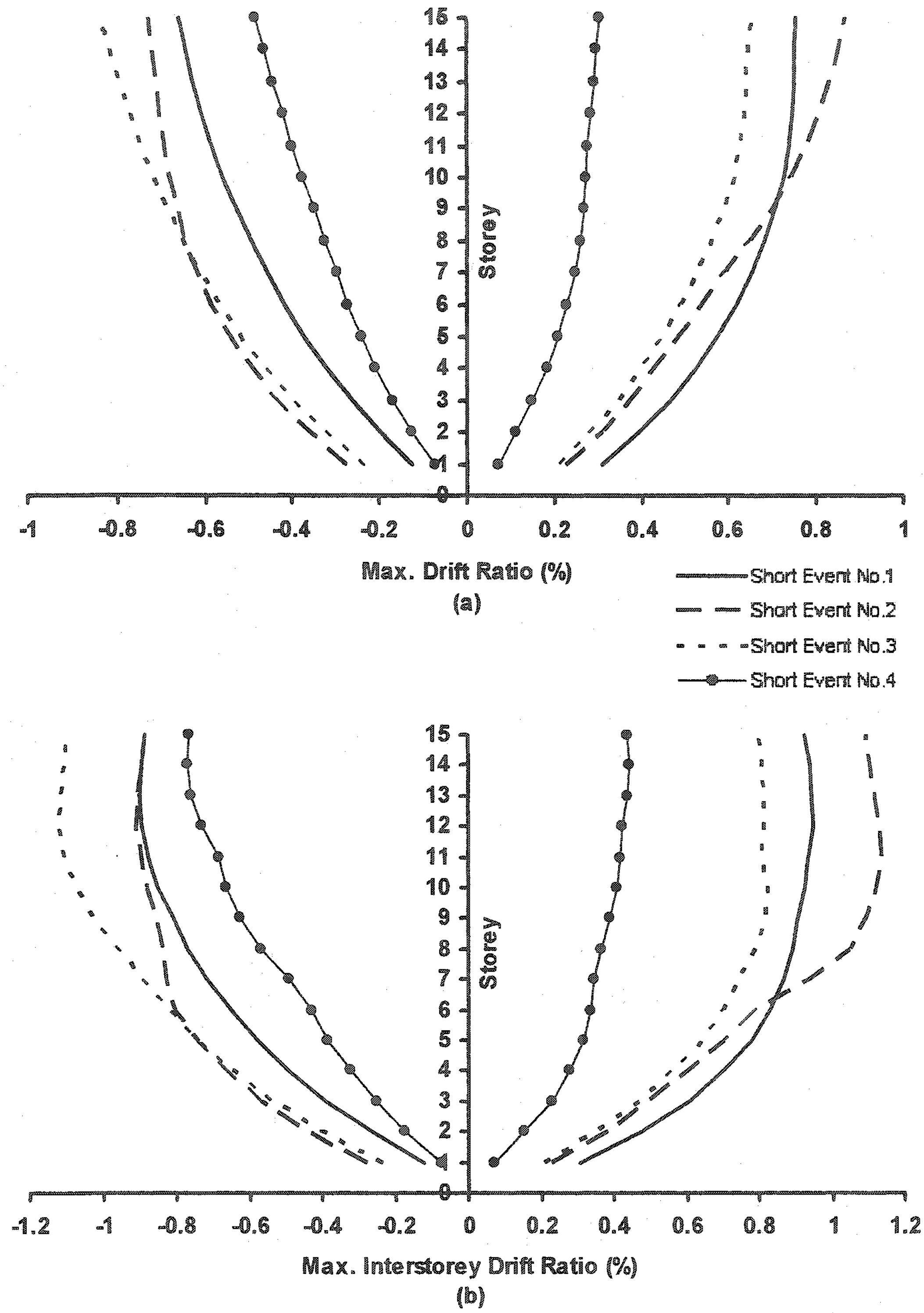

Fig. 4.50 Drift Response for 15-Storey SHW Subjected to Short Event Artificial Records for Vancouver

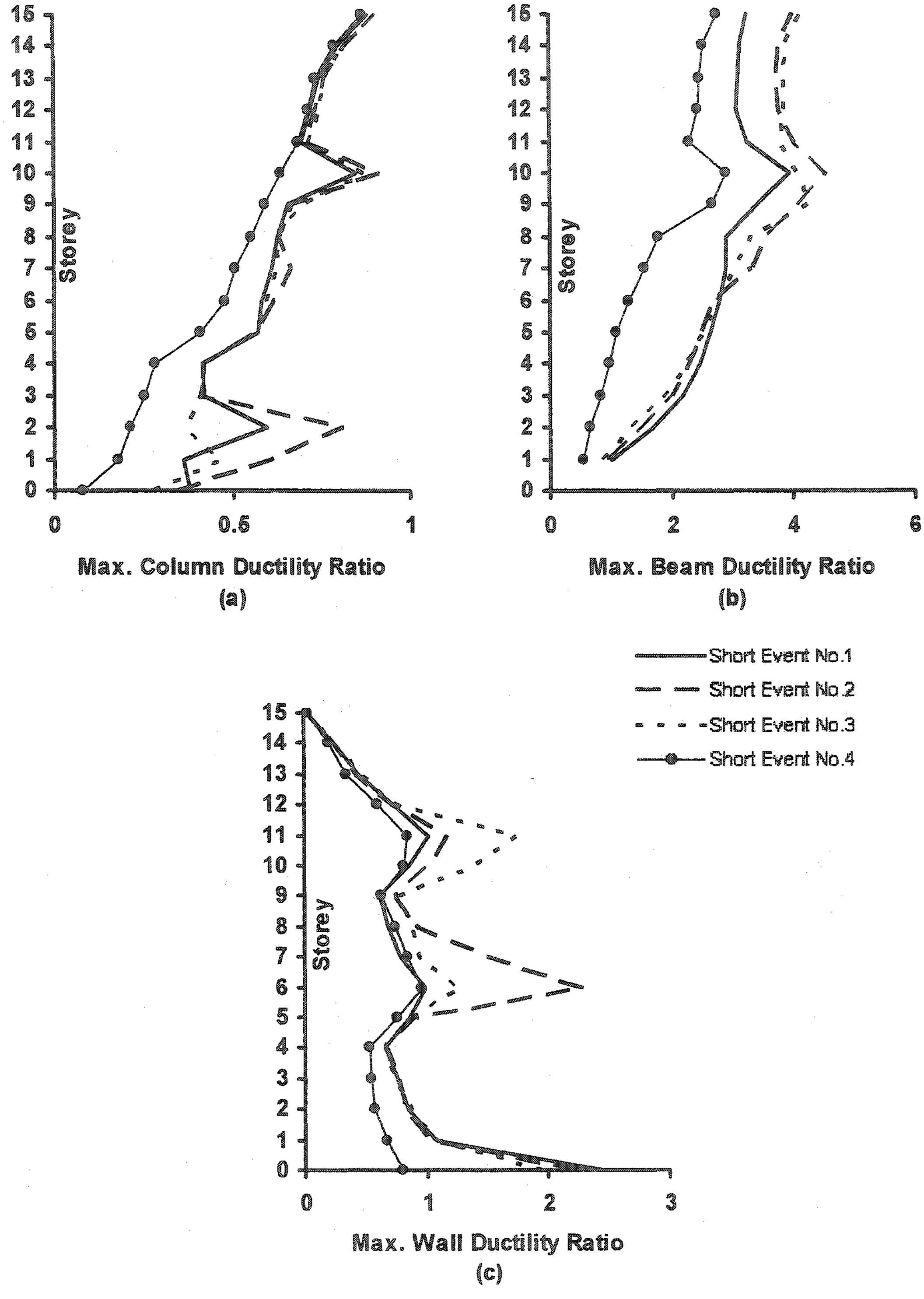

Fig. 4.51 Ductility Response for 15-Storey SHW Subjected to Short Event Artificial Records for Vancouver

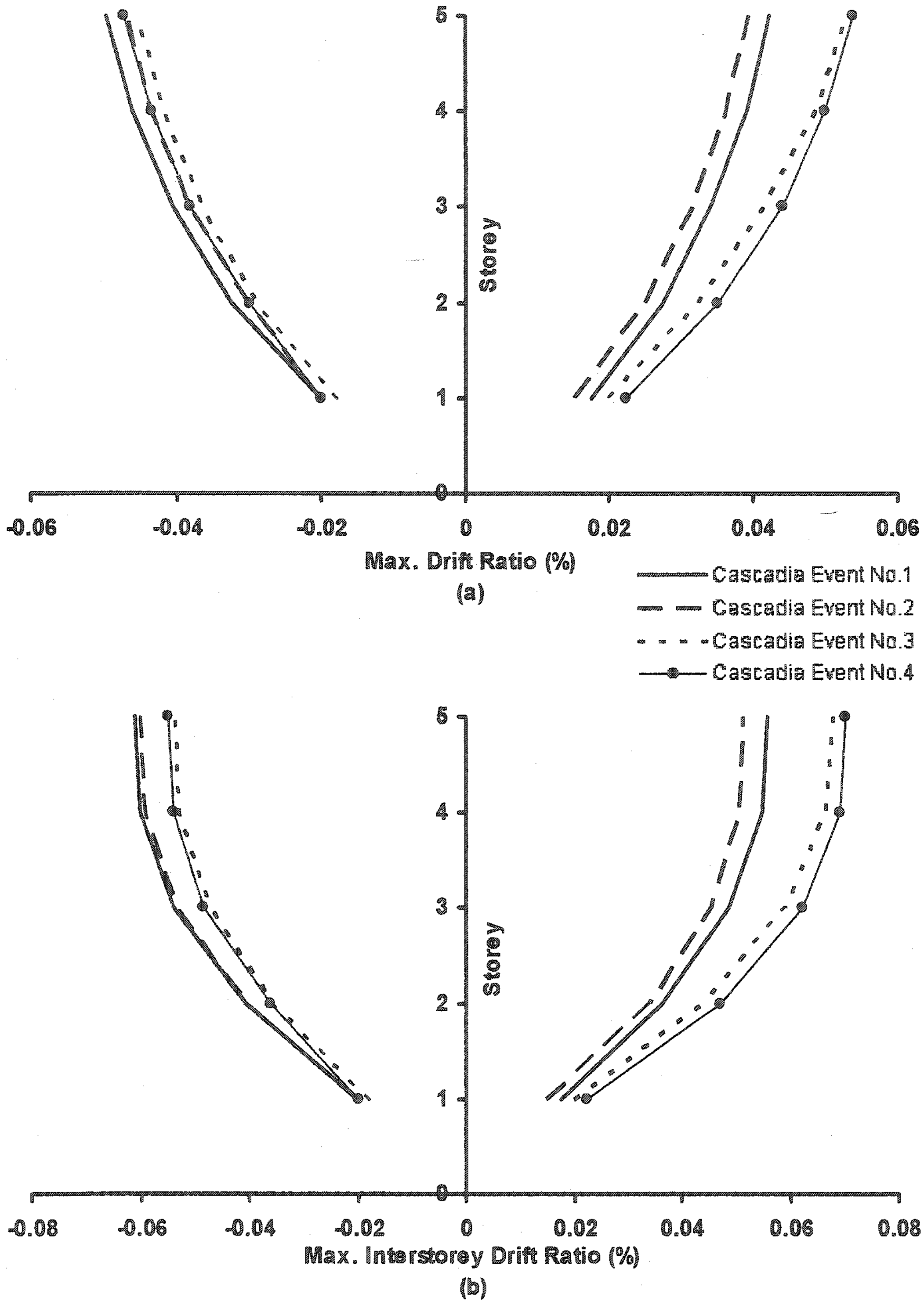

Fig. 4.52 Drift Response for 5-Storey CW Subjected to Cascadia Event Artificial Records for Vancouver

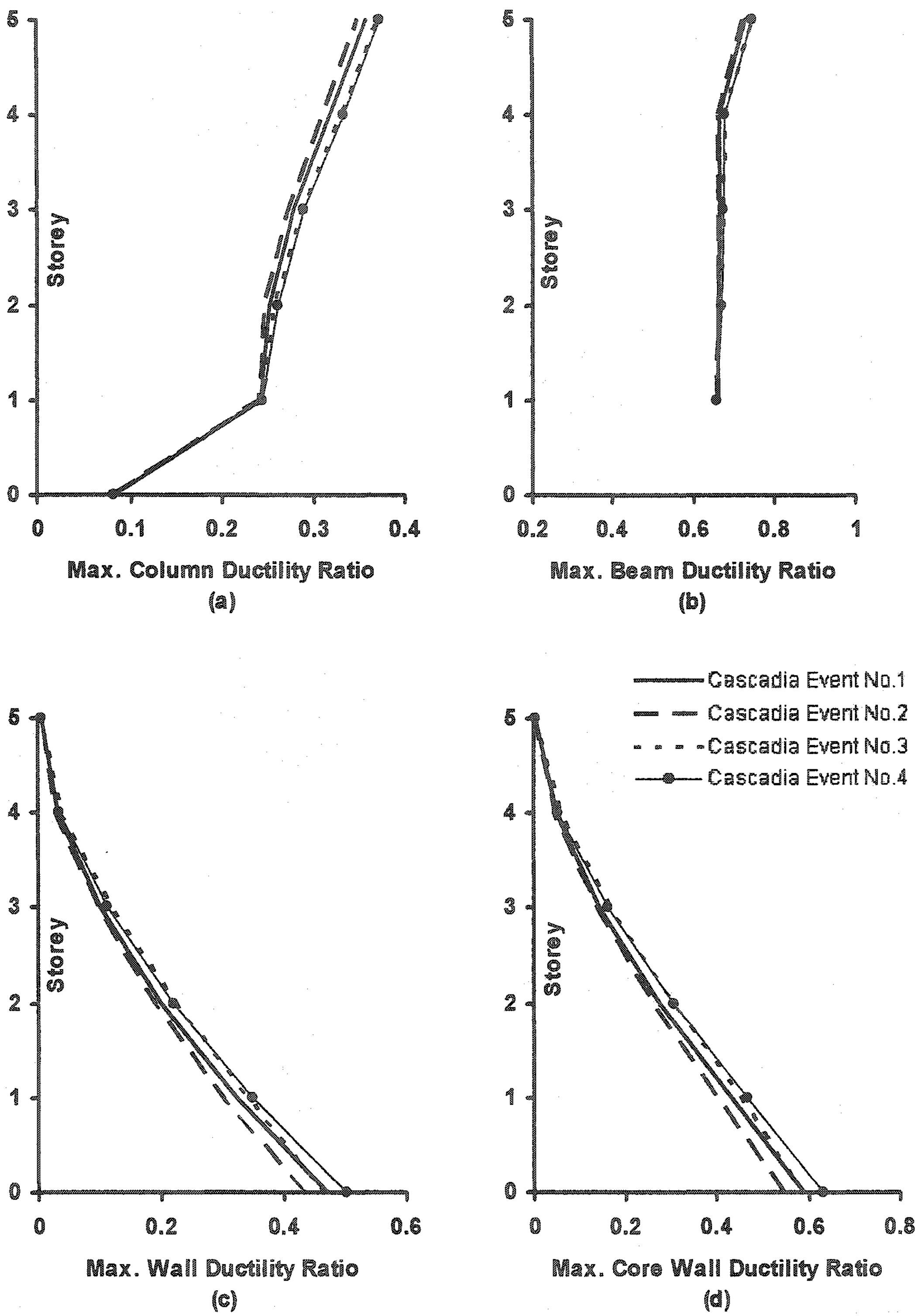

Fig. 4.53 Ductility Response for 5-Storey CW Subjected to Cascadia Event Artificial Records for Vancouver

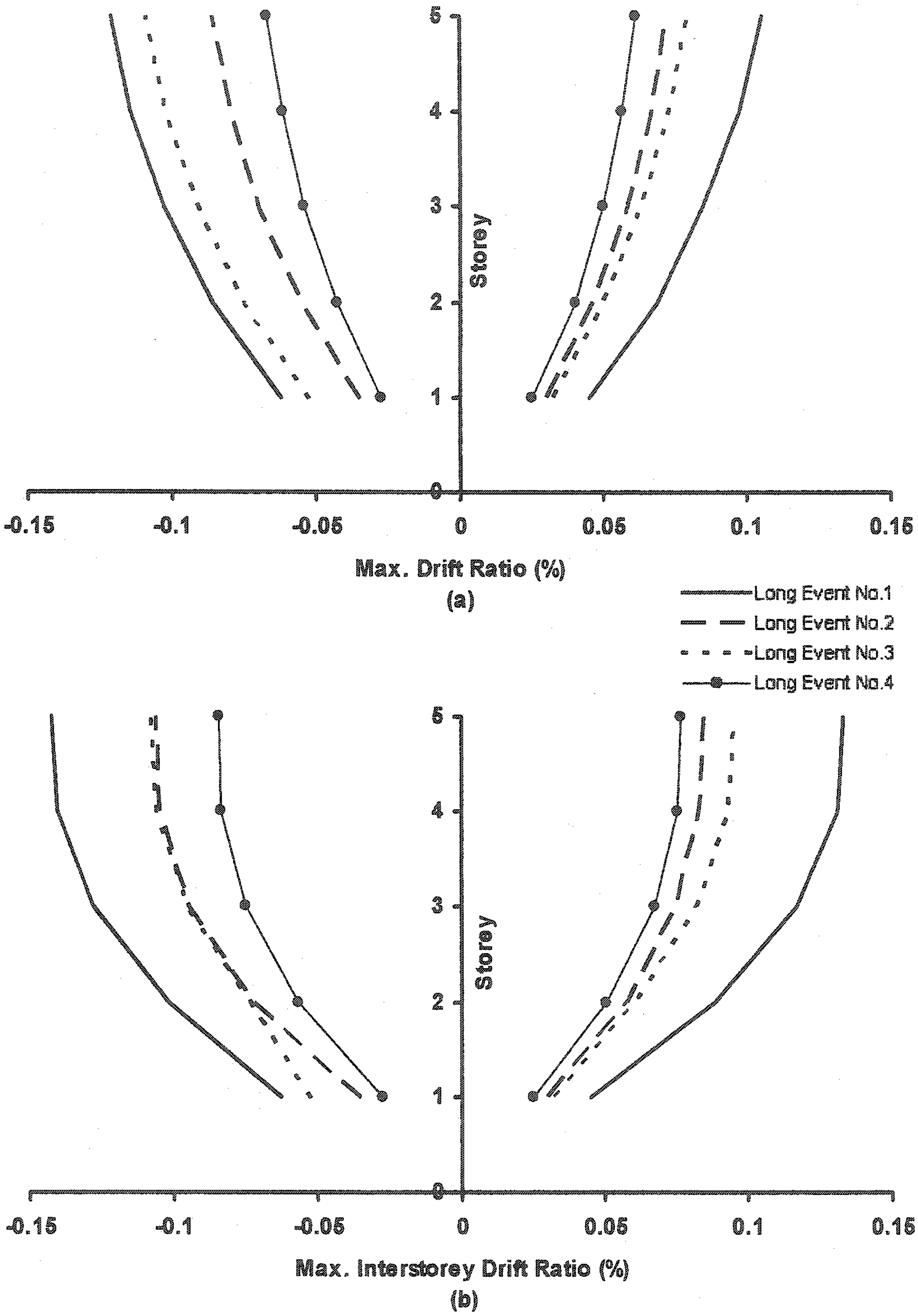

Fig. 4.54 Drift Response for 5-Storey CW Subjected to Long Event Artificial Records for Vancouver

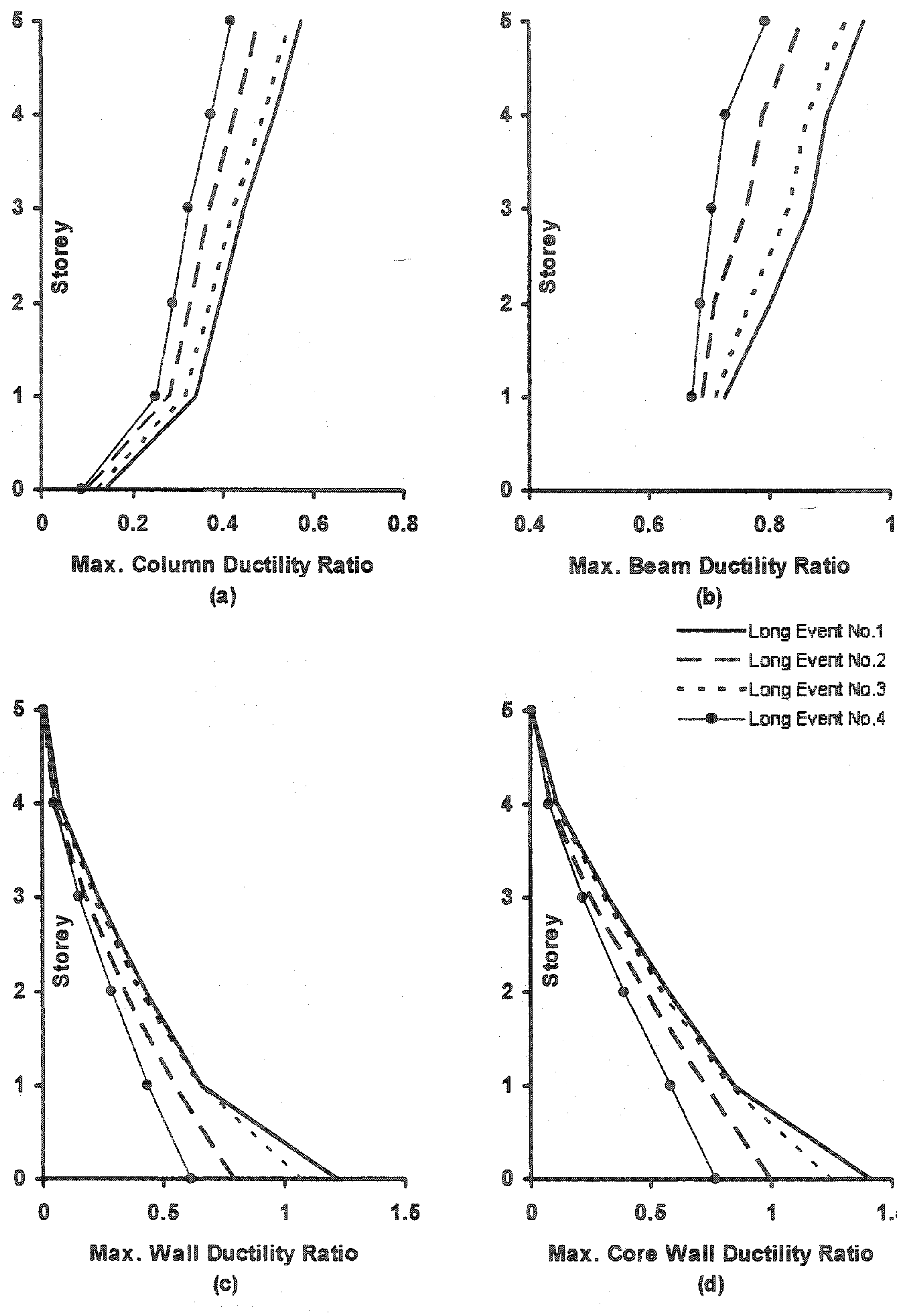

Fig. 4.55 Ductility Response for 5-Storey CW Subjected to Long Event Artificial Records for Vancouver

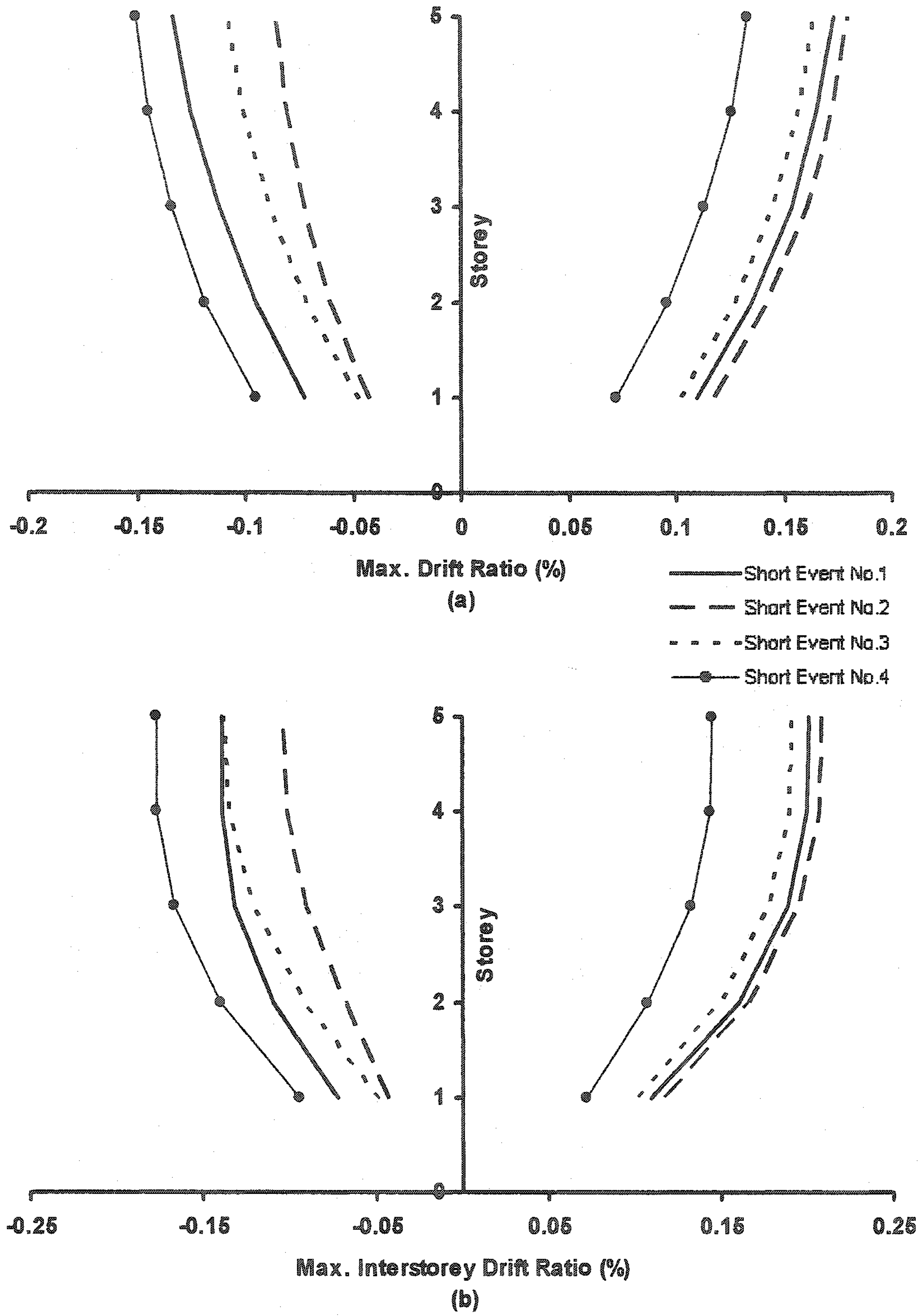

Fig. 4.56 Drift Response for 5-Storey CW Subjected to Short Event Artificial Records for Vancouver

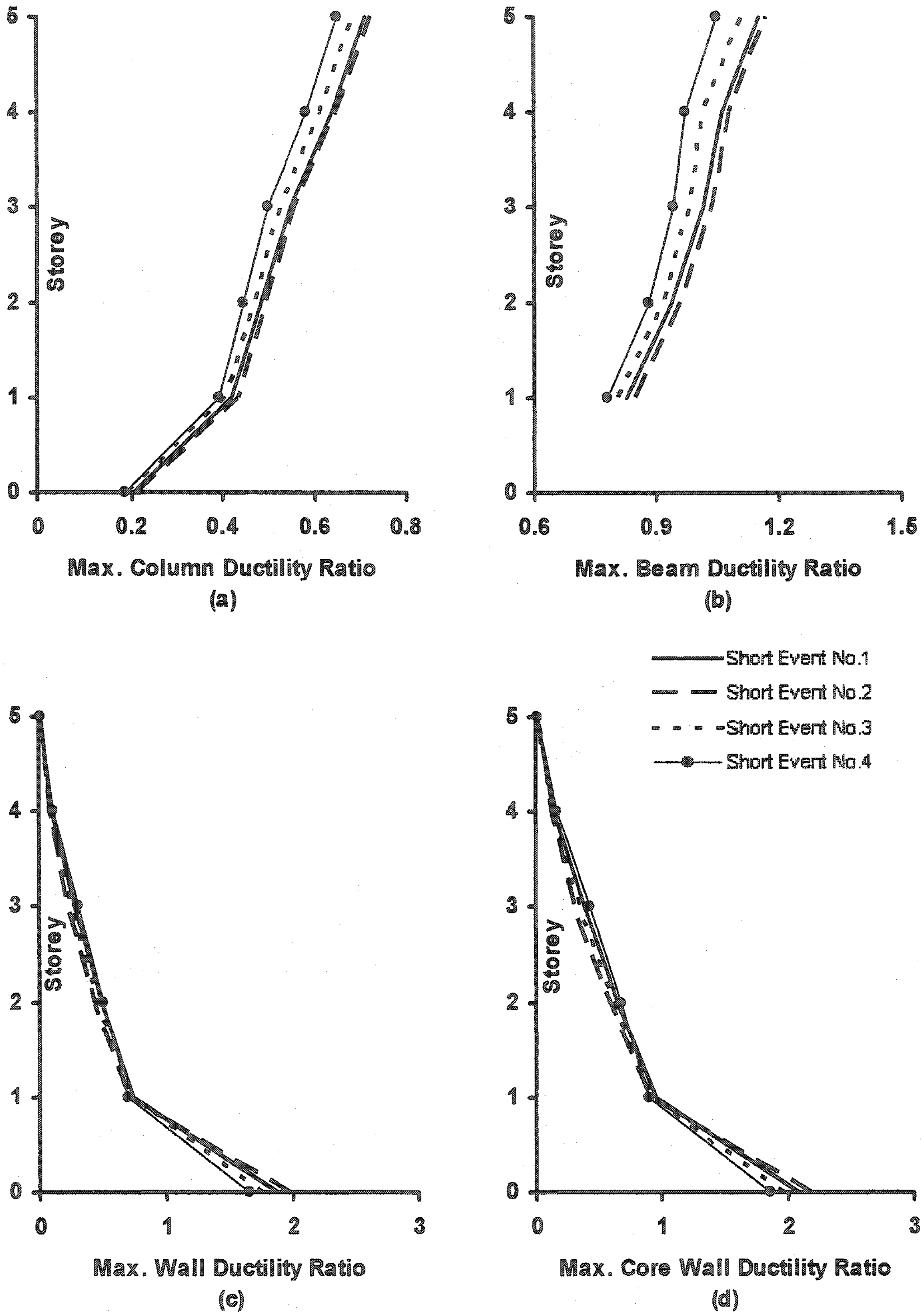

Fig. 4.57 Ductility Response for 5-Storey CW Subjected to Short Event Artificial Records for Vancouver

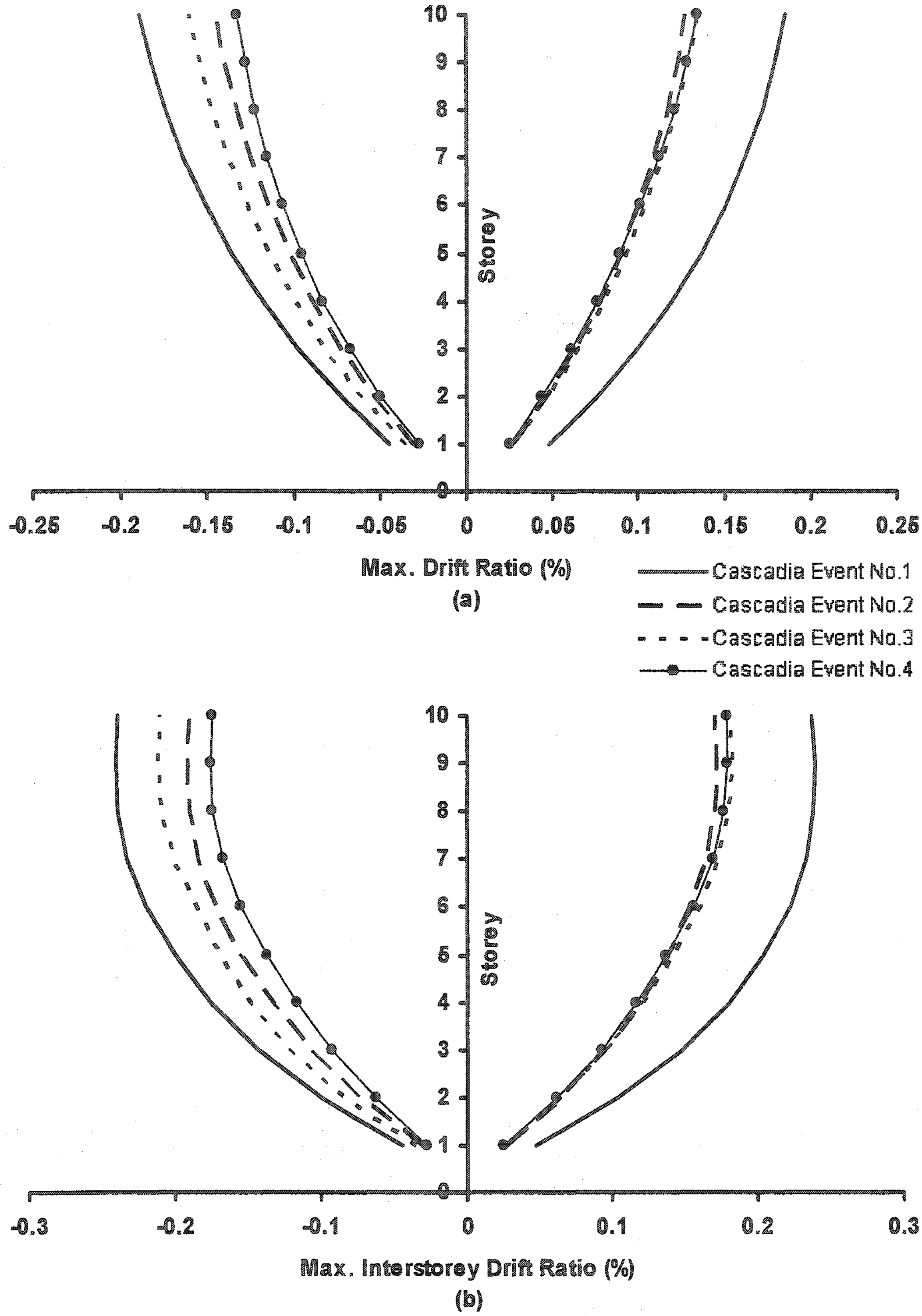

Fig. 4.58 Drift Response for 10-Storey CW Subjected to Cascadia Event Artificial Records for Vancouver

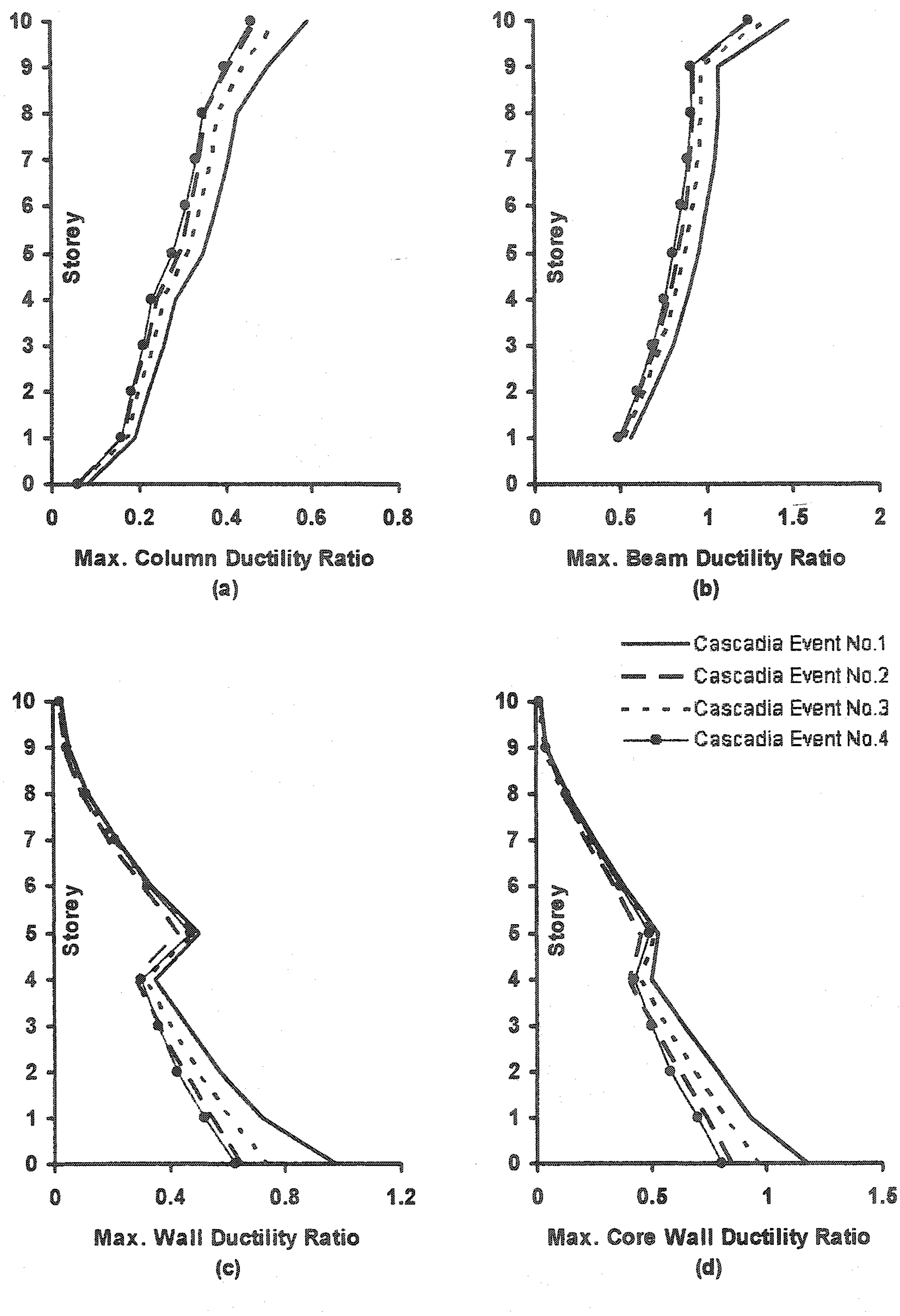

Fig. 4.59 Ductility Response for 10-Storey CW Subjected to Cascadia Event Artificial Records for Vancouver

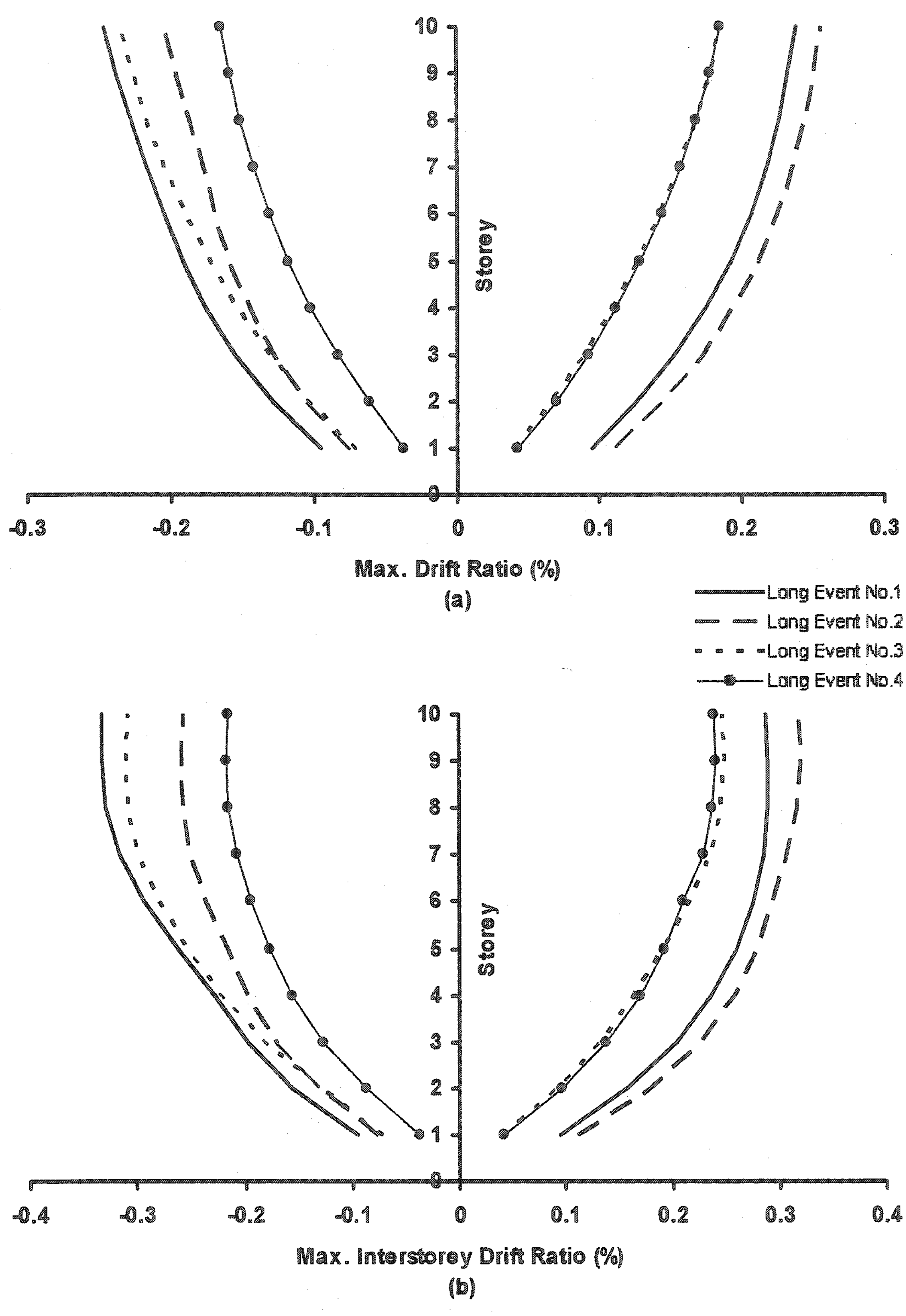

Fig. 4.60 Drift Response for 10-Storey CW Subjected to Long Event Artificial Records for Vancouver

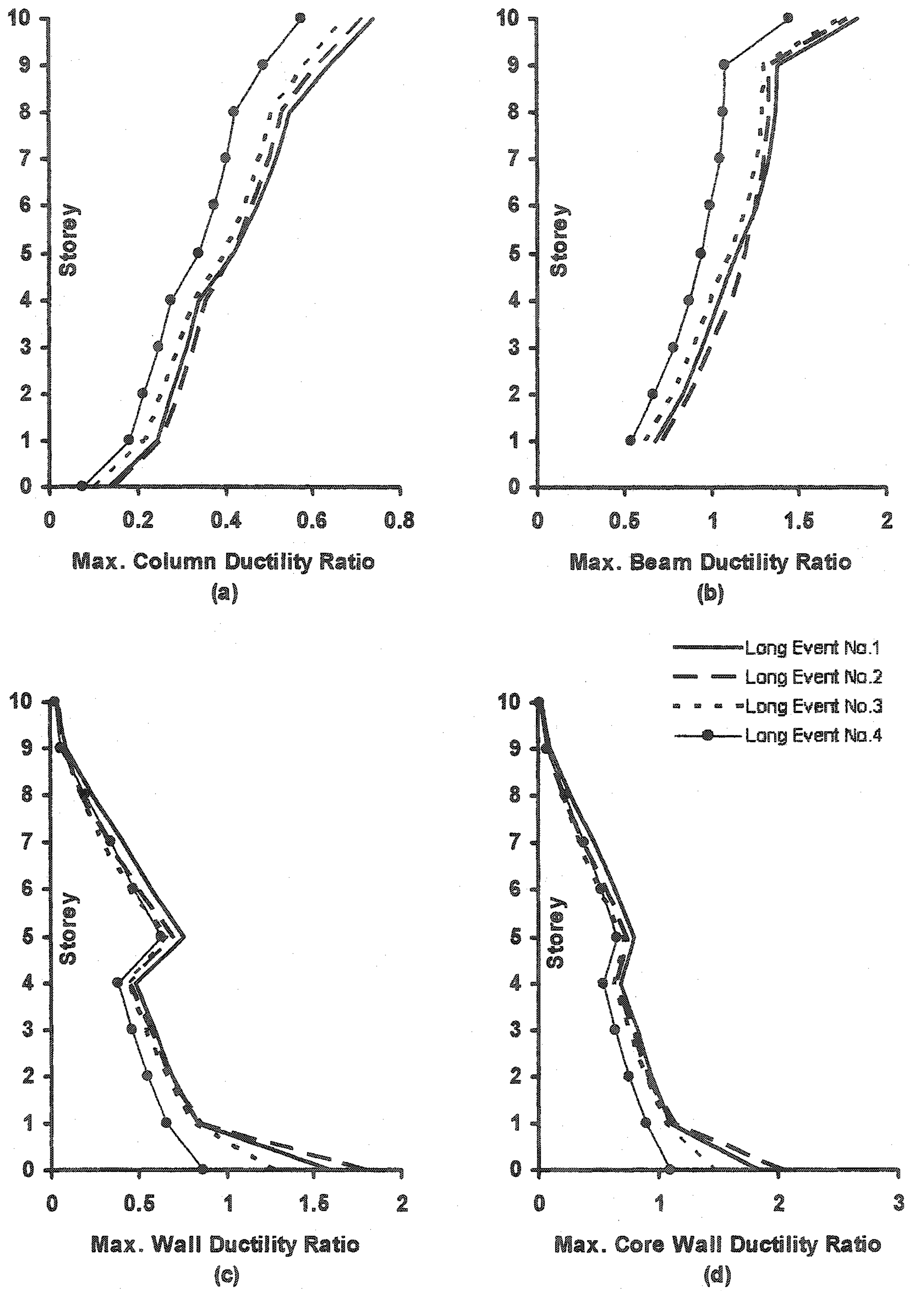

Fig. 4.61 Ductility Response for 10-Storey CW Subjected to Long Event Artificial Records for Vancouver

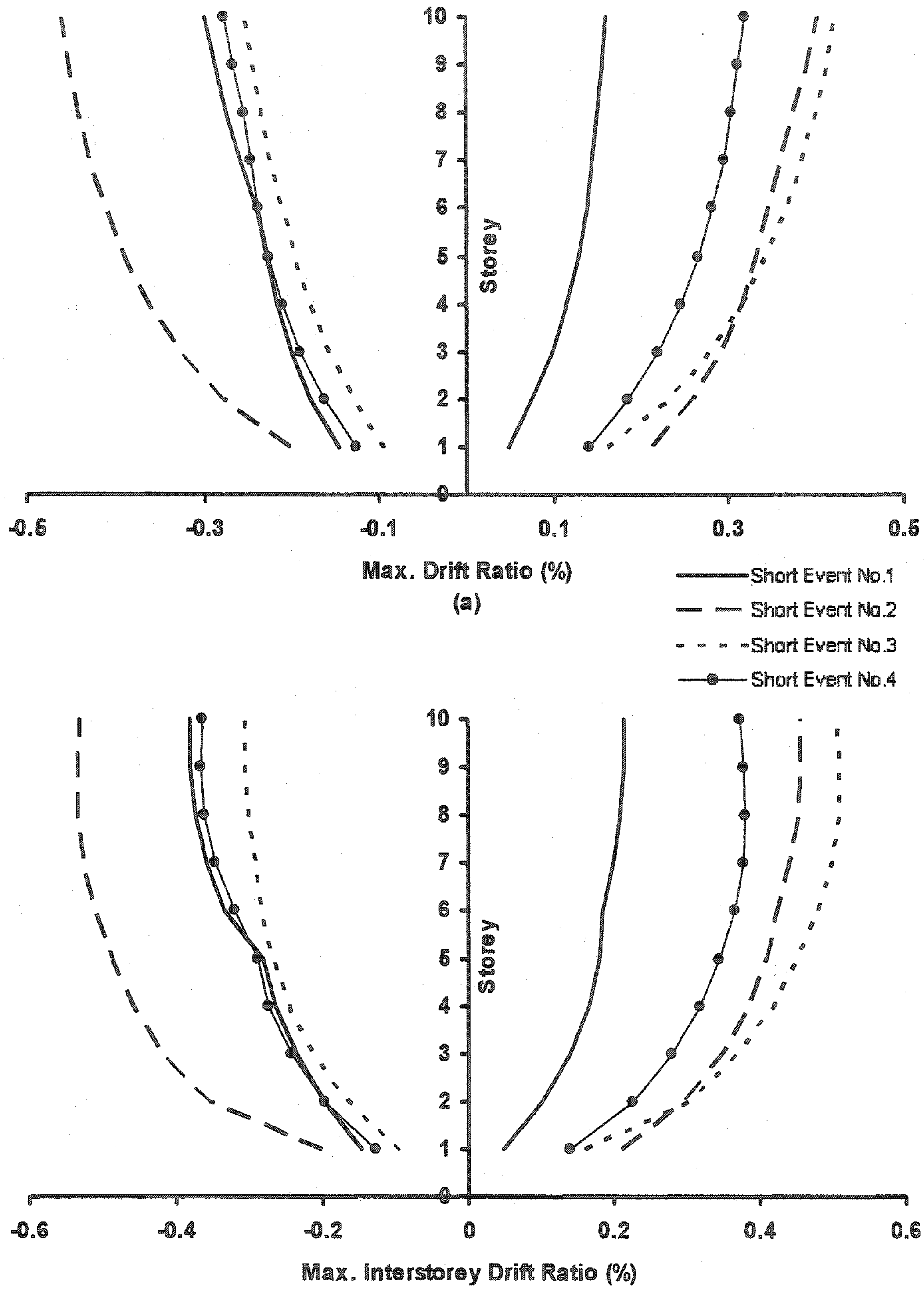

Fig. 4.62 Drift Response for 10-Storey CW Subjected to Short Event Artificial Records for Vancouver

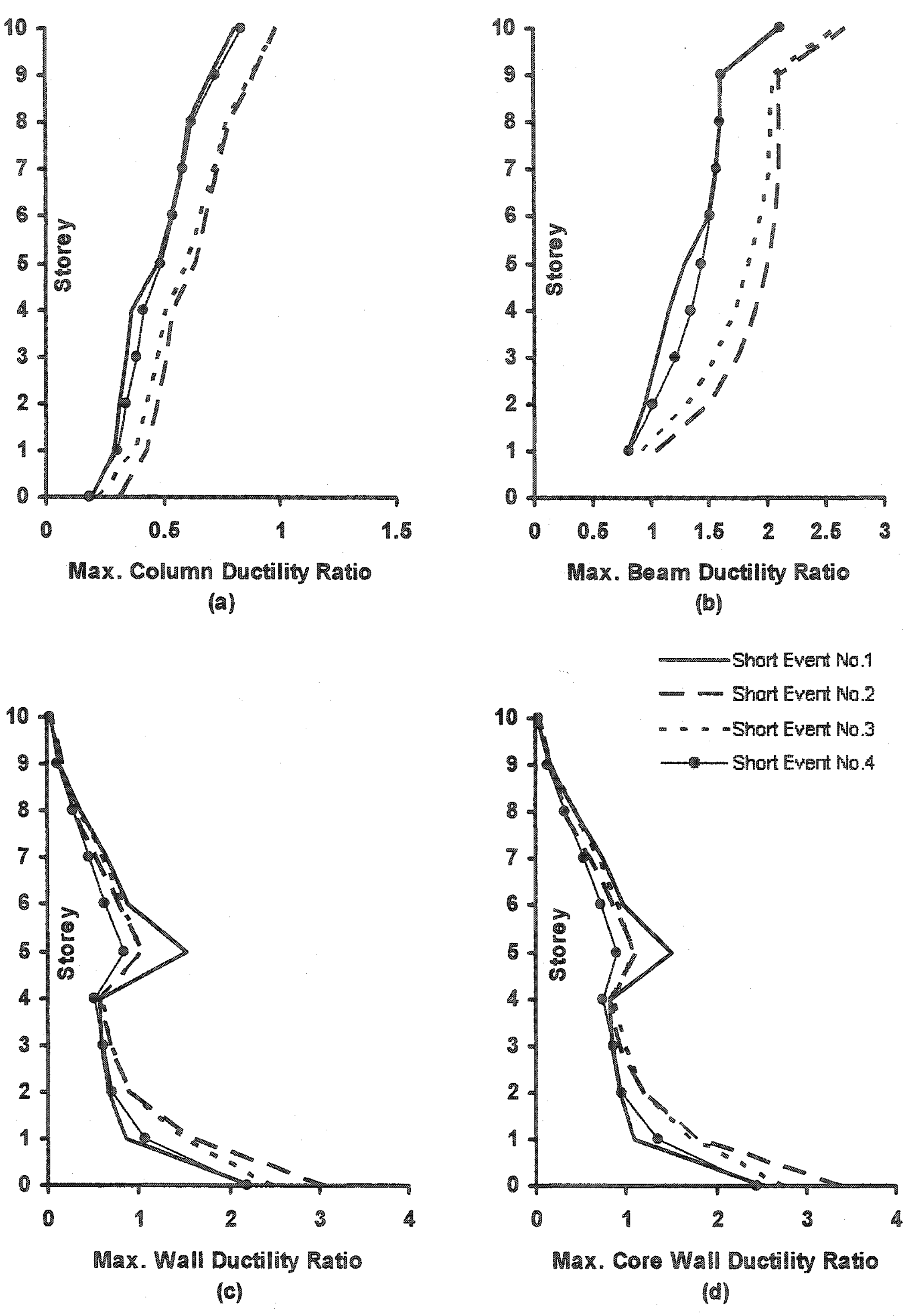

Fig. 4.63 Ductility Response for 10-Storey CW Subjected to Short Event Artificial Records for Vancouver

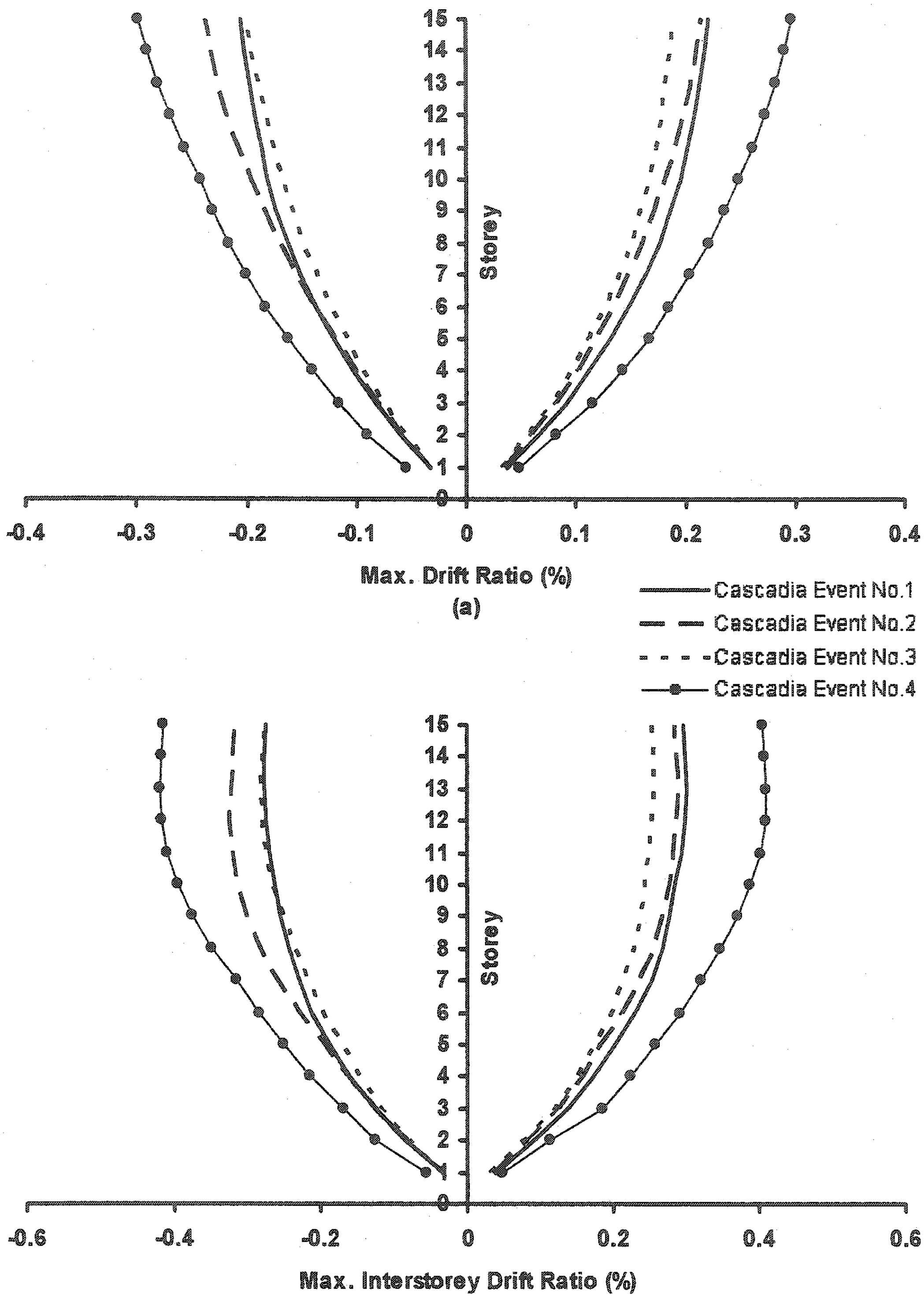

Fig. 4.64 Drift Response for 15-Storey CW Subjected to Cascadia Event Artificial Records for Vancouver

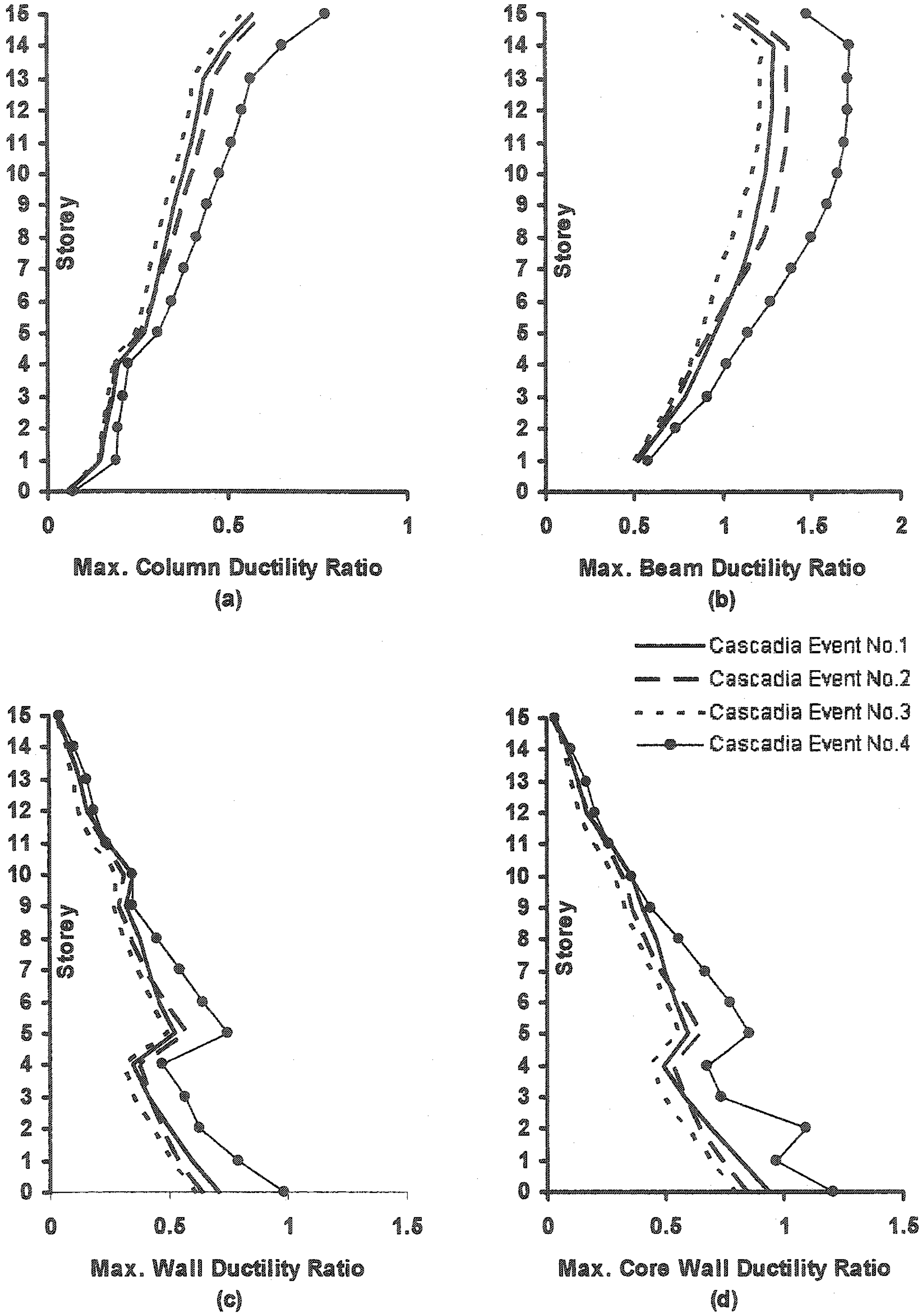

Fig. 4.65 Ductility Response for 15-Storey CW Subjected to Cascadia Event Artificial Records for Vancouver

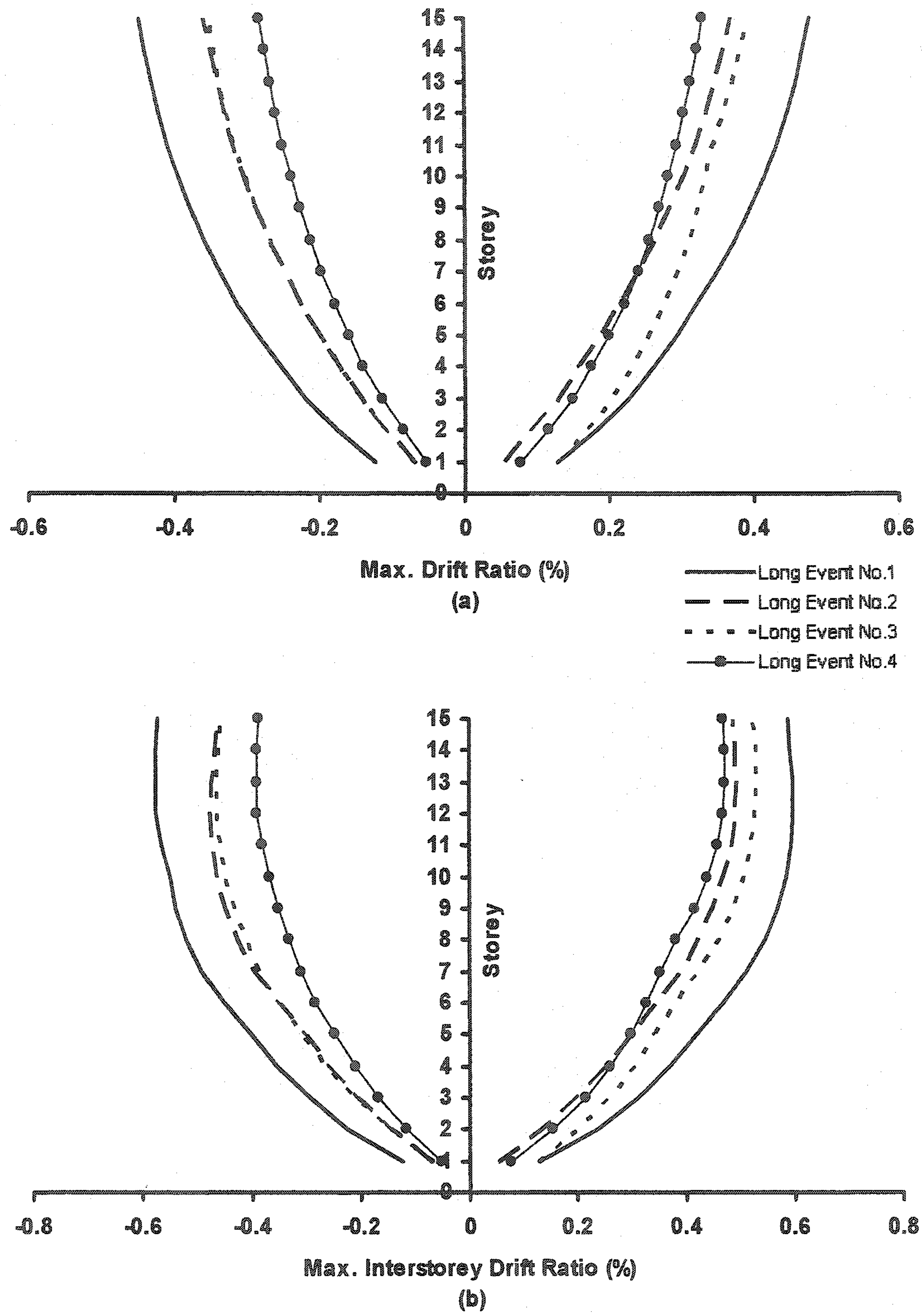

Fig. 4.66 Drift Response for 15-Storey CW Subjected to Long Event Artificial Records for Vancouver

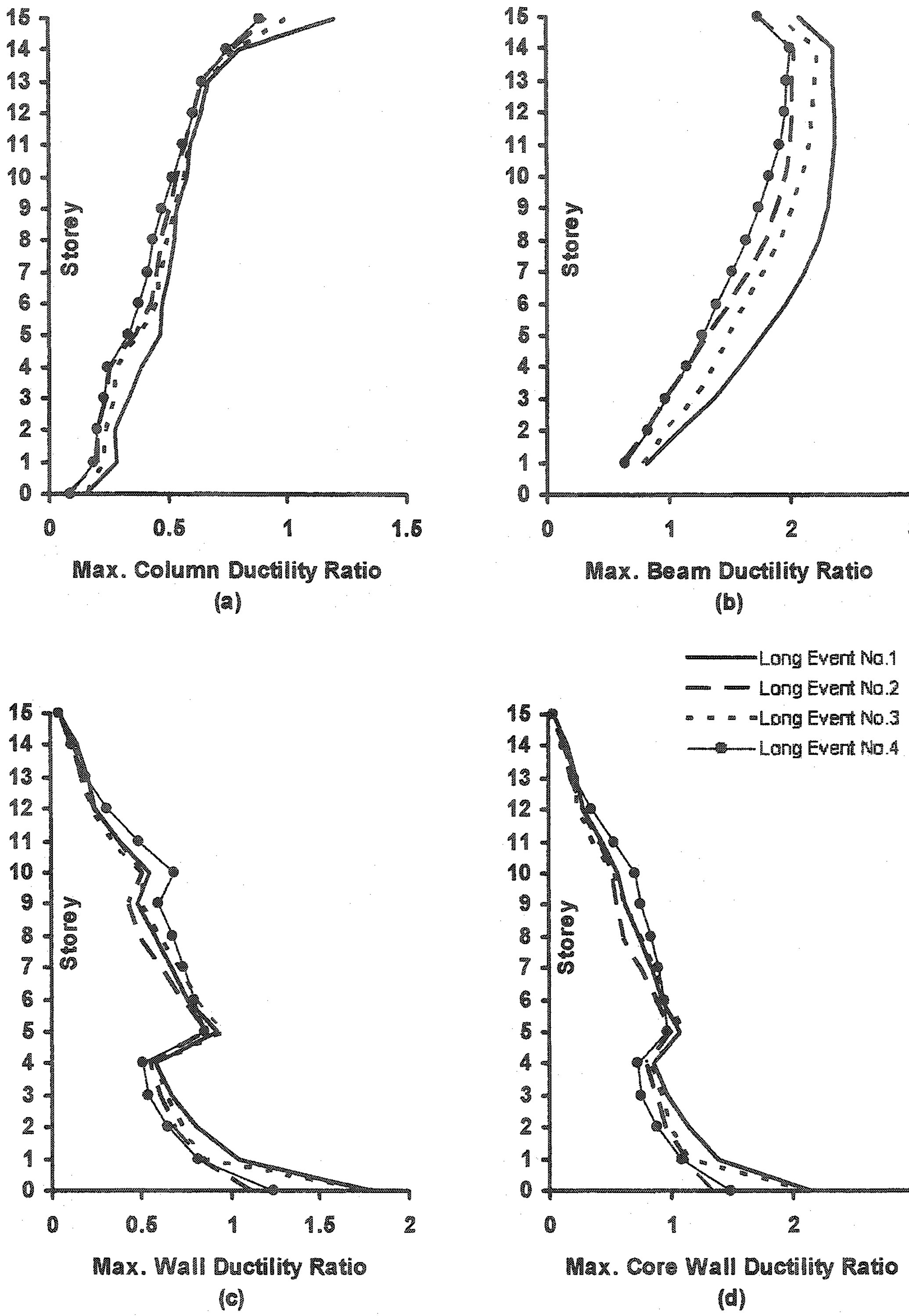

Fig. 4.67 Ductility Response for 15-Storey CW Subjected to Long Event Artificial Records for Vancouver

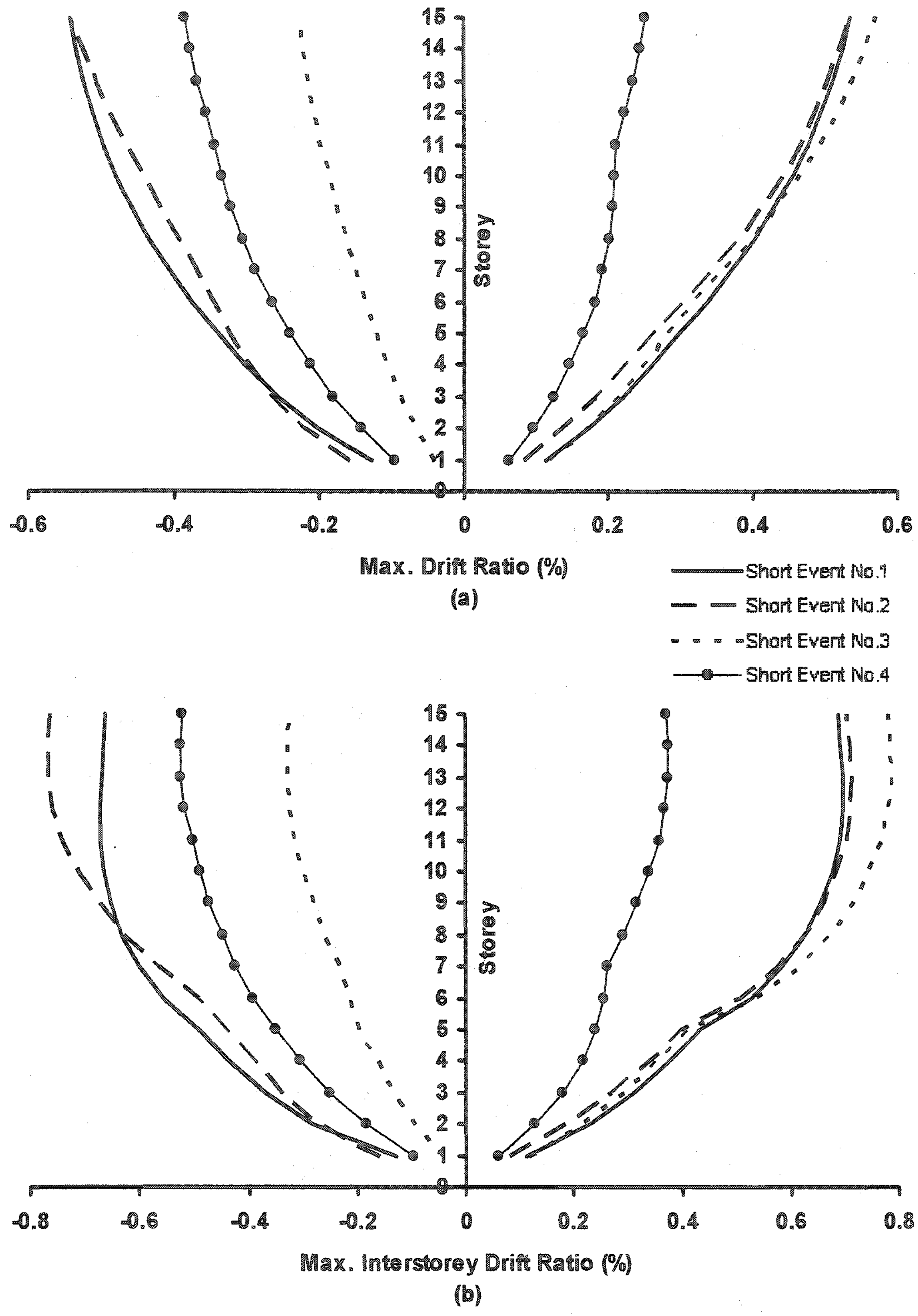

Fig. 4.68 Drift Response for 15-Storey CW Subjected to Short Event Artificial Records for Vancouver

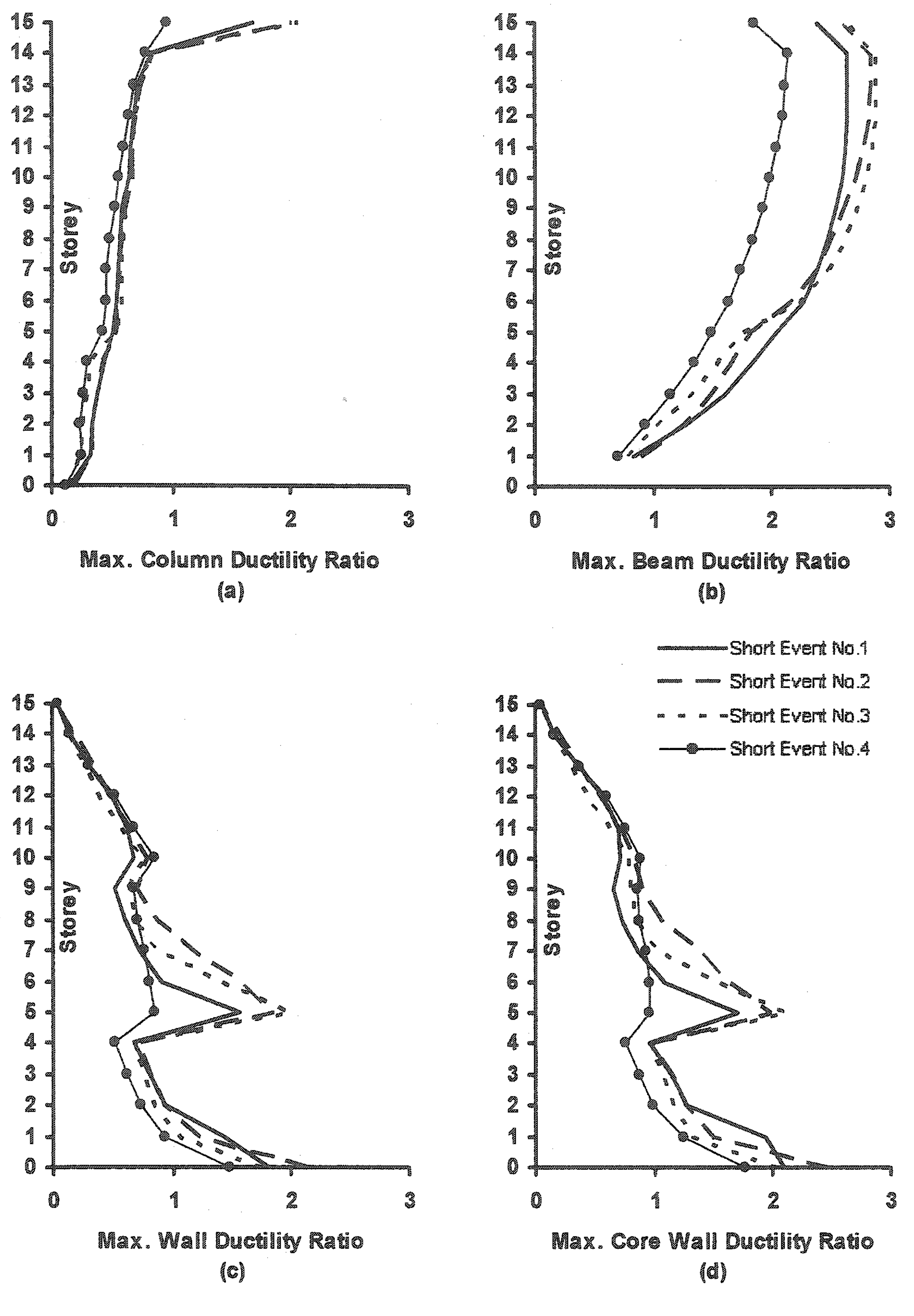

Fig. 4.69 Ductility Response for 15-Storey CW Subjected to Short Event Artificial Records for Vancouver

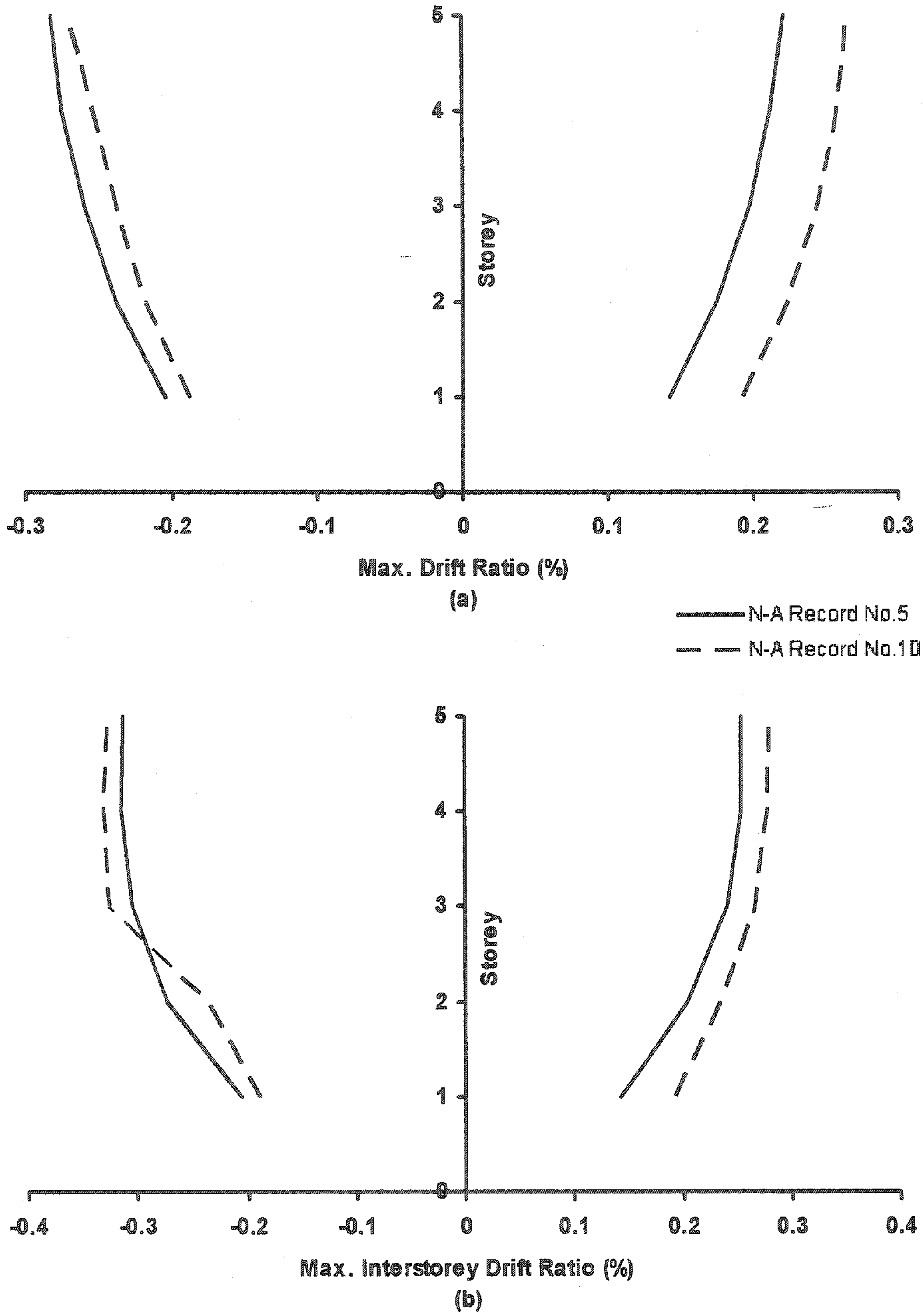

Fig. 4.70 Drift Response for 5-Storey SHW Subjected to N-A Artificial Records for Vancouver

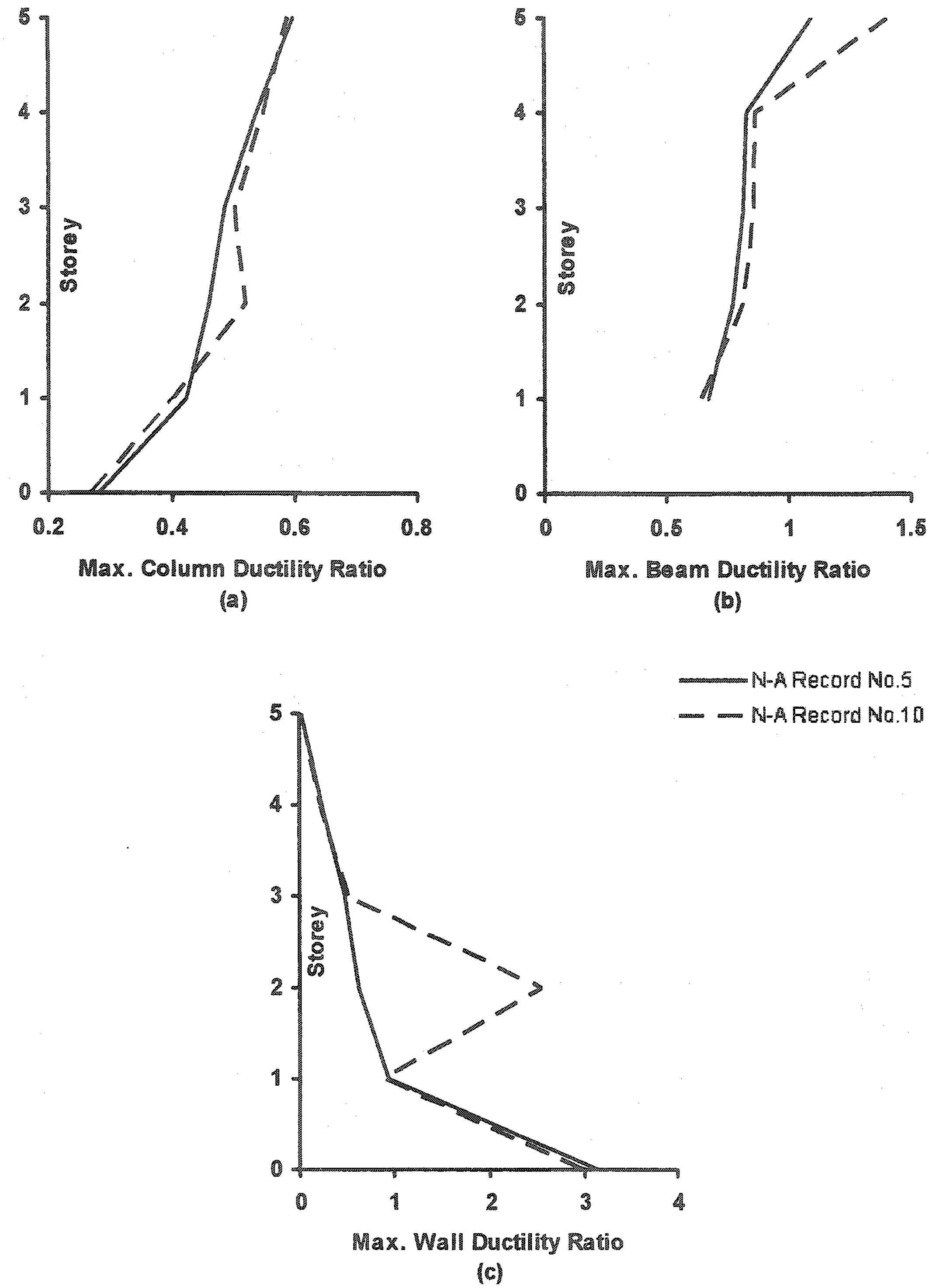

Fig. 4.71 Ductility Response for 5-Storey SHW Subjected to N-A Artificial Records for Vancouver

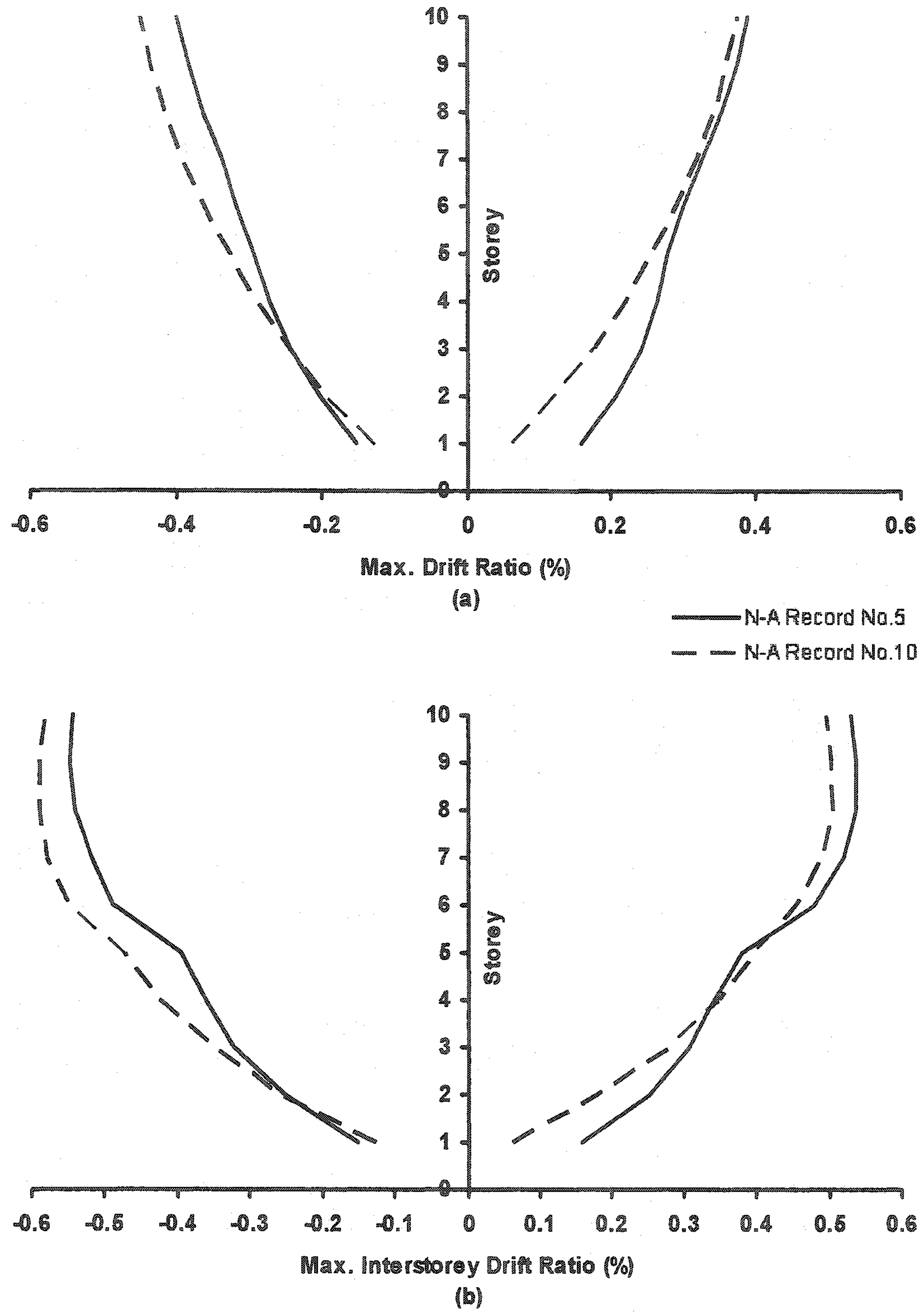

Fig. 4.72 Drift Response for 10-Storey SHW Subjected to N-A Artificial Records for Vancouver

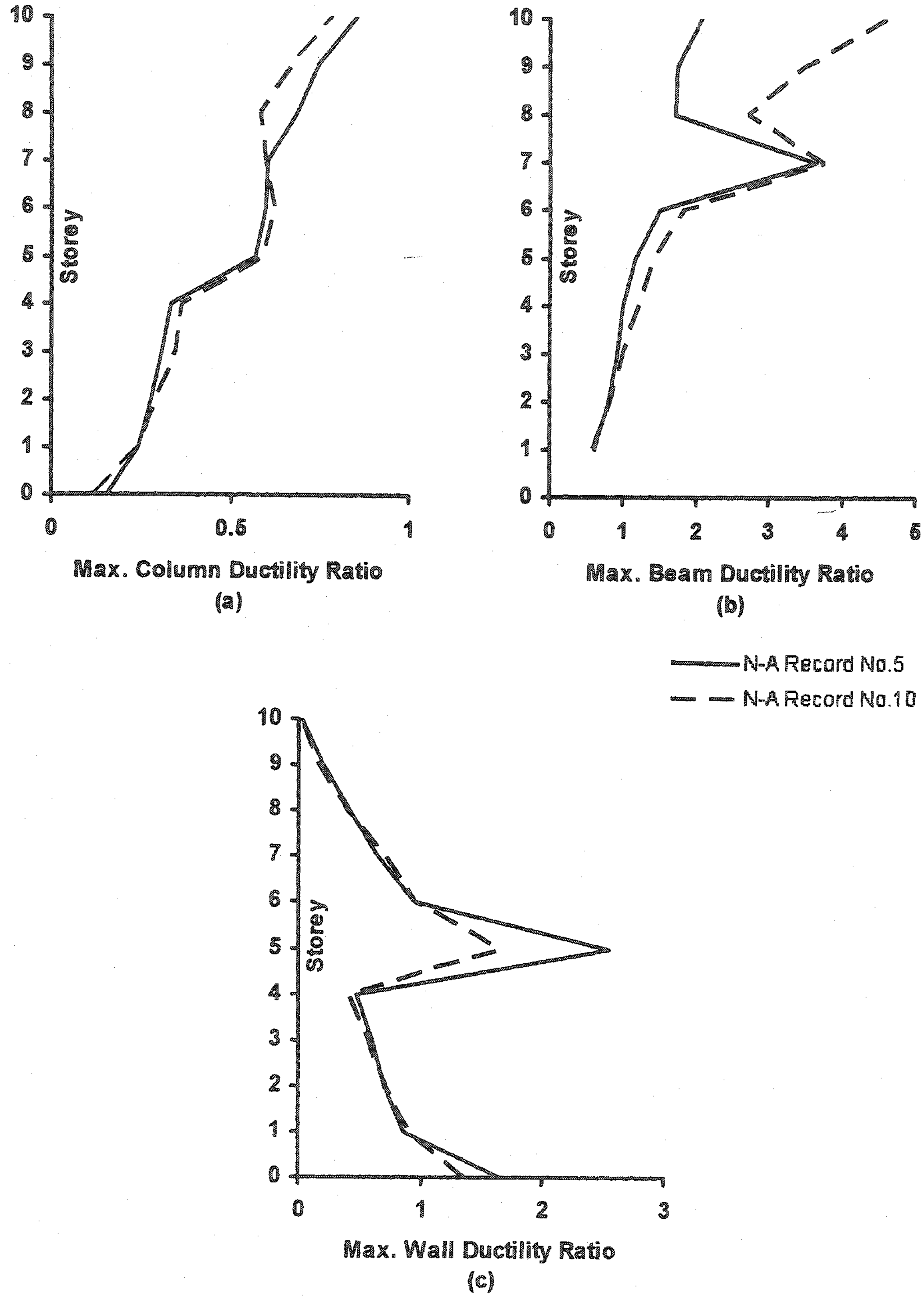

Fig. 4.73 Ductility Response for 10-Storey SHW Subjected to N-A Artificial Records for Vancouver

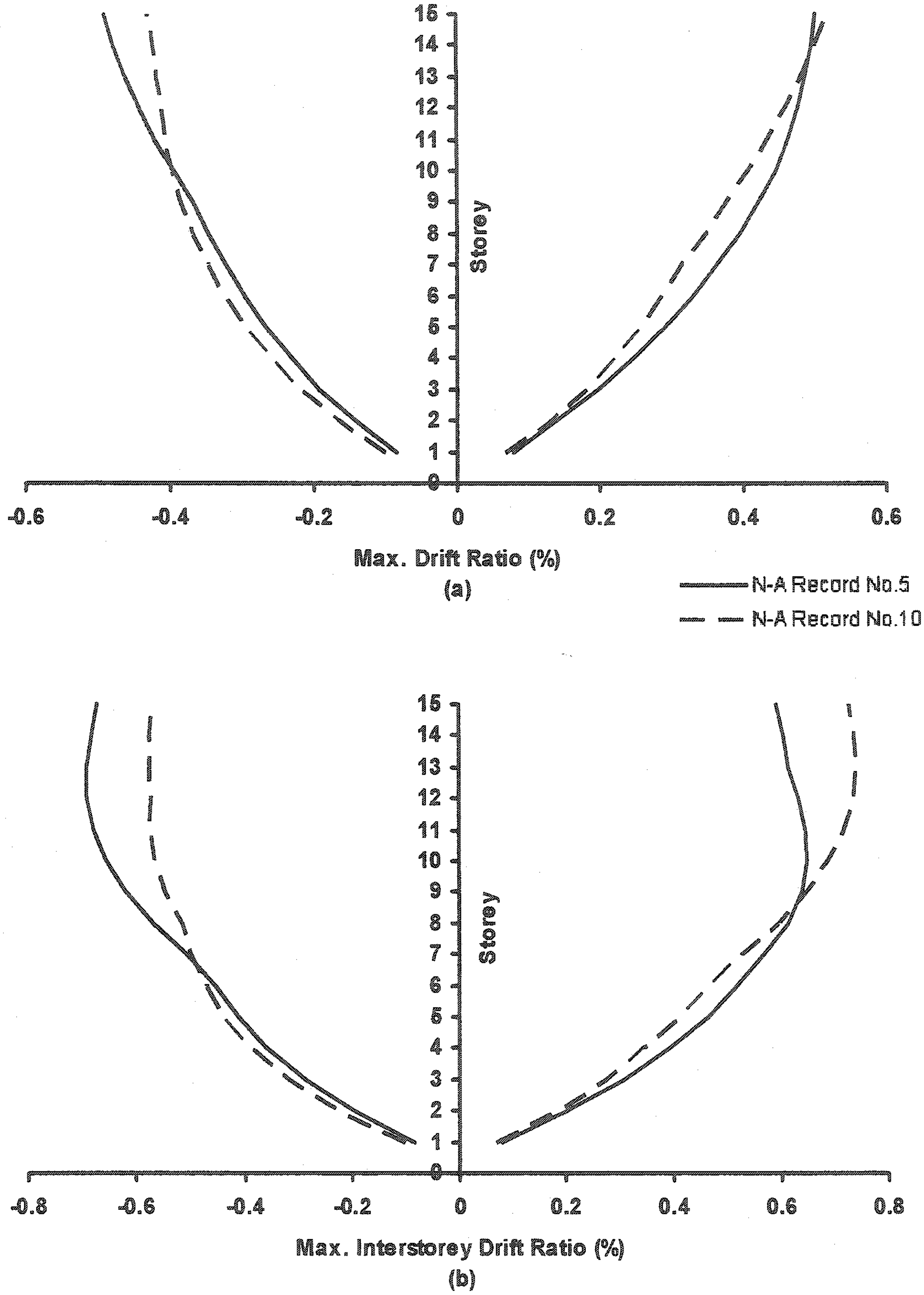

Fig. 4.74 Drift Response for 15-Storey SHW Subjected to N-A Artificial Records for Vancouver

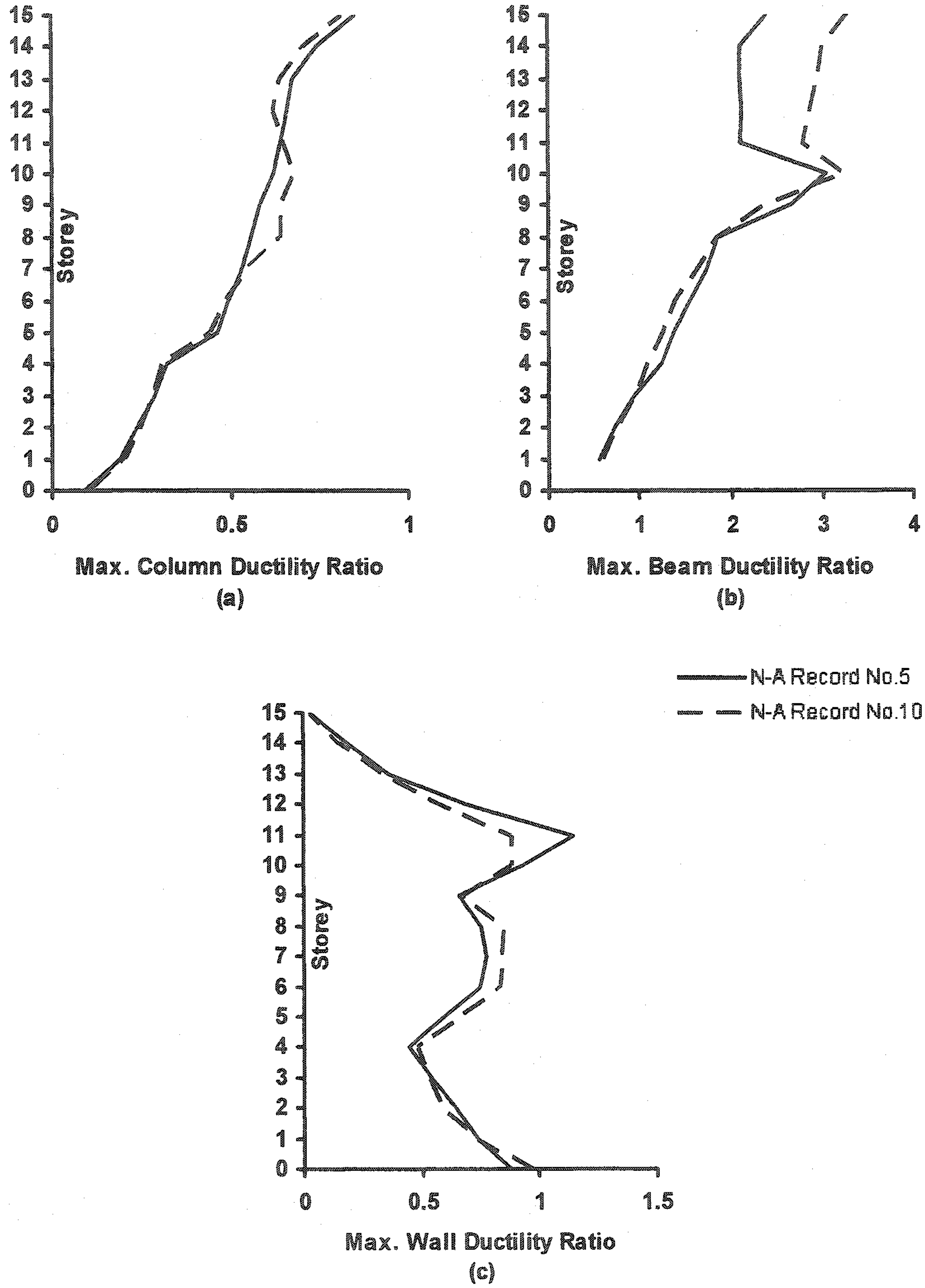

Fig. 4.75 Ductility Response for 15-Storey SHW Subjected to N-A Artificial Records for Vancouver

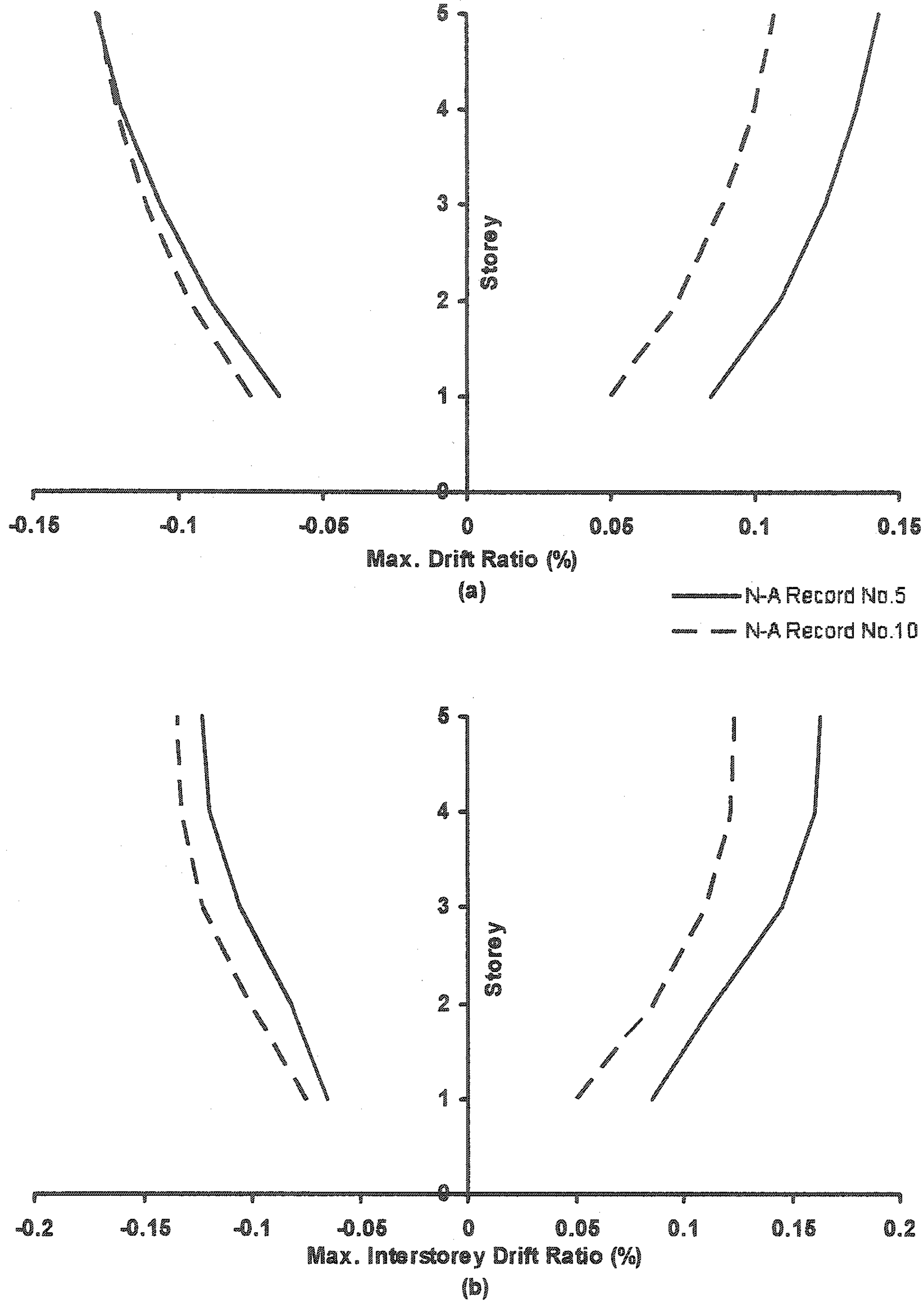

Fig. 4.76 Drift Response for 5-Storey CW Subjected to N-A Artificial Records for Vancouver

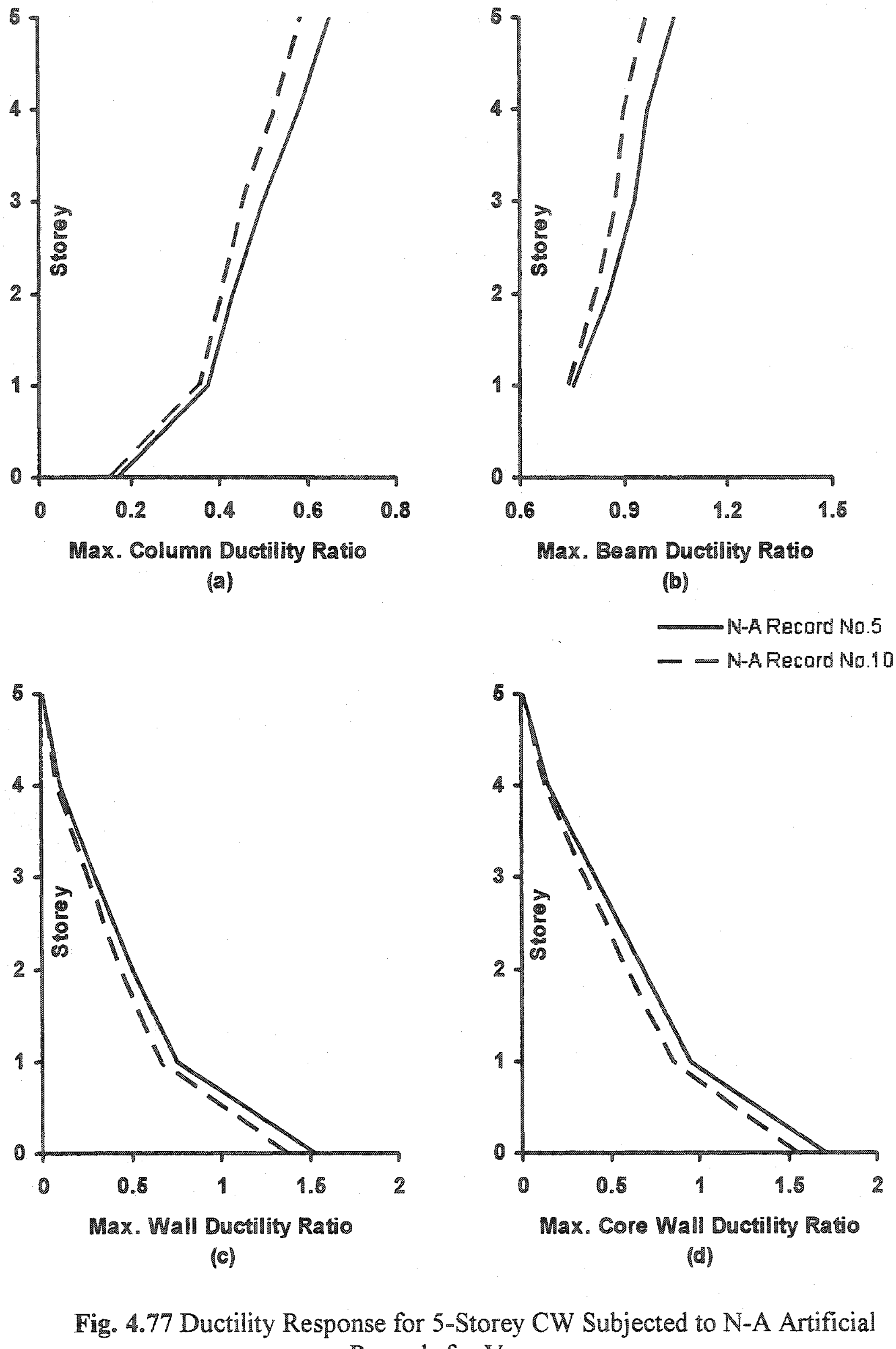

Fig. 4.77 Ductility Response for 5-Storey CW Subjected to N-A Artificial Records for Vancouver

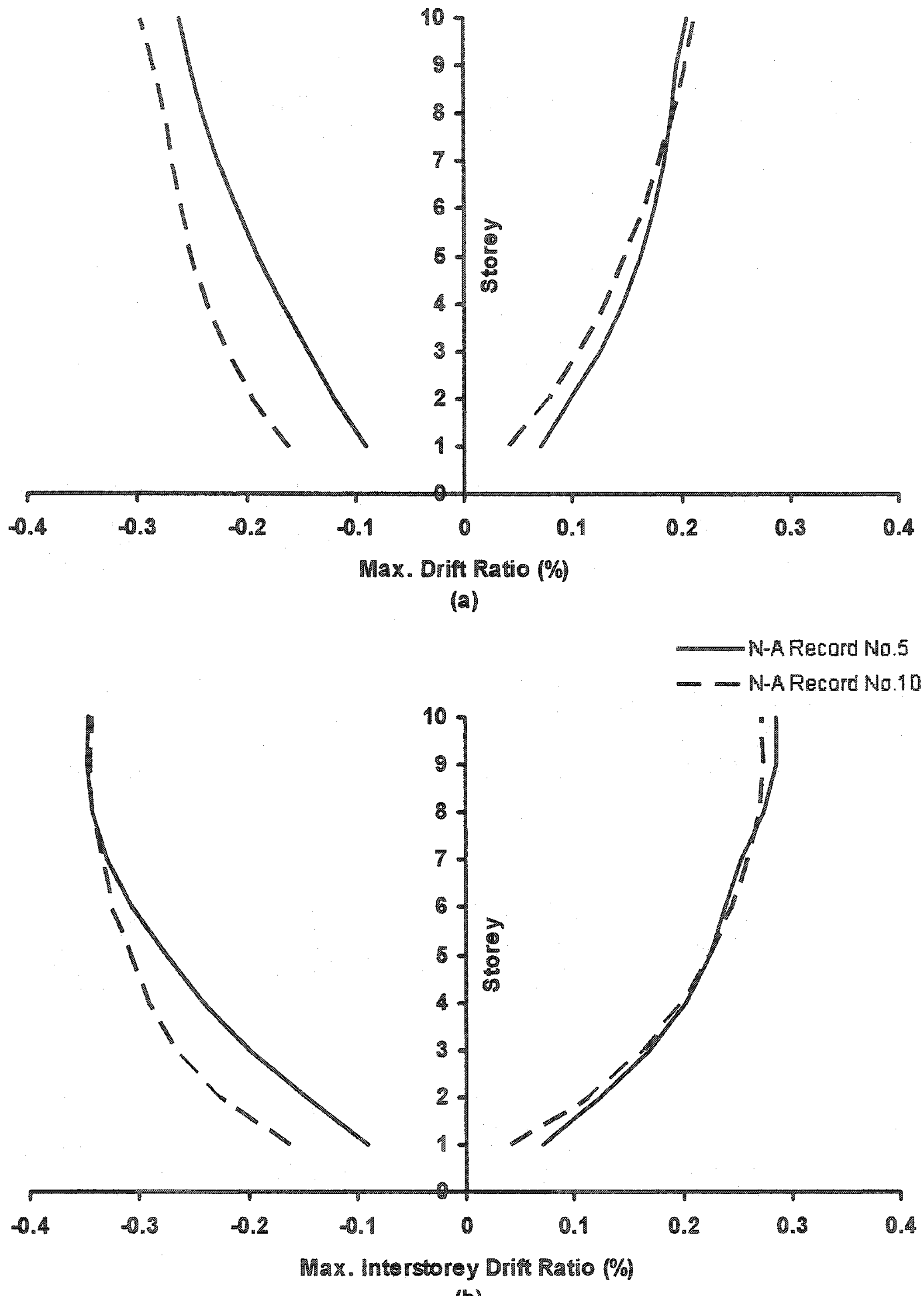

Fig. 4.78 Drift Response for 10-Storey CW Subjected to N-A Artificial Records for Vancouver

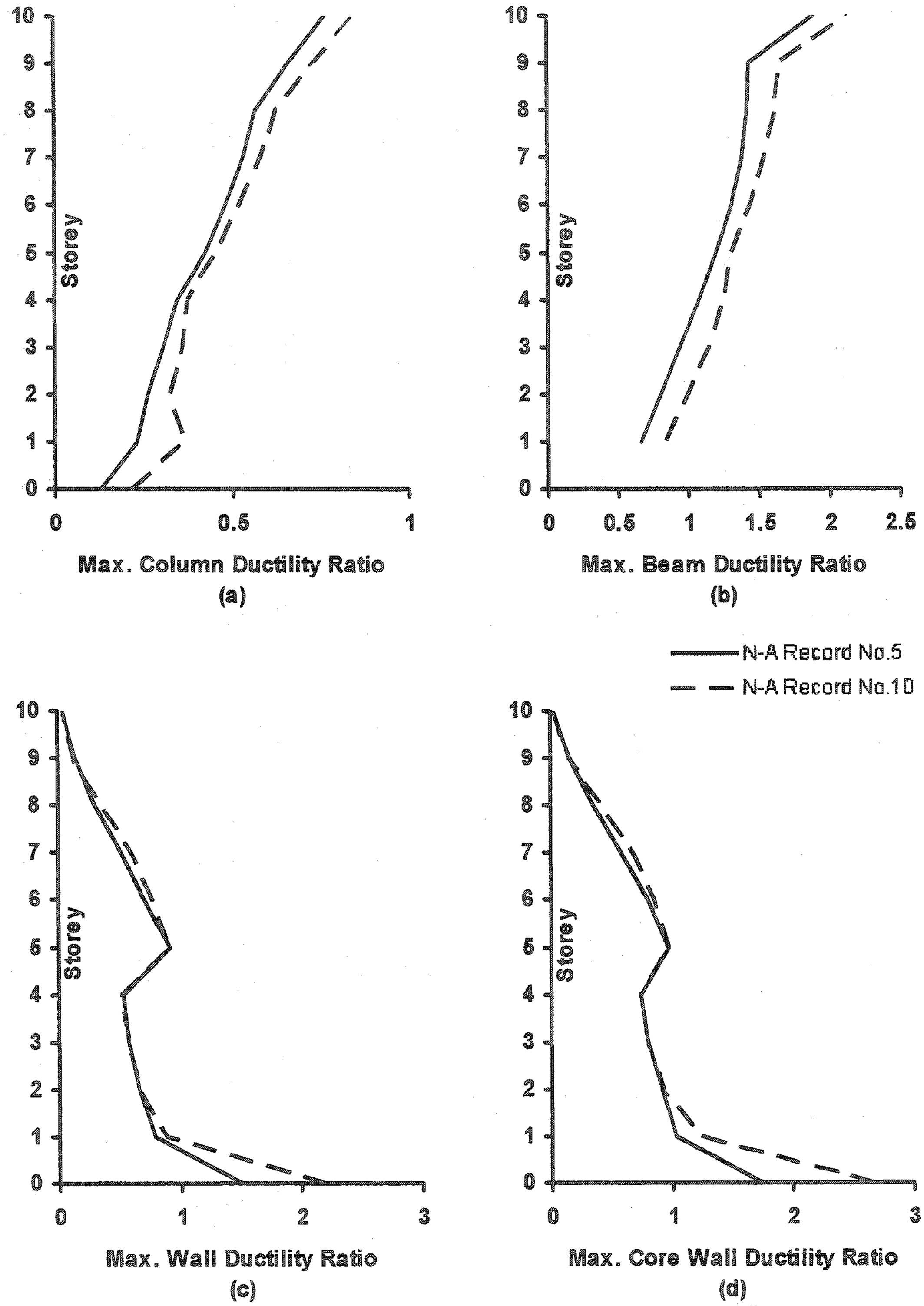

Fig. 4.79 Ductility Response for 10-Storey CW Subjected to N-A Artificial Records for Vancouver

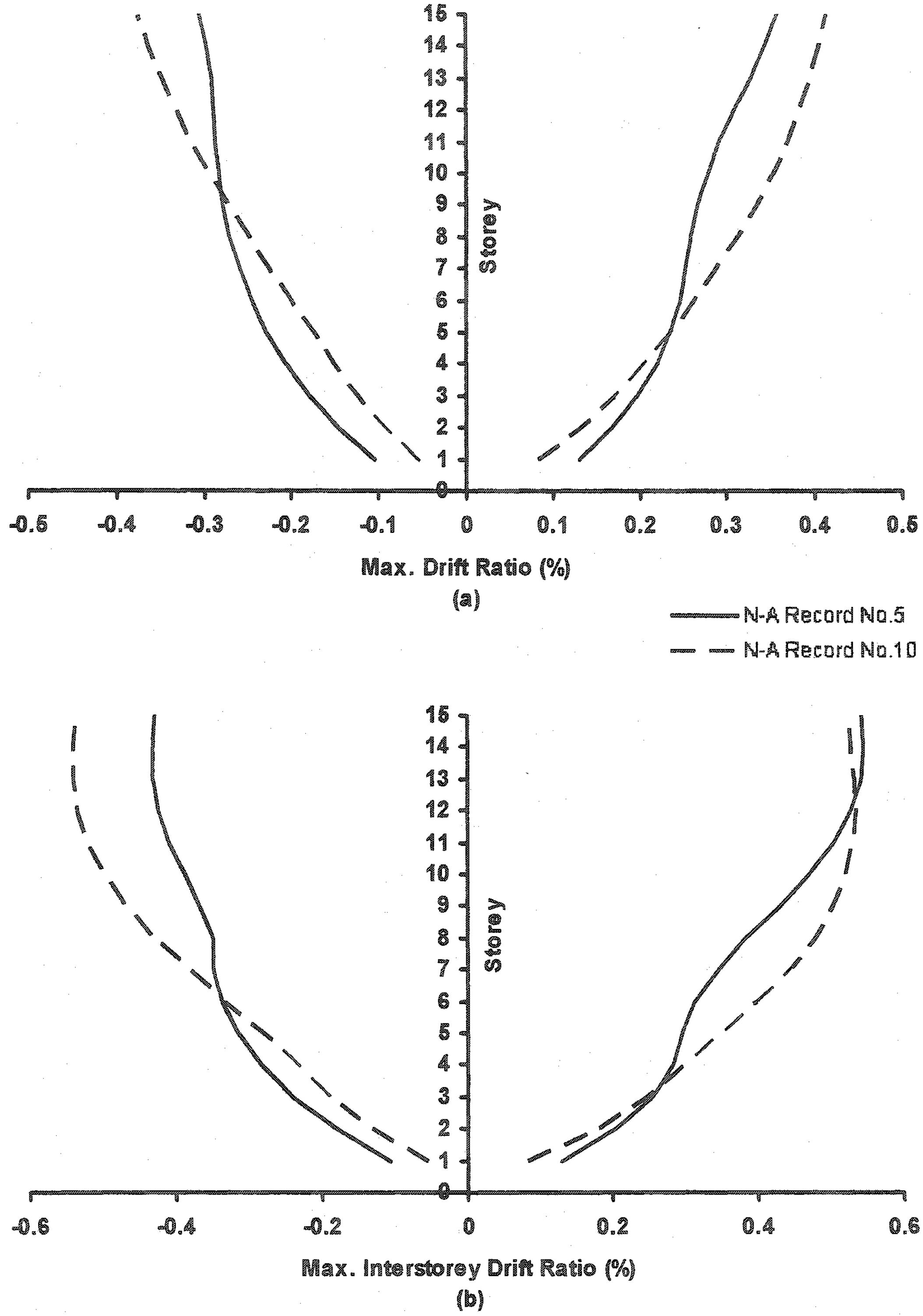

Fig. 4.80 Drift Response for 15-Storey CW Subjected to N-A Artificial Records for Vancouver

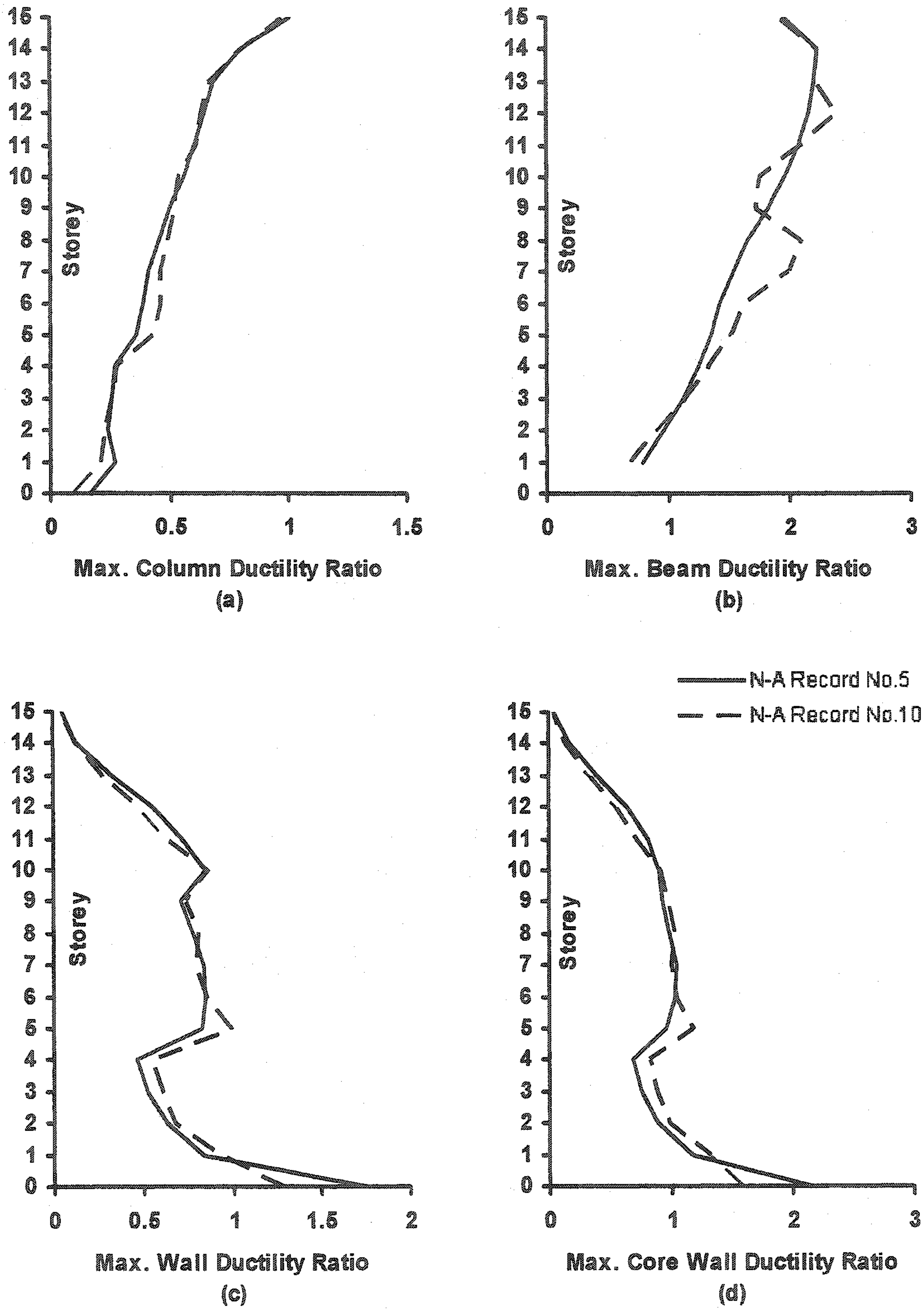

Fig. 4.81 Ductility Response for 15-Storey CW Subjected to N-A Artificial Records for Vancouver

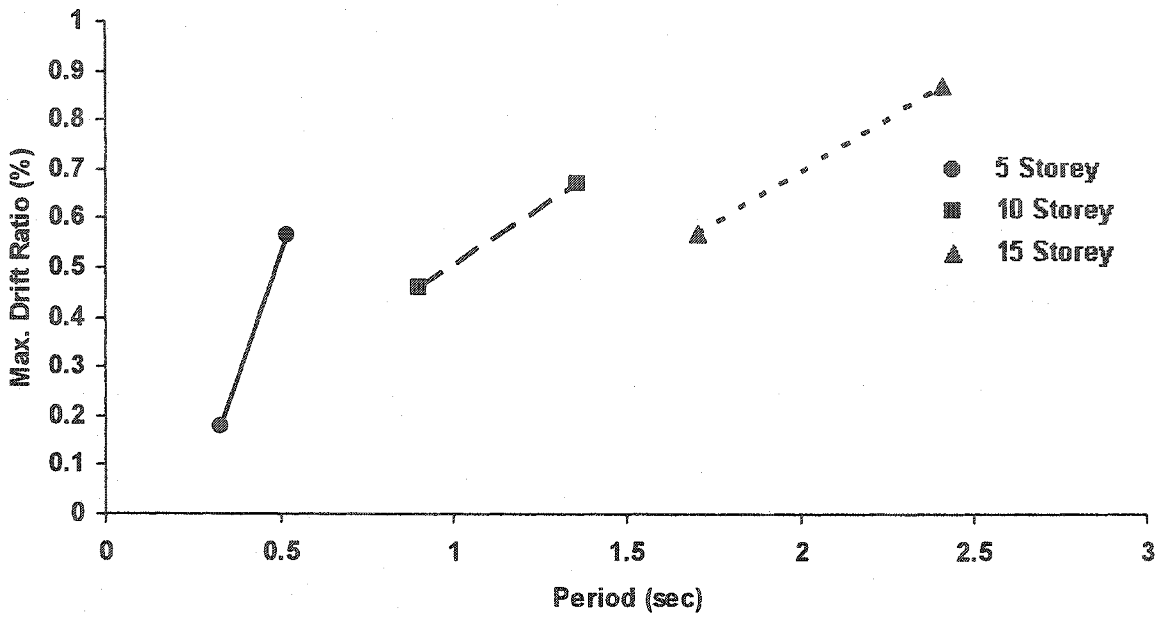

(a)

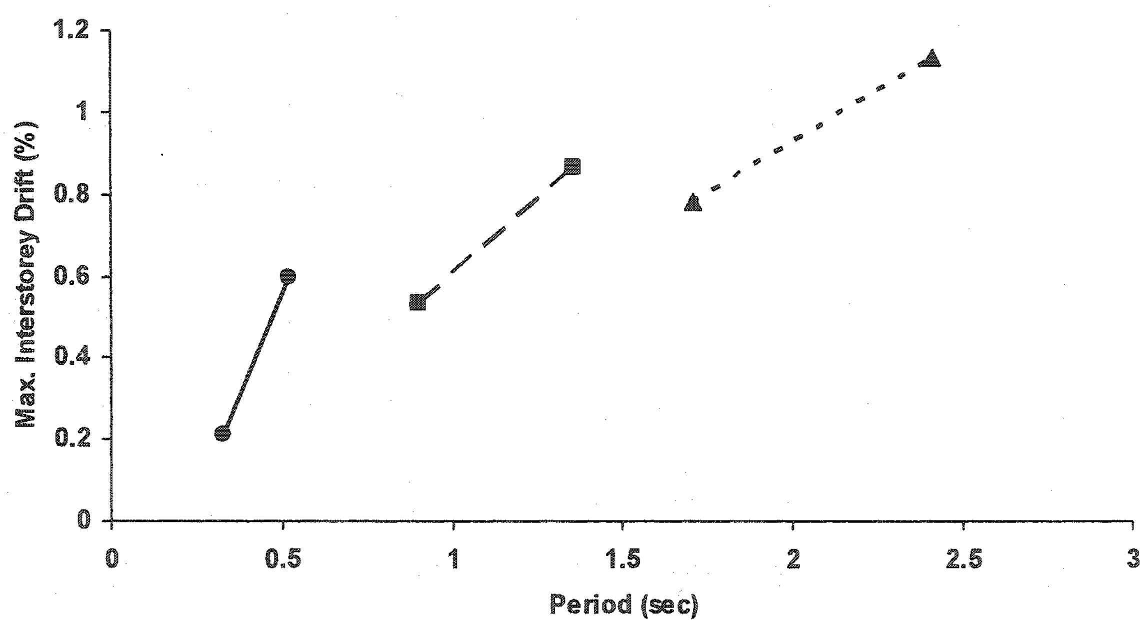

(b)

Fig. 4.82 The Relationship Between Maximum Drift Ratios and The Fundamental Period of Structures Subjected to A-B Artificial Records for Vancouver

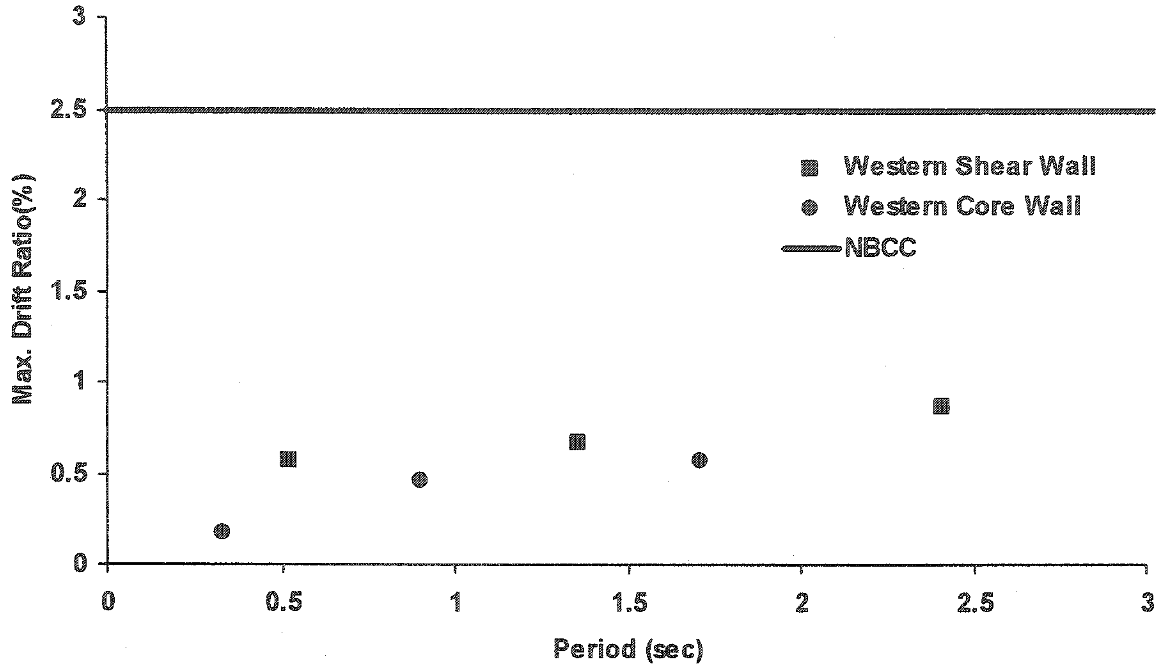

Fig. 4.83 The Relationship Between Computed Maximum Drift Ratios, NBCC Drift Limit and The Fundamental Period of Structures Subjected to A-B Artificial Records for Western Canada

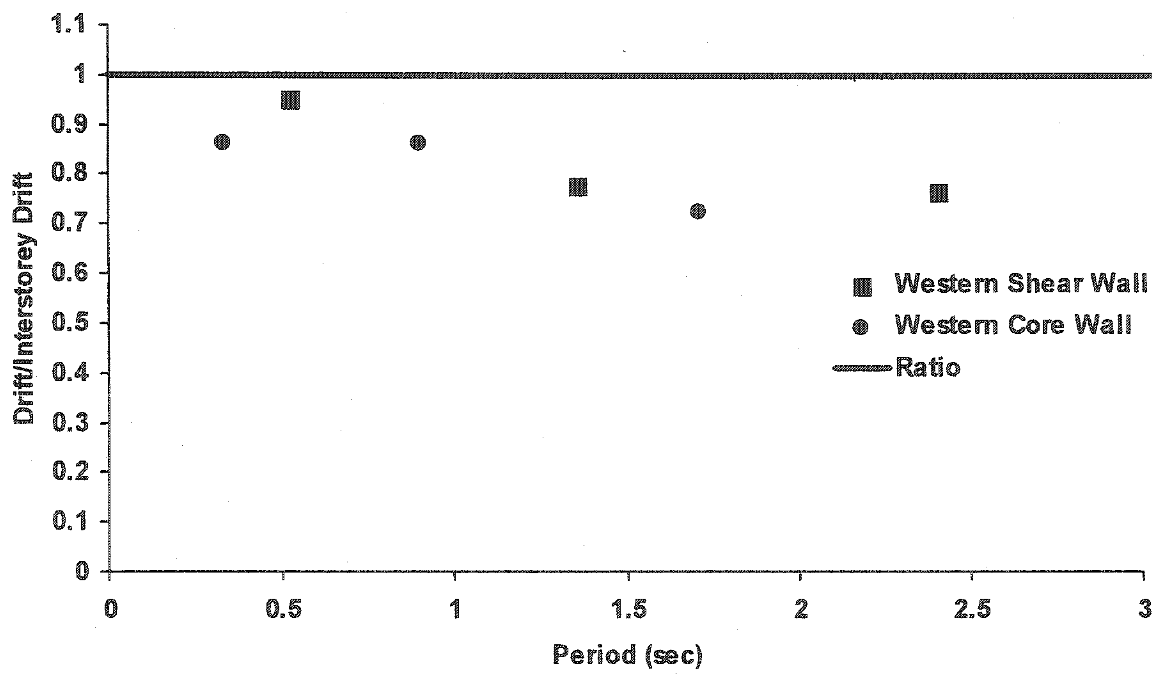

Fig. 4.84 The Relationship Between The Ratio of Drift to Interstorey Drift and The Fundamental Period of Buildings Subjected to A-B Artificial Records for Western Canada

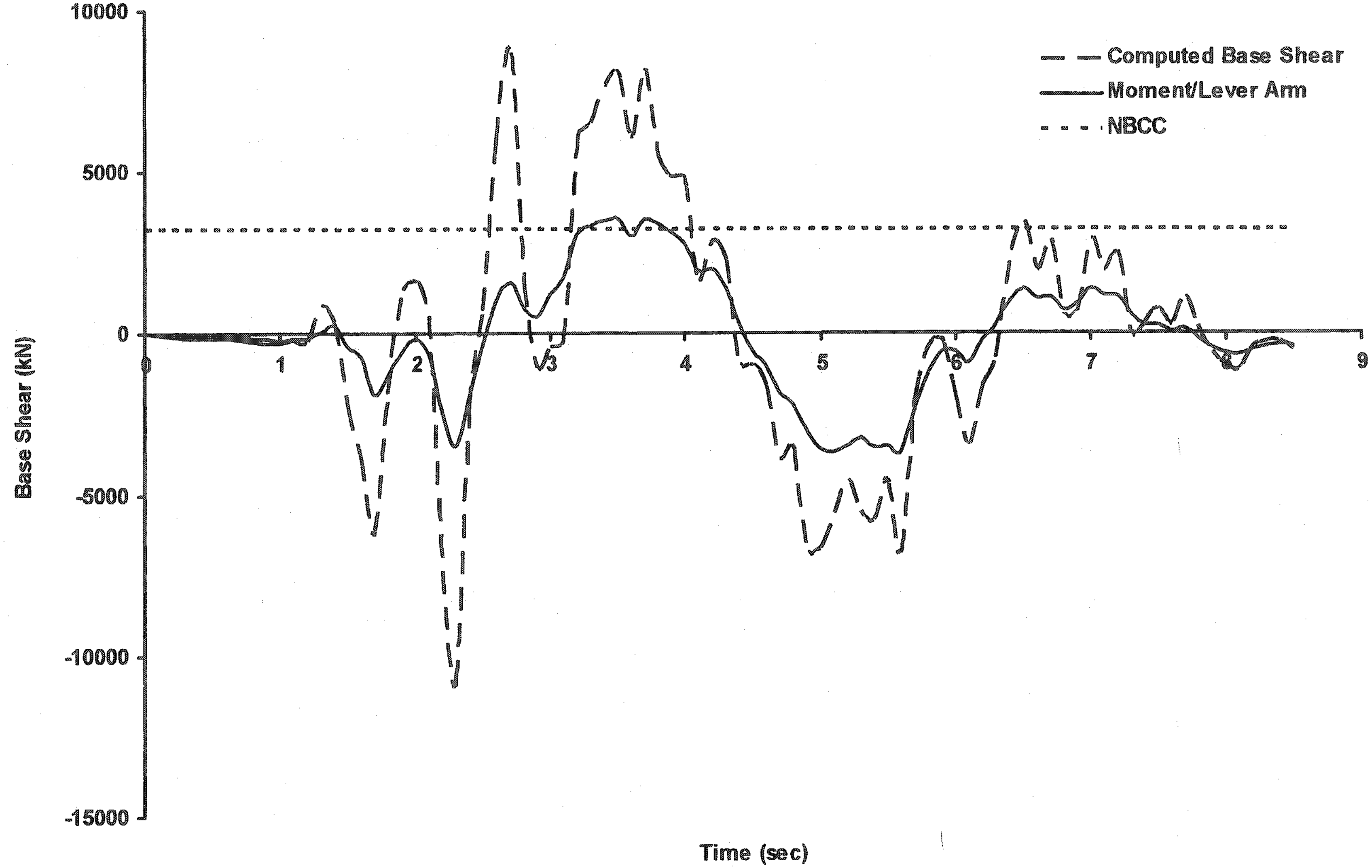

Fig.4.85 Comparison of Dynamic Base Shear Time Histories for Short Event No.3 Artificial Record and Static Base Shear Calculated due to NBCC Requirements for 15-Storey Shear Wall Building for Vancouver.

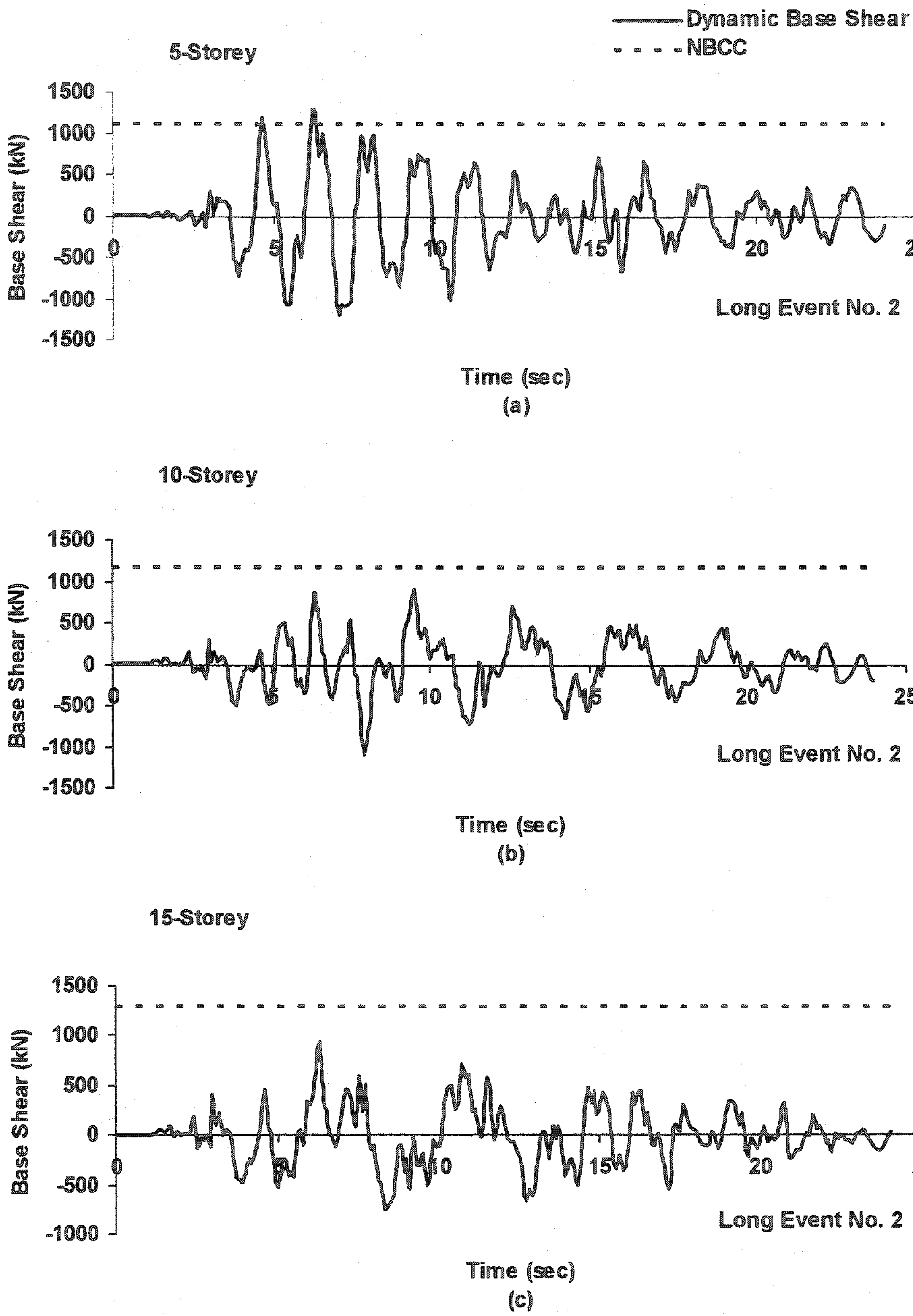

Fig. 4.86 Comparison of Dynamic Base Shear Time Histories and Static Base Shear Calculated due to NBCC Requirements for Frame Buildings in Ottawa

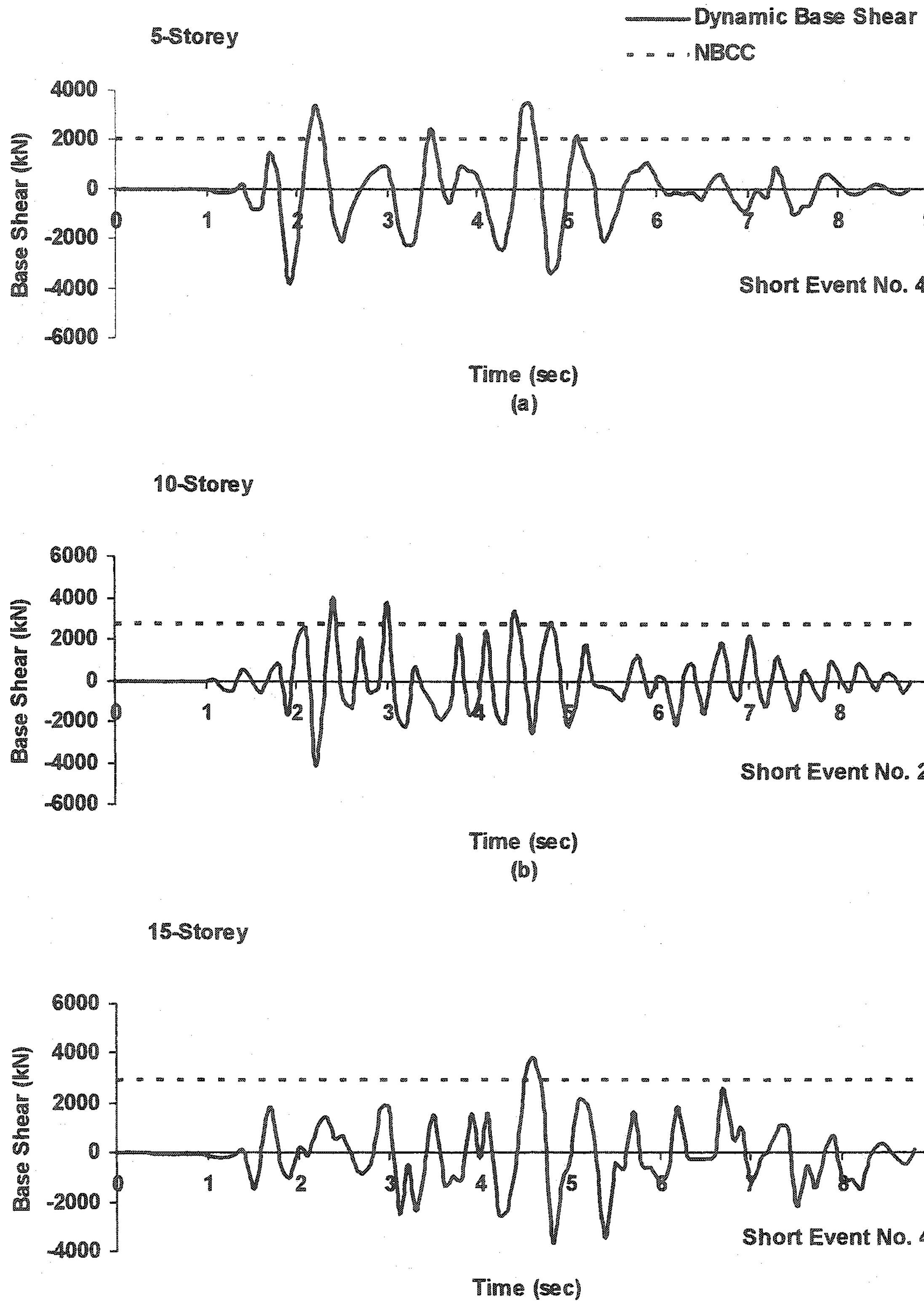

Fig. 4.87 Comparison of Dynamic Base Shear Time Histories and Static Base Shear Calculated due to NBCC Requirements for Frame-Shear Wall Buildings in Ottawa

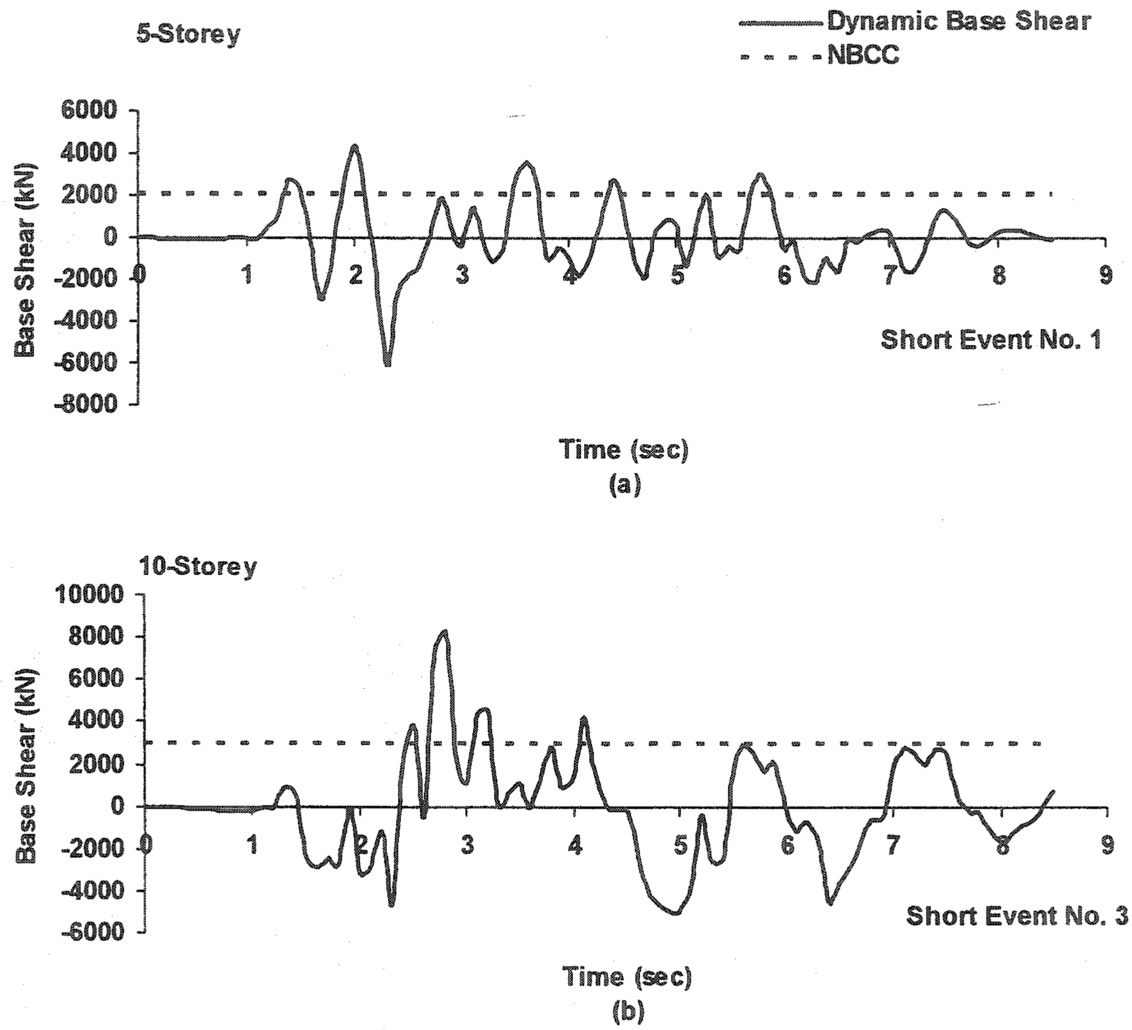

Fig. 4.88 Comparison of Dynamic Base Shear Time Histories and Static Base Shear Calculated due to NBCC Requirements for Frame-Shear Wall Buildings in Vancouver

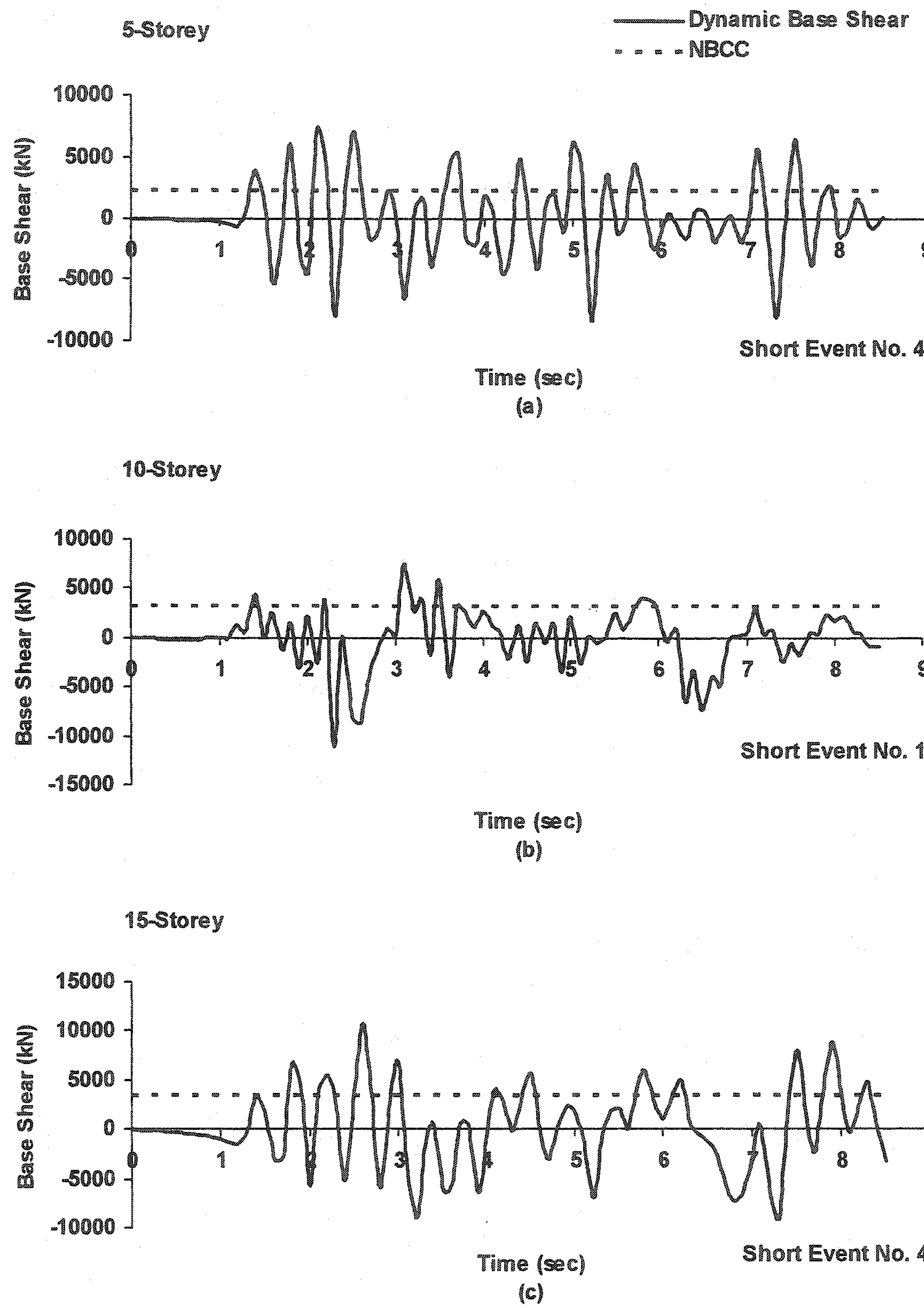

Fig. 4.89 Comparison of Dynamic Base Shear Time Histories and Static Base Shear Calculated due to NBCC Requirements for Core Wall Buildings in Vancouver

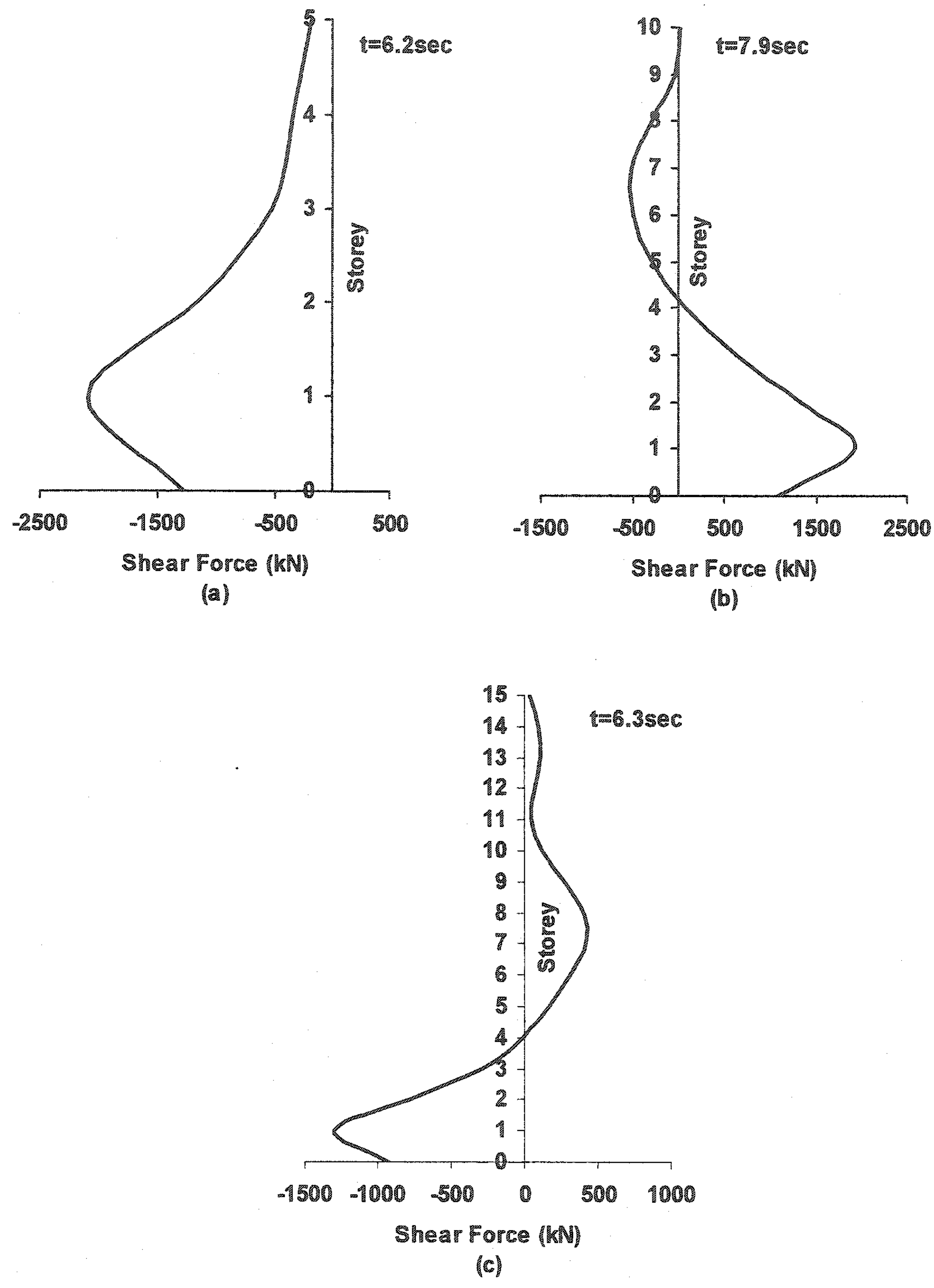

Fig. 4.90 Dynamic Shear Forces for Each Storey of Frame Buildings in Ottawa When Maximum Base Shear is Attained

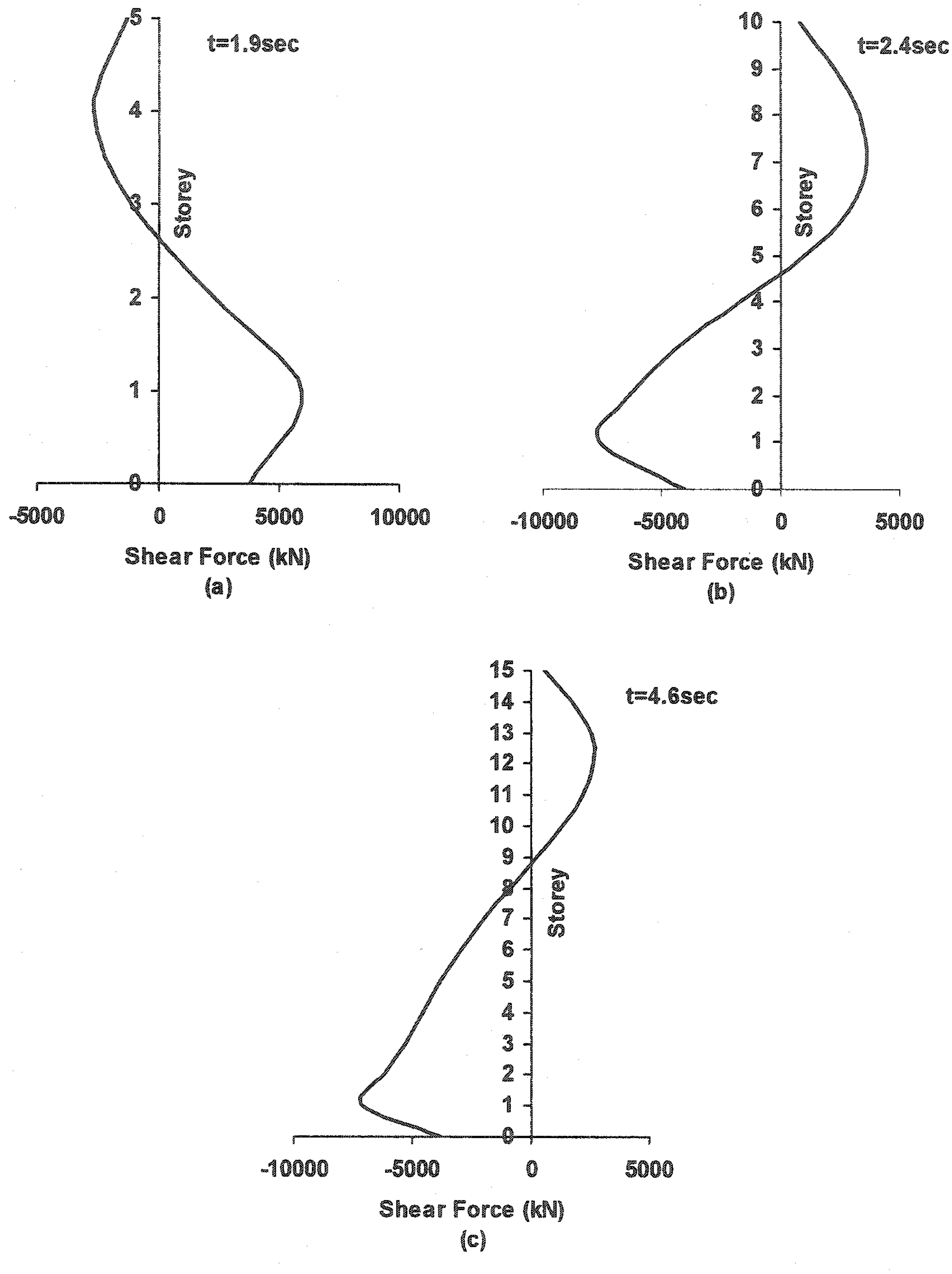

Fig. 4.91 Dynamic Shear Forces for Each Storey of Frame-Shear Wall Buildings in Ottawa When Maximum Base Shear is Attained

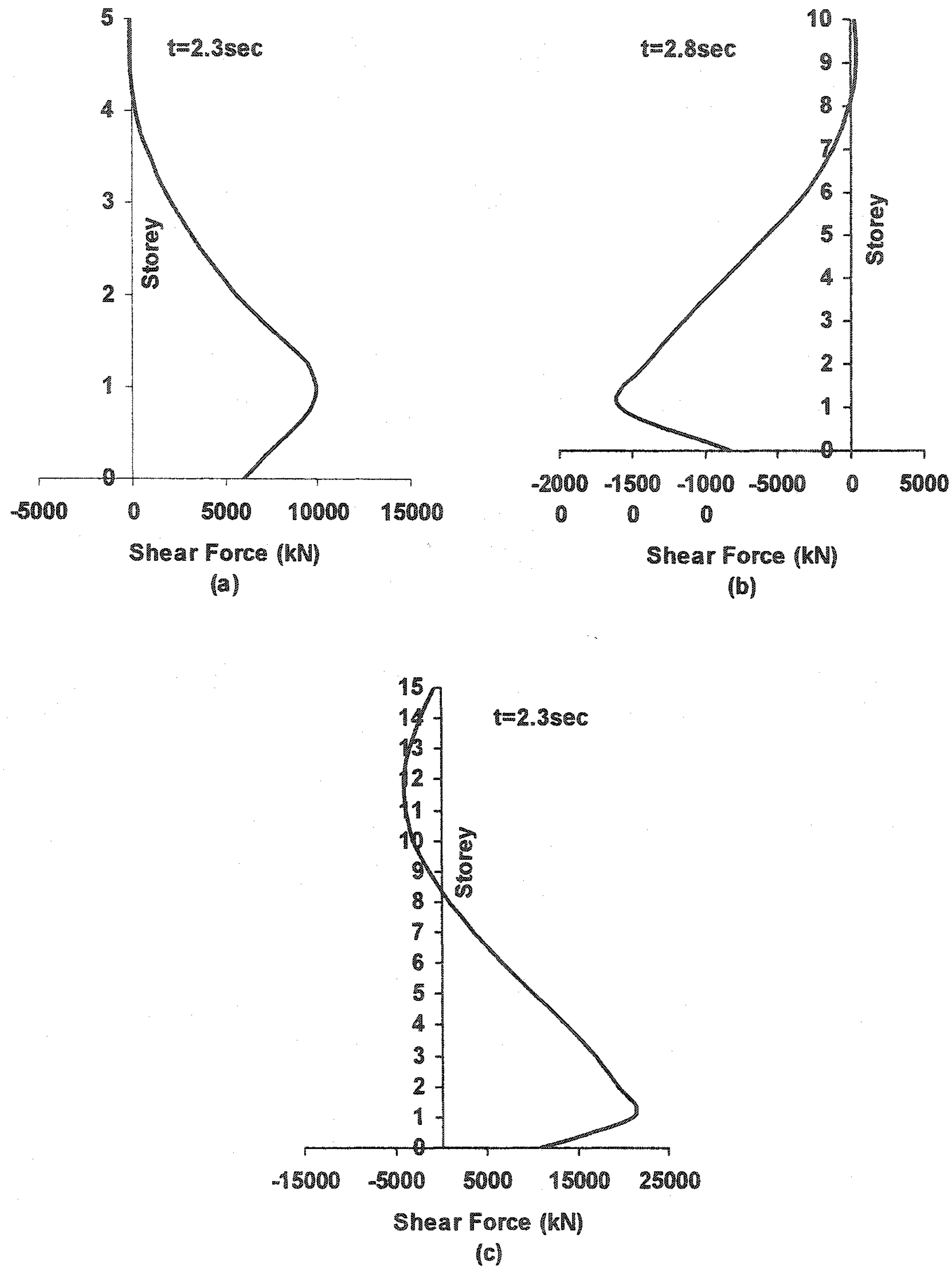

Fig. 4.92 Dynamic Shear Forces for Each Storey of Frame-Shear Wall Buildings in Vancouver When Maximum Base Shear is Attained

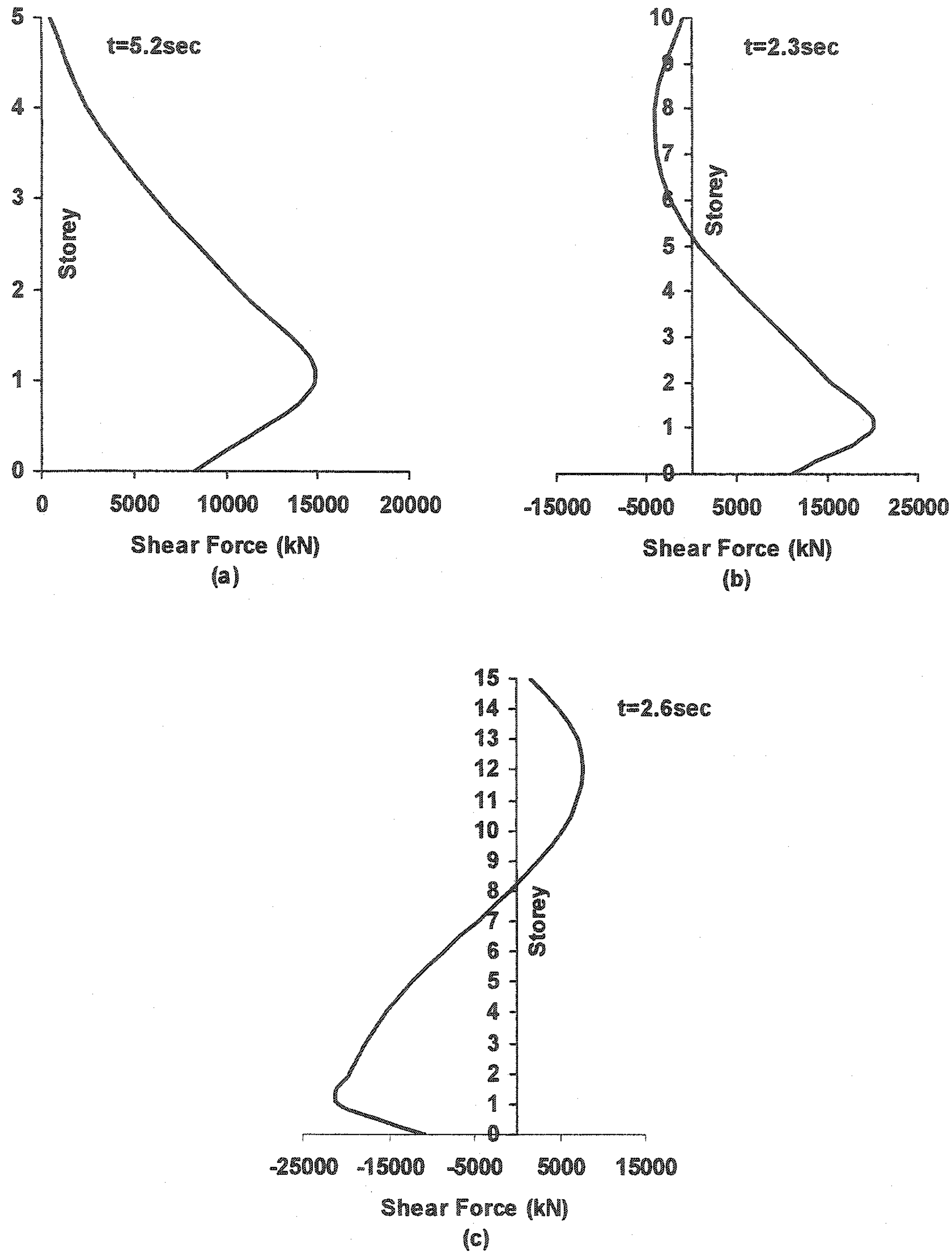

Fig. 4.93 Dynamic Shear Forces for Each Storey of Core Wall Buildings in Vancouver When Maximum Base Shear is Attained

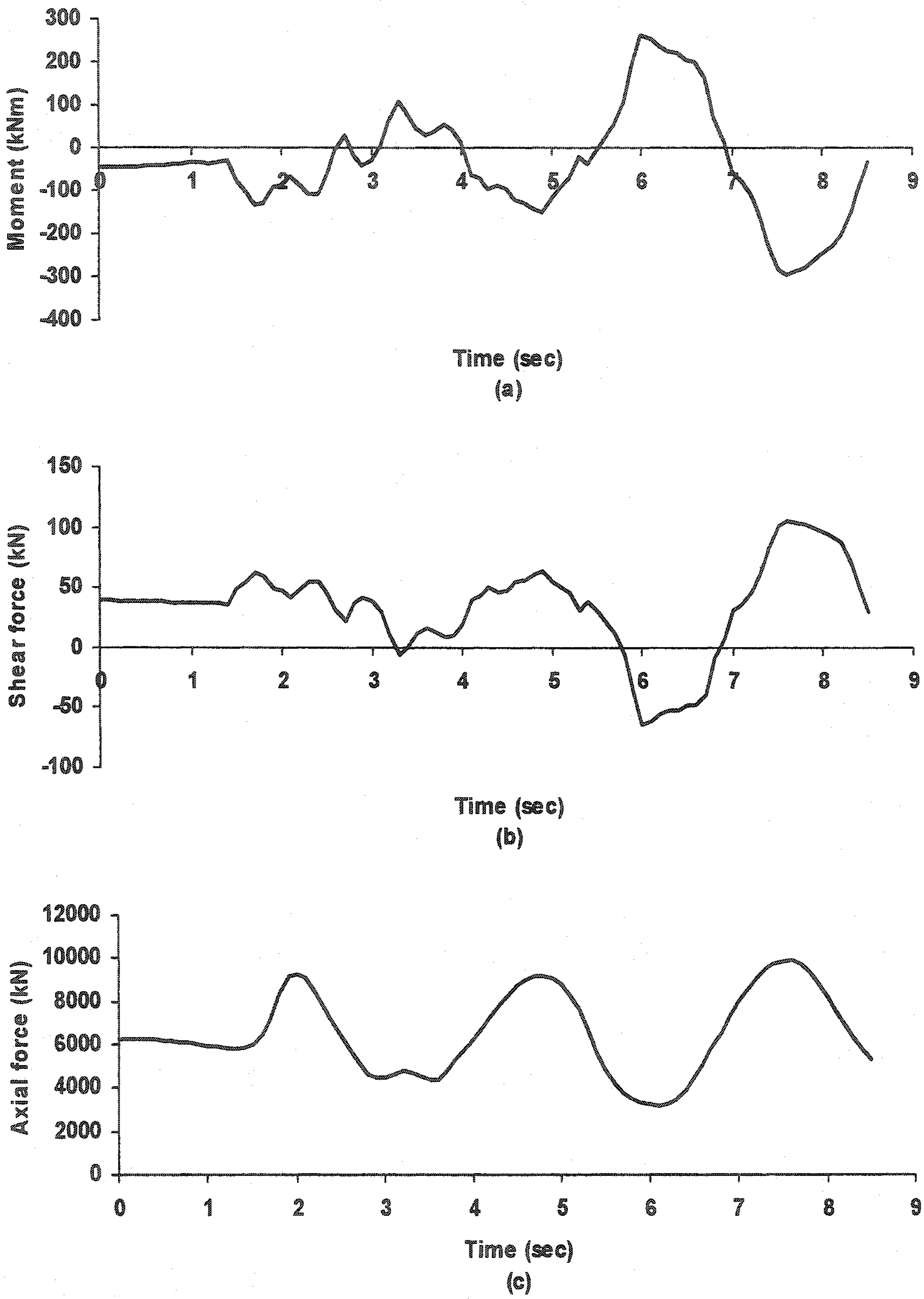

Fig. 4.94 Moment, Shear Force and Axial Force Time Histories of Short Event No.3 Artificial Record for First Storey Exterior Column of 15-Storey Shear Wall Building for Vancouver

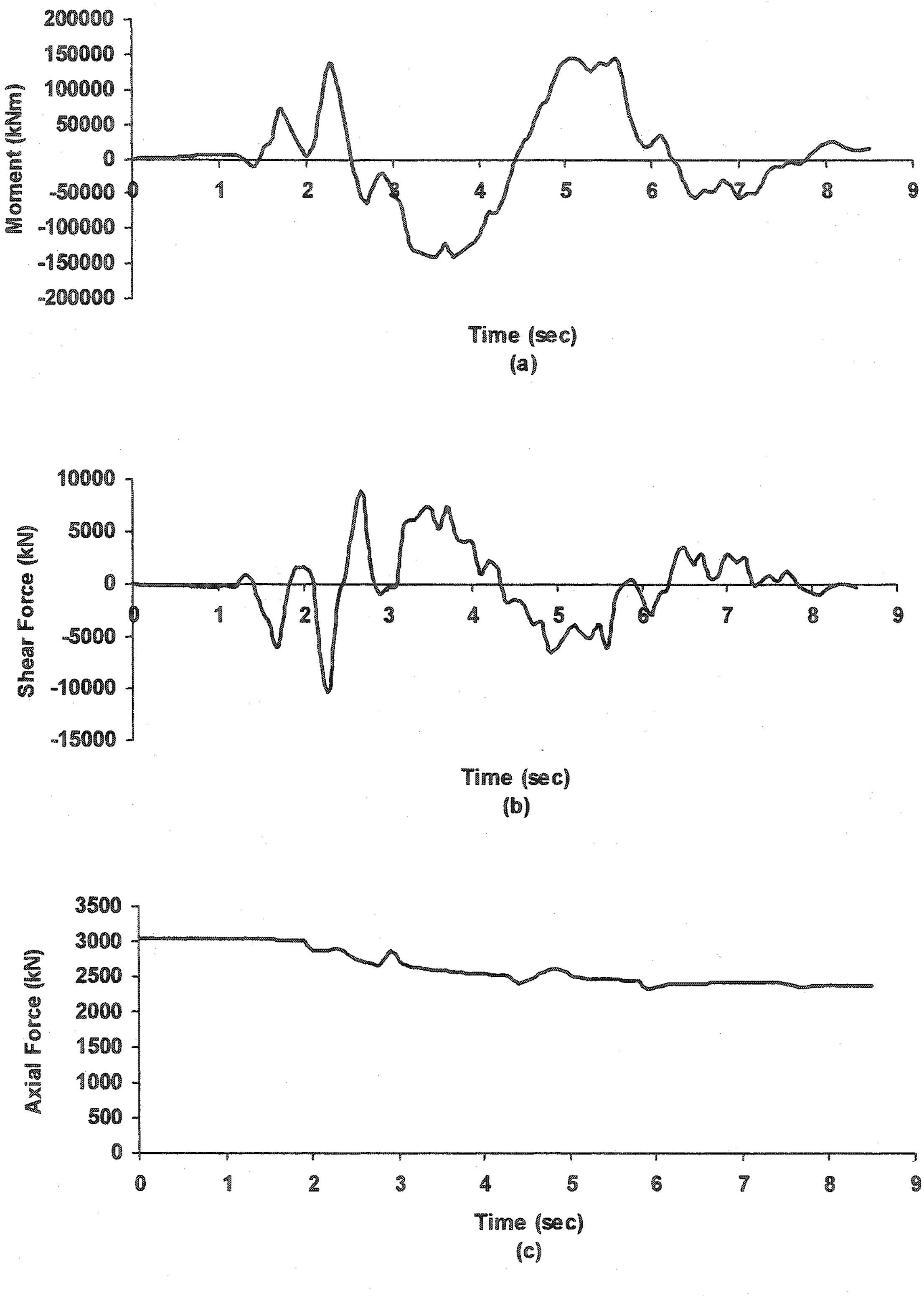

Fig. 4.95 Moment, Shear Force and Axial Force Time Histories of Short Event No.3 Artificial Record for First Storey Shear Wall of 15-Storey Shear Wall Building for Vancouver

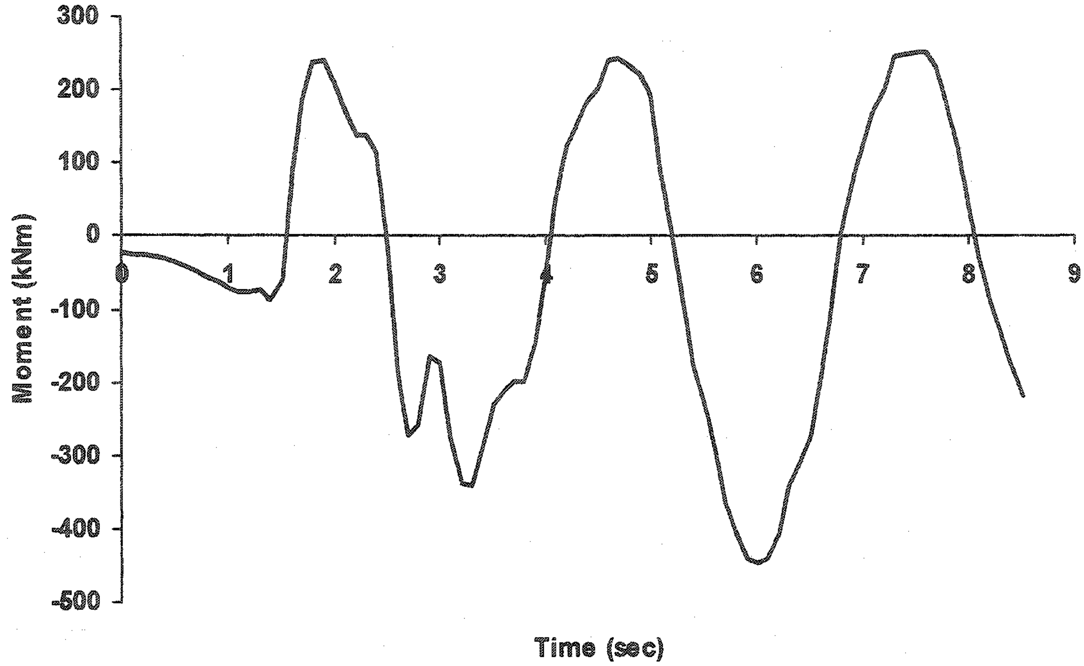

(a)

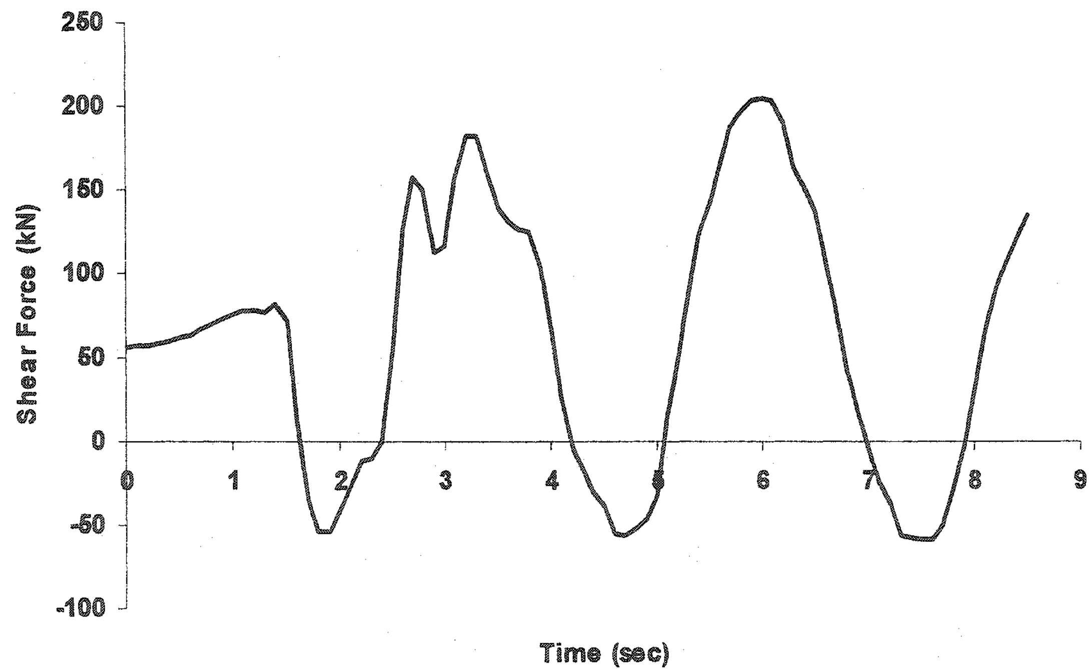

(b)

Fig. 4.96 Moment and Axial Force Time Histories of Short Event No.3 Artificial Record for Fifth Storey Yielded Beam of 15-Storey Shear Wall Building for Vancouver

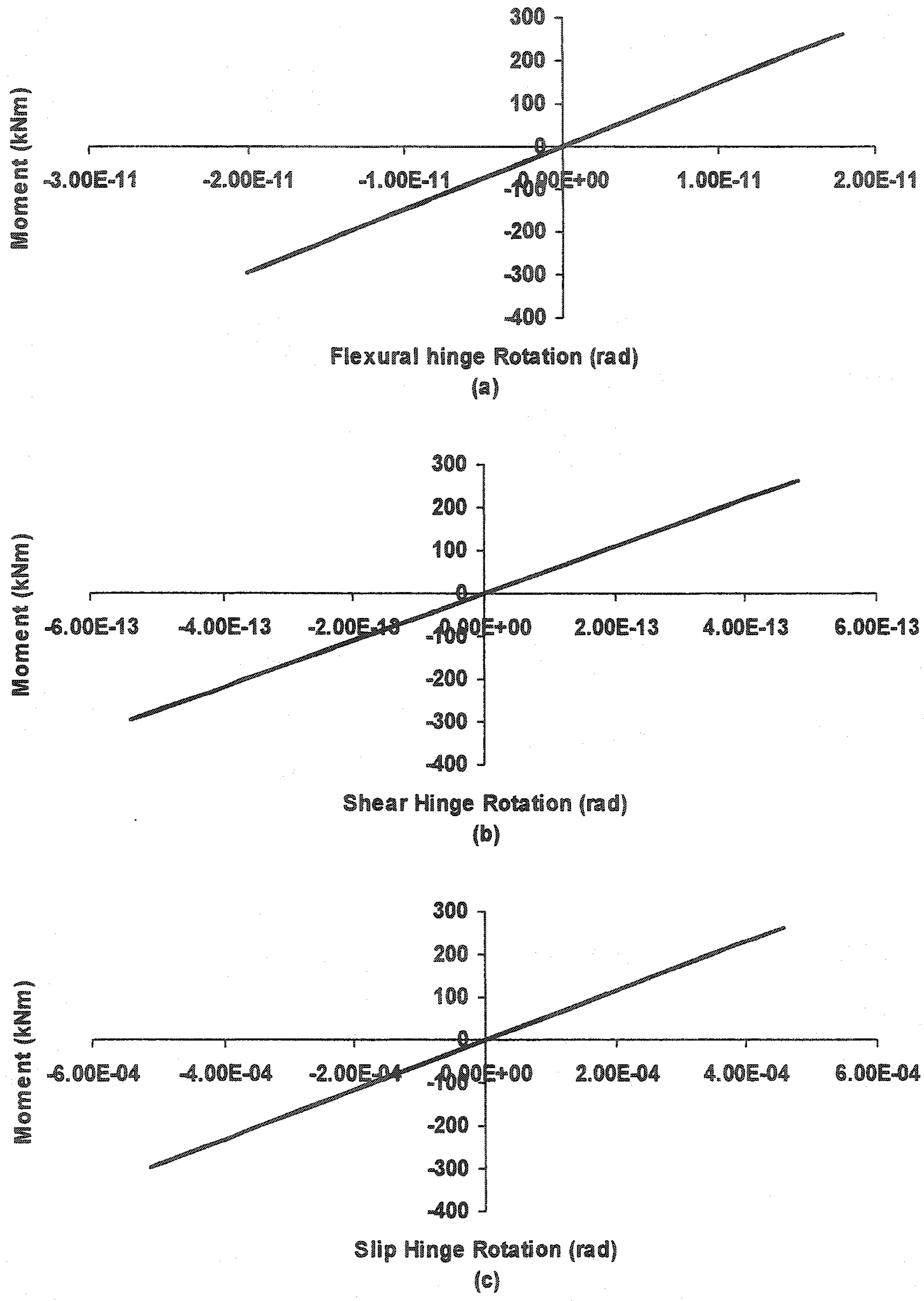

Fig. 4.97 Moment versus Flexure, Shear and Slip Hinge Rotations of Short Event No.3 Artificial Record for First Storey Exterior Column of 15-Storey Shear Wall Building for Vancouver

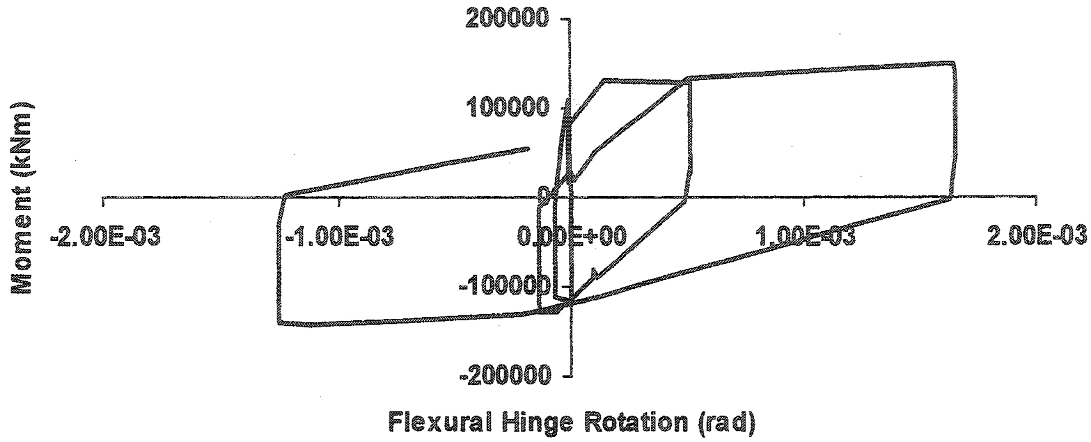

(a)

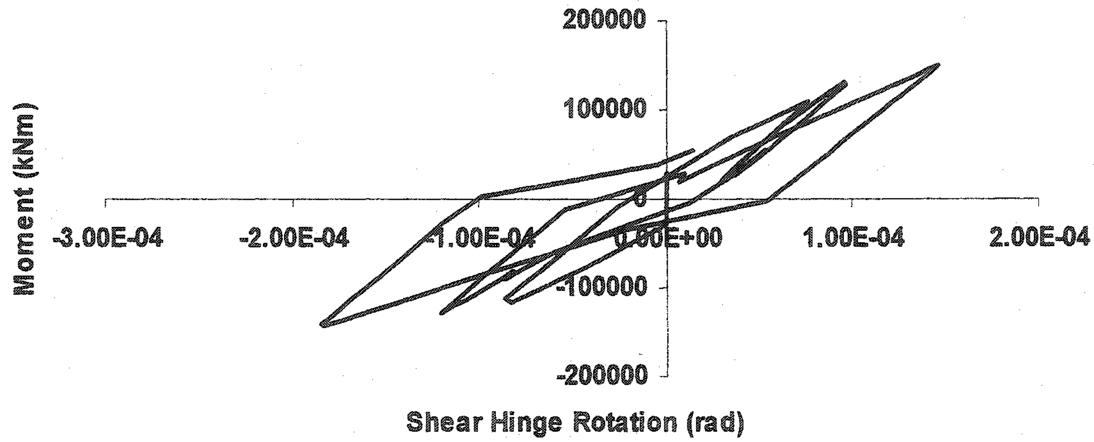

(b)

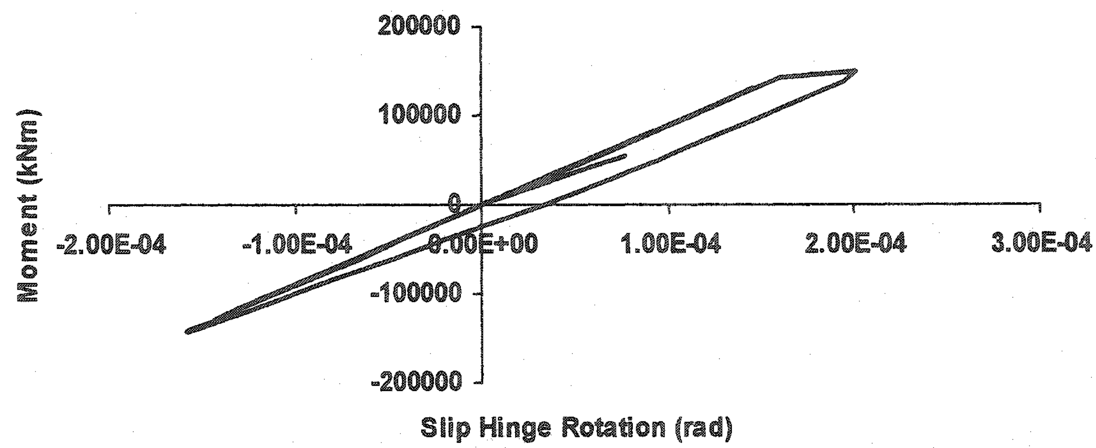

(c)

Fig. 4.98 Moment versus Flexure, Shear and Slip Hinge Rotations of Short Event No.3 Artificial Record for First Storey Shear Wall of 15-Storey Shear Wall Building for Vancouver

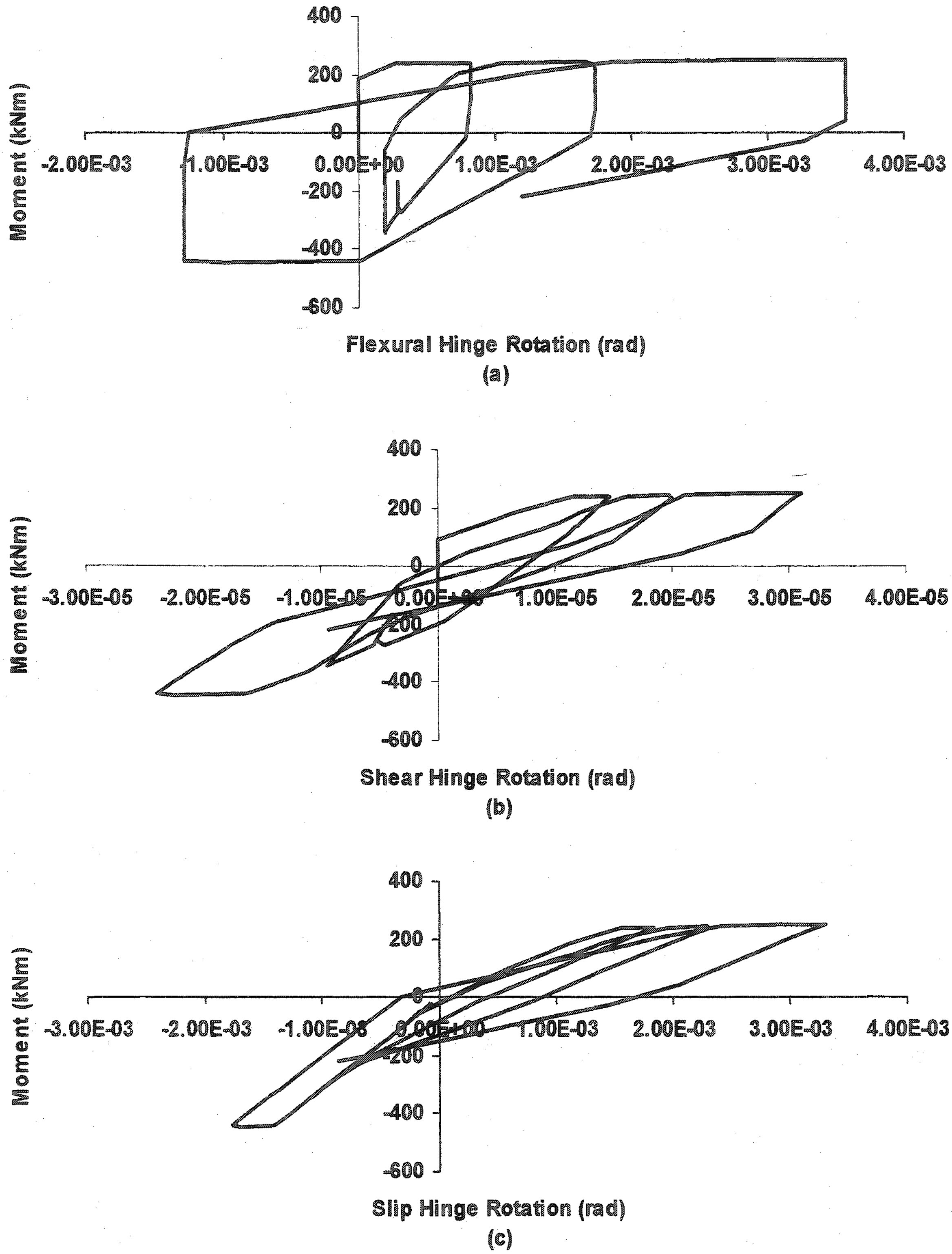

Fig. 4.99 Moment versus Flexure, Shear and Slip Hinge Rotations of Short Event No.3 Artificial Record for Fifth Storey Yielded Beam of 15-Storey Shear Wall Building for Vancouver

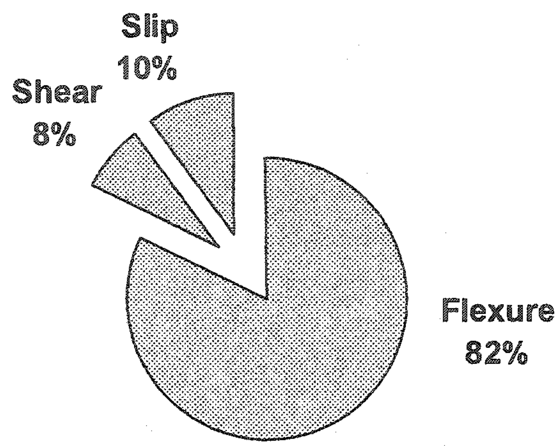

Fig.4.100 Contributions of Inelastic Flexure, Shear and Slip Deformation Components to The First Storey Shear Wall of the 15-Storey Shear Wall Building in Vancouver Subjected to Short Event No.3

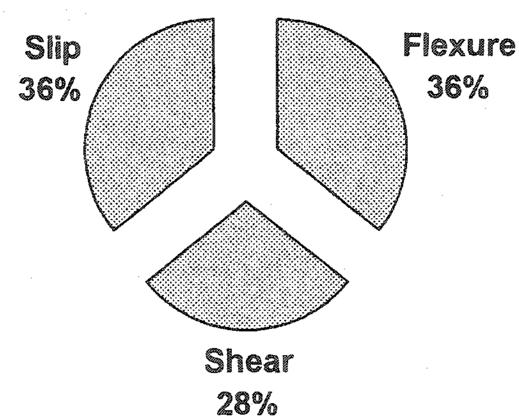

Fig.4.101 Contributions of Inelastic Flexure, Shear and Slip Deformation Components to The Fifth Storey Beam of the 15-Storey Shear Wall Building in Vancouver Subjected to Short Event No.3

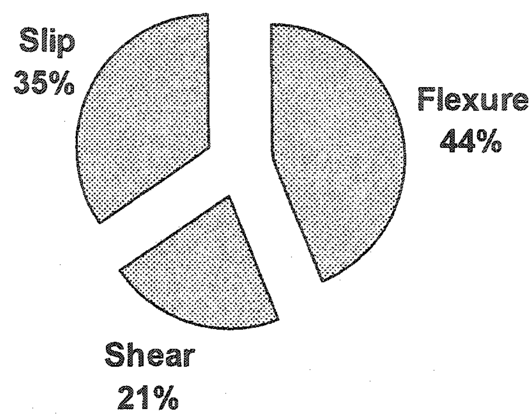

Fig.4.102 Contributions of Inelastic Flexure, Shear and Slip Deformation Components to The First Storey Exterior Column of the 15-Storey Shear Wall Building in Vancouver Subjected to Short Event No.3

Appendix A

USER'S GUIDE FOR DRAIN-RC

The input data for DRAIN-RC is entered using two types of windows. The first type is used to enter the data of general type, as in the case of specifying control nodes, and contains only two commend buttons, i.e., "OK" and "Cancel." After entering each item in text boxes, the user must click the OK button to save the data. The data is saved in a file with "TXT" extension. Clicking OK button completes the data entry and the user should then select another data entry window from the main menu in the Main Window. The Cancel button is only needed if the user wishes not to save the data entered, and close the window. The window also contains an icon for a text editor, for a possible updating and correcting the data entered. Clicking on the icon enables the "Notepad" text editor that is resident in the Windows environment. An example of the first type Window is shown below.

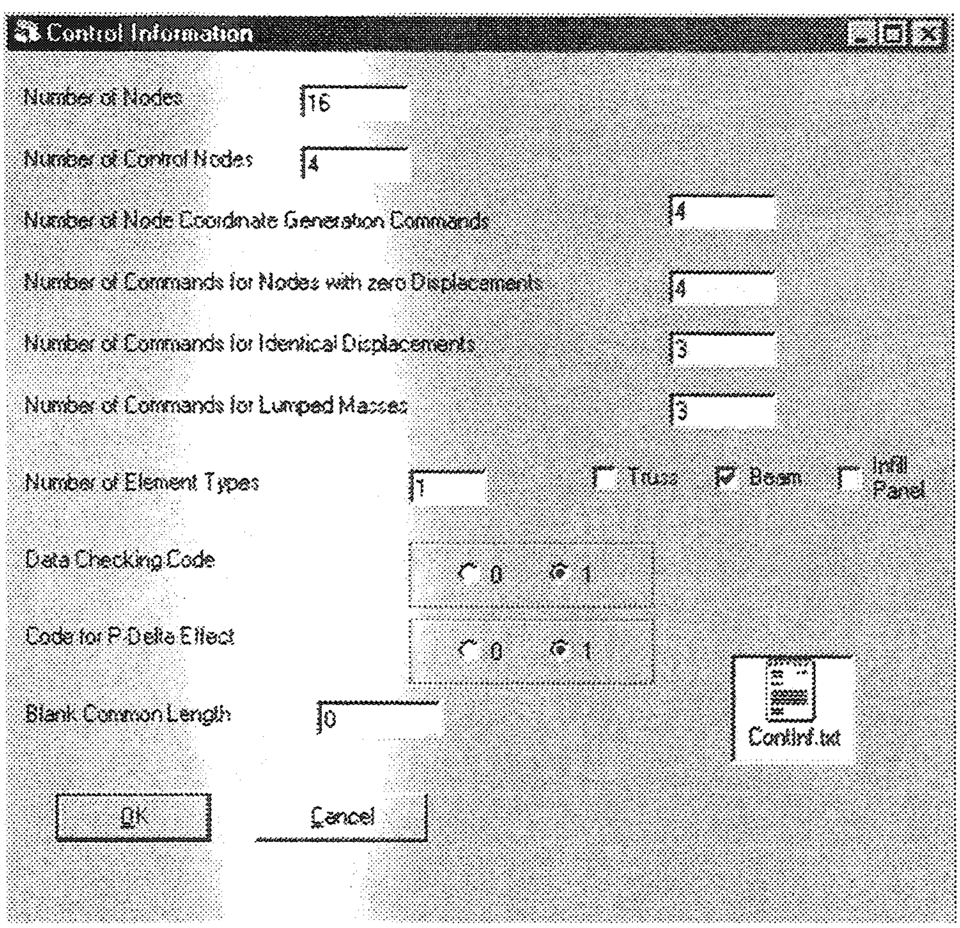

The second type of Window is used to enter detailed data with options to choose from. This type of Window provides the user with different buttons to execute different tasks. Upon selecting (a second type) data Window from the Main Menu, the user must click the "New" button to activate the entry of new data set (for a new project). This will enable data entry in a form that can be saved. After the "New" button is clicked to enter a new set of data, each data set is entered in text boxes. The user must click the "Add" button after the entry of a complete set of data to keep it temporarily in the memory and empty the text boxes for the next set entry. Once all data sets are entered, the user must click the "OK" button in the lower left frame (immediately below the "Add" button) to complete the data entry into the temporary memory. The data set may be given in any order, and need not follow a sequence (ex: node number 5 data may be entered before node number 2 data). The data is not saved until the "Last Save" button is clicked. Therefore, it is not possible to correct and/or update the data items in temporary memory until after they are saved by clicking the "Last Save" button. Clicking the main "OK" button (next to "Existing" button) closes the Window.

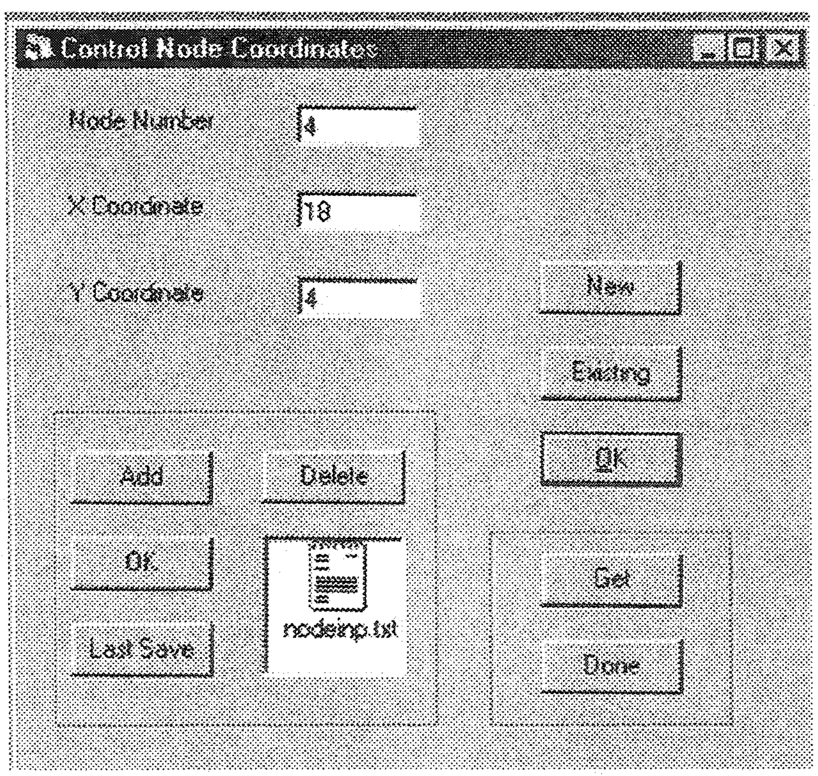

Updating or correcting data can be done either prior to exiting the data Window or by re-selecting it. If the data Window is open, entry of new (corrected) data set replaces the (old) existing data set, or inserted in place of a missing data set. Clicking "Add" and "Last Save" buttons complete the updating operation. Alternatively, the text editor (Notepad) can be activated by double clicking the text editor icon and the data set can be updated in the text edit mode. The "Delete" button is used to delete a data set during updating operation. If the data Window is re-selected for updating or correction, then clicking "Existing" button activates the previously entered and saved file. The updating process described above can then be followed to make changes/corrections in exactly the same manner. The previously entered data set can be reviewed either by using the text editor option or by using the "Get" and "Done" buttons. Each data set can be viewed by entering the control data in the first text box and clicking the "Get" button (ex: entering 4 for node number and clicking "Get" button displays x and y coordinates of 18 and 4). Clicking "Done" empties text boxes so that a new item can be displayed. The main "OK" button must be clicked to exit the Window.

The above two types of windows are used to enter data, which is itemized and described in the following paragraphs. Additional information is provided, when warranted, to further describe the operation of a data window, especially when new commend buttons are involved.

TITLE OF THE PROJECT

Title of the Problem Data: This title appears in the beginning of output file with '.INP' extension.

STRUCTURAL GEOMETRY INFORMATION

- **Control Information**

Number of Nodes: Total number of nodes required to define the structural system.

Number of Control Nodes: Number of control nodes in the structure for which coordinates are specified directly. Other nodes are internally generated following prescribed sequence.

Number of Node Coordinate Generation Commands: After specifying the coordinates of control nodes, the remaining node coordinates between these control nodes are generated using straight line generation commands. The control node coordinates must be defined with respect to the X, Y coordinate system.

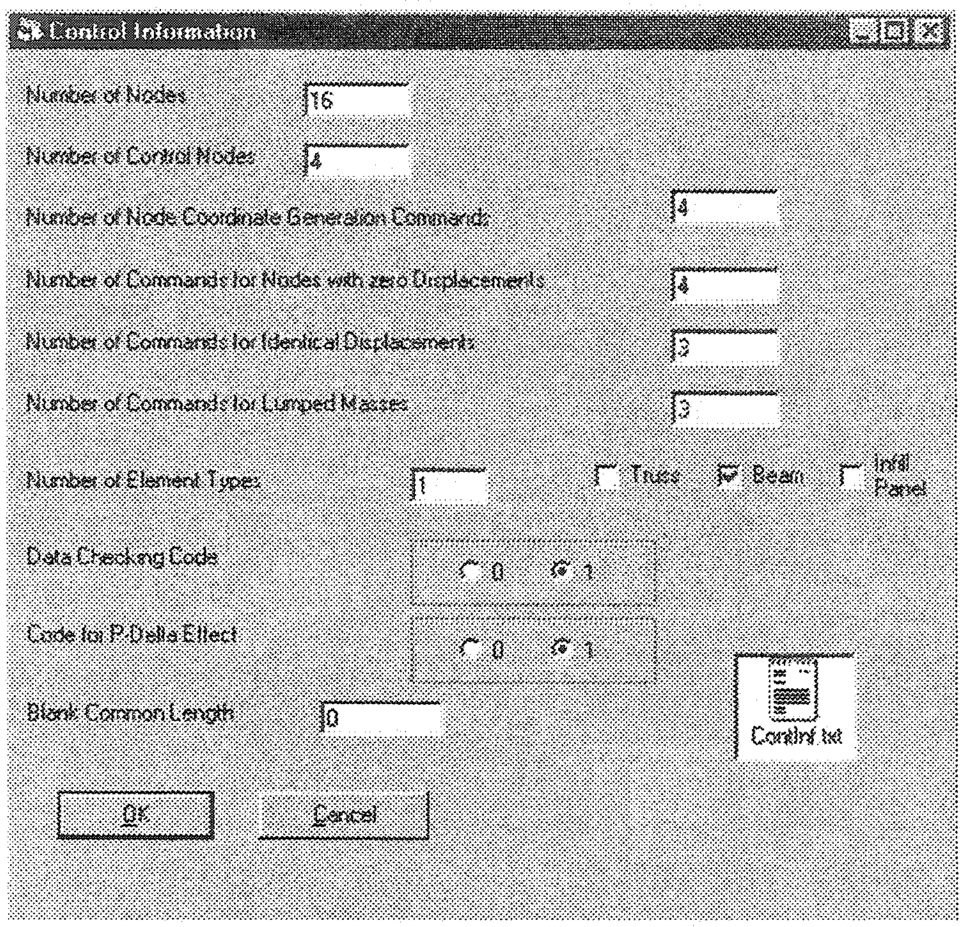

Number of Commands for Nodes with zero Displacements: In general, all nodes may have up to three degrees of freedom, namely X and Y displacements and rotations relative to the ground. In some cases, either certain nodes may be fixed relative to the ground in certain directions or they may be assumed to have a zero displacement.

Number of Nodes with Identical Displacements: In some cases, it may be assumed that certain nodes undergo identical displacements in a given direction, such as the nodes at a floor level when the rigid diaphragm assumption is employed.

Number of Commands for Lumped Masses: The mass of the structure is assumed to be lumped at the nodes. They should be input in units of mass, and not weight. If certain nodes are constrained to have an identical displacement, the mass associated with this displacement will be the sum of the masses specified for the individual nodes.

Number of Element Types: The program contains 3 different element types, used to model reinforced concrete structures. They consist of; i) truss, ii) reinforced concrete beam and iii) infill panel elements. After entering the number of different elements that are used in the analysis, the checkboxes should be checked to define the element type.

Data Checking Code: To check data only, '0' option box should be marked. This enables generation of all element information and stores them in '.INP' file. To execute the problem, '1' option box should be marked.

Code for P-Delta Effect: To consider the P-Δ effect, '1' option box must be marked whereas '0' option box is used to ignore this effect. The decision to use P-Δ effect should be made here. If it is entered as '0', the problem will be solved without this effect, even though geometric stiffness of elements are included in element generation part.

Blank Common Length: The program was originally designed to have dynamic allocation of arrays. During the execution of large data files, the same array may be used more than once for different variables. This is done by arranging the arrays in blocks. When one block of arrays are used, the arrays are utilized only once and no optimization of common block is done. Though this may have been a consideration when main-frame systems were used, it no longer has an important role. Therefore, the PC version of the program was modified to run with a single block of arrays. A default value of (3,000,000) is used for the "Blank Common Length" when '0' is entered. A lesser value may be specified for improved efficiency of execution time. The program executes correctly only if the specified common length is larger than that needed for a specific problem to execute using a single block of array. If the entered value is less than that required to form a single block, the results may not be correct. It is recommended to use the default blank common length, which is expected to be sufficiently large for most applications. When in doubt as to whether the specified length is sufficient or not, the user should check the output and make sure the required number of blocks is not greater than 1 (implying the specified value was sufficient to solve the problem in one block of storage area).

- **Control Node Coordinates**

Node Number: Node number for a control node.

X Coordinate: Coordinate of the node in X direction.

Y Coordinate: Coordinate of the node in Y direction.

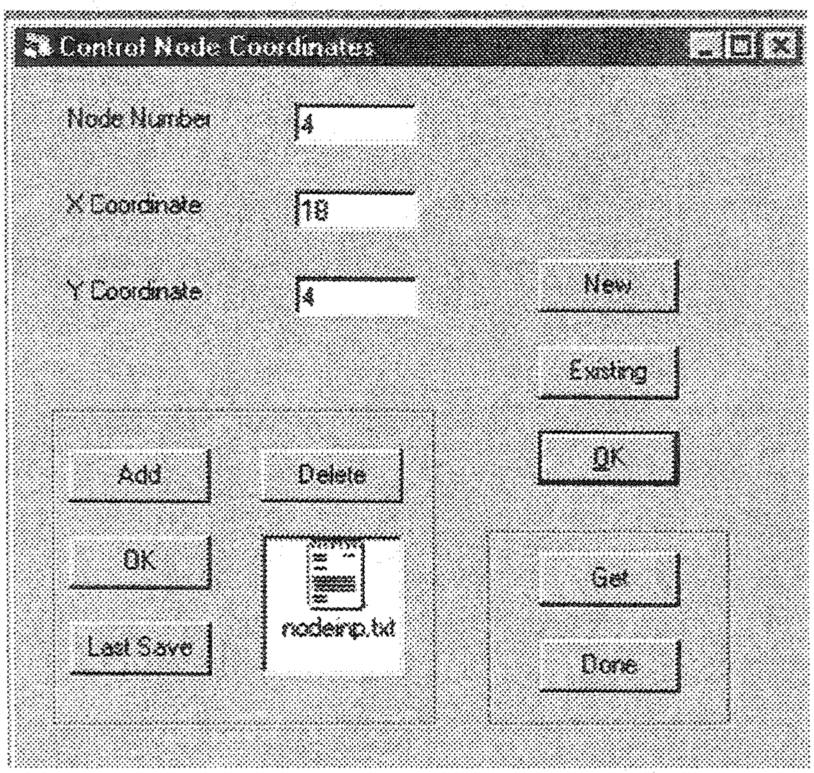

- **Line Generation of Node Coordinates**

Line Generation Number: Number defining the current line generation information. This number is not stored in the '.TXT' file. It is only used to identify the data set.

Node Number at Beginning: Node number at the beginning of the generation line.

Node Number at End: Node number at the end of the generation line.

Number of Nodes to be Generated: Number of nodes to be generated along one line

Node Number Difference: The difference between any two successive nodes on line. The node number difference between the nodes should be constant. If '0' is entered it means that the difference is equal to '1'.

Spacing Between Nodes: The spacing between the successive generated nodes are defined with codes. '0' means the nodes ate automatically spaced uniformly along the generation line. If a value less than '1' is specified, it is considered as the ratio of actual spacing to the length of generation line. The actual spacing may be defined by entering the value equal or greater than '1', representing the length between the nodes.

- **Nodes with Zero Displacement**

Zero Displacement Number: The number defining the current zero displacement information. This number is not saved in the '.TXT' file. It is used to identify the data set.

Number of First Node: Node number or number of first node in a series of nodes covered by this command.

Code for X Displacement: The code is "1" if the node has zero displacement (constrained) in X direction, '0' (unconstrained) otherwise.

Code for Y Displacement: The code is "1" if the node has zero displacement (constrained) in Y direction, '0' (unconstrained) otherwise.

Code for Rotation: The code is "1" if the node has zero rotation (constrained), '0' (unconstrained) otherwise.

Number of Last Node: If a series of nodes is considered, this will represent the last node of the series. If a single node is considered, '0' should be entered.

Node Number Difference: The difference between any two successive nodes on line. The node number difference between the nodes should be constant. If '0' is entered it means that the difference is equal to 1.

- **Nodes with Identical Displacements**

Identical Displacement Number: Number defining the identical displacement information. This number is not stored in the '.TXT' file. It is only used to identify the data set.

Displacement Code: If X displacements are identical for certain nodes, '1' should be entered. '2' is entered for identical displacements in Y direction. For identical rotations, '3' must be entered.

Number of Nodes: Number of nodes having identical displacements covered by this command. A maximum of 14 nodes may be specified by a single command.
List of Nodes: The nodes having identical displacements should be entered in increasing numerical order.

- **Lumped Masses at Nodes**

Lumped Mass Number: The number defining the current lumped mass information. This number is not stored in the '.TXT' file. It is only used to identify the data set.
Number of First Node: Node number or number of first node in a series of nodes covered by this command.
X Mass: Mass associated with X displacement. May be zero if no mass is associated with X displacement.
Y Mass: Mass associated with Y displacement. May be zero if no mass is associated with Y displacement.
Rotational Mass: Mass associated with rotation. May be zero if no mass is associated with rotation.
Number of Last Node: If a series of nodes is considered, this will represent the last node of series. If a single node is considered, '0' should be entered.
Node Number Difference: The difference between any two successive nodes on line. The node number difference between the nodes should be constant. If '0' is entered it means that the difference is equal to '1'.
Modifying Factor: The modification factor by which masses are to be divided. If the mass values are given in weights, this factor will typically be equal to 'g' gravitational acceleration. When this value is entered as '0', the value from the preceding command will be applied to all masses. Thus, specifying the factor for the first command is sufficient when the same factor is to be applied for all commands.

LOAD INFORMATION

- **Control Information**

Static Load Code: If static loads are applied prior to dynamic analysis, '1' should be selected. If there are no static loads, '0' option box should be checked.

Pushover Code: '0' is entered if pushover analysis is not to be performed. A positive value defines the number of load steps the lateral loads are divided by equally. For example, if 25 is entered, the structure is analyzed in 25 steps (4% of total load in each step). A negative value indicates the number of lines that define unequal division of lateral loads.

Number of Static Load Commands: Number of commands specifying static loads applied directly at nodes. If no static loads are applied directly at the nodes, '0' is entered.

Number of Integration Time Steps: Number of integration time steps to be considered in dynamic analysis.

Integration Time Step: The integration time step, Δt, which is used in the dynamic analyses.

Magnification Factor for X Acc.: Modification factor to be applied to ground accelerations specified for the X direction. The factors may be used to increase or decrease ground accelerations, or to convert from multiples of the acceleration due to gravity to acceleration units, or both. When the accelerations are scaled, the ground velocities and displacements are scaled by the same proportion.

Magnification Factor for X Time Scale: Modification factor to be applied to the time scale of ground acceleration record specified for the X direction. If a time scale factor is equal to 'k', all input times are multiplied by k before obtaining the interpolated accelerations at intervals equal to the integration time step. If the ground accelerations remain unchanged, the effect is to increase the ground velocities by k and the ground displacements by k^2, and to alter the frequency content of the earthquake.

Magnification Factor for Y Acc.: Magnification factor to be applied to ground accelerations specified for the Y direction. The comments given for X direction also apply to Y direction.

Magnification Factor for Y Time Scale: Magnification factor to be applied to the time scale of the ground acceleration record specified for the Y direction. The comments given for X direction also apply to Y direction.

Maximum Displacement: Absolute value of the maximum displacement permitted before the structure is assumed to be collapsed. The execution is terminated if this value is exceeded at any step. '0' should be entered to use the default value as '100000'.

- **Static Loads Applied Directly at Nodes**

Static Load Number: The number defining the current static load information. This number is not stored in the '.TXT' file. It is only used to identify the data set.

Number of First Node: Node number or number of first node in a series of nodes covered by this command.

Load in X Direction: Load in X direction. The same load is assumed to apply on all nodes in the series.

Load in Y direction: Load in Y direction. The same load is assumed to apply on all nodes in the series. Note that the Y direction will normally be positive upwards.

Moment Load: Moment specified about Z axis using the right hand screw rule. The same moment is assumed to apply on all nodes in the series. As normally viewed, counterclockwise is positive.

Number of Last Node: If a series of nodes is considered, this will represent the last node of the series. If a single node is considered, '0' should be entered.

Node Number Difference: The difference between any two successive nodes on line. The node number difference between the nodes should be constant. If '0' is entered it means that the difference is equal to '1'.

- **Dynamic Loads**

➢ ***Control Information***

Number of Time-Acc. for X Direction: Number of time-acceleration pairs defining ground motion in X direction. If there is no ground motion in this direction '0' should be entered.

Number of Time-Acc. For Y Direction: Number of time-acceleration pairs defining ground motion in Y direction. If there is no ground motion in this direction '0' should be entered.

Code for Printing Acc. as Input: '0' is entered for no output, and "1" is entered to get listing of acceleration records.

Code for Printing Interpolated Acc.: '0' is entered for no output, and "1" is entered to get listing of acceleration record as interpolated at intervals.

Title to Identify Records: This title is printed with output files to identify records.

➢ *Ground Acceleration Time History in X Direction*

Ground acceleration time histories are entered in the appropriate window. Once the window is selected from the main menu, a window with a blank (white) frame will appear. Double clicking on the blank frame activates Microsoft Word. This word processing software opens a document with the name of "AccX." The user should cut and paste the acceleration record from its original location to the Microsoft Word document. Once the data is entered, the Save As option within the MS Word program should be selected and 'Plain Text' should be defined in 'Save as Type' part. It means that the document is saved as a 'text' document instead of 'word' document. It is important not to change the name of the document.

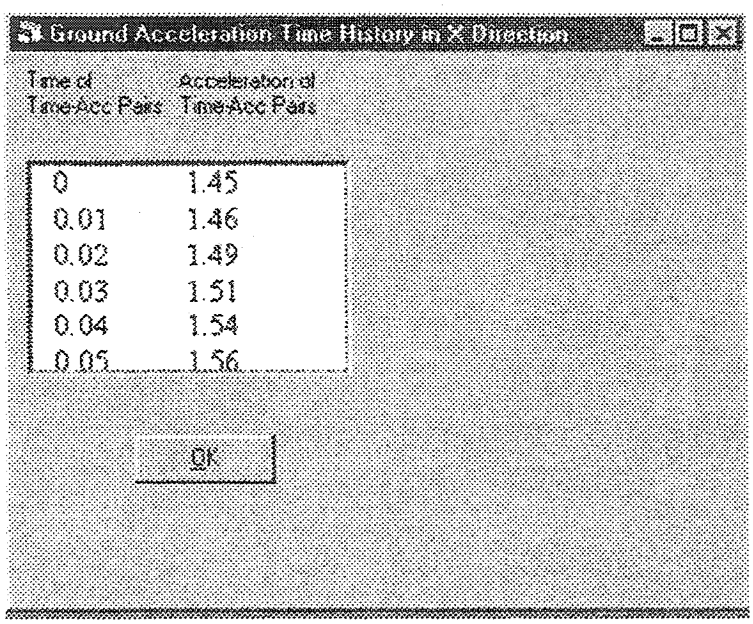

Time of Time-Acc. Pairs: The time corresponding to the acceleration record defined in X direction.

Acceleration of Time-Acc. Pairs: The acceleration corresponding to the acceleration record defined in X direction. This data is often entered in acceleration units (and not multiples of the acceleration due to gravity). Both the acceleration and time scales may then be scaled if desired. If the record is input in terms of the acceleration due to gravity, an acceleration magnification factor equal to g may be used to convert the input record to acceleration units.

> ***Ground Acceleration Time History in Y Direction***

Time of Time-Acc. Pairs: The time corresponding to the acceleration record defined in Y direction.

Acceleration of Time-Acc. Pairs: The acceleration corresponding to the acceleration record defined in Y direction. It is assumed to be in acceleration units (not multiples of the acceleration due to gravity).

- **Damping Information**

Mass Proportional Damping Factor, α: A viscous damping matrix $C = \alpha M$ is assumed, where M= mass matrix. If only mass dependent damping is assumed, damping equal to Ψ_i in the mode with period T_i can be obtained by specifying $\alpha = 4*\pi* \Psi_i / T_i$.

Stiffness Proportional Damping Factor, β: A viscous damping matrix $C = \beta K_T$ is assumed, where K_T = current tangent stiffness matrix. If only stiffness dependent damping is assumed, damping equal to Ψ_i in a mode with period T_i can be obtained by specifying $\beta = \Psi_i *T_i/ \pi$. If a damping matrix is assumed as a combination of stiffness and mass matrices $C= \alpha M+ \beta K_T$, the coefficients are defined as:

$$\alpha = 4*\pi*(T_i*\Psi_i-T_j*\Psi_j)/(T_i^2-T_j^2)$$

$$\beta = T_i*T_j*(T_j*\Psi_i-T_i*\Psi_j)/(\pi*(T_j^2-T_i^2))$$

Stiffness Proportional Damping Factor, β₀: A viscous damping matrix $C=\beta_0*K_0$ is assumed, where K_0 = original elastic stiffness matrix, ignoring the geometric stiffness.

Structural Damping Factor, δ: No viscous damping is assumed. Damping forces in any time step are applied, based on the member actions and rates of deformation existing at the end of the previous step.

ELEMENT SPECIFICATION

- **Truss Elements**

> ***Control Information***

Truss Elements: The type number of the truss element is '1'. If truss elements are included in the analyses, the check box must be checked.

Number of Elements: The total number of truss elements.

Number of Stiffness Types: Number of different element stiffness types. Maximum 40 different stiffness types may be used.

Number of Fixed End Forces: Number of different fixed end force patterns. Maximum 40 different fixed end force patterns may be used.

➢ ***Stiffness Types***

Stiffness Type Number: The number defining the current stiffness information. The number should be entered sequentially beginning with 1.

Young's Modulus of Elasticity:

Strain Hardening Modulus: This value should be entered as a proportion of young's modulus.

Average Cross-Sectional Area: The area of the defined member.

Yield Stress in Tension:

Yield Stress in Compression: The yield stress or elastic buckling stress in compression.

Buckling Code: If element buckles elastically in compression, '1' is entered. If the element yields in compression without buckling, '0' is entered.

➢ ***Fixed End Force Patterns***

Pattern Number: The number defining the current fixed end force pattern information

Axis Code: If the forces are in the element coordinate system, '0' is entered. If the forces are in the global coordinate system, '1' is entered.

Clamping Force F_i: The force in the X direction of the global or element coordinate systems at end i.

Clamping Force V_i: The force in the Y direction of the global or element coordinate systems at end i.

Clamping Force F_j: The force in the X direction of the global or element coordinate systems at end j.

Clamping Force V_j: The force in the Y direction of the global or element coordinate systems at end j.

The effects of static loads applied along the element length rather than at the nodes can be taken into account by specifying fixed end force patterns. The forces specified above are the forces on the element ends required to prevent them from displacing.

➢ ***Element Generation Command***

Element Number: The number of element, if the properties of a single element are defined. If elements will be generated, it refers to the first element in the series. Elements don't need to be entered in increasing numerical order.

Node Number at end i: The node number for specifying the element at end i.

Node Number at end j: The node number for specifying the element at end j.

Node Number Increment: Node number increment for element generation. If '0' is entered, the increment is taken as '1'.

Stiffness Type Number: The stiffness type number of the current element.

Code for Geometric Stiffness: To include geometric stiffness in the analyses, '1' should be entered whereas '0' is entered to ignore this property.

Time History Output Code: '1' is entered to obtain time histories of element results at the time intervals specified. If time histories of element results are not required for elements covered by this command, '0' should be put.

Fixed E.F. for DL: Fixed end force pattern number for static dead loads on elements. If there are no dead loads, '0' is put.

Fixed E.F. for LL: Fixed end force pattern number for static live loads on elements. If there are no live loads, '0' is put.

Scale F. for DL: Scale factor to be applied to fixed end forces due to static dead loads. If there are no dead loads, '0' is put.

Scale F. for LL: Scale factor to be applied to fixed end forces due to static live loads. If there are no live loads, '0' is put.

Initial Axial Force: If there is initial axial force defined on the element, it should be entered assuming that tension is positive

Number of Element Generation Commands: The total number of element generation commands should be entered to control the input data. This number will not appear in the '.TXT' files.

REINFORCED CONCRETE BEAM ELEMENTS WITH DEGRADING STIFFNESS

➢ *Control Information*

RC Elements: The type number of the reinforced concrete beam element is '6'. If RC elements are included in the analyses, the check box must be checked.

Number of Elements: The total number of RC elements.

Number of Stiffness Types: Number of different element stiffness types. Maximum 40 different stiffness types may be used.

Number of Rigid Offset Types: Number of different rigid end offset types. Maximum 15 different rigid offset types may be used.

Number of Yield Moments: Number of different yield moment values for cross sections. Maximum 40 different yield moments may be used.

Number of Fixed End Forces: Number of different fixed end force patterns. Maximum 34 different fixed end force patterns may be used.

Number of Initial Forces: Number of different initial element force patterns. Maximum 30 different initial forces may be used.

Number of M-P Interactions: Number of different axial force-bending moment interactions.

Code for Anchorage Slip: To consider the anchorage slip nonlinearity deformation during analysis, '0' option box should be selected. To ignore this kind of deformation in the behavior of the structure, '1' is selected.

Code for Shear: To consider the shear nonlinearity deformation during analysis, '0' option box should be selected. To ignore this kind of deformation in the behavior of the structure, '1' is selected.

Code for Shear and Slip Models: Select '0', if shear and slip yielding moments are not necessarily equal to flexural yielding moment and to be determined by the user. If shear and slip yielding moments are equal to initial flexural yielding moment even they are different in input file, select '1'.

➢ *Stiffness Types*

Beam Properties

Stiffness Type Number: The number defining the current stiffness information. The number should be entered in sequence beginning with 1.

EI: Reference flexural stiffness

EA: Effective axial stiffness

GA': Effective shear stiffness. Shear deformations are neglected if this value is entered '0'.

Flex. Stiff. Fac. k_{ii}: Flexural stiffness factor k_{ii}.

Flex. Stiff. Fac. kjj: Flexural stiffness factor k_{jj}

Flex. Stiff. Fac. kij: Flexural stiffness factor k_{ij}.

Strain Hardening at i: Strain hardening ratio that is defined for inelastic flexure at node i. If a non-zero hinge stiffness will be specified at node i for flexural behavior, this strain hardening ratio will apply directly to the hinge moment-rotation relationship. Otherwise, this ratio will apply to the overall beam end moment-rotation relationship or cantilever P-Δ relationship.

Strain Hardening at j: Strain hardening ratio that is defined for inelastic flexure at node j. As with node i, a zero or non-zero hinge stiffness for node j will control whether this ratio is directly applied to the hinge alone or to the beam as a whole.

Flexural Hinge Properties

Stiffness Type Number: The number defining the current stiffness information. The number should be entered in sequence beginning with 1. It is corresponding to the stiffness type number on the preceding beam properties.

Hinge Stiffness at Node i: If hinge properties are to be determined by the program, '0' should be entered and they are marked with * in the output files. The program calculates the hinge stiffness by multiplying the beam stiffness with 10^8. The hinge stiffness values for end i and j should be entered as a same manner (If zero is entered for end i, the following field for end j must also zero. If nonzero, the following field must also be nonzero).

Hinge Stiffness at Node j: If hinge properties are to be determined by the program, '0' should be entered and they are marked with * in the output files. The program calculates the hinge stiffness by multiplying the beam stiffness with 10^8.

Unloading Stiffness at i: α_i, unloading stiffness parameter for end i. For unloading according to Takeda model, '0' should be entered.

Unloading Stiffness at j: α_j, unloading stiffness parameter for end j. For unloading according to Takeda model, '0' should be entered.

Loading Parameter at i: β_i, loading parameter for end i. For reloading according to Takeda model, '0' should be entered.

Loading Parameter at j: β_j, loading parameter for end j. For reloading according to Takeda model, '0' should be entered.

Loading Exp. Parameter: N, loading exponential parameter. It is anticipated that a value N=1 will be used.

Anchorage Slip Hinge Properties

Slip Stiffness Type Number: The number defining the current slip stiffness information. The number should be entered in sequence beginning with 1.

Elastic (+) Stiffness at i: Elastic positive stiffness of slip model at end i.

Elastic (-) Stiffness at i: Elastic negative stiffness of slip model at end i.

(+) Strain Hard. at i: Positive strain hardening ratio of slip model at end i.

(-) Strain Hard. at i: Negative strain hardening ratio of slip model at end i.

Unl. Stiff. (+) / El. Stiff at i: Unloading stiffness at the positive control point of slip model at end i as a ratio of the elastic positive stiffness.

Unl. Stiff. (-) / El. Stiff at i: Unloading stiffness at the negative control point of slip model at end i as a ratio of the elastic negative stiffness.

Rotation Coor. (+) at i: Rotation coordinate of the positive control point of the slip model at end i.

Rotation Coor. (-) at i: Rotation coordinate of the negative control point of the slip model at end i.

Elastic (+) Stiffness at j: Elastic positive stiffness of slip model at end j.

Elastic (-) Stiffness at j: Elastic negative stiffness of slip model at end j.

(+) Strain Hard. at j: Positive strain hardening ratio of slip model at end j.

(-) Strain Hard. at j: Negative strain hardening ratio of slip model at end j.

Unl. Stiff. (+) / El. Stiff. at j: Unloading stiffness at the positive control point of slip model at end j as a ratio of the elastic positive stiffness.

Unl. Stiff. (-) / El. Stiff. at j: Unloading stiffness at the negative control point of slip model at end j as a ratio of the elastic negative stiffness.

Rotation Coor. (+) at j: Rotation coordinate of the positive control point of the slip model at end j.

Rotation Coor. (-) at j: Rotation coordinate of the negative control point of the slip model at end j.

Shear Hinge Properties

Shear Stiffness Type Number: The number defining the current shear stiffness information. The number should be entered in sequence beginning with 1.

(+) Post Crack. Stiff. / El. Stiff. at i: Positive post cracking stiffness of shear model at end i as a ratio of the elastic stiffness

(+) Post Yield Stiff. / El. Stiff. at i: Positive post yield stiffness of shear model at end i as a ratio of the elastic stiffness

(-) Post Crack. Stiff. / El. Stiff. at i: Negative post cracking stiffness of shear model at end i as a ratio of the elastic stiffness

(-) Post Yield Stiff. / El. Stiff. at i: Negative post yield stiffness of shear model at end i as a ratio of the elastic stiffness

(+) Post Crack. Stiff. / El. Stiff. at j: Positive post cracking stiffness of shear model at end j as a ratio of the elastic stiffness

(+) Post Yield Stiff. / El. Stiff. at j: Positive post yield stiffness of shear model at end j as a ratio of the elastic stiffness

(-) Post Crack. Stiff. / El. Stiff. at j: Negative post cracking stiffness of shear model at end j as a ratio of the elastic stiffness

(-) Post Yield Stiff. / El. Stiff. at j: Negative post yield stiffness of shear model at end j as a ratio of the elastic stiffness.

➢ *Rigid Offsets*

Rigid Offset Type Number: The number defining the current rigid offset type information. The number should be entered in sequence beginning with 1.

Length in X at i: The length of rigid offset in X direction at end i.

Length in X at j: The length of rigid offset in X direction at end j. This value must be entered negative.

Length in Y at i: The length of rigid offset in Y direction at end i.

Length in Y at j: The length of rigid offset in Y direction at end j. This value must be entered negative.

Plastic hinges in frames and coupled frame-shear wall structures will form near the faces of the connection rather than at the theoretical joint centerline. This effect can be approximated by postulating rigid and infinitely strong connecting links between the nodes (located at the joint centerlines) and the element ends. Rigid offsets are defined for this purpose.

➢ *Cross Section Yield Interaction Surfaces*

Yield Surface Number: The number defining the current yield surface information that should be entered in sequence beginning with 1.

(+) Flex. My: Positive flexural yield moment.

(-) Flex. My: Negative flexural yield moment.

(+) Shear My: Positive shear yield moment.

(-) Shear My: Negative shear yield moment.

(+) Slip My: Positive slip yield moment.

(-) Slip My: Negative slip yield moment.

(+) Shear Mcr: Positive cracking moment in shear model. The cracking moment estimated from moment-curvature analysis of the sections considering the presence of axial load.

(-) Shear Mcr: Negative cracking moment in shear model.

(+) Slip M_0: Positive zero strain moment in the slip model. In the presence of axial compression, the elastic deformation in steel is recovered prior to complete unloading of the bending moment. The residual deformation is computed at a moment that corresponds to zero force in tension reinforcement that is defined as M_0.

(-) Slip M_0: Negative zero strain moment in the slip model.

P: Static axial load in the member.

P_0: Axial load capacity of the member.

➢ *Fixed End Force Patterns*

Pattern Number: The number defining the current fixed end force pattern information that should be entered in sequence beginning with 1.

Axis Code: If the forces are in the element coordinate system, '0' is entered. If the forces are in the global coordinate system, '1' is entered.

Clamping Force F_i: The force specified in the X direction of the global or element coordinate systems at end i.

Clamping Force V_i: The force specified in the Y direction of the global or element coordinate systems at end i.

Clamping Moment M_i: The moment specified about the Z direction at end i.

Clamping Force F_j: The force specified in the X direction of the global or element coordinate systems at end j.

Clamping Force V_j: The force specified in the Y direction of the global or element coordinate systems at end j.

Clamping Moment M_j: The moment specified about the Z direction at end j.

Load Reduction: Live load reduction factor for computation of live load forces to be applied to nodes.

The effects of static loads applied along the element length rather than at the nodes can be taken into account by specifying fixed end force patterns. The forces specified above are the forces on the element ends required to prevent them from displacing.

➢ *Initial Element Force Patterns*

Pattern Number: The number defining the current initial element force pattern information

Initial Axial Force F_i: The initial force specified in the X direction of the global or element coordinate systems at end i.

Initial Shear Force V_i: The initial force specified in the X direction of the global or element coordinate systems at end i.

Initial Moment M_i: The initial moment specified about the Z direction at end i.

Initial Axial Force F_j: The initial force specified in the X direction of the global or element coordinate systems at end j.

Initial Shear Force V_j: The initial force specified in the Y direction of the global or element coordinate systems at end j.

Initial Moment M_j: The initial moment specified about the Z direction at end j.

For structures in which static analyses are carried out separately, initial member forces may be specified. These forces are not converted to loads on the nodes of the structure, but simply used to initialize the element end forces. They may be specified in addition to static nodal loads and element end clamping forces, in which case the element forces due to static loading are added to the initial forces.

➤ *Axial Force-Bending Moment Interaction Patterns*

Pattern Number: The number defining the current M-P interaction pattern information

(+) P_b: Axial Force for positive balanced point.

(+) M_b: Bending moment for positive balanced point.

(-) P_b: Axial force for negative balanced point.

(-) M_b: Bending moment for negative balanced point.

(+) M at P=0: Positive bending moment for zero axial force.

(-) M at P=0: Negative bending moment for zero axial force.

P_{tens} at M=0: Tension axial force for zero bending moment.

P_{comp} at M=0: Compression axial force for zero bending moment.

➤ *Element Generation Command*

Element Number: The number of element, if the properties of a single element are defined. If elements will be generated, it refers to the first element in the series. Elements don't need to be specified in increasing numerical order.

Node Number at i: The node number for specifying the element at end i.

Node Number at j: The node number for specifying the element at end j.

Node Number Increment: Node number increment for element generation. If '0' is entered, the increment is taken as '1'.

Stiffness Type Number: The stiffness type number of the specified element.

End Ecc. Type Number: If there is no end eccentricity, '0' should be entered.

Yield Surface Number at i: Yield surface number for the specified element end i.

Yield Surface Number at j: Yield surface number for the specified element end j.

Code for Geometric Stiffness: To include geometric stiffness in the analyses, '1' should be entered whereas '0' is entered to ignore this property.

Time History Output Code: '1' is entered to obtain time histories of element results at the time intervals specified. If time histories of element results are not required for elements covered by this command, '0' should be put.

Fixed E.F. for DL: Fixed end force pattern number for static dead loads on elements. If there are no dead loads, '0' is put.

Fixed E.F. for LL: Fixed end force pattern number for static live loads on elements. If there are no live loads, '0' is put.

Scale F. for DL: Scale factor to be applied to fixed end forces due to static dead loads.

Scale F. for LL: Scale factor to be applied to fixed end forces due to static live loads.

Initial Force Pattern Number: If there is initial axial force defined on the element, it should be entered assuming tension is positive

Scale F. for Initial Forces: Scale factor to be applied to initial element forces.

M-P at i: Axial Force-Bending Moment pattern number at element end i.

M-P at j: Axial Force-Bending Moment pattern number at element end j.

Number of Element Generation Commands: The total number of element generation commands should be entered to control the input data. This number will not appear in the '.TXT' files.

INFILL PANEL ELEMENTS

➢ Control Information

Infill Panel Elements: The type number of the infill panel element is '11'. If infill panel elements are included in the analyses, the check box must be checked.

Number of Elements: The total number of infill panel elements.

Number of Stiffness Types: Number of different element stiffness types. Maximum 40 different stiffness types may be used.

➢ Stiffness Types

Stiffness Type Number: The number defining the current stiffness information, which should be entered in sequence beginning with 1.

Modulus of Elasticity:

Average Cross-Sectional Area:

Yield Stress in Tension:

Yield Stress in Compression:

➢ Element Generation Command

Element Number: The number of element, if the properties of a single element are defined. If elements will be generated, it refers to the first element in the sequentially numbered series. Elements don't need to be entered in increasing numerical order.

Node Number at i: The node number for specifying the element at end i.

Node Number at j: The node number for specifying the element at end j.

Node Number Increment: Node number increment for element generation. If '0' is entered, the increment is taken as '1'.

Stiffness Type Number: The stiffness type number of the specified element.

Time History Output Code: '1' is entered to obtain time histories of element results at the intervals specified. If time histories of element results are not required for elements covered by this command, '0' should be put.

Number of Element Generation Commands: The total number of element generation commands should be entered to control the input data. This number will not appear in the '.TXT' files.

TIME HISTORY ANALSIS

- **Control Information**

Time Interval for printout of nodal displacement time histories: It is expressed as a multiple of time step Δt. For no printout, '0' should be entered.

Time Interval for printout of time histories of element results: It is expressed as a multiple of time step Δt. For no printout, '0' should be entered.

Time Interval for intermediate printout of envelope values: It is expressed as a multiple of time step Δt. For no printout, '0' should be entered.

Number of Nodes for X displ.: Number of nodes for which X displacement time histories are required.

Number of Nodes for Y displ.: Number of nodes for which Y displacement time histories are required.

Number of Nodes for Rotation: Number of nodes for which rotation time histories are required.

Number of Pairs for X displ.: Number of pairs of nodes for which time histories of relative X displacement is required.

Number of Pairs for Y displ.: Number of pairs of nodes for which time histories of relative Y displacement is required.

Print Code for Nodal Displacement Time Histories: To get time history printout only as the computation progress, '0' should be selected. By checking '1', both a printout as the computation progress and a re-ordered printout at the end of the computation is obtained. '2' is selected when only a re-ordered printout at the end of the computation is aimed.

Print Code for Relative Nodal Displacement Time Histories: The same codes (0,1,2) as defined previously are used.

Print Code for Element Results Time Histories: The same codes (0,1,2) as defined previously are used.

- **Nodes for X,Y Displacement and Rotation Time Histories**

The node numbers, for which displacements and rotation time histories are required as output, should be entered in text boxes sequentially, by separating them with commas.

The information is saved when the 'OK' button is clicked. 'Cancel' button may be used to close the form without a change.

Node Numbers for X Displacements: List of node numbers for which X displacement time histories are required.

Node Numbers for Y Displacements: List of node numbers for which Y displacement time histories are required.

Node Numbers for Rotations: List of node numbers for which rotation time histories are required.

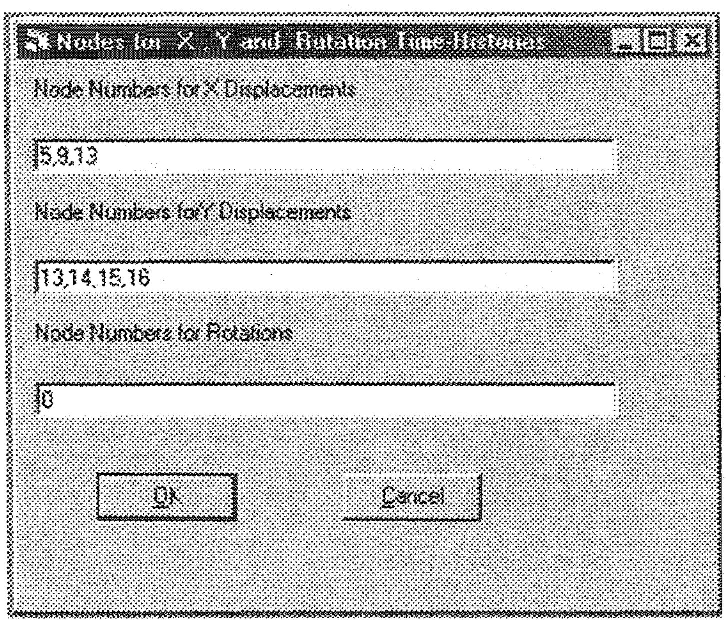

- ## <u>Nodes for Relative X and Y Displacement Time Histories</u>

Node Numbers for Relative X Displacements: The number of first and second nodes of pairs of nodes for which relative X displacement time histories are required. They should be entered sequentially in the same line separated by commas. The following pairs should also be entered in the same manner as the previous pairs and in the same line. The printed displacement is the displacement of the first node of any pair minus the displacement of the second node.

Node Numbers for Relative Y Displacements: The number of first and second nodes of pairs of nodes for which relative Y displacement time histories are required. They should be entered sequentially in the same line separated by commas. The following pairs should also be entered in the same manner as the previous pairs and in the same line.

PUSHOVER ANALYSIS

Number of Commands

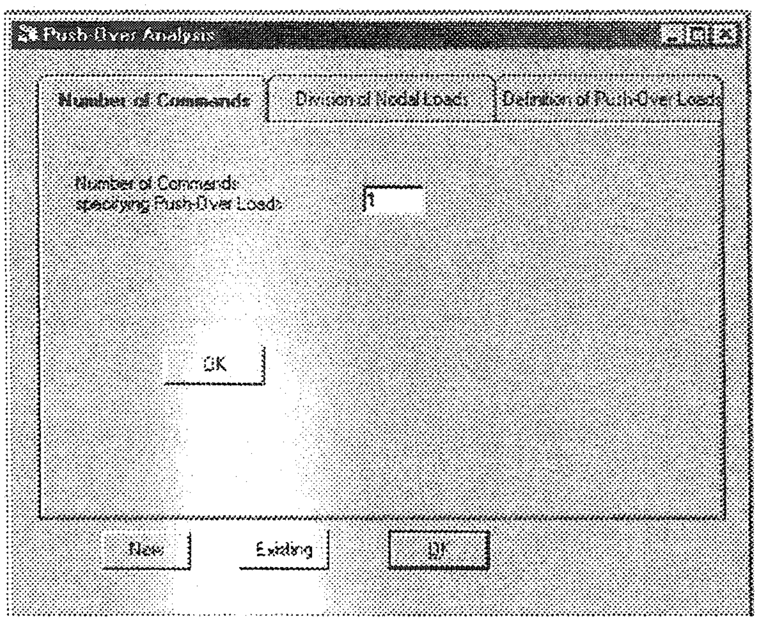

Number of Commands specifying Pushover Loads: This command specifies the pushover loads applied directly at the nodes.

Division of Nodal Loads

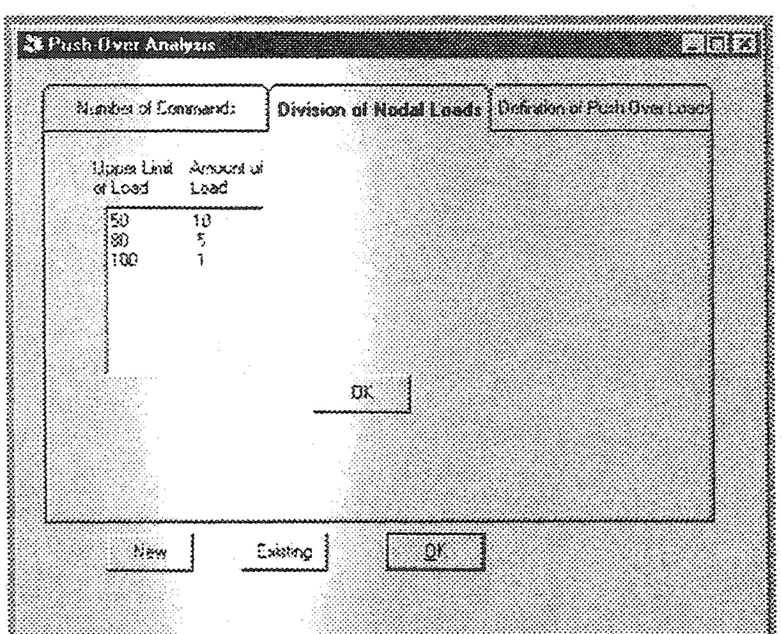

Upper Limit of Load: The percentage of pushover load that represents the end of a loading segment. The pushover load is applied up to the limit specified in this data entry in equal increment, where each increment is specified in percentage of pushover load in the next data entry (Amount of Load).

Amount of Load: The increment of pushover load specified in percentage of total load.

This section specifies the manner of division of nodal loads specified in Pushover analysis. If these loads are divided equally and Pushover code is positive, this section should be omitted. The number of lines in this section is equal to absolute value of '***Pushover Code***'.

Example: If '***Pushover Code***' is defined as '-3', it means in this section three lines must be specified. Assuming these three lines are put as following:

50,10

80,5

100,1

It means that up to 50% of load, in each loading stage 10% of total load will be applied. After that, up to 80%, in each loading stage 5% of total load and finally until 100%, in each loading stage just 1% of total load will be applied (totally 31 load stages).

<u>Definition of Pushover Loads</u>

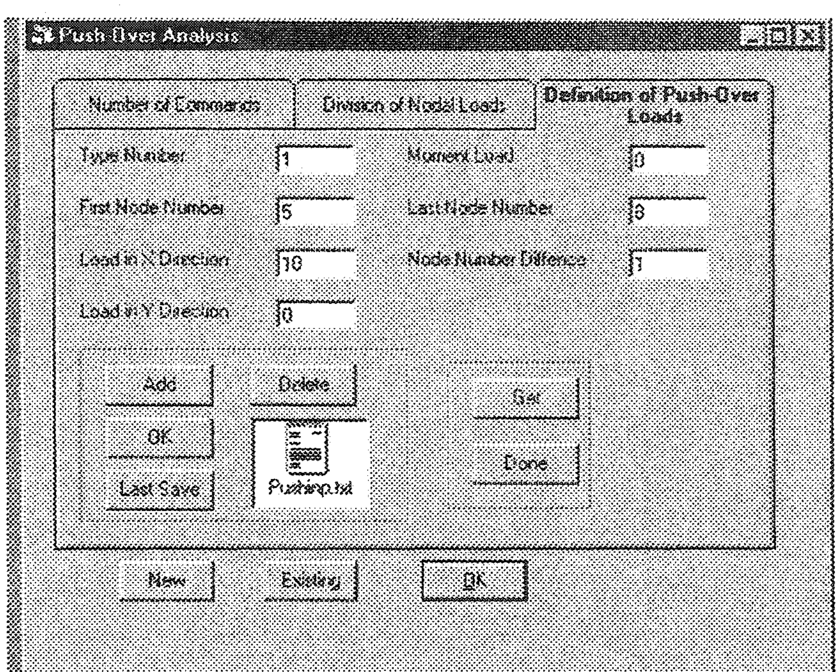

Type Number: The number defining the current pushover load information. This number will not be seen in the '.TXT' file. It is used to see the added information in the system.

First Node Number: Node number or number of first node in a series of nodes covered by this command.

Load in X Direction: The load that is specified on X direction. The same load is assumed on all nodes in the series.

Load in Y direction: The load that is specified on Y direction. The same load is assumed on all nodes in the series.

Moment Load: The moment load that is specified about Z axis using right hand screw rule. The same load is assumed on all nodes in the series. As normally viewed, counterclockwise is positive.

Number of Last Node: If a series of nodes is considered, this will represent last node of the series. If a single node is considered, '0' should be entered.

Node Number Difference: The difference between any two successive nodes on line. The node number difference between the nodes should be constant. If '0' is entered it means that the difference is equal to '1'.

When the Pushover Analysis window is opened, the 'New' or 'Existing' button should be pressed as described above. The input files are divided to three by using tab functions. To save the information entered in the first and second forms, 'OK' button on related tab should be pressed. The third form is executing as the same manner as defined earlier.

HOW TO EXECUTE THE PROGRAM?

All files related to the program are in a folder named 'aaa' that should be put directly under the 'C' part of the harddisk (C:\aaa). This folder contains DRAIN-RC.exe, which should be opened to input data and execute the program. It is the pre-processor of the program. The other executable file 'Drainrc_es.exe' ,is the original program that contains the source code. AccX.doc and AccY.doc files are also in that folder. After DRAIN-RC.exe is double clicked, it is opened and ready to enter data to the forms. When data input is finished, from the 'run' menu the 'start' option should be selected and the original program will execute. The input file is automatically named 'project' and the output files will appear in the same folder. They can be looked by using any text editor.

OUTPUT FILES

1. Output file with 'INP' extension. It contains echo of input file.
2. Output file with 'STA' extension. It contains static nodal displacement and results for all elements for time equal to zero (static analysis). If static analysis is not required, this file will not created.
3. Output file with 'REV' extension. It contains time history (if it is required) and results envelopes for all elements.
4. Output file with 'NDE' extension. It contains time history (if it is required) and results envelopes for nodal displacements for all nodes in X and Y direction.
5. Output file with 'HGR' extension. It contains hinge rotation results.
6. Output file with 'DCD' extension. It contains ductility demands results.
7. Output file with 'EGD' extension. It contains dissipated energy factors.
8. Output file with 'YIE' extension. It contains the information of yielded members.